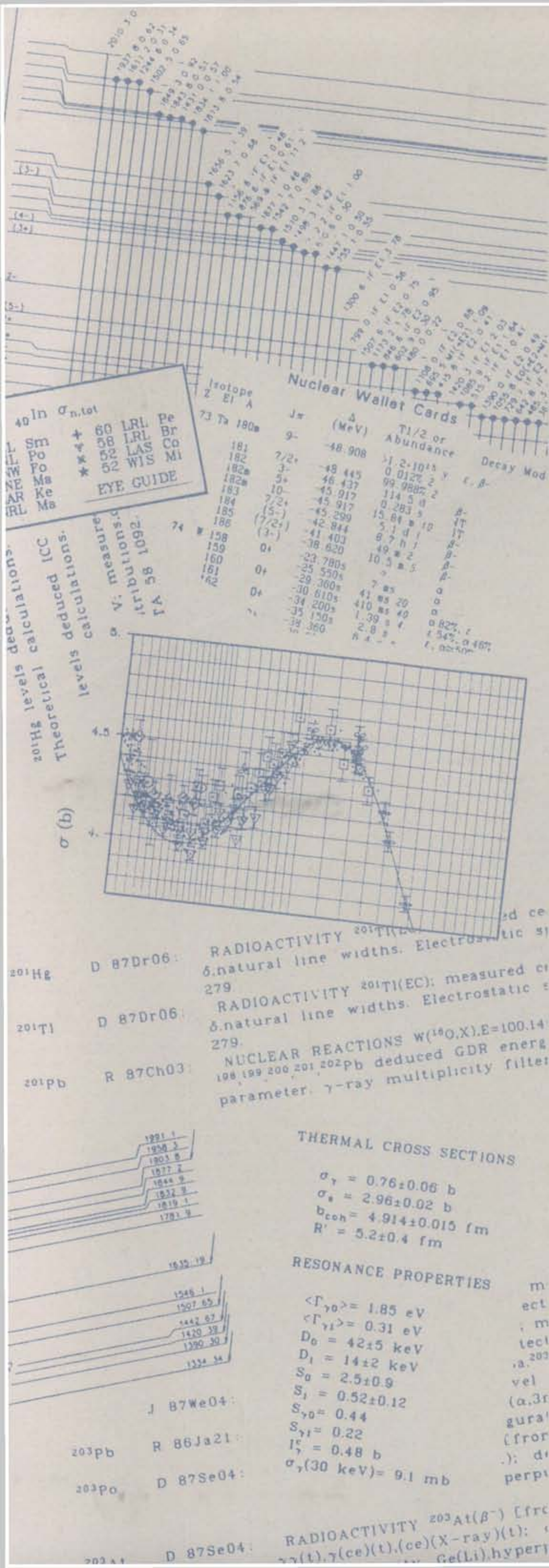

BNL-NCS-46173
DOE/NDC-58/U
NEANDC(US)-229/U
INDC(USA)-104/L
INFORMAL REPORT
LIMITED DISTRIBUTION

REPORTS TO THE DOE NUCLEAR DATA COMMITTEE

Compiled by the
NATIONAL NUCLEAR DATA CENTER
for the
U.S. Department of Energy
Nuclear Data Committee

May 1991

BROOKHAVEN NATIONAL LABORATORY
ASSOCIATED UNIVERSITIES, INC.
UPTON, LONG ISLAND, NEW YORK 11973

national
nuclear
data
Center

BNL-NCS-46173
DOE/NDC-58/U
NEANDC(US)-229/U
INDC(USA)-104/L
Informal Report
Limited Distribution

REPORTS TO
THE DOE NUCLEAR DATA COMMITTEE

MAY 1991

national
nuclear
data
Center

Compiled by the

NATIONAL NUCLEAR DATA CENTER
BROOKHAVEN NATIONAL LABORATORY
ASSOCIATED UNIVERSITIES, INC.

UNDER CONTRACT NO. DE-AC02-76CH00016 WITH THE
UNITED STATES DEPARTMENT OF ENERGY

Printed in the United States of America
Available from
National Technical Information Service
U.S. Department of Commerce
5285 Port Royal Road
Springfield, VA 22161

NTIS price codes:
Printed Copy: A08; Microfiche Copy: A01

PREFACE

The reports in this document were submitted to the Department of Energy Nuclear Data Committee (DOE-NDC) in April, 1991. The reporting laboratories are those with a substantial program for the measurement of neutron and nuclear cross sections of relevance to the U.S. applied nuclear energy program.

The authors of the Status Report contributions are responsible for collecting and editing individual contributions from their laboratory and are not necessarily the sole authors of the contributions. The scientists responsible for the work described in each individual contribution are listed at the beginning of the contribution.

The material contained in these reports is to be regarded as comprised of informal statements of recent developments and preliminary data. Persons wishing to make use of these data should contact the individual experimenter for further details. *The data which appear in this document should be quoted only by permission of the contributor and should be referenced as private communication, and not by this document number.* Appropriate subjects are listed as follows:

1. **Microscopic neutron cross sections** relevant to the nuclear energy program, including shielding. Inverse reactions, where pertinent, are included.

2. **Charged-particle cross sections**, where they are relevant to (1.) above, and where relevant to developing and testing nuclear models.

3. **Gamma ray production, radioactive decay, and theoretical developments** in nuclear structure which are applicable to nuclear energy programs.

4. **Proton and α-particle cross sections**, at energies of up to 1 GeV, which are of interest to the space program.

These reports cannot be regarded as a complete summary of the nuclear research efforts in the U.S. A number of laboratories whose research is less programmatically oriented do not submit reports; neither do the submitted reports reflect all the work related to nuclear data in progress at the submitting laboratory.

This compilation has been produced almost completely from master copies prepared by the individual contributors listed in the Table of Contents, and reports are reproduced *without change* from these master copies.

DOE STATUS REPORTS

1991

TABLE OF CONTENTS

ARGONNE NATIONAL LABORATORY

A. NEUTRON TOTAL AND SCATTERING CROSS-SECTION MEASUREMENTS

1. Elastic Neutron Scattering from ^{238}U and ^{232}Th. (P.T. Guenther, A.B. Smith and S. Chiba*)

The importance of the non-elastic cross sections in evaluations of the actinides has been clear for many years. Given the well-known total and fission cross sections, it is the only reasonable way of determining the remaining partial cross sections below the (n,2n) threshold, particularly the continuum inelastic-scattering cross sections. The key experimental problem is the precise determination of the elastic-scattering cross section from ≈ 2 to 10 MeV. That is difficult (or technologically impossible) over much of this energy range due to the inelastic excitation of the low-lying 2^+ and 4^+ rotational states of the ground-state rotational band. However, precise measurement of the "pseudo-elastic-scattering" cross section (elastic plus the inelastic contribution due to the first two levels), interpreted using rigorous fitting with a rotational coupled-channels model, will give the non-elastic cross sections corresponding to the neutron energy transfers of more than ≈ 150 keV, i.e., the non-elastic cross sections of applied importance above several MeV. The quality of the results depends upon the accuracy of the measurements. The latter have been completed from ≈ 4 to 8.5 MeV, at ≈ 0.5 MeV incident-energy intervals, and at $\geq$ 40 scattering angles. Care was taken to obtain the best possible angle and magnitude normalizations. The work is now being extended to 10 MeV, and the completed results will be fitted at JAERI (Japan) as a part of the NEANDC evaluation task force. The objective of 3% accuracies on the non-elastic cross section seems realistic at this point, implying similar accuracies for the evaluated continuum inelastic-scattering cross section.

---

* Visiting Scientist. Permanent address: Japan Atomic Energy Research Institute, Tokai, Ibaraki-ken, Japan.

2. Fast Neutron Total and Scattering Cross Sections of ^{58}Ni and Nuclear Models. (A.B. Smith, P.T. Guenther, J.F. Whalen and S. Chiba*)

The measurement aspects of this work were completed during the prior year. The associated model interpretation is now finished and a report has been drafted with the following abstract:

"The neutron total and scattering cross sections of ^{58}Ni were measured from ≈ 1 to > 10 MeV, using white-source techniques. Differential elastic-scattering cross sections were measured from ≈ 4.5 to 10 MeV, at ≈ 0.5 MeV intervals, with ≥ 75 differential values per angular distribution. Differential inelastic-scattering cross sections were also measured, corresponding to thirteen levels with excitations up to ≈ 4.8 MeV. The experimental results, combined with relevant values in the literature, were interpreted in terms of optical-statistical and coupled-channels models, using both vibrational and rotational coupling schemes. The physical implications of the experimental results, and their interpretations, are discussed in the contexts of the optical-statistical, dispersive-optical, and coupled-channels models."

Various aspects of the above interpretations should prove useful to anyone attempting to provide nickel data for applied purposes.

---

* Visiting Scientist. Permanent address: Japan Atomic Energy Research Institute, Tokai, Ibaraki-ken, Japan.

3. <u>Neutron Scattering from Elemental Indium: Optical Model and Bound Potential</u>. (S. Chiba*, P.T. Guenther, R.D. Lawson and A.B. Smith)

The experimental aspects of this work were previously reported. The interpretation is now also complete and the totality of these results has been published[1]. The abstract of the paper is:

"Neutron elastic-scattering cross sections of indium are measured from 4.5 to 10 MeV, at intervals of ≈ 500 keV. Seventy or more differential values are obtained at each incident energy, distributed between ≈ 18^{o} and 160^{o}. These are combined with lower-energy data previously obtained at this laboratory, and with 11- and 14-MeV results in the literature, to form a comprehensive elastic scattering data base extending from ≈ 1.5 to 14 MeV. These data are interpreted in terms of a conventional spherical optical model. The resulting potential is extrapolated to the bound-state regime. It is shown that, in the middle of the 50 - 82 neutron shell, the optical potential derived from the scattering results adequately describes the binding energies of particle states, but does not do well for hole states. The latter shortcoming is attributed to hole states having occupational probabilities sufficiently different from unity so that the exclusion principle becomes a factor, to rearrangement of the neutron core, and to the fact that the shell-model potential was assumed to have an energy independent-geometry. The systematic behavior of the real optical potential is discussed, and it is shown that the isovector strength deduced from neutron scattering is consistent with nucleon-nucleon scattering data when a mass dependence of the radius is used."

---

* Visiting Scientist. Permanent address: Japan Atomic Energy Research Institute, Tokai, Ibaraki-ken, Japan.

1 S. Chiba, P.T. Guenther, R.D. Lawson and A.B. Smith, Phys. Rev. C42, 2487 (1990).

4. Ambiguities in the Elastic Scattering of 8-MeV Neutrons from Adjacent Nuclei. (R.D. Lawson, P.T. Guenther and A.B. Smith)

This work, cited in the previous report of this series (Reports to the DOE Nuclear Data Committee, May 1990), has now been formally published[1].

---

1 R.D. Lawson, P.T. Guenther and A.B. Smith, Nuclear Phys. A519, 487 (1990).

5. Differential Neutron Scattering from Elemental Calcium ($\approx$ 97% ^{40}Ca). (A.B. Smith, S.Chiba*, P.T. Guenther and R.D. Lawson)

Physical interpretation of the very extensive set of neutron scattering measurements ($\approx$ 1.5 to 10 MeV), together with those in the literature as has been cited previously, is continuing. This is proving to be a very difficult problem since there clearly is very anomalous behavior of the nuclear absorption in the few-MeV region. This tendency was somewhat evident at the outset from the sparse few-MeV data in the literature, but it became very apparent from examination of the comprehensive data from this laboratory. It is a particularly interesting issue in view of the attention ^{40}Ca has received in the interpretation of dispersive optical potentials, which are found to be sensitive to neutron absorption processes in this low-energy region.

---

* Visiting Scientist. Permanent address: Japan Atomic Energy Research Institute, Tokai, Ibaraki-ken, Japan.

6. Elastic and Inelastic Neutron Scattering from Elemental Scandium.
(S. Chiba*, P.T. Guenther and A.B. Smith)

In view of the problems associated with understanding those calcium results already discussed in Item A.5, neutron scattering from neighboring scandium was measured from ≈ 1.5 to 10 MeV. This work employed techniques identical to those for the calcium measurements. The results of a preliminary optical-statistical model analysis are quite conventional, with some scatter observed for the model parameters at low energies due to incomplete averaging of resonance structure. There is no evidence of the sort of anomalies evident in the calcium analysis. These results suggest that the problems with the calcium physical interpretations are of a fundamental physical nature, and are not associated with the experimental data.

---

* Visiting Scientist. Permanent address: Japan Atomic Energy Research Institute, Tokai, Ibaraki-ken, Japan.

7. Fast-Neutron Interaction with Elemental Zirconium, and the Dispersive Optical Model. (S. Chiba*, P.T. Guenther, A.B. Smith and R.D. Lawson)

The physical interpretation of those measurements cited in the previous report of this series (Reports to the DOE Nuclear Data Committee, May 1990) is now complete. A draft report of the work has been prepared, with the following abstract:

"Differential neutron elastic- and inelastic-scattering cross sections of elemental zirconium are measured from ≈ 1.5 to 10 MeV. The measurements are made at these incremental incident-neutron energies: Below 3 MeV, ≈ 100 keV; from 3 to 4 MeV; ≈ 200 keV; at higher energies, ≈ 500 keV. The angular range of these measurements is ≈ 18^{o} to 160^{o}, with up to ≈ 100 differential values per angular distribution. This comprehensive data base, augmented with a 24-MeV elastic-scattering distribution from the literature, is used to develop a phenomenological optical-statistical model which considers the dispersion relationship connecting real and imaginary portions of the potential. The resulting potentials are consistent with the systematics previously reported from this laboratory. It is shown that the potential geometries are energy dependent, and that the dispersion relationship primarily effects the real-potential strength. It adds an energy-dependent contribution to the Hartree-Fock component over the energy range of the neutron interpretations, in a manner consistent with the concept of the Fermi Surface Anomaly. The dispersive potential deduced from the neutron observations is compared with the shell-model potential describing particle- and hole-states. The form of the bound-state potential, including Hartree-Fock and dispersive components, is discussed."

The use of the dispersive optical model does not remove the energy dependence of the the model parameters. It is also shown that the imaginary isovector strength in this region of the N = 50 shell closure is positive, rather than negative as conventionally given by "global" models.

---

* Visiting Scientist. Permanent address: Japan Atomic Energy Research Institute, Tokai, Ibaraki-ken, Japan.

8. Inelastic Neutron Excitation of the Yrast 2^+ Levels of the Even Cadmium Isotopes. (A.B. Smith, P.T. Guenther and R.D. Lawson)

Preliminary high-resolution measurements of cadmium inelastic-scattering cross sections have be made at incident neutron energies from ≈ 7 to 9 MeV. Very comprehensive electromagnetic decay studies of these isotopes have been reported in the literature by researchers at the University Rochester. These decay properties are being used to calculate those matrix elements governing the inelastic-scattering process. Preliminary results are encouraging. That is, good agreement in both magnitude and angular-dependent shape are observed when comparing experimental and calculated results. More detailed measurements are planned in the near future. These will be made with a longer flight path in order to obtain better energy resolution.

B. CONTINUUM NEUTRON STUDIES

1. Double-Differential Inelastic-Neutron Emission Measurements. (P.T. Guenther and A.B. Smith)

The results of measurements previously reported have been distributed to the participants of an IAEA-sponsored CRP on level densities. This was done in a standardized, comprehensive library, including documentation and error analysis. These data are currently contributing to testing of pre-equilibrium and level density models in an international effort. In the past year, efforts have been made to improve experimental technique. Among these were more exacting procedures to determine energy scales, elimination of target-neutron contaminants through a new gas target design, and design and construction of more sensitive, larger volume scintillator detectors. Upgrading of the ten-angle fast neutron spectrometer, reported elsewhere (Item I.1), will result in a significant increase in efficiency in measuring these low-count-rate scattering processes.

C. STANDARDS MEASUREMENTS

1. International Comparisons of the Dosimetry Cross Section Standards $^{58}Ni(n,p)^{58}Co$ and $^{93}Nb(n,2n)^{92m}Nb$. (D.L. Smith, J.W. Meadows, R.C. Haight*, W. Mannhart**, H. Vonach***, G. Winkler*** and M. Wagner***)

Precision measurements of the $^{58}Ni(n,p)^{58}Co$ and $^{93}Nb(n,2n)^{92m}Nb$ cross sections have been made for neutron energies below 10 MeV and in the Be(d,n) neutron spectrum produced by deuterons of 7 MeV. This work was done as part of an international exercise whose purpose is to intercompare the data correction procedures associated with these measurements at several different laboratories. This project is being conducted under the auspices of the NEANDC Working Group on Activation Cross Sections. The measurements at each of these laboratories were made using nickel and niobium samples which had been fabricated from the same batch of material. The $^{238}U(n,f)$ cross-section standard was used to measure neutron fluence, and the laboratories participating in the exercise employed uranium fission deposits which had been previously intercalibrated[1]. Finally, each laboratory counted a common sample for its gamma-ray activity in order to intercompare counting facilities and methodologies. The neutron irradiations and about half of the counting of the activated nickel and niobium samples had been completed at Argonne as of December 1990. Analysis of these data was also in progress at this time.

---

* Los Alamos National Laboratory.

** Physikalisch-Technische Bundesanstalt, Braunschweig, Germany.

*** Institut fuer Radiumforschung und Kernphysik, University of Vienna, Vienna, Austria.

1 J.W. Meadows, D.L. Smith, G. Winkler, H. Vonach and M. Wagner, "Intercomparison of ^{238}U Deposits Employed for Neutron Fluence Determination in Neutron Activation Cross Section Measurements", Proceedings of a Specialists' Meeting on Neutron Activation Cross Sections for Fission and Fusion Energy Applications, Argonne National Laboratory, 13-15 September 1989, Report NEANDC-259 "U", eds. M. Vonach and H. Wagner, p. 153 (1989).

2. Characteristics of the Samples in the FNG Fission Deposit Collection. (J.W. Meadows)

Information concerning the samples in the Fast Neutron Generator (FNG) Group's fission deposit collection has been assembled and published in a Laboratory report[1]. This includes the physical dimensions, isotopic analyses, half-lives, alpha emission rates, specific activities and deposit weights. These calibrated fission deposits represent a very valuable resource of this Group, providing a vital calibration link to work done at other laboratories in the U.S. and in foreign countries.

---

1 J.W. Meadows, Report ANL/NDM-118 (1990).

D. ACTIVATION AND OTHER REACTION CROSS SECTION MEASUREMENTS

1. Microscopic Integral Cross Section Measurements in the Be(d,n) Neutron Spectrum for Applications in Neutron Dosimetry, Radiation Damage and the Production of Long-Lived Radionuclides. (D.L. Smith, J.W. Meadows, and L.R. Greenwood*)

Integral neutron-reaction cross sections have been measured, relative to the ^{238}U neutron fission cross-section standard, for 27 reactions which are of contemporary interest in various nuclear applications (e.g., fast-neutron dosimetry, neutron radiation damage and the production of long-lived activities which affect nuclear waste disposal). The neutron radiation field employed in this study was produced by bombarding a thick Be-metal target with 7-MeV deuterons from an accelerator. The experimental results are reported along with detailed information on the associated measurement uncertainties and their correlations. These data are also compared with corresponding calculated values, based on contemporary knowledge of the differential cross sections and of the Be(d,n) neutron spectrum. Some conclusions are reported on the utility of this procedure for neutron-reaction data testing[1].

---

* Battelle Pacific Northwest Laboratory.

1 Seventh ASTM-EURATOM Symposium on Reactor Dosimetry, Strasbourg, France, August 27-31, 1990.

2. A Search for Neutron-Induced Long-Lived Activities in Copper, Silver, Hafnium, Europium and Terbium. (J.W. Meadows, D.L. Smith, L.R. Greenwood*, R.C. Haight**, Y. Ikeda*** and C. Konno***)

Work continued on this IAEC Coordinated Research Program during 1990. Cross sections were obtained for a number of these reactions after applying corrections for background neutrons from the target assemblies and room-return neutrons from the general laboratory environments at each of the facilities where irradiations were performed (Argonne, JAERI-Japan and Los Alamos). It remains to coordinate the results from data analyses at the other laboratories, and to adjust the cross sections for any changes in the decay half lives which are decided upon by the participating laboratories. Final results from this project will be reported at a meeting of the CRP which is to take place in Vienna in late 1991.

---

* Battelle Pacific Northwest Laboratories.

** Los Alamos National Laboratory.

*** Japan Atomic Energy Research Institute, Tokai, Ibaraki-ken, Japan.

3. Measurement of the $^{89}Y(n,p)^{89}Sr$ Cross Section. (G. Piccard*, D.L. Smith and J.W. Meadows)

All the neutron irradiations and sample beta counting for this experiment have been completed. Most of the data analysis is finished for this investigation, which spans the neutron-energy range from threshold to about 10 MeV as well as integral studies in the Be(d,n) spectrum for 7-MeV deuterons. This project has been adopted as a Master's thesis project for one of the authors (GP). This work should be completed by late 1991.

---

* University of Michigan, Ann Arbor.

4. Cross-Section Measurements for the $^{9}Be(d,n)^{8}Be$ Reaction in the Be(d,n) Neutron Spectrum. (D.L. Smith, J.W. Meadows, L.R. Greenwood*, D.W. Kneff** and B.M. Oliver***)

Measurements of the helium content in the neutron-irradiated beryllium samples were completed in 1990. The amount of helium found in these samples was enough to provide helium-production accuracies of a just a few percent. The data analysis commenced in 1990 and continues into 1991. It is planned to complete this project before the end of 1991. The objective of this work is to settle an important question concerning neutron multiplication in the beryllium blanket of fusion reactors.

---

* Battelle Pacific Northwest Laboratories.

** Rocketdyne Division, Rockwell International Corporation.

E. NEUTRON SPECTRUM INVESTIGATIONS

1. Investigation of the Neutron Spectra from Bombardment of Thick Be-Metal Targets with Protons and Deuterons. (J.W. Meadows)

The bombardment of thick beryllium metal targets with protons or deuterons at energies of a few MeV provides intense neutron sources with broad energy spectra. The dependence of spectrum shape on the energy of the incident particle opens the possibility of tailoring (within limits) the spectra for specific applications. Such spectra have a number of uses. A very important one is the production and testing of neutron reaction data. Precise characterization of these spectra is necessary for such quantitative applications, but reliable data are available for only a few energies. Consequently, measurements involving time-of-flight techniques are in progress at the FNG to provide information on those spectra produced by incident proton and deuterons with energies between 3 and 7 MeV. ^{235}U and ^{238}U fission chambers were chosen as the detectors because of their relatively flat and well-determined cross sections. Emphasis has been placed on the lower-energy range of the $^{9}Be(d,n)$ spectra (i.e., < 2 MeV) because many of the applications in this laboratory are sensitive to these neutrons. Measurements of the higher energy portions of these spectra are now in progress, using ^{238}U detectors at longer flight paths, in order to obtain better resolution for the middle energies, and to provide normalization data for very high resolution measurements with scintillation detectors at still longer flight paths. Less extensive measurements of the same nature for $^{9}Be(p,n)$ spectra are also in progress.

F. NUCLEAR DATA EVALUATION ACTIVITIES

1. Comprehensive Evaluated Neutronic Data File for Indium. (A.B. Smith, S. Chiba*, D.L. Smith, J.W. Meadows, P.T. Guenther, R.D. Lawson and R.J. Howerton**)

This work, cited in the previous report of this series (Reports to the DOE Nuclear Data Committee, May 1990), has now been formally published[1] and accepted for ENDF/B-VI.

---

* Visiting Scientist. Permanent address: Japan Atomic Energy Research Institute, Tokai, Ibaraki-ken, Japan.

** Lawrence Livermore National Laboratory.

1 A.B. Smith, S. Chiba, D.L. Smith, J.W. Meadows, P.T. Guenther, R.D. Lawson and R.J. Howerton, Report ANL/NDM-115 (1990).

2. Comprehensive Evaluated Neutronic Data File for Zirconium. (A.B. Smith, D.L. Smith, J.W. Meadows, P.T. Guenther, R.D. Lawson and R.J. Howerton*)

This file nears completion as the measurement program, cited in Item A.7, is finished. The remaining portions of the file are several small (n,X) reaction cross sections and the photon production files.

---

* Lawrence Livermore National Laboratory.

3. Evaluated Fast-Neutron Cross Sections of ^{58}Ni. (A.B. Smith, P.T. Guenther and J. W. Meadows)

Work is in progress on this limited-scope evaluation, with the objective of putting those results of measurements described in Item A.2 into a format useful for applications. This information should be valuable for updating the existing ENDF/B-VI file.

4. Evaluated Neutron Total, Nonelastic and Continuum Inelastic Scattering Cross Section of ^{238}U and ^{232}Th. (S. Chiba*, P.T. Guenther and A.B. Smith)

This work will make use of the measurements cited in Item A.1, and their interpretation, to give new accuracies to the evaluated total, nonelastic and continuum inelastic-scattering cross sections. The latter have been a major uncertainty for many years. The work is a part of the NEANDC/NEACRP Coordinated Evaluation Program.

---

* Visiting Scientist. Permanent address: Japan Atomic Energy Research Institute, Tokai, Ibaraki-ken, Japan.

5. An Evaluation of the $^{93}Nb(n,n')^{93m}Nb$ Dosimeter Reaction for ENDF/B-VI. (D.L. Smith and L.P. Geraldo*)

An evaluation of the differential cross section for the $^{93}Nb(n,n')^{93m}Nb$ dosimetry reaction from threshold to 20 MeV has been prepared for ENDF/B-VI and published as a Laboratory report[1]. This evaluation was obtained by adjusting the results of nuclear model calculations using published differential cross section information. Uncertainties for the measured differential cross sections were derived from information provided in the literature. The uncertainties associated with the model-calculated curve were estimated indirectly through consideration of the total cross section and all other prominent reaction channels. Experimental and model-calculated information was then merged by means of the least-squares method to provide a final evaluation and its covariance matrix.

---

* Visiting Scientist. Permanent address: Divisao Fisica Nuclear, IPEN, C.P. 11049-Pinheiros, 01000 Sao Paulo, Brazil.

1 D.L. Smith and L.P. Geraldo, Report ANL/NDM-117 (1990).

G. NUCLEAR THEORY, MODELS AND CODES

1. The Real Optical- and Shell-Model Potentials. (R.D. Lawson, S. Chiba*, P.T. Guenther and A.B. Smith)

From the fits to neutron scattering data over a wide range of nuclei it is shown that r_v, the reduced radius of the real optical-model potential, decreases with increasing A. The value of the isovector part of the real potential is discussed and a simple argument is given for its magnitude. The dispersion relationship and the method of moments are used to extrapolate the scattering potential to the bound-state regime. The possibility of deducing the spin-orbit strength from the observed single-particle binding energies is discussed.

---

* Visiting Scientist. Permanent address: Japan Atomic Energy Research Institute, Tokai, Ibaraki-ken, Japan.

H. ANALYTICAL METHODS DEVELOPMENT

1. Fast-Neutron Scattering Support Software. (P.T. Guenther)

With the introduction of the new ten-angle spectrometer interface and the 386-based on-line PC, significantly more sophisticated on-line processing has become possible. In addition, a greater integration of the various off-line data-reduction steps can now promise the elimination of a host of tedious and error-prone intermediate data manipulation steps. With this in mind, a significant effort was made to design and implement a user-friendly, library-file oriented processing environment. The data acquisition is now handled with program NEW-AGE. It is task oriented. Each function is command-line initiated, using a free-format input, and output files directly compatible with the off-line spectrum analyzing program SCATTER, which has been previously reported. The processing stream will be closed with the completion of the detector efficiency and cross section codes now under development.

2. Probability, Statistics and Data Uncertainties in Nuclear Science and Technology. (D.L. Smith)

An NEANDC monograph bearing this title is nearing completion. This work is intended as a text for students and a general reference volume for laboratory researchers. A draft version of the manuscript was distributed to a number of reviewers in the U.S. and in foreign countries in October 1990. By the end of December 1990, extensive comments had been received from most of the reviewers and work was in progress on the final revisions to the manuscript. The draft was generally very well received by the reviewers, and their comments were quite constructive. This work is to be published as a single-author book by the American Nuclear Society (probably around September 1991).

3. Some Thoughts on the Determination of Covariance Matrices for Nuclear Data Evaluations. (S. Chiba* and D. L. Smith)

Modern nuclear data evaluation methodology is largely based on statistical inference, with the least squares technique commonly used to generate estimators for physical quantities and their uncertainties. It has been observed that evaluations which employ covariance matrices involving absolute errors derived directly from the experimental data tend to produce values which are too low. This problem is alleviated by employing, instead, effective data uncertainties calculated from percentage errors and prior estimates for the evaluated quantities. Such an approach leads to more realistic weighting of the experimental data and, thus, to better evaluated results. One shortcoming of the method is that iteration may be required to converge on the best evaluated results. Examples are provided to illustrate the basic problem and to demonstrate the approach suggested for its resolution. This work has been reported at a conference.[1]

---

* Visiting Scientist. Permanent address: Japan Atomic Energy Research Institute, Tokai, Ibaraki-ken, Japan.

1 S. Chiba* and D. L. Smith, Bull. Amer. Phys. Soc. 35, No. 6, 1395 (1990).

I. INSTRUMENTATION DEVELOPMENT

1. Upgrade of Time-of-Flight System at the FNG Laboratory. (A.B. Smith, J.W. Meadows and P.T. Guenther)

For more than a quarter of century, the ANL neutron time-of-flight spectrometer has been a major source of fast-neutron scattering data. After this extended period of operation, it became clear that a general upgrade of the system was in order. The work was actually initiated several years ago, and proceeded as the resources to do so became available. Three generic areas have been addressed: i) pulsed-source intensity, ii) data acquisition and processing, and iii) neutron detection. The work is now essentially complete, and initial measurements indicate that it has been very successful.

In neutron time-of-flight measurements, pulsed intensity is a major concern. Increases in pulsed intensity of about a factor of 2 have been obtained, with a burst duration of $\approx$ 1 nsec, by the installation of a harmonic bunching system. The same method has been exploited at heavy ion facilities, but at much higher frequencies than are useful for neutron work (e.g., at the ANL-ATLAS facility). The system used in this laboratory was installed at modest cost and it has proven to be very reliable.

Many years ago, this Group recognized the importance of small digital computers in data acquisition, data processing, and instrument control. It first installed such a system in the early 1960s. Equally important has been the continuing development of an extensive software system that permitted effective handling of large masses of incoming information. Recently, an older computer data acquisition system (and the associated interfacing) has been replaced with new components based on a 386 PC computer. As described in Item H.1, software and data manipulations with the new system are largely carried out in FORTRAN, in contrast to the ridged machine-language programs of the older system. The software has been completely re-written so as to provide far greater capability in a user friendly environment. It is interesting to note that the data-acquisition computer which was first installed in the 1960s cost $\approx$ \$100,000 (1960 dollars), while the far more powerful recent replacement system sold for $\approx$ \$3,500 (1991 dollars). Some things have become more economical with the passing years!

In the past, two distinct neutron detector systems, comprised of at least ten detectors each, were used in neutron scattering experiments. One of these systems was designed for neutron energies of less than $\approx$ 1 MeV. The other was optimized for neutron energies in the range $\approx$ 1 - 5 MeV. However, for the last few years the measurement program has given primary emphasis to neutron scattering in the 4 - 10 MeV range. An optimal detector system for the latter energy range was not available. The present upgrade remedies this shortcoming. Tests show an increased sensitivity in this higher-energy range by about a factor of 3 relative to that of the detector system which was previously used for work in this energy range. This was achieved with no significant deterioration in either pulse-shape performance or time resolution. Therefore, the overall system sensitivity (including the contributions of the harmonic buncher) has been increased by about a factor of 6 by this system upgrade program.

1. BROOKHAVEN NATIONAL LABORATORY

A. TWO PHONON COLLECTIVITY IN DEFORMED NUCLEI AND PAULI BLOCKING: GRID STUDY OF ^{168}Er

One of the outstanding questions in nuclear structure for the last thirty years has been whether two-phonon vibrational states can exist in deformed nuclei, or whether Pauli blocking will lead to their complete fragmentation. Soloviev and co-workers, for example, have long argued the latter position while Piepenbring and others maintain that the collectivity will persist. This dichotomy arises because complete calculations are impossible and different theoretical truncation schemes give widely different results. The question is of fundamental importance in nuclear physics because it directly relates to the interplay of single particle quantal states and collectivity. These are unique features of the atomic nucleus since, as opposed to other many-body systems, only a few constituents (e.g., 10-30 nucleons) are really "active." Hence, Pauli effects are critical, collectivity and correlations are sensitive to single particle effects, and "phase transitions" in such finite systems show fascinating fluctuations absent from their abrupt counterparts in other mediums. In the present case, this question can actually be addressed and quantitatively assessed.

The way to do so empirically is to identify a good candidate for a two-phonon vibration and measure its decay B(E2) value to the one-phonon level. The best candidate has long been known (indeed, from our well known study of ^{168}Er): it is the 4^+ level at 2055 keV in ^{168}Er which decays predominantly to the γ band and would therefore be a double γ K = 4 vibration. Until now, however, it has been impossible to measure its lifetime or to reach it in Coulomb excitation. This is now changed with the advent of the GRID technique, and the appropriate GRID experiment has been done at the ILL. The result is that the $4^+_{\gamma\gamma} \rightarrow 2^+_\gamma$ B(E2) value is indeed collective. All models (Piepenbring, IBA with g bosons, the pseudo-SU(3) and symplectic group approaches of Draayer, the models of Kumar and Matsuo) that give this state two-phonon character are in excellent agreement with the data while Soloviev's model has predicted a B(E2) value three orders of magnitude lower. (Incidentally, though our result seriously impacts Soloviev's work of the last decades, he has called this study the most important experimental result in nuclear structure in the last several years: he is now re-examining the assumptions and approximations in his model to try to reformulate it. It appears tentatively that a number of neglected terms in the matrix element add coherently: if this is so, it would be equally important to carry out similar studies in other rare earth nuclei.)

B. EXPERIMENTAL STUDY OF ^{214}Pb(0^+) $\rightarrow$ ^{214}Bi β DECAY AND MESON EXCHANGE ENHANCEMENTS

These shell model studies of the Pb region near ^{208}Pb lead to the possibility of predictions for the nucleus ^{214}Bi by exploiting the generalized seniority scheme to extrapolate from ^{210,212}Bi. In one of the very few experimental studies actually carried out at the HFBR during this time, the TRISTAN instrumentation was used to study the decay of radioactive $^{214}Pb(\beta) \rightarrow ^{214}Bi$. The main result, which coincided with the original motivation for the study, was to search for J = 0 states that could be the final states for $0^+ \rightarrow 0^-$ β decay. A state previously assigned 1^- was in fact discovered to be 0^- and, thus, combining both theoretical and experimental components of this project, the very large nonnucleonic enhancements of first forbidden β decay in the lead region were found to extend to A = 214 as well.

A side benefit of these studies resulted from the need for accurate shell model interactions in this region. This led to a detailed appraisal of the adequacy of the Kuo-Herling interaction and to a discussion of possible modifications to it, for example to the core-polarization component.

C. ANTI-ALIGNED COEXISTING OBLATE DECOUPLED BAND STRUCTURE IN ^{191}Os

A long term study of ^{191}Os was finally completed this year with the further reanalysis of GAMS and BILL data from the ILL. This is a collaborative BNL-ILL-Munich study involving (at BNL) both ARC and γ-γ coincidence data. Its completion was held up for some years by the inability to place 3 of the 7 strongest γ rays. Finally, this obstacle was overcome, and a rare example of anti-aligned decoupled band states was observed. Since these states were populated in (n,γ) from an even-even $J = 0^+$ target state, they must be low K. In addition, the interconnecting transitions, $\Delta J = 2$ sequences of intense E2 transitions which cascade upwards in spin, show virtually no depopulation outside this family of levels. All of this clearly points towards a decoupled band structure and the observation of the favored and unfavored anti-aligned states. But, ^{191}Os is a nearly prolate rotor with nearly filled major shells, and hence the Fermi surface is near the high K abnormal parity levels. The only way a decoupled band structure can arise is in a coexisting oblate minima. Details in particle rotor calculations confirmed the essential oblate nature of the levels ($\gamma \approx 43°$) and also explained their anomalously strong population in (n,γ): these levels, and especially those most strongly fed, are dominated by low K wave function amplitudes (mostly K = 1/2 and 3/2). This is one of only a couple of known extensive sets of anti-aligned decoupled states (another is ^{109}Pd, previously studied in a BNL-ILL collaboration). The negative parity levels (22 states of $1/2^-$, $3/2^-$) disclosed in ARC helped round out earlier interpretations of the evolution of the fragmentation of Nilsson strength in this region that is due to changing quadrupole and hexadecapole deformation and the interplay of $\Delta N = 2$ and Coriolis mixing.

D. ARC STUDY OF ^{124}Te AND COMPETING INTERPRETATIONS

The Te isotopes are enigmatic: just 2 protons away from Z = 50, they seem to display both single particle (shell model) and collective behavior. The even isotopes have been variously interpretated in terms of vibrator (or U(5)) and γ-soft (or U(6)) studies, along with some claims for the presence of intruder states. A key to a resolution of these issues is the knowledge of a complete set of low-spin low-energy states, especially 0^+ states. However, there have been conflicting experimental results for these levels. Hence, an ARC study was carried out and completed just prior to the HFBR shutdown. The results show that 0^+ states at 1156 and 1290 keV do not exist and that the set of $0^+,2^+$ states proposed by robinson is in fact complete up to 2500 keV, thus ruling out any interpretations (e.g., vibrator plus intruder) that require extra 0^+ states. This study is an excellent example of the benefits that occur from the guarantee of completeness that ARC can provide; there is a subtle yet important distinction between a level scheme where the known levels form a complete set and the case where it is explicitly known that this set is complete. The former case does not preclude that new levels will be discovered, the second case does, and therefore strictly constrains the allowable nuclear degrees of freedom.

E. National Nuclear Data Center

1. Cross Section Evaluation Working Group (CSEWG)

CSEWG held one meeting in 1990, its 24th year of activity. The release of the ENDF/B-VI data file is nearly complete. Only the decay data, the fission product yields and the charged particle sublibraries remain to be completed. Some errors in the released file have been reported. We hope to produce an updated version of ENDF/B-VI with the errors corrected and a few new or revised evaluations included in the next 18 months. The ENDF-6 Formats and Procedures Manual has been released and the Summary Documentation for ENDF/B-VI is ready for review.

Data testing has been slow but some encouraging results have been obtained. Thermal reactor data testing results have been obtained only for ^{235}U assemblies. ENDF/B-VI results are similar to ENDF/B-V except the trend of increasing eigenvalue as a function of epithermal leakage and epithermal fission fractions has significantly improved. In the fast reactor area, results show a slight improvement, although there are still areas of concern. For example, k_{eff} for larger assemblies such as BIG-10, ZPR-6/7 appear to be about 1% high, although there is greater consistency between ^{235}U and ^{239}Pu assemblies. The k_{eff} for Pu-fueled assemblies has increased and is close to 1.0. The ^{238}U capture to ^{235}U fission ratio and to ^{239}Pu fission ratio have improved. The dosimetry reaction evaluations do not perform as well as in ENDF/B-V, in particular, the ^{58}Fe and ^{59}Co (n,γ) reactions.

The NEACRP/NEANDC Working Group on Evaluation cooperation has been in operation for 18 months. Seven subgroups have been formed to investigate tapes of mutual interest. Three of these groups will present papers at the Juelich conference.

The organizing committee for the Symposium on Nuclear Evaluation Methodology which will be held in September 992 at BNL has been formed. The committee will meet during the Juelich conference to set responsibilities for the symposium sessions and begin to advertise for papers.

2. Nuclear Data Sheets

The NNDC has been producing the Nuclear Data sheets at the rate of about an issue a month. of these, nine issues a year are devoted to nuclear structure evaluation and the remaining three to the publication of Recent References.

The Center evaluated A=45, 67, 143, 145, 150, 165 and 211 and submitted them for publication; A=48, 57, 94 and 212 are being evaluated.

A new edition of the Nuclear Wallet Cards was published and distributed in July 1990.

A program AEGIS is currently under development on an IBM-compatible PC. This program is intended to help the evaluator to prepare an adopted data set for a given nuclide from the source decay and reaction data sets which have been included in the data base.

The U.S. is a part of an international network of evaluators contributing recommended values of nuclear structure information to the Evaluated Nuclear Structure Data file (ENSDF). Publication of the Nuclear Data Sheets proceeds directly from this computerized file. In addition to the U.S., evaluations have been received or are anticipated from the Federal Republic of Germany, U.S.S.R., France, Japan, Belgium, Kuwait, Sweden, the People's Republic of China and Canada.

Use of the concise format for the published A-chains in the Nuclear data sheets is functioning smoothly. This format reduces the size of the publication without omitting essential information and improves its readability.

3. <u>On-line Services</u>

For approximately 4 1/2 years, the NNDC has offered on-line access to several of its nuclear data bases. This service is available on the NNDC's VAX-11/780 and 8820 computers via ESNET, INTERNET or over telephone lines. Approximately one-half of the queries have been to the NSR data base (see Table 1).

All retrieval programs in the online service now have video as well as sequential node user interaction. The photon atomic data base of Hubbell et al has been added to the service. This program also contains the ability to calculate polarized scattering cross sections as seen by a detector after scattering of a finite sized photon beam from a material. The ENDF/B-VI form factors are used in this calculation. Work has begun on a user document for the system.

<u>Table 1</u>

<u>On-line Access Statistics 1986-1990</u>

Year	Runs	Retrievals	NSR	ENSDF	NUDAT	CINDA	CSISRS	ENDF
1986	648	1621	814	142	536	129	--	--
1987	1275	4263	2521	863	815	60	--	--
1988	2264	8748	5022	1303	1492	285	459	187
1989	3374	8406	3253	850	1841	522	1649	150
1990	5436	12067	5613	1256	2204	187	1623	1019

COLORADO SCHOOL OF MINES

1. Radiative capture of protons by light nuclei at low energies. Our study of the (p,γ) reactions on light nuclei is completed. We have made direct measurements of gamma ray to charged particle branching ratios for proton bombardments on ^{6}Li, ^{7}Li, ^{9}Be and 11B between bombarding energies of 25 and 180 keV. These branching ratios have been used to infer radiative capture cross sections and astrophysical S-factors based upon previously published values of the S-factors for the corresponding charged particle reactions. Our results have been published in summary form[1] and a complete report has been submitted for publication[2]. Our results have been compared to distorted-wave Born approximation calculations[3] assuming unit final state spectroscopic factors. As seen in Fig. 1, the calculated cross sections agree remarkably well with the measured values in each case except ^{6}Li for which C^2s = 0.2.

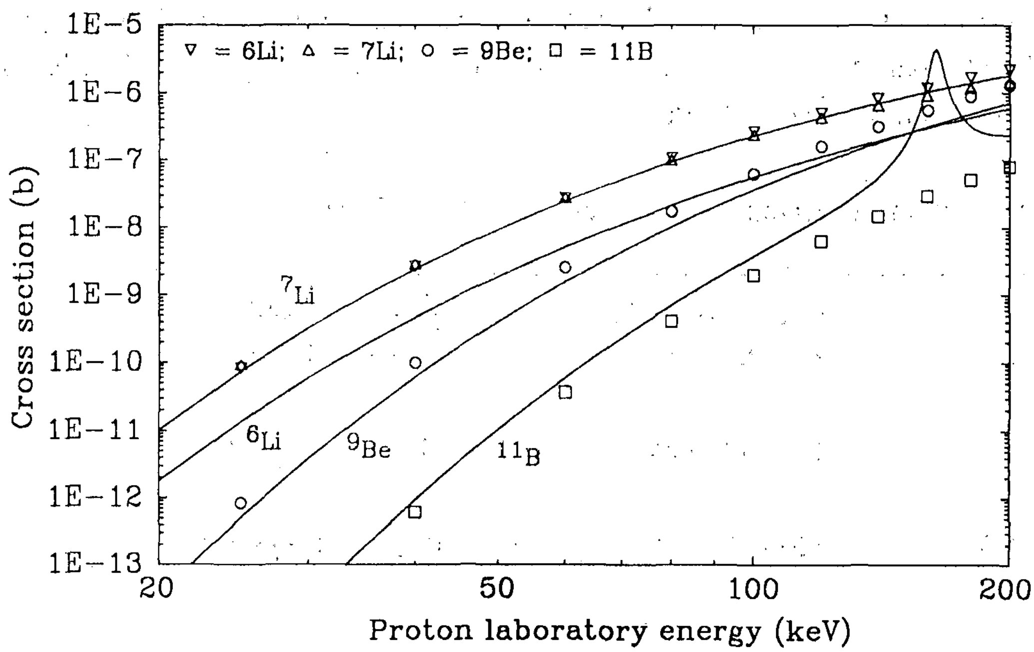

Figure 1. Comparison of measured and calculated cross sections for radiative capture of protons on ^{6}Li, ^{7}Li, ^{9}Be and ^{11}B. The symbols are the calculated cross sections and the solid lines are the cross sections inferred from the experimentally determined astrophysical S-factors.

2. Radiative capture of deuterons by light nuclei at low energies. As an extension of our earlier measurements of the reactions $D(d,\gamma)^4He$, $T(d,\gamma)^5He$ and $^3He(d,\gamma)^5Li$ and as a continuation of the program in radiative capture discussed above, we have completed a series of preliminary measurements of deuteron capture by ^2H, ^6Li and ^{10}B between center-of-mass energies of 20 and 160 keV. As in the case of our measurements of proton radiative capture, the deuteron capture studies consisted of thick-target gamma-ray to charged-particle branching ratio measurements. These deuteron capture reactions are extraordinarily exothermic, producing 23.8, 22.3 and 25.2 MeV gamma rays respectively. In the case of the reaction $^6Li(d,\gamma)^8Be$, care was taken to prevent deuterium build-up in the target as such build-up could cause the observation of the 22.3 MeV gamma ray from the ^6Li capture reaction to be obscured by the 23.8 MeV gamma ray from the ^2H capture reaction. The gamma-ray to charged particle branching ratios for the three reactions are roughly independent of energy and are given in Table 1. The charged particles to which the gamma ray yields are compared are, respectively, the 3.1 MeV proton from the reaction $^2H(d,p)T$, the 11.2 MeV alpha particle from the reaction $^6Li(d,\alpha)^4He$ and the 11.8 MeV alpha particle from the reaction $^{10}B(d,\alpha 0)^8Be$.

Table 1. Summary of Deuteron Radiative Capture Measurements.

Reaction	$E_{deuteron}$ (lab)	Branching ratio
$d + {}^2H$	40 - 80 keV	$(1.0 +/- 0.2) \times 10^{-7}$
$d + {}^6Li$	110 - 140 keV	$(2.0 +/- 0.4) \times 10^{-7}$
$d + {}^{10}B$	120 - 150 keV	$(2.0 +/- 0.3) \times 10^{-4}$

3. The Oppenheimer-Phillips (O-P) effect in low energy deuteron induced reactions on light nuclei. We have examined three reactions in an effort to observe the enhancement of (d,p) reactions at low energies resulting from the electric polarization of the deuteron by the electrostatic field of the target nucleus. The reactions which we

considered were the D-D, the D-^{6}Li and the D-^{10}B reactions. In the case of the D-D reactions we were able to compare the reactions ^{2}H(d,p)^{3}H and ^{2}H(d,n)^{3}He by observing the recoil triton and ^{3}He directly in a windowless ruggedized ORTEC silicon surface barrier detector as shown in Figure 2.

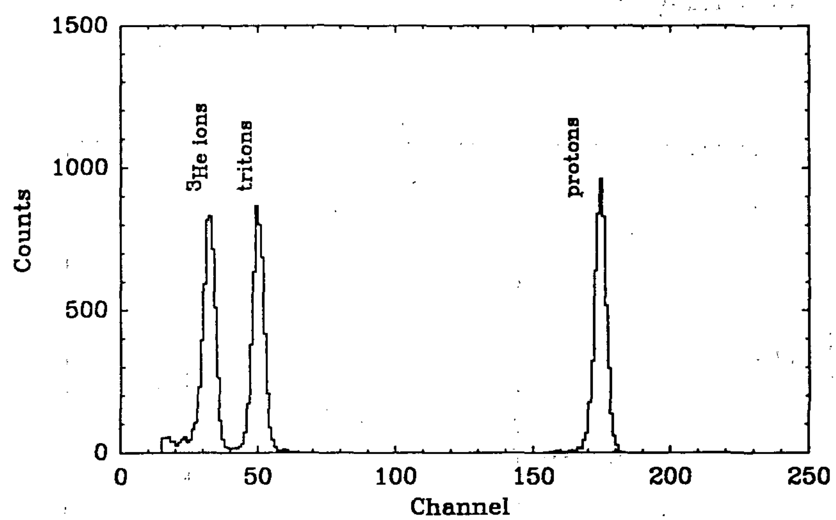

Figure 2. Spectrum of d-d reaction at $E_{c.m.}$ = 10 keV

The ratio of the yields were measured down to a c.m. energy of 3 keV and are plotted in Figure 3 where we find no evidence of an enhancement of the (d,p) reaction. In this Figure, the (d,n)/(d,p) ratio is compared to measurements at higher energies by Krauss et al.[4] and Jarmie et al.[5] The measured ratio is likewise compared in this figure to R-matrix calculations of these reactions.[6]

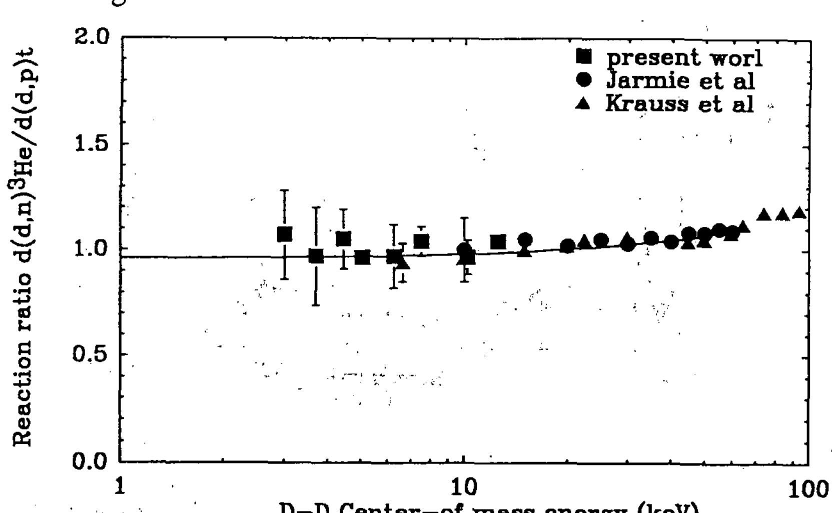

Figure 3. Measured (d,n)/(d,p) reaction ratio for deuteron bombardment of ^{2}H.

In the case of our studies of deuteron interaction with ^{6}Li and ^{10}B, it was not possible to observe the recoil nuclei due to the intense fluxes of Rutherford back-scattered deuterons and consequently we compared the (d,p) and (d,α) reactions on the assumption that the (d,α) reactions would not be affected by the O-P process. Typical spectra are shown in Figure 4.

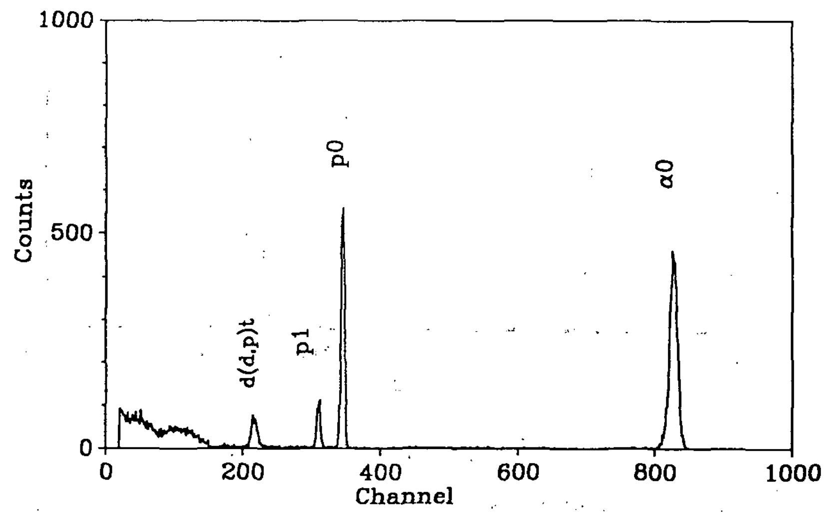

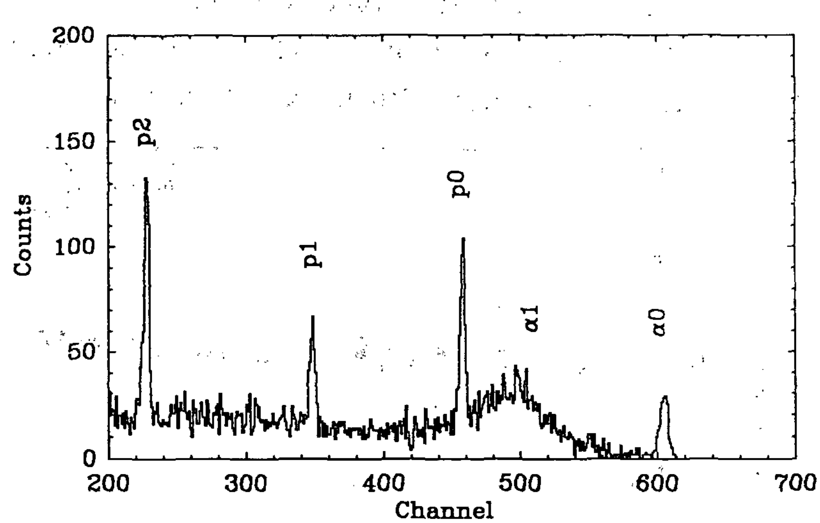

Figure 4. Energy spectra of charged particles during the bombardment of isotopically enriched ^{6}Li(top) and ^{10}B(bottom) targets.

In both cases we compared the states labeled "p0" to the ground state alpha transition. The yield ratios are given in Figures 5. In the case of the d-^{6}Li reaction, there appears to be a small but statistically significant enhancement of the (d,p)/(d,α) ratio. In the case of the d-^{10}B reaction, the enhancement appears significantly greater but with poorer statistics. Further work on this reaction is underway to improve the statistics and possibly extend the measurements to lower bombarding energies.

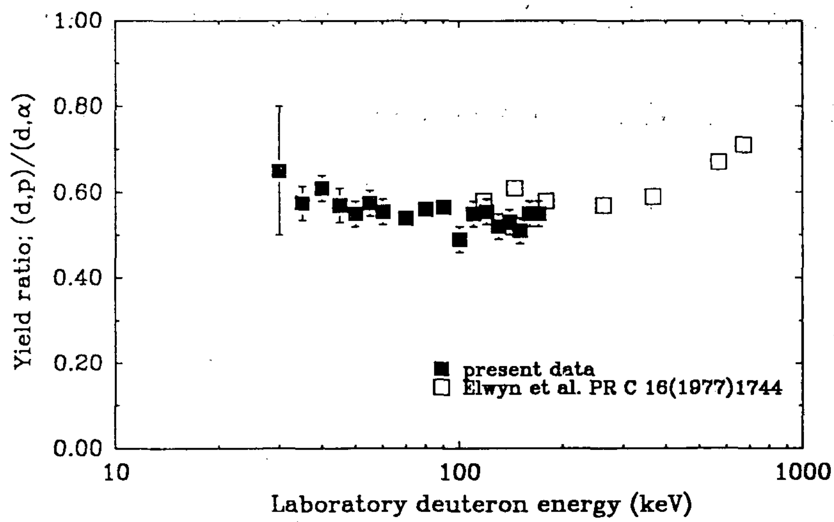

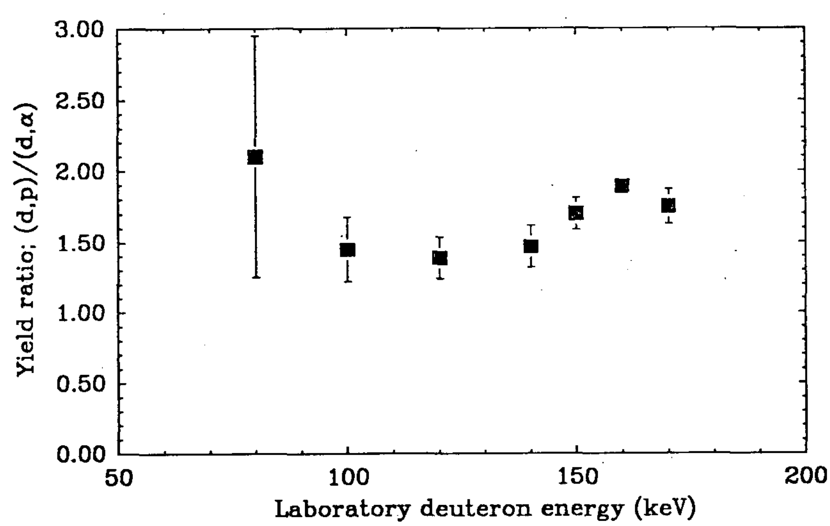

Figure 5. Ratio of the yields of the reactions (d,p0)/(d,α0) for deuteron bombardment of isotopically enriched ^{6}Li(top) and ^{10}B(bottom).

References.

1. F.E. Cecil, H. Liu, J.C. Scorby and S.S. Medley. Rev. Sci. Instruments 61 3223,(1990).

2. F.E. Cecil, D. Ferg, H. Liu, J.A. McNeil and P.D. Kunz. Nuclear Physics A, submitted for publication (1991).

3. J.A. McNeil and P.D. Kunz, private communication (1990).

4. A. Krauss, H.W. Becker, H.P. Trautvetter, C. Rolfs and K. Brand. Nuclear Physics, A465, 150 (1987).

5. Nelson Jarmie and Ronald E. Brown. Nucl. Instrum. and Methods, B10/11, 405 (1985).

6. G.M. Hale, private communication (1991).

CROCKER NUCLEAR LABORATORY AND DEPARTMENT OF PHYSICS UNIVERSITY OF CALIFORNIA, DAVIS

A. MEASUREMENTS

1. The $^{12}C(n,p)^{12}$B Reactions at 60 and 65 MeV.*# (F.P. Brady, T.D. Ford, G.A. Needham♡ J.L. Romero, E.L. Hjort, D. Sorenson, C.M. Castaneda, J.L. Drummond, B. McEachern, N.S.P. King♣, and D.J. Millener**◇)

The $^{12}C(n,p)^{12}$B reaction has been studied at 60 and 65 MeV. Cross sections for the 1^+ ground state, the 2^+ first excited state at 0.95 MeV, an unresolved pair of 2^- and 4^- states at 4.4. MeV and the analogs of the giant electric dipole and spin-dipole resonances around 7.7 MeV have been extracted and compared with previous data at 56 MeV and with microscopic Distorted Wave Born Approximation (DWBA) calculations. The shapes of angular distributions out to $q \sim 2fm^{-1}$ are well reproduced by the calculations. A comparison of (n,p), (p,n) and (p,p') cross sections near 60 MeV is made, and a value for $|J_{\sigma\tau}|$ (the volume integral of the central, spin-isospin part of the effective nucleon-nucleon interaction) is extracted. The magnitudes of cross sections for negative-parity states can be qualitatively understood when the loose binding of the *sd*-shell neutron in the final state and the effect of ground-state correlations on the dipole and spin-dipole strengths are taken into account.

* Supported by NSF grant PHY 87-22008.
# Accepted for publication in Phys. Rev. C (1991).
♡ Permanent address: Rockwell International, Canoga Park, CA 91304.
♣ Permanent address: P15, Los Alamos National Lab., Los Alamos, NM 87545.
** Supported by DOE contract DE-AC02-76CH00016
◇ Brookhaven National Laboratory, Upton, NY 11973.

2. Elastic and Inelastic Neutron Scattering at 65 MeV.♠♯ (Eric Lance Hjort)

Elastic scattering cross sections for 65 MeV neutrons have been obtained for natural targets of C, Si, Ca, Fe, Sn and Pb at center of mass angles of up to 45°. Inelastic scattering cross sections have been measured for natural Fe, Sn and Pb. A unique experimental system was utilized for all of these measurements using wire chambers in conjunction with a CH_2 converter. The system is simple, compact and relatively inexpensive. The counting rate and energy resolution of the system are adequate for the desired measurements. Data analysis is outlined with emphasis on those aspects which were developed specifically for these experiments.

The giant resonance regions of the $(n, n'x)$ spectra are compared with earlier $(p, p'x)$ results and macroscopic model analyses are used to extract the ratio of neutron to proton matrix elements M_n/M_p. The ratio is found to be consistent with the hydrodynamic model, $(M_n/M_p \approx N/Z)$ and inconsistent with $(\pi^{\pm}, \pi^{\pm\prime})$ scattering results. The elastic scattering cross sections include lab angles from 6° to 45°. Microscopic models are used to derive optical model potentials. Cross sections obtained from these potentials are found to describe the experimental results accurately.

3. $^3H + d \rightleftharpoons \vec{n} + ^4He$ Measurements and Absolute Neutron Polarization Determination at 50 MeV.* ◇ (A.L. Sagle,† B.E. Bonner,+ F.P. Brady, N.S.P. King,♣ M.W. McNaughton,‡ J.L. Romero, and J.L. Ullmann♣)

The reaction $^3H(d, \vec{n})^4He$ is used to produce polarized neutrons, which at $\Theta_n = 29.7°$ lab are analyzed in the inverse reaction $^4He(\vec{n}, d)^3H$. At $\Theta_d(\text{deut}) = 25°$ lab the two reactions are time reversed (or more specifically, reciprocal), corresponding to the same cm angles and energies, so that the neutron polarization, P, and the (inverse reaction) neutron-^4He analyzing power, A, are equal. Thus the measured asymmetry $e = P^2$ and the absolute neutron polarization is determined as $P = 0.480 \pm 0.016$. $A(\Theta_d)$ and $\sigma_d(\Theta_d)$ are also measured.

♠ Supported by NSF grant PHY87-22008 and by a Associate Western University fellowship.

♯ Ph.D. thesis, UC Davis, 1990.

* Supported by NSF grant PHY 87-22008.

◇ Accepted for publication in Nuclear Physics (1991).

† Present Address: Perking-Elmer Corporation, 411 Clyde Ave., Mountain View, CA.

+ Present Address: Department of Physics, Rice University, Houston, TX 77251.

♣ Present Address: Physics Division, Los Alamos National Laboratory, Los Alamos, NM 87545.

‡ Present Address: MP Division, Los Alamos National Laboratory, Los Alamos, NM 87545

4. The Response of $NaI(Tl)$ to 30-60 MeV Z=1 Particles[†♣] (J.L. Romero, G.A. Needham,[♡] F.P. Brady, C.M. Castaneda and T.D. Ford)

Measurements are reported for the light output response on a $NaI(Tl)$ detector for protons, deuterons, and tritons with energies between 30 and 60 MeV. The stopping power region covered by this data overlaps previous data taken with electrons and protons. The new data around 60 MeV is interesting in that the light output is greater for deuterons (and tritons) than that for protons by the equivalent of ≈ 1 MeV. A comparison is made with the model of Murray and Meyer for light output response in inorganic crystals.

5. The Energy Dependence of the Gamow-Teller Transition for $^6Li(n,p)$, $^{12}C(n,p)$ and $^{13}C(n,p)$ from bombarding energies of 65 to 250 MeV.[*#] (D.S. Sorenson,[♠] X. Aslanoglou,[△] F.P. Brady, J.R. Drummond, R.C. Haight,[♠] C.R. Howell,[♭] N.S.P. King[♠] A. Ling,[♠] P.W. Lisowski[♠], C.L. Morris[♠], B.K. Park[△], J. Rapaport[△], J.L. Romero, W. Tornow,[♭] J.L. Ullmann[♠].)

Cross sections from 0 to 10 degrees (lab) have been measured for ground state Gamow-Teller transitions for the reactions $^6Li(n,p)$, $^{12}C(n,p)$, and $^{13}C(n,p)$ from 65 to 250 MeV. The 90 meter station at the W.N.R. facility at Los Alamos was used to obtain these data. Unit cross sections and volume integrals ($J_{\sigma\tau}$) for the spin-flip isospin-flip part of the effective nucleon-nucleon interaction were obtained using the expression[1]:

$$\frac{d\sigma}{d\Omega}(q=0) = K\ N^D_{\sigma\tau}|J_{\sigma\tau}|^2\ B_{\rm GT}$$

where K is a kinematic factor, N^D is the distortion factor and $B_{\rm GT}$ is the Gamow-Teller transition strength which is obtained from measured logft values. Microscopic distorted wave calculations using the code DW81 are compared to the data. Finally, a comparison between (n,p) and the corresponding (p,n) data will be presented.

---

† Supported by NSF grant PHY 84-19380

♣ Accepted for publication in Nuc. Instr. & Meth. (1991).

♡ Permanent Address: Rockwell International, Canoga Park, CA 91304.

$*$ Supported by the U.S. DOE, DOD, and NSF.

\# Abstract submitted for the Spring Meeting of the American Physical Society, April 22-25, 1991.

♠ Los Alamos National Laboratory, Los Alamos, NM.

△ Ohio University, Athens, OH.

♭ Duke University, Durham, NC.

1 T.N. Taddeucci et al., Nucl. Phys. (1987) 125.

6. The Energy Dependence of the $T^{>}$ Gamow-Teller Strength in p-shell Nuclei Observed in The (n,p) Reaction.* ♡ (Danny Scott Sorenson.)

Cross sections have been measured for the transitions to the ground state of the residual nucleus using the (n,p) reaction on the targets $^{6}Li,^{12}C$, and ^{13}C. A "white" continuum neutron source allows cross sections to be measured for neutron energies from 60 to 260 MeV simultaneously. Charged particles are detected using a facility developed over the last few years which makes use of five "target" wire chambers, four x and y multiwire drift chambers, a 5 kilo gauss magnet which deflects the charged particles out of the neutron beam, a wall of 15 CsI calorimeters, and a large-area plastic delta E detector. This arrangement allows four targets to be run simultaneously, and with magnet-on, scattering angles betweeen 0 and 15 degrees can be measured concurrently as well. Angular distributions for the Gamow-Teller transitions are made and are extrapolated to q=0. At q=0 a simple expression relates the cross section to the volume integral for the effective nucleon-nucleon (N-N) interaction ($J_{\sigma\tau}$) , and the inverse β-decay matrix element ($B_{\mathrm{GT}} \uparrow$). For all transitions considered here B_{GT} can be obtained from measured half-lifes and so the cross section measurements can be used to calculate $J_{\sigma\tau}$ from 60 to 260 MeV.

$J_{\sigma\tau}$ should be a smooth function of A, however, (p,n) experiments were done where cross sections were measured for the isobaric analog states of the transitions that are considered in this thesis and were found to vary by as much as 40 percent as in the case of $^{12}C(p,n)$ and $^{13}C(p,n)$. This discrepancy will not be seen to exist in the (n,p) direction.

The code DW81 is used to make microscopic distorted wave calculations for angular distributions and are compared to the data. These calculated curves are also used to extrapolate the data to zero momentum transfer where $J_{\sigma\tau}$ can be found.

* Supported by NSF grant PHY87-22008 and by DOE.
♡ Ph.D. thesis, UC Davis, 1990.

B. NUCLEAR DATA EVALUATION AND MODEL

1. Summary of Monoenergetic Neutron Beam Sources for Energies > 14 Mev .†♣ (F.P. Brady and J.L. Romero.)

The production of neutron beams for energies between $\sim$ 20 and 100 MeV is reviewed. Considerations for obtaining monoenergetic beams as well as some of the limiting factors, such as energy resolution, are examined. Production cross sections at 0 deg are reviewed for proton- and deuteron-induced reactions on light elements. Some current facilities in the context of neutron beams obtained by collimation, by the associate particle method, and by the use of a beam swinger are also discussed.

2. Microscopic Optical Model Analysis of Neutron Scattering Cross Sections at 65 MeV over a Wide Range of A Values.* ◇ ♡ (L.F. Hansen,♠ E.L Hjort, F.P. Brady, J. Drummond, B. McEachern, G.H. Osborne and J.L. Romero.)

The neutron differential cross sections for C, Si, Ca, Fe, Sn, and Pb measured at 65 MeV between 6° and 47° using a wire chamber based neutron detector[1], are compared with calculations done with the microscopic OM potentials of JLM (with M3Y spin-orbit interaction) and Yamaguchi et al. The fits to the measurements were obtained with only three parameters: the normalization constants for the real (λ_V) and imaginary (λ_W) parts of the central potential, and for the real SO potential (λ_{SO}) The latter has a constant value of 1.3 for all the targets. The quality of the agreement with the measurements is very close for both calculations and also with fits obtained earlier[2] with phenomenological potentials for a much larger number of parameters. The A dependence of λ_V and λ_W will be discussed.

---

† Supported by NSF grant PHY 84-19380.
♣ Published in Nuclear Science and Engineering 106 (1990) 318.
* Work performed under the auspices of USDOE, Contract W-7405-ENG-48.
◇ Supported by NSF grant PHY 87-22008.
♡ Bulletin of the American Physical Society 35 (1990) 1650.
♠ Lawrence Livermore National Laboratory
1 F.P. Brady et al., Nucl. Instr. & Meth. 228, 89 (1984).
2 E.L. Hjort, BAPS, 34, 1831 (1989).

A. EXPERIMENTAL STUDIES

1. Beta-Decay Strength Functions for Fission Isotopes

(R. C. Greenwood, R. G. Helmer, M. A. Oates, M. H. Putnam, D. A. Struttmann, K. D. Watts)

The initial studies of the use of the total absorption gamma-ray spectrometer (TAGS) system with ISOL operation to measure beta-feeding (strength) distributions of fission-product nuclides have concentrated on selected fission-product isotopes of Cs, Ba, La and Ce with complex but reasonably well understood decay schemes, to serve as "validation cases" for the technique. Specifically, beta-feeding distribution measurements using the TAGS system in ISOL operation have been completed for ^{138g}Cs, ^{138m}Cs, ^{139}Cs, ^{140}Cs, ^{141}Cs, ^{141}Ba, ^{142}Ba, ^{143}La, ^{144}La, ^{145}La, and ^{145}Ce. In several of these cases it has been necessary to correct a specific nuclide spectrum for daughter-product grow-in. This was accomplished using a computer program SPANAL, which was written to allow both singles and coincidence-gated gamma spectra to be corrected for daughter grow-in (or parent-decay) as well as for the background gamma spectrum observed with the NaI(Tl) sum crystal spectrometer.

During the course of the year an increased noise was noted in the 300-mm^2 diameter x 1.0-mm thick Si detector, which is a component (for beta particle detection) of the total absorption gamma-ray spectrometer. This led to a re-evaluation of the Si beta-particle detection configuration. As a result, it was determined that a Si detector having a thickness of 1.5 mm would be sufficient to allow beta gates to be unambiguously set as high as 360 keV, with all possible internal conversion electron components being <5%. With such a detector, the probability for gamma rays causing a"beta" gate is still <5% for up to multiplicity-four cascades. In consequence, the following two new beta particle detectors have been obtained: a 300 mm^2 x 1.0 mm Si detector as a direct replacement of the present one; and a 300 mm^2 x 1.5 mm Si detector for use with those higher-Z fission-product isotopes where higher beta energy discrimination gates must be set to minimize false coincident events resulting from internal conversion.

In parallel with this measurement activity to obtain beta-strength-function distributions utilizing the total gamma-ray absorption spectrometer, there was a continuing effort to implement and upgrade the methods and computer codes necessary to analyze the spectra obtained. The methodology is based on the generation of Monte Carlo calculated response functions for the NaI(Tl) detector at various gamma-ray energies. These response functions can then be used to simulate the observed spectra for various sequences of coincident gamma rays, and these can be combined to simulate the complete spectrum for any assumed decay scheme. The principal systematic uncertainties in this analysis were: (1) the ambiguity in the choice of the number of cascades, the cascade gamma-ray energies, the associated multiplicities, and the intensity of each cascade for the new levels that are added to the decay scheme; (2) similar ambiguities for known levels, when the deduced beta feeding differs from the reported value; (3) any contribution from random summing; and (4) any contribution from bremsstrahlung that is counted in the NaI detector.

During this process of analyzing the fission-product radionuclides, it has been found necessary to add some new types of components to the response functions for single gamma rays and sum coincidences. First, a crude representation of the random summing has been generated. Second, it has been found necessary to generate a component to represent bremsstrahlung response functions. This component appears in both the measured singles and coincidence spectra. It occurs in the latter when the beta interacts in the Si detector and produces a gate for coincident photons which in this case are bremsstrahlung photons, rather than gamma rays. (The same process can occur for betas to excited states and the bremsstrahlung photons will sum in the NaI with the coincident gamma rays.) Third, it has been found that for the measured spectra the detector resolution is often poorer than that used in generating the gamma-ray response functions. Therefore, a convolution routine with a variable Gaussian convolution function has been developed to degrade the resolution of the simulated spectra to correspond to the resolution of each measured spectrum. Fourth, it is necessary to correct the results of the analyses of the beta-gamma coincidence spectra (but not the singles spectra) for the fact that a gate on the beta counter discards pulses below the preset energy (normally between 75 and 360 keV). As a result, the gamma-ray cascades from the high-energy levels are suppressed relative to those from the low-energy levels. This rejection of beta-gated coincident events occurs for both betas with energies less than the gate energy and betas with initial energies greater than the gate energy but which are scattered out of the Si detector resulting in only partial energy deposition. To correct for this effect, response functions for monoenergetic electrons interacting in the Si detector have been computed using the CYLTRAN Monte Carlo code, and these are used to compute correction factors for each of the excited states fed by beta decay in a nuclear decay.

As additional total gamma-ray absorption spectra are measured, they are being used (1) to compare with simulated spectra computed, using the codes and methodology developed to date, from the published decay scheme and (2) to refine the simulated spectra to more closely compare to the actual measured spectra and thereby deduce information about the multiplicity of the gamma cascades together with the beta feeding distributions. In these analyses, the measured spectra are matched to the simulated spectra by adding additional (new) levels to the decay scheme (each with its specific gamma-ray cascade sequence). In fact, the actual level energies are not known, rather the analysis shows that a certain beta feeding exists to levels in a certain energy range. However, once a specific new level has been proposed in a future decay scheme study, this analysis of the TAGS spectral data will place an upper limit on the beta feeding to it.

The first "final" analysis was carried out for the decay of ^{141}Ba (18 min) which has a decay energy of 3.2 MeV. In the decay scheme in Nuclear Data Sheets there are three levels above 2.0 MeV, namely 2.29, 2.47, and 2.74 MeV with beta feedings of 1.5, 0.5, and 0.5%, respectively. Comparison of the simulated spectrum, based on the decay scheme, with the measured TAGS spectrum showed that the 2.74 MeV level has a beta feeding of at least a factor of five less than that proposed. Furthermore, in order to obtain a fit to the TAGS spectrum, several new lower lying levels had to exist. This result is somewhat surprising considering the decay energy and relatively long half-life of this activity.

2. <u>Ground-State Beta-Branching Intensities for Fission Isotopes</u>
(R. C. Greenwood, D. A. Struttmann, K. D. Watts)

In order to obtain absolute beta-strength function values from the distribution of relative beta feeding intensities to excited states measured with the TAGS system, it is necessary to have available the corresponding values of ground-state beta-branching intensities, B_{gs}. (Where here, B_{gs} is defined as the sum of all beta-branching intensities to levels below the gamma-spectral discrimination level of the TAGS system, normally set at 50 keV.) For many of the short-lived fission-product nuclides for which beta-strength distribution measurements are planned with this spectrometer, B_{gs} values either do not exist or they may be viewed as suspect. This results from the fact that such nuclei, having large beta decay energies and complex decay schemes, represent a particular challenge for traditional nuclear spectroscopic methods of determining B_{gs} values; involving beta spectral unfolding or by determining transition feeding and de-exciting intensity imbalances for each excited state. This latter approach, depending as it does on the availability of a detailed knowledge of the decay scheme, including any significant internal electron conversion coefficients, is particularly time consuming for complex nuclear decay processes and furthermore, in such cases, is inherently subject to error resulting from missing weak gamma transitions, the so called "Pandemonium" problem.

On the other hand, using the TAGS system in the beta-gamma coincidence mode as a $4\pi\gamma$-β spectrometer, a ground-state beta-branching intensity is obtained in a rather straightforward manner from ratios of the beta-gamma coincidence to beta singles counting rates without the necessity of having an <u>a priori</u> knowledge of the specifics of the decay scheme. In order to obtain the most precise values for B_{gs} using this method, small (generally) correction terms must be evaluated to account for (1) non-detection in the NaI(Tl) detector of any member of a gamma-ray cascade de-exciting a level and, (2) betas detected in the Si detector with energies below that of the common beta-gating discriminator level, G_β.

The first correction term, for gamma-ray escape, can be computed if sufficient details of the nuclide decay scheme are already known or it can be estimated from the measured (with the TAGS system) distribution of beta-feeding to excited states together with estimates of average cascade multiplicities. This multiplicity information can be inferred both from fits to the measured "sum" spectrum and by comparing the "sum" spectrum to a "singles" spectrum measured with the source located external to the NaI(Tl) well. The second correction term, for missing betas below G_β, is quite straightforwardly calculated using the measured distribution of beta-feeding intensities to excited states and the ground state. In the computation of this correction term, it is necessary to have available sets of beta response functions for the Si detector, covering all beta energies of interest. The electron and photon Monte-Carlo code CYLTRAN was used to obtain these response functions. From these response functions, values of the fractional beta detection probability, above G_β, could be generated as a function of beta energy and folded into the beta spectral distributions, to the ground state and to the excited states, to obtain an appropriate correction factor.

Preliminary results obtained in this work, with the TAGS system, for "ground-state" branching intensities are summarized in Table A-1 and

TABLE A-1 Preliminary values of ground-state beta-branching intensities obtained using the TAGS system.

Fission Isotope	$\frac{N_{\beta\gamma}}{N_\beta}$	Estimated Correction Factor	Ground-State β-Branch(%) Measured	Previous Work[a]
^{138g}Cs	0.913	1.056	4(2)	0
^{138m}Cs	0.936	1.032	3(2)	0
^{139}Cs	0.190	1.165	78(1)	82(7)
^{140}Cs	0.630	1.043	34(1)	14, 40(4)
^{141}Cs	0.604	1.077	35(1)[b]	~50, 57(4)
^{141}Ba	0.946	1.033	2(2)	<10, 4.4(22)
^{142}Ba	0.896	1.064	4(2)[c]	0
^{142}La	0.731	1.090	20(3)	16.5(19)
^{143}La	0.240	1.142	73(1)[d]	~84
^{144}La	0.975	1.006	2(1)	0
^{145}La	0.862	1.070	5(2)[e]	52
^{145}Ce	0.905	1.066	3(2)[f]	0,6,24

[a] References to previous work from Nuclear Data Sheets.
[b] Ground state defined to include 48.5 and 55.0 keV levels.
[c] Ground state defined to include 77.6 keV level.
[d] Ground state defined to include 18.9 and 42.3 keV levels.
[e] Ground state defined to include 64.3, 70.0, and 118.2 keV levels.
[f] Ground state defined to include 62.7 keV level.

compared to current literature values. The uncertainty values associated with the present B_{gs} values in Table A-1 are statistical uncertainties (1σ) and contain no contribution from any systematic effects.

For those cases including ^{138}Cs, ^{139}Cs, ^{142}La, and possibly ^{142}Ba and ^{144}La, where prior work has provided B_{gs} values of sufficient certainty to compare with the present data, we note an acceptable degree of agreement. For those cases where B_{gs} values are known to be zero, ^{138}Cs, probably ^{144}La and possibly ^{142}Ba, we note that in each case our B_{gs} results show small positive values which, however, are not inconsistent with zero. A systematic bias towards such small positive values in such cases, in the present method, might be anticipated because the measured $N_{\beta\gamma}/N_{\beta}$ ratios are themselves constrained to values ≤ 1 by the coincidence triggering circuitry.

3. Beta-Decay Energies Measured for Fission-Product Isotopes
(R. C. Greenwood, R. G. Helmer, M. A. Oates, M. H. Putnam, K. D. Watts)

Measurement of beta end-point energies in decay to known levels in neutron-rich nuclides has provided a convenient method of deriving Q_{β} values, that is energy (mass) differences between neighboring isobars. Since nuclide masses close to the line of beta stability are generally known with good accuracy, such measurements allow nuclide masses in isobaric chains to be determined out to the limits of practical neutron-rich nuclide production in fission.

As one moves further off the line of beta stability, nuclei have higher Q_{β} values and more complex beta-decay schemes. Thus, in order to reliably utilize beta end-point energies to obtain Q_{β} values, it is generally necessary that such end-point values be derived from beta spectra measured in coincidence with the corresponding de-exciting gamma rays. (Furthermore, it is essential that details of the decay scheme be sufficiently well understood to know which levels in the daughter nuclide are directly fed in the beta-decay process.)

Such a beta-gamma coincidence system, for beta end-point measurements, has been developed in conjunction with the INEL ISOL facility. In order to allow for measurement of beta end-point energies of up to ~10 MeV, a 200-mm^2 x 10-mm intrinsic Ge detector with a thin Be window was selected for beta spectral measurements. In order to minimize the total window thickness through which the betas must pass, this detector is mounted directly into the vacuum system of the collection tape transport line. With this arrangement, based upon measurements using ^{137}Cs and ^{207}Bi internal conversion electron sources, electron energy loss values, in the total window thickness, of 27.0, 24.6, and 23.0 keV were obtained at electron energies of 481.7, 624.2 and 975.6 keV, respectively, with the electron peaks being broadened to ~10.5 keV (FWHM).

Initial tests of the Ge spectrometer with beta sources of ^{133}Xe, ^{32}P, ^{90}Sr-^{90}Y and ^{144}Pr demonstrated that acceptable beta end-point energy values could be obtained using only the raw counting data, without correction for detector response to electrons, provided that the Fermi-Kurie fit range was confined to an energy range > 80% of the end-point value, E_o.

In many cases in an ISOL operation, involving weak sources of short-lived fission-product isotopes with complex decay schemes which necessitate the use of beta-gamma coincidence spectroscopy to select out relevant beta branches, it is found necessary to utilize a much wider energy region, from $0.5E_o$ - E_o, to obtain an acceptable Fermi-Kurie plot. In these cases, if undistorted values are to be obtained for end-point energies, it is essential that the Ge detector response and peak efficiency for detection of betas be corrected for. To do this, a standard gain scale of 16 keV per channel was established for the beta spectrometer, and a complete library of response distributions for monoenergetic betas, at 16 keV intervals, was computed with the CYLTRAN Monte-Carlo photon and electron transport code (obtained from Sandia National Laboratory). These response functions are subsequently used in a simple beta spectrum stripping code ENDPT to correct for beta-peak detection efficiencies and beta response functions. With this same code, Fermi-Kurie plots (appropriately corrected with the Fermi functions) and least-squares fits to compute end-point energies can be made.

TABLE A-2 Preliminary values of Q_β deduced from beta end-point energy measurements.

Fission Isotope	Q_β Value (keV) This Work	Q_β Value (keV) 1983 Mass Evaluation
^{140}Cs	6150 ± 25	6218 ± 13
^{151}Pr	4048 ± 30	3800 ± 300[a]
^{153}Pm	1869 ± 8	1900 ± 16
^{154}Nd	2666 ± 25	2700 ± 300[a]
^{154}Pm (1.7 min.)	4060 ± 70	4000 ± 100
^{155}Nd	4263 ± 60	4400[b]
^{155}Pm	3201 ± 25	3100 ± 200[a]
^{155}Sm	1601 ± 20	1627.5 ± 2.1
^{157}Sm	2704 ± 20	2600 ± 200
^{158}Sm	1995 ± 15	2050 ± 220[a]

[a] Q_β prediction based on the systematics of atomic masses.[1]
[b] Q_β prediction based on the systematics of atomic masses.[2]

1. A. H. Wapstra and G. Audi, Nucl. Phys. A432, 1 (1985).
2. A. H. Wapstra, G. Audi, and R. Hoekstra, At. Data Nucl. Data Tables 39, 281 (1988).

Initially, one interest of this work has been to establish Q_β values for some of the most recently identified rare-earth fission-product isotopes. A summary of preliminary Q_β values obtained for several of these isotopes is shown in Table A-2, in comparison to current literature values representing data obtained from both measurement and from predictions based upon the systematics of atomic masses.

4. The Standardization of ^{93m}Nb for Use as a Reference Material for Reactor Neutron Dosimetry (R. J. Gehrke, JW Rogers, L. D. Koeppen)

Neutron dosimetry by means of radiometric monitors provides the principal experimental method of assessing the fluence spectra of neutrons incident on power-reactor pressure vessels and other structures. Two desirable features of nuclear reactions used in radiometric monitors are: an activation cross section whose neutron energy dependence resembles that for displacement damage in iron; and a radioactive product with sufficiently long half-life to provide effective integration over exposure durations of several years.

Niobium-metal dosimeters are widely used in nuclear reactors for measuring the neutron fluence. The activation reaction employed is ^{93}Nb(n,n′)^{93m}Nb. The distinct advantages of this reaction are: it has a threshold energy below 1 MeV, and therefore sees a large fraction of fast neutrons; and it has a fairly long half-life, and is therefore useful as a neutron-fluence monitor. The number of atoms, n, of ^{93m}Nb in a post-irradiation foil or wire is related to the measured K X-ray emission rate N_{KX} by

$$n=\frac{(N_{KX})\,(T_{1/2})}{(P_{KX})\,(ln2)}$$

where P_{KX} and $T_{1/2}$ are the K X-ray emission probability and half-life, respectively. Thus, apart from the neutron cross section, the accuracy of the neutron-fluence measurements using niobium dosimeters will be limited by the uncertainty in these two parameters. Measurements of the half-life at the Centre d'Etudes Nucleaires-Grenoble ((16.11 ± 0.19) y)[1] and the Central Bureau for Nuclear Measurements (CBNM) in Geel ((16.13 ± 0.15) y)[2] have reduced the uncertainty resulting from this latter quantity. However, the uncertainties in previously measured values for P_{KX} are large and result in an unacceptably large uncertainty in the number of Nb atoms in the irradiated fluence monitor. The present study was undertaken to reduce the uncertainty in the value for P_{KX} so that the number of ^{93m}Nb atoms could be accurately measured.

1. R. Lloret, Radiochem. Radioanal. Lett. 50, 113 (1981).
2. R. Vaninbroukx, Int. J. Appl. Radiat. Isot. 34, 1211 (1983).

A solution of ^{93m}Nb in 1M HF + 1M HNO_3 was dispensed into teflon containers and distributed to several laboratories to allow a definitive measurement of the emission probability for the 17-keV K X-rays. The material was characterized for stability, activity concentration, and K X-ray emission rate. The activity concentration was measured by liquid-scintillation counting, with an estimated uncertainty (one standard deviation) of 0.76%. The K X-ray emission rate was measured in five laboratories using three different detector types: a defined solid-angle photon detector; a 4π pressurized proportional counter; and calibrated semiconductor photon spectrometers. The K X-ray emission-rate value for the five laboratories had an estimated uncertainty (one standard deviation) of 1.9%. Combining the activity and emission-rate values gives a K X-ray emission probability of 0.1112 ± 0.0022. The combined result of the five laboratories was published in Nuclear Instruments and Methods in Physics Research.[1]

5. Measurements of Fission Spectrum Averaged Cross Sections for the ^{93}Nb(n,n')^{93m}Nb Reaction (JW Rogers, R. J. Gehrke, J. D. Baker, F. J. Wheeler)

Neutron dosimetry by means of radiometric monitors provides the principal experimental method of assessing the fluence spectra of neutrons incident on power reactor pressure vessels and other structures. Two desirable features of nuclear reactions used in radiometric monitors are that the activation cross section have a neutron energy dependence that resembles that for displacement damage in iron, and that the radioactive product have a sufficiently long half-life to provide effective integration over exposure durations of several years. The ^{93}Nb(n,n')^{93m}Nb reaction meets these criteria more nearly than any other practically applicable reaction, with the possible exception of the ^{237}Np fission reaction, which is also widely used for this purpose. Many papers describing the use of niobium as a radiometric monitor and the relevant nuclear data have been published.

The cross section for ^{93}Nb(n,n')^{93m}Nb is difficult to measure using monoenergetic neutrons because the combination of its long half-life and small cross section make it difficult to produce enough activity to measure. Large niobium target masses cannot be effectively used because of the weakly penetrating nature of the product radiation. Recent measurements by Gayther _et al._[2] are the only ones available for which the

1. B. M. Coursey, R. Vaninbroukx, D. Reher, J. M. R. Hutchinson, P. A. Mullen, K. Debertin, R. J. Gehrke, JW Rogers, L. D. Koeppen, and D. Smith, Nucl. Instr. & Methods in Phys. Research A290, 537 (1990).

2. D. B. Gayther, M. F. Murphy, K. Randle, W. H. Taylor, and C. A. Uttley, "The Determination of the ^{93}Nb(n,n')^{93m}Nb Excitation Function Using Foil Activation", in Proceedings of the International Conference on Nuclear Data for Basic and Applied Science, Santa Fe, 13-17 May, 1985 (Gordon and Breach, New York, 1986), Vol. I, pp. 521-524.

activation method has been used with monoenergetic neutrons in the range 1-6 MeV. Uncertainty values, which include significant contributions from counting statistics, were provisionally estimated as ±10% at each energy used.

Spectrum-averaged values of the cross section reported here provide an integral check of the energy-dependent cross section, and may be used for normalization of the excitation function and benchmarking of dosimetry in fission neutron-driven systems. More accurate measurements are possible for spectrum-averaged cross sections than for monoenergetic cross sections because of the availability of higher neutron fluences, which are also more accurately known. The ^{252}Cf spontaneous-fission spectrum and the thermal neutron-induced ^{235}U fission spectrum are the best-known neutron spectra in the relevant energy range.

The measurements reported here were undertaken with the objective of reducing the contribution of cross-section uncertainties in niobium dosimetry to the range (about ± 5%) considered acceptable for reactor dosimetry. The target accuracy for the measured spectrum cross-section values was ±4%. The four principal contributors to the uncertainty were anticipated to be: neutron fluence determination; correction for scattering effects perturbing the ideal free-field conditions; x-ray detector calibration; and counting statistics. Our aim was to limit each of these to approximately ±2%.

The spectrum-averaged cross sections of the ^{93}Nb(n,n')^{93m}Nb reaction in two standard fission-neutron spectra have been measured by the activation method. The two standard spectra were the ^{252}Cf spontaneous-fission neutron spectrum and the thermal neutron-induced neutron spectrum of ^{235}U. Effective free-field neutron fluences were established by neutron source-strength calibration against the national standard Ra-Be source, fluence transfer from intermediate standard sources, and Monte Carlo scattering corrections. Activity measurements were performed by x-ray counting using a variety of Ge and Si(Li) spectrometers, with sources prepared by deposition of niobium fluoride on analytical paper discs.

The spectrum-averaged cross section for ^{93}Nb(n,n')^{93m}Nb in the ^{252}Cf fission-neutron spectrum was calculated using the specific activity value measured in this study, the number of atoms per mg for niobium (6.4818×10^{18}), the saturation factor (0.01056 ± 0.93%), the source emission rate at the end of the irradiation (4.477×10^{10} ± 1.5%) and the data from the Monte Carlo results. A bias factor of 1.00 ± 0.58% due to source and detector positioning uncertainty in the irradiation was also used. The cross-section value found was 150.6 mb ± 2.6%.

The cross section in the ^{235}U fission neutron spectrum was calculated using the specific-activity value, the number of atoms per mg, the factor (0.9982) for decay during irradiation, the free-field neutron fluence

(1.00 x 10^{17} ± 2.1%), the scattering correction (1.016 ± 0.56%), and the half-life (16.13 ± 0.15) y[1].

The results of this study were presented at the 5th ASTM EURATOM Symposium on Reactor Dosimetry held in Jackson, Wyoming, June 1987 and the proceedings of this meeting were recently published.[2]

6. IAEA Coordinated Research Program on Decay Data for Ge Detector Efficiency Calibration: Measurement (R. G. Helmer)

As a part of our participation in the IAEA Coordinated Research Program on Decay Data for Ge Detector Efficiency Calibration, we have been involved in both the measurement and the evaluation of nuclear decay data. In response to a need identified at one of the meetings of the participants in this CRP, we measured the relative emission probabilities of the two most intense gamma rays from the decay of ^{207}Bi. The value measured for the ratio of the emission rates of the 1063 and the 569-keV gamma rays was 0.764 ± 0.005. This agrees reasonably well with the value 0.7579 ± 0.0039 reported by Yoshizawa *et al*. [Nucl. Instrum. Methods 174, 109 (1980)]. Our result has been published in Applied Radiation and Isotopes 41, 791 (1990).

B. NUCLEAR DATA EVALUATION ACTIVITY

1. Mass-Chain Evaluations for the Nuclear Data Sheets (R. G. Helmer, C. W. Reich)

As part of our involvement in the work of the International Nuclear Structure and Decay Data Evaluation Network, which carries out the evaluation of basic nuclear-physics data for publication in the Nuclear Data Sheets, we have historically had the evaluation responsibility for the ten mass chains in the region $153 \leq A \leq 162$. However, with the recent withdrawal of the German evaluation group from the network, we have been given permanent evaluation responsibility for one of this groups's mass chains, namely that with A=87. In addition, we have previously carried out, through a temporary assignment, the evaluation of data for A=206, which was one of the mass chains assigned to the Nuclear Data Project at ORNL. Our

1. R. Vaninbroukx, Int. J. Appl. Radiat. Isot. 34, 1211 (1983).

2. J. G. Williams, C. O. Cogburn, L. M. Hodgson, S. C. Apple, E. D. McGarry, G. P. Lamaze, F. J. Shima, JW Rogers, R. J. Gehrke, J. D. Baker, and F. J. Wheeler, "Measurements of Fission Spectrum Averaged Cross Sections for the ^{93}Nb(n,n')^{93m}Nb Reaction", Reactor Dosimetry Methods, Applications, and Standardizations, H. Farrar IV and E. P. Lippincott, Editors; publication of American Society for Testing and Materials (ASTM), STP1001, Philadelphia, PA 19103, (1989) pp 235-244.

policy for the evaluation of these mass chains continues to be to work on them in order of time since the previous publication, with those most out of date at any given time being evaluated.

The current status of the A-chain evaluations within our area of responsibility (including the temporary assignment of A=206) is as follows:

A-chain	status (according to currency)
160	evaluation under way; last published in NDS 46 (1985)
156	evaluation underway; last published in NDS 49 (1986)
162	submitted for publication
87*	in process of being published
206†	Nuclear Data Sheets 61 (1990)
153	Nuclear Data Sheets 60 (1990)
161	Nuclear Data Sheets 59 (1990)
158	Nuclear Data Sheets 56 (1989)
157	Nuclear Data Sheets 55 (1988)
159	Nuclear Data Sheets 53 (1988)
154	Nuclear Data Sheets 52 (1987)
155	Nuclear Data Sheets 50 (1987)

* This evaluation was done by the German evaluation group
† Temporary assignment from the Nuclear Data Project at ORNL

As is evident from this listing, the current status of our mass-chain evaluations satisfies one of the objectives of the international evaluation network, namely a cycle time of about 5 years.

During the past year, an evaluation of recent data on the A=161 mass chain was carried out in the so-called "update mode". THis new system is designed to make the Evaluated Nuclear Structure Data File (ENSDF) more current without the necessity of preparing a complete new publication in the Nuclear Data Sheets. This represents the first case in which this new procedure has been used. It will help identify any problems associated with this process and thus help identify those items that will enhance its practicality in the future.

2. Evaluation of Decay Data for ENDF/B-VI (C. W. Reich)

Within the framework of the Cross Sections Evaluation Working Group, we have the responsibility for the evaluated experimental decay data in ENDF/B. During this past year, decay data evaluations were carried out for the following nine nuclides that were identified as being needed for the Activation file of ENDF/B-VI: ^{6}He, ^{8}Li, ^{16}N, ^{19}O, ^{23}Ne, ^{32}P, ^{44m}Sc, ^{49}Cr, and ^{195}Au. With the completion of these evaluations, the INEL-based evaluation work has essentially been completed; and a final checking of the ENDF/B-VI decay data has been going on. The "final" numbers of nuclides for which INEL-evaluated decay data will be included in the various subfiles of ENDF/B-VI are as follows: Activation File (158 nuclides); Actinide File (108 nuclides); and Fission Product File (510 nuclides).

3. IAEA Coordinated Research Program on Transactinium Nuclide Decay Data (C. W. Reich)

As a follow-up to the IAEA Coordinated Research Program (CRP) on Transactinium Isotope Nuclear Decay Data Measurement and Evaluation, which took place from 1978 through 1984, the IAEA Nuclear Data Section convened a meeting of the participants in that CRP at IAEA Headquarters in November, 1989. This meeting was called to consider the present status of data on these nuclides, which have important applications in many aspects of the fast reactor fuel cycle. A number of important new data were identified. Because of those new data and the widespread acceptance of the final report of this CRP (issued as No. 261 in the IAEA Technical Reports Series), it was decided to revise the contents of this report and to issue an updated version of it. The INEL participant was assigned responsibility for re-doing the evaluation of the ^{237}Np decay data. At present, the proposed revisions to CRP report are being reviewed; and it is expected that the revised report will be issued sometime during this calendar year.

4. Additional Activities (R. G. Helmer)

The evaluation work related to the IAEA Coordinated Research Program on Decay Data for Ge Detector Efficiency Calibration, discussed in our report for last year, has continued. In addition, R. G. Helmer has continued to serve as the Coordinator of the Gamma- and Beta-Ray Spectrometry Working Group of the International Committee for Radionuclide Metrology (ICRM).

A. STUDIES OF FISSION PRODUCTS WITH THE TRISTAN SEPARATOR

Neutron-rich nuclides far from stability are mass separated and studied using the TRISTAN separator on-line to the High Flux Beam Reactor (HFBR) at Brookhaven National Laboratory. The nuclides are produced by thermal neutron fission of ^{235}U and studied using the techniques of γ-ray spectroscopy. We measure γ singles, $\gamma\gamma$ coincidences, and angular correlations. The FEST β-γ-γ fast-timing system is used to measure lifetimes of nuclear excited states as short as a few picoseconds. The research at TRISTAN is carried out by a team consisting of the Ames group at Iowa State University and scientists from Brookhaven and Clark University. The HFBR has been shut down since April 1989 and is not available for research. We thus have less to report than in past years.

1. Decay of ^{74}Cu to Levels in Even-Even ^{74}Zn (Winger et al.)

The decay of high- and low-spin isomers of ^{74}Cu to levels in ^{76}Zn was studied. Half-lives for the ^{76}Cu isomers were 0.57 ± 0.06 s and 1.27 ± 0.30 s, respectively. Twelve γ rays were attributed to the decay of ^{76}Cu. Eleven of these were placed in a level scheme for ^{76}Zn with 8 excited states up to 3 MeV. The excitation energy of 599 keV for the 2_1^+ state is the lowest known for even-A Zn isotopes. Shell-model calculations of the even-A neutron-rich isotopes were carried out with active protons in the $1f_{5/2}$, $2p_{3/2}$, $2p_{1/2}$, and $1g_{9/2}$ orbitals. Reasonable agreement is obtained between theory and experiment below 2 MeV excitation. The dominant proton components for states below 2.3 MeV in ^{76}Zn are $1f_{5/2}$ and $2p_{3/2}$. This work has been published in *Phys. Rev. C*.[1]

2. Decay of ^{102}Y to Levels in ^{102}Zr (Hill et al.)

The decay of high- and low-spin isomers of ^{102}Y to levels in ^{102}Zr was studied at the JOSEF separator at the KFA, Jülich, Germany, and at the TRISTAN separator, respectively. Based on γ singles and $\gamma\gamma$ coincidence measurements, decay schemes for both isomers were deduced. The half-life of the low-spin isomer of ^{102}Y was measured at TRISTAN to be 0.30 ± 0.01 s. Six γ rays were assigned to the decay of the low-spin isomer and 8 to the high-spin isomer. Levels were postulated for ^{102}Zr with excitation energies up to about 2 MeV. Of special interest is a new level at 894 keV that we tentatively postulate to be the 0_2^+ state. This 0^+ state could be either an essentially

[1] Winger, Hill, Wohn, Warburton, Gill, Piotrowski, Schuhmann, and Brenner, *Phys. Rev. C* **42**, 954 (1990).

"spherical" state or the band head of a β vibration of the highly deformed core. Additional experiments are needed to differentiate between these two possibilities. This material will be published in *Phys. Rev. C.* in the spring or summer of 1991.[2]

3. B(E2;$0_1^+ \rightarrow 2_1^+$) rates in ^{90,92,94,96}Sr (Wohn et al.)

Lifetimes of low-lying levels in ^{90,92,94,96}Sr were measured at TRISTAN using the FEST system. B(E2;$0_1^+ \rightarrow 2_1^+$) values for ^{90,92,94,96}Sr were found to be 0.10(3), 0.09(4), 0.10(4), and 0.17(9), in e^2b^2, respectively. These B(E2) values, which fill the N=52-58 gap in the known B(E2;$0_1^+ \rightarrow 2_1^+$) values for $^{78-100}$Sr, are exceptionally low. They provide direct evidence for strong Z=38 subshell closure from N=50 to N=58. Also, these B(E2) strengths establish a close similarity between $^{88-96}$Sr and $^{90-98}$Zr, which form a region of lowest B(E2) values (for nuclei with A>56) second only to $^{204-210}$Pb. A dramatic change in the Sr collectivity occurs at N=60, where B(E2;$0_1^+ \rightarrow 2_1^+$) abruptly increases by a factor of 15. A change in nuclear shape of such abruptness occurs only for Sr and Zr nuclei. These results, which include a comparison with recent laser spectroscopic studies and also discusses the octupole vibrational collectivity of nuclei in this region, is in press for publication in *Nucl. Phys. A*.[3]

[2] Hill, Schwellenbach, Wohn, Winger, Gill, Ohm, and Sistemich, *Phys. Rev. C* (accepted).

[3] Mach, Wohn, Molnár, Sistemich, Hill, Moszyński, Gill, Krips, and Brenner, *Nucl. Phys. A* (in press).

A. NEUTRON SCATTERING

1. Separation of Neutron and Proton Dynamics (M.T. McEllistrem)

a. Scattering from ^{48}Ca (S.F.Hicks, S.E. Hicks, and M.T. McEllistrem)

The study of neutron scattering from ^{48}Ca at incident energies from 2 to 8 MeV, involving both neutron and γ-ray detection in separate experiments,[1,2] led to the determination that the strong, intermediate-structure $d_{5/2}$ resonances at low energies were the result of p-wave neutrons coupled to two 3^- core excitations of ^{48}Ca. The two scattering studies also allow us to show very strong separation of neutron and proton dynamics in collective ^{48}Ca levels.

b. Scattering from Shape-transitional Nuclei (S.E. Hicks, G.R. Shen, and M.T. McEllistrem)

Similar neutron scattering studies[3-5] in the shape-transitional nuclei near A = 190 also demonstrate marked variations in target nucleus proton and neutron dynamics; neutrons and protons are not strongly coupled to each other in excitations of either magic or shape-transitional nuclei. Further examination of separate neutron and proton collective nuclear dynamics will correlate them with separate effective charges of protons and neutrons needed for description of bound state structures of the same nuclei, within both Interacting Boson Models and Fermion Dynamical Symmetry Models.

2. Five Even-A Sn Isotopes (J.L. Weil, M.C. Mirzaa, and A.A. Naqvi)

The analysis of the neutron scattering and total cross sections[6-8] of $^{116\text{-}124}$Sn is essentially complete. The most recent step has been to do a spherical optical model (SOM) analysis of the 4,11 and 24 MeV differential scattering cross sections, and to compare the dispersion corrected SOM potentials with those previously obtained from a coupled channel (CC) analysis. The differences are small. A publication is being written.

---

[1] Hicks, Hicks, Shen, and McEllistrem, Phys. Rev. **C41**, 2560 (1990).

[2] Vanhoy, Hicks, McEllistrem, Gatenby, Baum, Johnson, Molnár and Yates, submitted to Physical Review C.

[3] Hicks, Delaroche, Mirzaa, Hanly, and McEllistrem, Phys. Rev. **C36**, 73 (1987).

[4] Clegg, Haouat, Delaroche, Lagrange, Hicks, Shen, McEllistrem, Phys. Rev **C40**, 2527 (1989).

[5] Mirzaa, Delaroche, Weil, Hanly, and McEllistrem, Phys. Rev. **C32**, 1488 (1985).

[6] Harper, Weil and Brandenberger, Phys. Rev. **C30**, 1454 (1984).

[7] Rapaport, Mirzaa, Hadizadeh, Bainum and Finlay, Nucl. Phys. **A341**, 56 (1980).

[8] Harper, Godfrey and Weil, Phys. Rev. **C26**, 1432 (1982).

3. Projected Work in Neutron Scattering

a. Exploration of E3 Excitations (M.T. McEllistrem, D. Wang, P. Zhang, and J.L. Weil)

The presence of strong E3 excitations in collective nuclei, or instability to E3 deformations, has often been considered to be indicated by abnormally strong E1 amplitudes in γ-ray decay patterns. This is an indirect signature, owing to interference between E3 and the more common E2 susceptibility or deformations. The E1 intensity is a necessary signature for the many cases in which the direct ground state E3 transitions cannot compete with E1 cascades.

Calculations of expected electric dipole moments arising from macroscopic E3 strengths, based on the Myers and Swiatecki droplet model,[9] show rather small macroscopic, or collective, contributions because the large charge redistribution term is nearly cancelled by the comparably large neutron skin term.[10] Many nuclei near shape-transitional regions have large particle-hole E3 amplitudes,[10] which can make viewing the collective E3 susceptibility quite difficult.

Neutron scattering cross sections will be strongly enhanced when E3 strengths are large, just as the better known E2 enhancements produce large cross sections, even at low neutron energies.[4] Thus, we can see the E3 strengths directly, provided we can achieve adequate resolution of levels in the scattering experiment. To assure this, we will combine the observation of strong enhancements in neutron detection data with the high resolution capabilities available in γ-ray detection, as we did quite successfully for scattering in ^{48}Ca.[1,2] The task will be harder in the more complex collective nuclei, but should be feasible with our new pulsed- and bunched-beam system.

We plan to first examine E3 excitations in ^{196}Pt. In previous experiments in this laboratory[11] we examined the level and γ-ray decay schemes of ^{196}Pt, but only at low incident neutron energies. We will study the inelastic scattering spectra of 7 and 8 MeV neutrons, and supplement that with new γ-ray data taken at higher energies than taken previously. We expect the electromagnetic decay rates observed in γ-ray decays to be tens to hundreds of femtoseconds, within the range of lifetimes detectable here using DSAM methods. Part of this work, particularly the γ-ray decay studies, will be in collaboration with Paul Cottle of Florida State University who has a strong interest in E3 decay strengths in collective nuclei.

We will attempt the same approach in ^{140}Ce, where the advantage would be that the E3 strength should be much less fragmented, as the E2 strength is much weaker than in other collective nuclei. Further, the level density in the vicinity of the E3 excitations should be much lower because of the semi-magic character of ^{140}Ce.

b. Separate Neutron and Proton Dynamics (P. Zhang, D. Wang, and M. T. McEllistrem)

We have compared neutron scattering to collective levels in shape-transitional Pt and Os nuclei to electromagnetic excitation of those levels. These comparisons have shown clearly a very strong separation of neutron and proton dynamics in the target nuclei. These should be interpretable in terms of different effective charges used to represent bound state decays in the IBM-2 model. This question of the relation of bound state effective charges to the hadron dependence of scattering for the same collective levels will be explored during the following year in

[9] W.D. Myers, *Droplet Model in Atomic Nuclei* (IFI/Plenum Data, New York) (1977); Möller, Myers, Swiatecki, and Treiner, Atomic Data Nucl. Data Tables **39**, 225 (1988).

[10] P.A. Butler, in *Proc. Int'l. Conf. High Spin Physics and Gamma-Soft Nuclei*, Pitt/Carnegie Mellon, Pittsburgh, PA., Sept. 17-21 (1990).

[11] A.A. Khan, PhD dissertation, University of Kentucky (unpublished) (1985).

a more complete way; we will also attempt to interpret dynamical differences between neutrons and protons[12] in terms of the Fermion Dynamical Symmetry Model, to see which of these models most naturally accommodates varying roles for valence neutrons and protons in collective nuclei.

The same sort of dynamical differences are quite strongly expected for E3 excitations. Indeed, if the particle-hole effects and neutron skin effects projected to affect E3 amplitudes are as sensitive as expected,[10] we may well see stronger hadron dependence of scattering to those levels than to E2 collective levels. The whole subject of E3 amplitudes, the causes of them and the way they manifest themselves in nuclear structure, is a very interesting topic at this juncture.

c. Neutron Scattering from Five Even-A Sn Isotopes (J.L. Weil, M.C. Mirzaa, and A.A. Naqvi)

The remaining calculations of the dispersion theory corrections to the optical potentials for describing neutron scattering from $^{116\text{-}124}$Sn were completed during the past year. A comparison can now be made between the dispersion corrected potentials for a spherical optical model (SOM) analysis and a coupled channel optical model (CCOM) analysis. This comparison is now under way, and a manuscript is in preparation.

The dispersion correction paper will be submitted in the Spring of 1991. Following that, attention will turn to the task of completing the writing of the much longer paper describing the complete elastic and inelastic scattering results from these five nuclei. This is now possible, since the work on making resonance self-shielding corrections to the total cross sections is complete, and the needed information on level densities of highly excited states in Sn is well enough in hand for us to be able to do a reasonable job of making the statistical model calculations necessary for a very detailed analysis of the inelastic scattering cross sections.

B. <u>NUCLEAR STRUCTURE STUDIES</u>

1. <u>Probing Collective Excitations with the (n,n'γ) Reaction</u>

a. Two-phonon Octupole Vibrations (R.A. Gatenby, E.L. Johnson, G. Molnár and S.W. Yates)

While the role of surface vibrational excitations in nuclei has been a subject of study for many years, our knowledge of these fundamental modes remains incomplete. One way in which vibrations in nuclei can be better understood is by the observation of multiphonon excitations. In closed shell nuclei, the octupole vibrations have relatively low excitation energies and compete successfully with the quadrupole mode; in two heavy nuclei, ^{146}Gd and ^{208}Pb, the 3^- state lies lower than the quadrupole phonon, and is the first excited state in each. These features have stimulated a number of searches for a two-phonon octupole quadruplet of states with spins and parities of 0^+, 2^+, 4^+, and 6^+ at about twice the energy of the 3^- state in these nuclei, but no clear-cut identification has emerged in either nucleus.

Despite the failure of attempts to identify two-phonon octupole excitations in ^{146}Gd, stretch-coupled states of this type have been identified[13,14] in the neighboring nuclei ^{147}Gd and ^{148}Gd. Serendipitously, these states occur as yrast states and decay by characteristic cascades of two E3 transitions because lower multipolarity decays are not

---

[12] M.T. McEllistrem, in *Proc. Int'l. Conf. High Spin Physics and Gamma-Soft Nuclei*, Pitt/Carnegie Mellon, Pittsburgh, PA., Sept. 17-21 (1990).

[13] Kleinheinz, Styczen, Piiparinen, Blomqvist and Kortelahti, Phys. Rev. Lett. **48**, 1457 (1982).

[14] Lunardi, Kleinheinz, Piiparinen, Ogawa, Lach and Blomqvist, Phys. Rev. Lett. **53**, 1531 (1984).

possible. Since these states involve the coupling of one or two neutrons to the two-phonon octupole excitation ($\nu f_{7/2}\otimes 3^-\otimes 3^-$ in ^{147}Gd $\nu f^2\otimes 3^-\otimes 3^-$ and in ^{148}Gd), their descriptions are not straightforward, and the search for a *complete* two-phonon octupole multiplet has continued.

The nucleus ^{96}Zr has been shown to display many of the properties of a closed-shell nucleus.[15] At the same time, there are indications[16] of strong susceptibility to octupole deformations; recent measurements[17,18] of the lifetime of the first 3^- state yield an E3 transition rate of about 70 Weisskopf units (W.u.), making this $3^- \rightarrow 0^+$ transition the fastest known. We have identified two nuclei in measurements[15,19] recently reported, ^{96}Zr and ^{144}Sm, with possible octupole-octupole (and also quadrupole-octupole) coupled level-multiplets based on the observations of clusters of levels of the correct spins and parities, and with strong γ-ray decays to the one-phonon 3^- level. At somewhat less than twice the one-phonon octupole energy in each nucleus, a quartet of positive parity states which decay to the 3^- phonon with large E1 transition rates was observed. As shown by Kusnezov *et al.*,[20] within the framework of the *spdf* IBM, large E1 rates can be taken as evidence of transitions from two-phonon octupole states at least in the nucleus ^{96}Zr. Unfortunately, mixing between the octupole-octupole states and other quadrupole states can be substantial, and the octupole strength can be greatly fragmented; thus these identifications remain tenuous.

The nucleus ^{144}Sm is only two protons removed from ^{146}Gd, which has been shown by Kleinheinz and coworkers[21] to exhibit many of the properties of a doubly closed-shell nucleus, and B(E3;$3^- \rightarrow 0^+$) has recently been measured[22] to be 38 ± 3 W.u. Based on the DSAM lifetime measurements and γ-ray branchings,[23] evidence for a complete two-phonon octupole quartet and a quintet of quadrupole-octupole coupled states was obtained. Only a 4^+ level at 3494.1 keV and a 2^+ state at 3523.7 keV were observed to decay solely by E1 transitions to the 3^- octupole phonon, and can be confidently assigned[19] as members of the two-phonon multiplet. A striking observation of this work[19] and an accompanying study[23] of the N = 82 isotone ^{142}Nd, however, is that nearly *all* of the observed E1 transitions are fast. We are forced to question, therefore, whether E1 transition rates can be regarded as unambiguous signatures of octupole character in this mass region, or alternatively, whether octupole susceptibility might be a fairly common feature near closed shells and subshells.

b. Collective Magnetic Dipole States (E.M. Baum, D. Diprete and S.W. Yates)

The discovery of a new class of low-lying collective magnetic dipole excitations observed in inelastic electron and photon scattering experiments (see the excellent review by Richter[24]) has stimulated considerable

[15]Molnár, Belgya, Fazekas, Veres, Yates, Kleppinger, Gatenby, Julin, Kumpulainen, Passoja and Verho, Nucl. Phys. **A500**, 43 (1989).

[16]W. Nazarewicz, in *Proc. Intl. Conf. on High Spin and Gamma-Soft Nuclei*, Pitt/Carnegie-Mellon, Pittsburgh, PA, Sept. 17-21, (1990).

[17]Ohm, Liang, Molnár, Raman, Sistemich and Unkelbach, Phys. Lett **241B**, 472 (1990).

[18]Mach, Cwiok, Nazarewicz, Fogelberg, Moszynski, Winger and Gill, Phys. Rev. **42**, R811 (1990).

[19]Gatenby, Vanhoy, Baum, Johnson, Yates, Belgya, Fazekas, Veres and Molnár, Phys. Rev. **C41**, R414 (1990).

[20]Kusnezov, Henry and Meyer, Phys. Lett. **228B**, 11 (1989).

[21]Kleinheinz, Broda, Daly, Lunardi, Ogawa and Blomqvist, Z. Phys. **A290**, 279 (1979).

[22]A.F. Barfield *et al.*, Z. Phys. **A332**, 29 (1989).

[23]R.A. Gatenby, Ph.D. Dissertation, University of Kentucky, (unpublished) (1990).

[24]A. Richter, *Contemporary Topics in Nuclear Structure Physics*, World Scientific, (Singapore, 1988) pp. 127-164.

experimental and theoretical interest. This M1 excitation, commonly referred to as the "scissors mode", has been observed in deformed nuclei from ^{46}Ti to ^{238}U, and its energy scales as $E_x = 66\delta A^{-1/3}$, where δ is the nuclear deformation parameter. Many theoretical approaches, from macroscopic to microscopic, have been developed to explain the M1 scissors mode, and it is now generally agreed that, in any successful description of these states, protons and neutrons must be treated as distinguishable, and that this is predominantly an orbital magnetic mode.

In a study of two-quasiproton configurations of the form $7/2^-[523] \otimes 5/2^-[532]$ in ^{164}Dy with the ^{165}Ho(t,α) reaction, Freeman *et al.*[25] found that the 2539-keV state observed previously in inelastic electron and photon scattering with a large M1 strength, 1.67 μ_N^2, is in fact dominated by this two-quasiparticle configuration. This observation appears inconsistent with a collective interpretation of this state. Additional states in ^{164}Dy near 3.1 MeV which were also found in (e,e') and (γ,γ) reactions[26,27] to exhibit large M1 strength (3.15 μ_N^2) were not observed in this proton transfer reaction, a result which could either be taken as evidence that the higher-lying states are the true isovector M1 states or that these states do not involve quasiproton components accessible with the reaction employed. Interestingly, recent intermediate energy proton scattering measurements[28] suggest that ^{164}Dy may be unique in having a significant (15%) spin admixture in the nuclear wavefunctions of the scissors M1 excitations. Clearly, a number of questions remain about the nature of M1 scissors mode states.

In an effort to address the inconsistencies noted above, we have initiated INS studies of ^{162}Dy and ^{164}Dy. In our measurements on these nuclei, we have observed *all* of the excited 1^+ states suggested as scissors states in these nuclei. The strong population of all low-spin levels in INS leads to the extreme complexity of these spectra; this makes the analysis difficult, particularly when attempting to determine the lifetimes from the small Doppler shifts. At the energies of our measurements, the maximum shifts in the γ-ray energies are about 1.5 keV. On the other hand, the identification of collective M1 transitions should be relatively straightforward, even if we are not able to determine the lifetimes with high precision. In addition to measuring the lifetimes of these states, from the line-shifts in the INS reaction, we have tentatively observed transitions other than the known decays to the ground and first 2^+ states from several scissors mode states. These new γ-rays have, of course, lower energies than the ground-state transitions and are typically obscured in nuclear resonance fluorescence measurements by the intense low-energy bremsstrahlung. We believe our measurements hold the best possibility for observing the complete γ-ray branchings from these isovector M1 excitations, and for sorting out the configurations responsible for them.

Most of the studies of collective magnetic dipole (or in the IBM language, mixed-symmetry) states have dealt with deformed nuclei having the SU(3) dynamical symmetry. Earlier, we had examined[29] the mixed-symmetry states in the O(6) nucleus ^{134}Ba where the lowest of these excitations are 2^+ rather than 1^+ states. In more recent measurements, we have been determining the lifetimes of these states.

c. (n,n'γ) Studies of Even-A Sn Isotopes (J.L. Weil, Z. Gacsi, and A.V. Ignatyuk)

Level Scheme: The first phase of the work on the extensive ^{116}Sn(n,n'γ) study has been completed. Based on our (n,n'γ) results and the (n,γ) results of S. Raman of ORNL, a complete level scheme for ^{116}Sn up to 4.0 MeV excitation has been constructed. The level scheme contains 101 levels up to 4.5 MeV, and over half of these have unique spin-parity assignments. In collaboration with K. Allaart of the Free University of Amsterdam,

[25] S.J. Freeman *et al.*, Phys. Lett. **222B**, 347 (1989).

[26] Bohle, Küchler, Richter and Steffen, Phys. Lett. **148B**, 260 (1984).

[27] C. Wesselborg *et al.* Phys. Lett. **207B**, 22 (1988).

[28] D. Frekers, *et al.*, Phys. Lett. **218B**, 439 (1989).

[29] Molnár, Gatenby and Yates, Phys. Rev. **C37**, 898 (1988).

we have compared these levels to the predictions of the two-broken pair model of Bonsignori and Allaart,[30] the Interacting Boson Model, and the deformed collective model.[31] In particular, nine new members of a proton quasi-rotational band structure[31] lying in three previously unobserved bands have been identified. In addition, several states have been phenomenologically identified as proton 1p-1h and collective quadrupole-octupole two-phonon excitations. It is concluded that all expected states of these models have been experimentally identified, and that no experimental states fall outside of these models, to a first approximation. It is on this basis that it is believed that a complete level scheme up to 4.0 MeV excitation has been established for ^{116}Sn.

In collaboration with J. Shriner, we have carried out a statistical analysis of the level spacings of these 101 states to investigate whether the distribution of spacings gives evidence for chaos in this quantum system.[32] The spacing distribution is found to be intermediate between that described by a Gaussian orthogonal ensemble and that which has a Poisson behavior, leaving us with no definitive answer regarding the chaotic properties of the system. Unfortunately, this seems to be typical of the evidence being found from such level spacing distributions. All this work, including the level scheme and the interpretation, was recently published by The Physical Review C.[33]

Level Densities: With a complete level scheme now available for ^{116}Sn, and newly determined information on the density of s-wave resonances at the neutron binding energy,[34] it is now possible to test whether generally accepted theories[35] are able to account successfully for the energy dependence of the level density of a given nucleus over a wide range of excitation. It was found that neither of the most commonly used level density formulas, the Fermi-gas model and the constant temperature approximation, were capable of simultaneously describing the level density of ^{116}Sn in the bound state region and in the neutron resonance region. When fitted to the density in one region, both models predicted a density in the other region which was incorrect by at least an order of magnitude. Both of these models are quite dated, and are based on rather simple physical assumptions, so this result is not too surprising.

In recent years a more sophisticated model of level density incorporating effects of pairing, collectivity, and shell structure has been put forward by Ignatyuk and coworkers.[36,37] Known as the Generalized Superfluid Model (GSM), it has enjoyed much success in explaining the energy dependence of level density over a wide energy range above the neutron binding energy. However, until the present time it has not been carefully tested for its applicability all the way down to the bound state region of excitation.

Dr. A. V. Ignatyuk, of the Physics and Energy Institute, Obninsk, USSR was invited to work with us on this problem and spent six weeks at our University in Lexington this fall applying his new model of level densities to the present ^{116}Sn data. The GSM was found to work very well in simultaneously describing the energy dependence of the level

[30]Bonsignori, Savoia, Allaart, van Egmond and Te Velde, Nucl. Phys. **A432**, 389, (1985).

[31]Wenes, van Isacker, Waroquier, Heyde, and van Maldegham, Phys. Rev. **C23**, 2291 (1981).

[32]Mitchell, Bilpuch, Endt and Shriner, Phys. Rev. Lett. **61**, 1473 (1988).

[33]Raman, Walkiewicz, Kahane, Jurney, Sa, Gácsi, Weil, Allaart, Bonsignori and Shriner, Phys. Rev. **C43**, 521 (1991).

[34]Timokhov, Bokhovko, Isakov, Kazakov, Kononov, Manturov, Poletaev and Pronyaev, Sov. J. Nucl. Phys. **50**, 375 (1989).

[35]A. Gilbert and A.G.W. Cameron, Can. J. Phys. **43**, 1446 (1965).

[36]A.V. Ignatyuk, *Statistical Properties of Excited Atomic Nuclei*, IAEA Report INDC(CCP)-233/L, (1985).

[37]Ignatyuk, Istekov and Smirenkin, Sov. J. Nucl. Phys. **29**, 450 (1979).

density over several MeV of excitation in the bound state region and the level density in the neutron resonance region. It does so with essentially only one free parameter, the other parameters being well determined by systematics of their values for many other nuclei. After some additional fine tuning, this work will be submitted for publication.

Lifetimes: The data reduction for the extraction of Doppler shifts from the (n,n'γ) angular distributions in ^{116}Sn was continued, and shifts for sixty γ-rays have been determined so far. From these shifts, the lifetimes of over 40 levels have been extracted. It is thought that with careful analysis, at least 10 more lifetimes can be determined. A preliminary report of this work was given at the Fall, 1990 Nuclear Division Meeting in Urbana-Champaign.

2. Projected Work in Nuclear Structure

a. Excitations in ^{140}Ce and ^{142}Ce (J.R. Vanhoy (U.S. Naval Academy), S.F. Hicks (U. of Dallas), S.W. Yates, and M.T. McEllistrem)

The initial experiments carried out with Sally Hicks, Jeffrey Vanhoy and University of Dallas students were very successful; however, because we had to use initially a natural isotopic abundance sample, we found some lifetimes for supposed collective M1 transitions in ^{142}Ce which appeared to be much slower than expected. It is not clear that we found the "scissors mode" states, or magnetic 2^+ excitations, but levels of the correct spins in the expected excitation energy region were discovered. However, the small abundance of ^{142}Ce made it difficult to achieve adequate accuracy. It is planned to return to lifetime measurements with an isotopically separated ^{142}Ce sample during the summer of 1991. We will also continue the study of the excitations of ^{140}Ce begun last summer, both with the natural sample and with the separated ^{140}Ce sample.

The advantage of working with both natural and enriched samples flows from the fact that the natural sample is a metal, while the isotopically enriched samples are Cerium dioxide powder. The effects of using compounds in powder form for lifetime measurements can be explored with the two types of sample, thus enabling us to have confident lifetimes when working only with the enriched powder oxide samples.

b. Collective Magnetic Dipole Modes (S.W. Yates, T. Belgya, E.L. Johnson, D. DiPrete and E.M. Baum)

As noted above, lifetimes of M1 collective excitations are expected to be well within the range that we can deal with using DSAM methods. Hence, the studies of magnetic 1^+ and 2^+ excitations in ^{164}Dy and ^{162}Dy will be continued. Several candidates for transitions have already been identified in the dysprosium nuclei; complications were expected and have been found because of the complex decay spectra from these nuclei. However, we expect to be able to complete several lifetime measurements.

The initial surveys looking for ground state transitions indicating 1^+ or 2^+ levels in ^{88}Sr have been successful in identifying several such levels with excitation energies near 4 MeV. The character of these levels will be the subject of intensive exploration during the next year. We will also be looking for M1, isoscalar modes near 8 to 9 MeV with the new 55% efficient Ge detector we have ordered for use in conjunction with our large BGO anti-Compton shield.

c. Gamma-ray Studies in ^{56}Fe and Other Sn Isotopes (J.L. Weil and students)

After completing some additional calculations with the Generalized Superfluid Model (GSM),[36,37] on the energy dependence of level densities in ^{116}Sn, we will submit a paper on these new results. Additional work on the lifetimes of the ^{116}Sn levels must be completed, and then a paper will be prepared describing the lifetime results, as well as the procedures used in determining the spin-parity assignments for this nucleus. As time permits, new level and lifetime results on ^{56}Fe will also prepared for publication. The next step in this program on the Sn isotopes will be to complete the investigation of the collective states observed in the nucleus ^{124}Sn. Following that, the analysis of a large data set on ^{120}Sn(n,n'γ) will be completed.

C. NUCLEAR ASTROPHYSICS

1. Mass Differences for Possible Solar Neutrino Detection Reactions (M.T. McEllistrem, J.R. Vanhoy (U.S. Naval Academy), K. Williams, and O. Gruter (University of London))

The possible use of either ^{81}Br or ^{127}I as targets for solar neutrino detection makes it useful to know, within $\leq$ 1 keV, the mass difference between ^{81}Br and ^{81}Kr and also that between ^{127}I and ^{127}Xe. The mass difference determination for the former reaction is nearly complete; the results should be available within a few months. These mass differences are being determined through analysis of the energy releases in the ^{81}Br(p,n)^{81}Kr and the ^{127}I(p,n)^{127}Xe reactions.

Another planned study deals with the structural properties of low-lying levels of ^{127}Xe which could participate in solar neutrino capture. This part of the solar neutrino detection reaction project calls for measuring and analyzing the ^{127}I(p,nγ)^{127}Xe angular correlations. Preliminary measurements have been made for this reaction, showing that the study is quite feasible. However, long experimental runs are necessary to accumulate adequate statistics in order to have good correlation information. This study will be pursued during the coming year, since feasibility tests were successful.

D. OPTICAL POTENTIAL STUDIES

1. Proton Induced Reactions in A=40-70 Nuclei (C.E. Laird, Q. Shen, S. Arole, S. Rucker, B. Rose, M. Hackworth and P. Esterle)

This project is a study of the systematic behavior of proton-induced nuclear reactions in the mass 40 to 70 region, and of the interpretation of these reactions using the optical potential. It involves the collection and analysis of data on reaction and scattering experiments on fifteen or more nuclei. Analysis of data taken last year was continued, resulting in the calculation of cross sections for (p,n), elastic and inelastic scattering, and radiative capture reactions on ^{52}Cr, ^{63}Cu and ^{65}Cu targets. A paper on proton-induced reactions on ^{52}Cr was presented at the Fall Meeting of the Nuclear Physics Division of the APS.

Recent measurements have been made on ^{46,47,49,50}Ti and ^{62}Ni targets. The data collection on the ^{62}Ni target for the four reactions given above is complete and is currently being analyzed. The (p,n) data for the titanium targets for energies below 7 MeV is sufficiently complete for initial analysis. This analysis involves separating the contributions from the (p,n) reactions of contaminating Ti isotopes present at levels of a few percent. This separation should be completed soon. In addition to the (p,n) data on the titanium targets, proton elastic scattering data was taken on ^{47}Ti along with initial γ-ray data for inelastic scattering and radiative capture. The data collection on all titanium targets for all reactions studied should be completed during the summer of 1991.

A. NUCLEAR DATA EVALUATION (E. Browne, R.B. Firestone, A.O. Macchiavelli, V.S. Shirley, and C.M. Baglin)

The LBL Isotopes Project has permanent responsibility for evaluating 33 mass chains with $89 \leq A \leq 93$ and $167 \leq A \leq 194$; temporary responsibility for 8 mass chains with A=59, 81, 83, 210, 215, 219, 223 and 227; and is responsible for converting $33 \leq A \leq 44$ to ENSDF format. Evaluation of mass chains A=90 and A=177 have been temporarily reassigned to Sweden and Japan, respectively. A summary of the current evaluation status of LBL mass chains is given in the following table.

The Isotopes Project contributed approximately 2.5 full-time equivalent (FTE) effort into mass-chain evaluation in 1990. This includes Dr. C.M. Baglin who evaluates for LBL from her residence in Morgan Hill, Ca. The group has achieved a stable production rate of more than 2.5 mass-chain evaluations per FTE/year. Nine evaluations (compared to seven produced last year) were completed in 1990. One LBL evaluator, Virginia Shirley, spent a year at the Free University of Berlin, between October 1989 and September, 1990 where she continued evaluating mass chains for the Isotopes Project while on professional leave.

B. ISOTOPES PROJECT PUBLICATIONS

1. Table of Isotopes, 8th Edition (R.B. Firestone)

The computer codes for generating the tabular and graphical presentations for the Table of Isotopes are nearly completed. Attached is a sample mass chain for A=237, reduced to 80%. The sample was computer generated from the Evaluated Nuclear Structure Data File (ENSDF). The skeleton decay scheme drawing is very similar to the style of the 7th edition. Complete tables of levels, their properties (energy, J^π, half-life, moments, and cross-references to reactions and decay), and deexcitation transition data (energies, intensity branching ratios, and multipolarities) are presented for each nucleus. Additional tables of radiations and their intensities are included for all radioactive decays. Combined decay scheme drawings, similar to those in the 7th edition, and rotational band drawings are also presented.

2. Electronic Table of Isotopes (R.B. Firestone)

Before the Table of Isotopes is published, advanced copies of the book will become available electronically. The sample shown in this report was generated from a POSTSCRIPT command file on a laserprinter. As mass chains are processed, they will become available by E-mail. Additional information on how to access this information will be available later this year. Future plans include regularly updating the electronic file as new ENSDF publications appear and periodic updated publication of the book.

Status of LBL Mass-Chain Assignments		
Mass Chain	Publication Year	Status
33-44[a]	1978	Sent to BNL 1987 (LBL)
59[bc]	1983	Published (Sweden)
81[c]	1985	(Germany)
83[c]	1986	(Germany)
89	1989	Published (Germany)
90[b]	1975	(Sweden)
91	1990	Published (Germany)
92	1980	Submitted 1990 (LBL)
93	1988	Published (Germany)
167	1989	Published (LBL)
168	1988	Published (LBL)
169	1982	Submitted 1990 (LBL)
170	1987	Published (China)
171[b]	1984	Published (LBL)
172	1987	Published (China)
173	1988	Published (LBL)
174	1991	Published (LBL)
175	1976	Submitted 1990 (LBL)
176	1990	Published (LBL)
177	1975	(Japan)
178	1988	Published (LBL)
179	1988	Published (LBL)
180	1987	Published (LBL)
181	1991	Published (LBL)
182	1988	Published (LBL)
183	1987	Submitted 1990 (LBL)
184	1989	Published (LBL)
185	1989	Published (LBL)
186	1988	Published (LBL)
187	1991	Published (LBL)
188	1990	Published (LBL)
189	1990	Published (LBL)
190	1990	Published (LBL)
191	1989	Published (LBL)
192	1983	Submitted 1991 (LBL)
193	1990	Published (LBL)
194	1989	Published (LBL)
210[bc]	1981	Published ORNL
215[c]	1977	Submitted 1990 (LBL)
219[c]	1977	Submitted 1990 (LBL)
223[c]	1977	Submitted 1990 (LBL)
227[c]	1977	Submitted 1990 (LBL)

[a] A=33-44 was published in 1990 and will be entered into ENSDF in 1991.
[b] To be evaluated in 1991.
[c] Temporary assignment

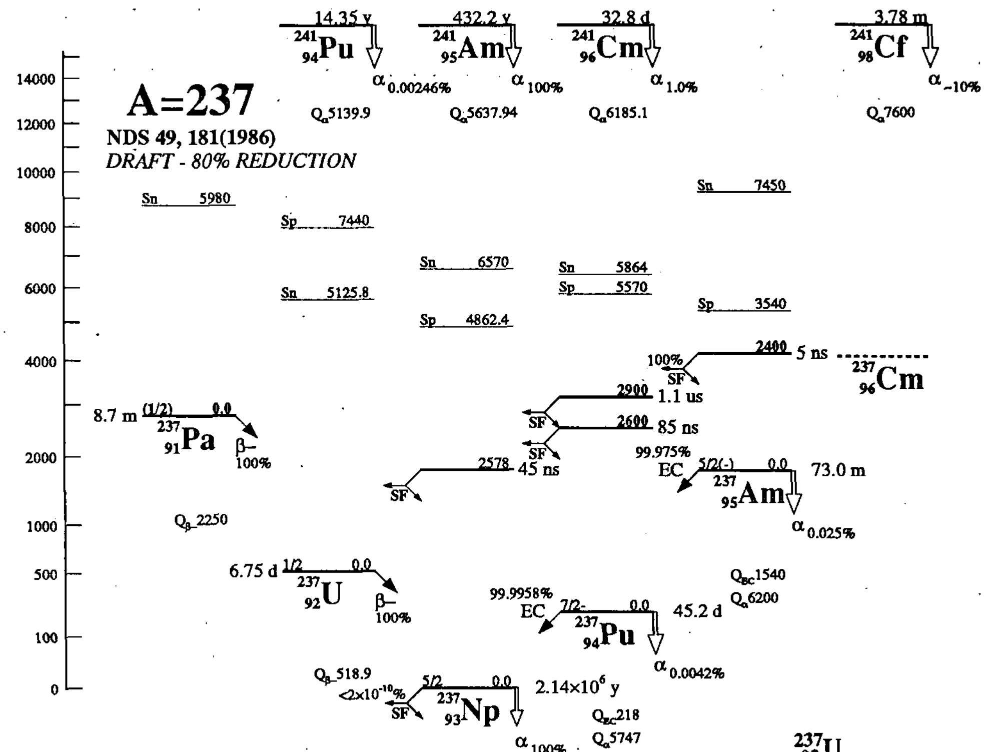

$^{237}_{92}$U

$^{237}_{91}$Pa

Q$_\alpha$4957.5

Reactions and References

238U(T,A) E=15 MEV 77TH04

Adopted levels and γ rays:

0.0, (1/2$^+$), 8.7 m 2, %β^-=100
35 2, (3/2$^+$)
90 3, (3/2$^-$)
105 5, (9/2$^+$)
147 6, (7/2$^-$)
158 6, (13/2$^+$)
202 6
258 4
319 4
364 4, (3/2$^+$)
393 6, (5/2$^+$)
491 4
554 8
577 8
624 4
686 8
714 8
741 8
972 8
1025 6
1112 4

γ(^{237}U) ^{237}Pa(0.0) β^- decay, 8.7 m<*norm: 0.34 3*> *45.0 5*, *179.1 2* (†$_\gamma$0.5 1), *310.1 2* (†$_\gamma$5.1 7), *498.7 2* (†$_\gamma$7.1 9), *529.4 2* (†$_\gamma$43.6 44), *540.7 2* (†$_\gamma$27.3 27), *543.6 5* (†$_\gamma$0.7 3), *554.9 2* (†$_\gamma$4.5 5), *701.0 5* (†$_\gamma$0.4 2), *722.6 2* (†$_\gamma$2.4 4), *734.0 2* (†$_\gamma$1.9 4), *847.1 5* (†$_\gamma$1.5 5), *853.7 2* (†$_\gamma$100), *865.0 2* (†$_\gamma$45.6 46), *1333.2 5* (†$_\gamma$0.50 25), *1344.8 5* (†$_\gamma$0.30 15), *1395.9 5* (†$_\gamma$0.50 25), *1407.5 5* (†$_\gamma$0.30 15).

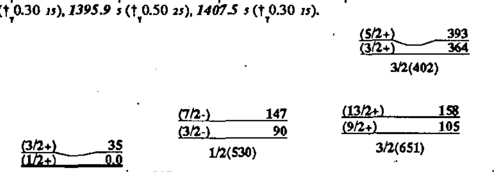

$^{237}_{91}$Pa Rotational Bands

Reactions and References

A 237PA B- DECAY
B 241PU A DECAY
C 236U(N,G) RES:PRIMARY 79VO05
D 236U(N,G) RES:SECONDARY G'S 79VO05
E 236U(D,P) E=11.96 MEV 65BR22
F 238U(D,T) 70BO31,72ER03
G 238U(3HE,A) E=30 MEV 70VO03

Adopted levels and γ rays:

0.0, 1/2$^+$, 6.75 d 1, *[ABCDEF]*, %β^-=100
11.39 2, 3/2$^+$, *[ABCDEFG]* γ_0*11.39* 2 (†$_\gamma$100)
56.30 4, 5/2$^+$, *[ABCDF]* γ_{11}*44.86* 10 (†$_\gamma$33 4) γ_0*56.32* 10 (†$_\gamma$100 7)
82.86 6, 7/2$^+$, *[BDEFG]* γ_{56}*26.6* γ_{11}*71.6* 2 (†$_\gamma$100)
159.96 2, 5/2$^+$, 3.1 ns 1, *[BCDF]* γ_{83}*77.10* 10 (†$_\gamma$11.4 4) γ_{56}*103.680* 5 (†$_\gamma$54.8 7) γ_{11}*148.567* 10 (†$_\gamma$100 2) γ_0*159.955* 20 (†$_\gamma$3.53 8)
163 2, 9/2$^+$, *[EFG]*
204.19 9, 7/2$^+$, *[BDF]* γ_{160}*44.20* 10 (†$_\gamma$100 4) M1+E2 γ_{83}*121.2* 2 (†$_\gamma$16.5 18)
205 4, 11/2$^+$, *[FG]*
260.95 14, 9/2$^+$, *[BEFG]* γ_{204}*56.76* 10 (†$_\gamma$100)
274.0 10, (7/2)$^-$, 155 ns 6, *[B]* γ_{160}*114.0* 10 (†$_\gamma$100) E1
316 5, (9/2$^-$), *[B]*
327 3, 11/2$^+$, *[BG]*
367 3, (11/2$^-$), *[BFG]*
426.15 6, (7/2$^+$), *[D]* γ_{160}*266.17* 6 (†$_\gamma$100)
432 10, *[G]*
482 1, (9/2$^+$), *[EF]*
506 2, (15/2$^-$), *[FG]*
530 4, *[F]*
540.62 5, 1/2$^-$, *[ACDF]* γ_{11}*529.26* 5 (†$_\gamma$100 7) γ_0*540.61* 5 (†$_\gamma$62 5)
551 2, (11/2$^+$), *[EG]*
554.98 6, 3/2$^-$, *[ACD]* γ_{56}*498.62* 5 (†$_\gamma$100 8) γ_{11}*543.68* 6 (†$_\gamma$12.5 11) γ_0*555.02* 9 (†$_\gamma$95 9)
578.01 6, (5/2$^-$), *[DF]* γ_{83}*495.09* 6 (†$_\gamma$80 7) γ_{56}*521.53* 11 (†$_\gamma$6.8 14) γ_{11}*566.65* 6 (†$_\gamma$100 8)
632 3, (13/2$^+$), *[G]*
657 3, *[E]*
664.27 20, 3/2$^+$, *[CDF]* γ_{160}*504.32* 10 (†$_\gamma$24 4) γ_{83}*581.90* 20 (†$_\gamma$28 6) γ_{11}*652.87* 6 (†$_\gamma$100 8) γ_0*664.21* 6 (†$_\gamma$<170)

666.45 10, $(5/2^{+})$, [CD] γ_{56}610.29 11 ($\dagger_{\gamma}$28 5) γ_{11}654.80 20 ($\dagger_{\gamma}$16 5) γ_{0}666.41 9 ($\dagger_{\gamma}$100 12)
677.59 10, $3/2^{+},5/2^{+}$, [CD] γ_{426}251.20 20 ($\dagger_{\gamma}$14 6) γ_{204}473.42 7 ($\dagger_{\gamma}$81 9) γ_{160}517.50 10 ($\dagger_{\gamma}$53 9) γ_{83}594.60 20 ($\dagger_{\gamma}$58 14) γ_{56}621.37 7 ($\dagger_{\gamma}$100 12)
688 2, [G]
697.65 6, $(5/2^{+})$, [CDE(*)F] γ_{160}537.61 9 ($\dagger_{\gamma}$27 4) γ_{83}614.86 10 ($\dagger_{\gamma}$32 5) γ_{56}641.34 6 ($\dagger_{\gamma}$84 8) γ_{11}686.29 8 ($\dagger_{\gamma}$100 10)
698 2, [E(*)]
718 6, []
720.45 10, $3/2^{-}$, [CDG] γ_{56}664.21 ($\dagger_{\gamma}$<592) γ_{11}709.06 12 ($\dagger_{\gamma}$100 17) γ_{0}720.44 12 ($\dagger_{\gamma}$68 11)
734.34 10, $(1/2^{-})$, [ACD] γ_{555}179.5 3 ($\dagger_{\gamma}$32 9) γ_{11}722.88 6 ($\dagger_{\gamma}$100 9) γ_{0}734.42 7 ($\dagger_{\gamma}$68 7)
758.16 6, $(3/2^{-})$, [CD] γ_{56}701.87 6 ($\dagger_{\gamma}$100 9) γ_{11}746.80 20 ($\dagger_{\gamma}$14 4) γ_{0}758.15 6 ($\dagger_{\gamma}$68 6)
798 2, $(9/2^{+})$, [FG]
832.45 14, $(5/2^{+})$, [CD] γ_{160}672.51 6 ($\dagger_{\gamma}$100 9) γ_{11}820.4 3 ($\dagger_{\gamma}$33 9)
846.94 15, $(1/2^{+})$, [CDE(*)] γ_{160}687.5 3 ($\dagger_{\gamma}$11 5) γ_{0}846.89 9 ($\dagger_{\gamma}$100 8)
848 1, $(11/2^{+})$, [E(*)G]
865.0 2, $1/2^{-}$, [ACDE(*)FG] γ_{555}310.2 2 ($\dagger_{\gamma}$5.1 7) γ_{11}853.6 2 ($\dagger_{\gamma}$100 9) γ_{0}865.1 2 ($\dagger_{\gamma}$46 5)
866 3, [E(*)]

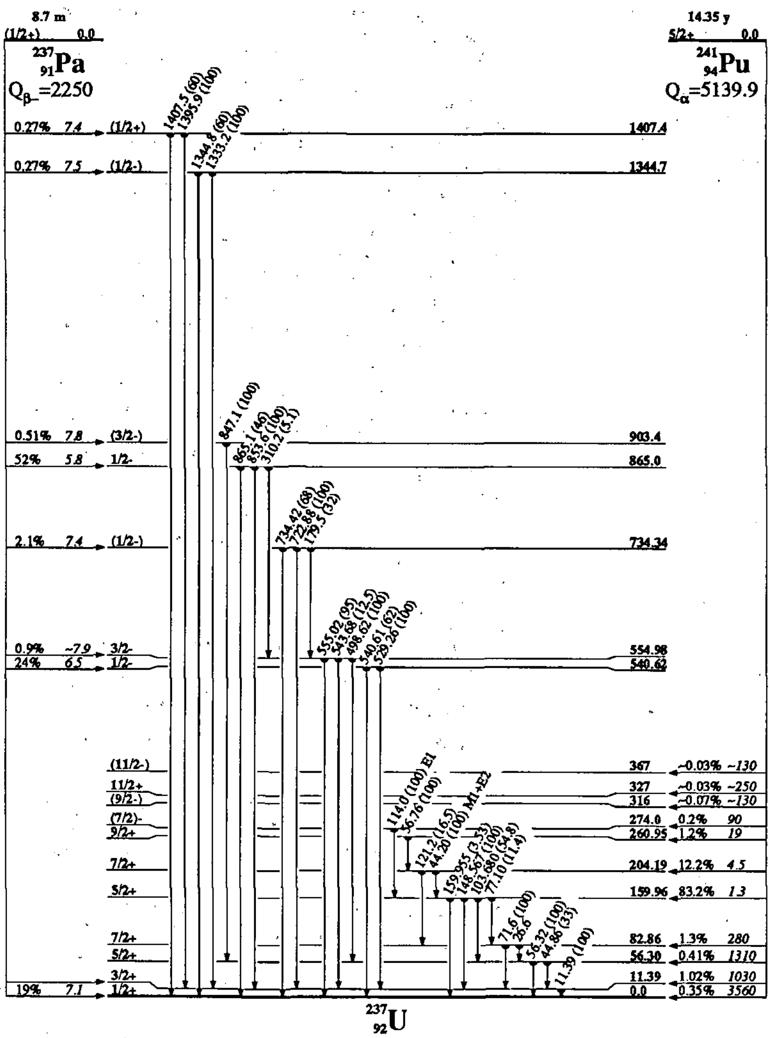

872.15 14, $(3/2^{+})$, [CD] γ_{555}317.14 ($\dagger_{\gamma}$<12) γ_{541}331.2 3 ($\dagger_{\gamma}$6 4) γ_{205}667.5 3 ($\dagger_{\gamma}$17 7) γ_{160}712.10 20 ($\dagger_{\gamma}$15 4) γ_{56}815.95 9 ($\dagger_{\gamma}$100)
893.43 20, $(5/2^{+})$, [CDE] γ_{56}837.14 14 ($\dagger_{\gamma}$100 18) γ_{11}882.00 20 ($\dagger_{\gamma}$87 15)
903.4 5, $(3/2^{-})$, [A] γ_{56}847.1 5 ($\dagger_{\gamma}$100)
905.7 2, $(1/2^{+})$, [CD] γ_{56}849.45 13 ($\dagger_{\gamma}$49 8) γ_{11}894.14 10 ($\dagger_{\gamma}$100 10) γ_{0}906.01 12 ($\dagger_{\gamma}$87 12)
909.4 3, $(1/2^{-},3/2^{-})$, [CDF] γ_{0}909.34
911 4, $(5/2^{-})$, [G]
920.6 2, $(3/2^{+})$, [CD] γ_{56}864.00 20 ($\dagger_{\gamma}$100 18) γ_{11}909.34 11 ($\dagger_{\gamma}$<107)
946 2, $(9/2^{+})$, [FG]
947.85 20, $(5/2^{+})$, [CD] γ_{664}283.40 γ_{426}521.53 γ_{83}865.1 γ_{11}936.40 20 ($\dagger_{\gamma}$90 17) γ_{0}947.97 14 ($\dagger_{\gamma}$100 20)
952 2, [E]
971 2, [G]
981.26 10, $(3/2^{+})$, [CDE(*)] γ_{698}283.40 20 ($\dagger_{\gamma}$10 4) γ_{664}317.14 12 ($\dagger_{\gamma}$25 5) γ_{578}403.16 7 ($\dagger_{\gamma}$38 4) γ_{555}426.33 8 ($\dagger_{\gamma}$51 7) γ_{541}440.69 6 ($\dagger_{\gamma}$100 9)
984 4, [(*)F]
987 3, [E]
1013 4, [F]
1033 2, [C]
1040 1, $(11/2^{+})$, [G]
1050.0 10, $(1/2^{+},3/2^{+})$, [CE]
1068 2, $(1/2^{+},3/2^{+})$, [C]
1078 1, $(1/2^{+},3/2^{+},5/2^{+})$, [C]
1085.0 10, $(1/2^{+},3/2^{+})$, [CE]
1094.7 10, $(5/2^{+})$, [C]
1108.8 3, $(1/2^{-},3/2^{-})$, [C]
1110 2, [EF(*)]
1112 3, [F(*)]
1122.8 3, $(1/2^{-},3/2^{-})$, [C]
1126 2, [E]
1128.0 10, $(5/2^{+})$, [C]
1140 3, $(13/2^{+})$, [G]
1155 3, [F]
1162 2, [E]
1175.3 3, $(1/2^{-},3/2^{-})$, [C]
1183.0 3, $(1/2^{+},3/2^{+})$, [C]
1189 3, [F(*)G]
1192 2, [EF(*)]
1201 1, $(1/2^{-},3/2^{-})$, [C]
1208 4, [F]
1215 2, [C]
1229 1, $(1/2^{+},3/2^{+})$, [C]
1235 3, [E]
1247 3, [F]
1259 2, $(15/2^{-})$, [G]
1268 2, $(1/2^{+},3/2^{+},5/2^{+})$, [C]
1287 1, $(1/2^{+},3/2^{+})$, [C]
1299 3, [G(*)]
1301 2, [CG(*)]
1344.7 5, $(1/2^{-})$, [AC] γ_{11}1333.2 5 ($\dagger_{\gamma}$100 50) γ_{0}1344.8 5 ($\dagger_{\gamma}$60 30)
1372 3, [E]
1375 3, [F]
1380.4 10, $(1/2^{+},3/2^{+})$, [C]
1407.4 5, $(1/2^{+})$, [AC] γ_{11}1395.9 5 ($\dagger_{\gamma}$100 50) γ_{0}1407.5 5 ($\dagger_{\gamma}$60 30)
1424.0 10, $(1/2^{-},3/2^{-})$, [C]

1441 2, [C]	1738 2, [C]	2061 2, [C]
1485 2, [C]	1741 4, [F]	2063 2, [C]
1488 2, [C]	1755 2, [C]	2069 2, [C]
1493 2, [C]	1757 2, [C]	2076 2, [C]
1508 2, [C]	1760 2, [C]	2079 2, [C]
1527 2, [C]	1798 2, [C]	2092 2, [C]
1531 2, [G]	1803 2, [C]	2101 2, [C]
1550 2, [C]	1823 2, [C]	2108 2, [C]
1561 3, [G(*)]	1838 2, [C]	2133 2, [C]
1563 2, [CG(*)]	1849 2, [G]	2136 2, [C]
1567 2, [C]	1864 2, [C]	2139 2, [C]
1579 2, [C]	1873 2, [C]	2148 2, [C]
1583 3, [F]	1883 2, [C]	2154 2, [C]
1588 2, [C]	1888 2, [G]	2171 2, [C]
1605 3, [G]	1889 2, [C]	2176 2, [C]
1612 3, [F]	1896 2, [C]	2211 2, [C]
1622 2, [C]	1900 2, [C]	2221 2, [C]
1634 2, [C]	1915 2, [C]	2226 2, [C]
1647 2, [C]	1929 2, [C]	2237 2, [C]
1651 2, [C]	1940 2, [C]	2244 2, [C]
1659 2, [C]	1955 2, [C]	2255 2, [C]
1667 2, [C]	1961 2, [C]	2263 2, [C]
1694 2, [C]	1962 2, [C]	2274 2, [C]
1696 2, [C]	1968 2, [C]	2282 2, [C]
1698 2, [C]	1977 2, [C]	2297 2, [C]
1712 2, [C]	1990 2, [C]	2308 2, [C]
1717 4, [F]	1999 2, [C]	
1719 2, [C]	2004 2, [C]	
1727 2, [C]	2039 2, [C]	
1733 2, [C]	2057 2, [C]	

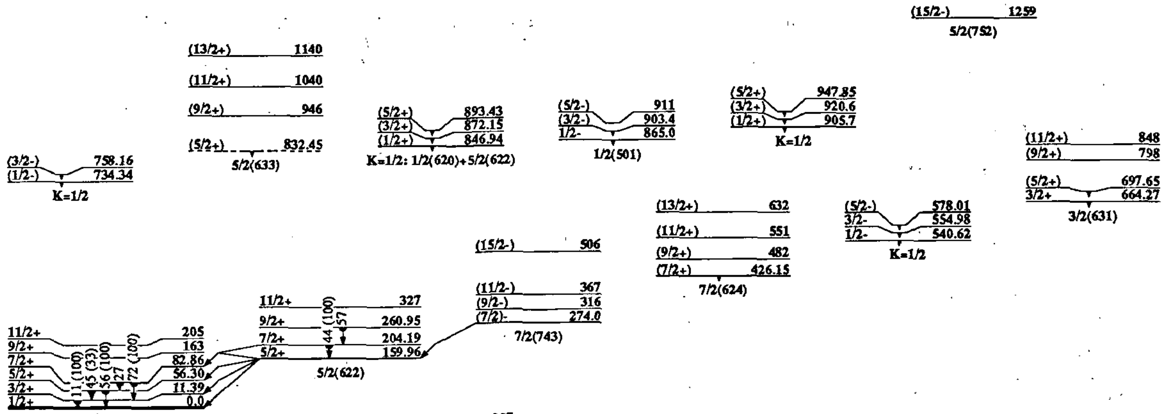

$^{237}_{92}$U Rotational Bands

$^{237}_{92}$U (Continued)

γ(^{237}Np) ^{237}U(0.0) β$^-$ decay, 6.75 d<norm: 1.0>2.3, 13.81 2 (†$_\gamma$0.099 4) M1+E2 δ=0.0321 10, 26.348 10 (†$_\gamma$2.43 6) E1, 33.195 11 (†$_\gamma$0.130 5) M1+E2 δ=0.13 3, 38.54 3 (†$_\gamma$0.4) (M1+E2), 42.73 5, 43.423 20 (†$_\gamma$0.0240 20) M1+E2 δ=0.41 2, 51.01 3 (†$_\gamma$0.340 10) E1, 59.536 3 (†$_\gamma$34.5 7) E1, 64.83 2 (†$_\gamma$1.28 2) E1, 69.76 3 (†$_\gamma$0.00095 19) (E1), 75.8 2, 102.98 2 (†$_\gamma$0.0064 9) E1, 114.09 5, 164.61 2 (†$_\gamma$1.852 18) E2, 208.000 10 (†$_\gamma$21.14 23) M1+E2 δ=+0.156 5, 221.80 4 (†$_\gamma$0.0212 7) E2, 234.40 4 (†$_\gamma$0.0205 7) M2, 267.54 4 (†$_\gamma$0.710 20) E1+M2 δ=0.490 15, 292.7 1 (†$_\gamma$0.0025 7), 309.1 (†$_\gamma$0.00027), 332.36 4 (†$_\gamma$1.195 20) E2, 335.38 4 (†$_\gamma$0.095 2) M1+E2 δ=0.46 17, 337.7 2 (†$_\gamma$0.0089 5) (E2), 340.45 (†$_\gamma$0.00165 33), 368.59 4 (†$_\gamma$0.040 2) M1(+E2) δ<0.31, 370.94 4 (†$_\gamma$0.107 2) M1+E2 δ=0.43$^{+47}_{-21}$.

$^{237}_{93}$Np

Reactions and References

A 237U B- DECAY
B 237PU EC DECAY
C 241AM A DECAY
D 236U(3HE,D), 236U(A,T) 70EL02
E 237NP(D,D') E=16 MEV 76TH01
F COULOMB EXCITATION

Adopted levels and γ rays:

0.0, 5/2$^+$, 2.14×10^6 y 1, [ABCEF], %α=100, %sf≤2×10^{-10}, μ=+2.5 3, Q=+4.1 7
33.192 2, 7/2$^+$, 54 ps 24, [ABCDEF] $\gamma_0$33.195 11 (†$_\gamma$100) M1+E2 δ=0.13 3
59.537 1, 5/2$^-$, 67 ns 2, [ABC], μ=+1.34 12, Q=+4.1 7 γ_{33}26.345 1 (†$_\gamma$6.71 14) E1 $\gamma_0$59.537 1 (†$_\gamma$100) E1
75.89 5, 9/2$^+$, ~56 ps, [ABCDEF] γ_{33}42.73 5 (†$_\gamma$100 15) $\gamma_0$75.8 2 (†$_\gamma$~11)
102.96 2, 7/2$^-$, 80 ps 40, [ABCD] γ_{76}27.03 γ_{60}43.423 10 (†$_\gamma$100 11) M1+E2 δ=0.41 2 γ_{33}69.76 5 (†$_\gamma$4.0 6) (E1) $\gamma_0$102.98 2 (†$_\gamma$26.7 2) E1
130.00 6, 11/2$^+$, [CDEF] γ_{33}96.7 (†$_\gamma$100)
158.51 2, 9/2$^-$, [BCDE] γ_{103}55.56 2 (†$_\gamma$89 9) M1+E2 δ=0.46 4 γ_{60}98.97 2 (†$_\gamma$100 2) E2 γ_{33}125.30 2 (†$_\gamma$20.1 2)
191.5 2, 13/2$^+$, [CDEF] γ_{76}115.5 1 (†$_\gamma$100)
225.96 5, 11/2$^-$, [CE] γ_{159}67.45 5 (†$_\gamma$42 10) (M1+E2) δ=0.46 12 γ_{103}123.01 2 (†$_\gamma$100 1) E2 γ_{76}150.04 5 (†$_\gamma$7.40 15)
267.54 2, 3/2$^-$, 5.2 ns 2, [ACD] γ_{103}164.61 2 (†$_\gamma$8.6 2) E2 γ_{60}208.00 1 (†$_\gamma$100 1) M1+E2 δ=+0.156 5 γ_{33}234.40 4 (†$_\gamma$0.097 10) M2 $\gamma_0$267.54 4 (†$_\gamma$3.36 10) E1+M2 δ=0.490 15
269.9, 15/2$^+$, [EF] γ_{130}139.9 (†$_\gamma$100)
281.35 2, 1/2$^-$, [AC] γ_{268}13.81 2 (†$_\gamma$21.4 8) M1+E2 δ=0.0321 10 γ_{60}221.80 4 (†$_\gamma$100 4) E2
305.06 4, 13/2$^-$, [C] γ_{159}146.55 3 (†$_\gamma$100 2) E2 γ_{130}175.07 4 (†$_\gamma$3.9 3)
316.8 2, [C] $\gamma_0$316.8 2
324.42 5, (7/2$^-$), [CDE] γ_{159}165.81 6 (†$_\gamma$54.7 24) γ_{103}221.46 3 (†$_\gamma$100 2) γ_{76}249.00 15 (†$_\gamma$1.3) γ_{60}264.89 6 (†$_\gamma$21.2 10) γ_{33}291.30 20 (†$_\gamma$7.3 8)
332.36 5, 1/2$^+$, <1.0 ns, [AC] γ_{281}51.01 5 (†$_\gamma$93.4 16) E1 γ_{268}64.83 2 (†$_\gamma$100 2) E1 $\gamma_0$332.36 4 (†$_\gamma$26.6 8) E2
348.5, 17/2$^+$, [DEF] γ_{191}157.0 (†$_\gamma$100)
359.7 1, (5/2$^-$), [C] γ_{60}300.13 6
368.59 3, 5/2$^+$, [ACD] γ_{76}292.77 6 (†$_\gamma$2.86 11) γ_{60}309.1 3 (†$_\gamma$0.28) γ_{33}335.38 3 (†$_\gamma$100 1) M1+E2 δ=0.46 17 $\gamma_0$368.59 4 (†$_\gamma$43.7 2)
370.93 3, 3/2$^+$, [AC] γ_{332}38.54 3 (M1+E2) γ_{33}337.7 2 (†$_\gamma$8.3 5) (E2) $\gamma_0$370.94 3 (†$_\gamma$100 1) M1+E2 δ=0.43$^{+47}_{-21}$
395.52 5, 15/2$^-$, [C] γ_{226}169.56 3 (†$_\gamma$100 2) E2 γ_{191}204.06 6 (†$_\gamma$1.68 11)
434.12 10, (11/2$^-$), [CD] γ_{324}109.70 7 (†$_\gamma$74) γ_{305}129.2 γ_{159}275.77 8 (†$_\gamma$100 7) γ_{130}304.21 20 (†$_\gamma$15 4) γ_{76}358.25 20 (†$_\gamma$18 4)
452.53 4, 9/2$^+$, [CE] γ_{191}260.80 15 (†$_\gamma$0.87 14) γ_{130}322.52 3 (†$_\gamma$110 1) (M1+E2) δ~0.6 γ_{76}376.65 3 (†$_\gamma$100 1) (M1) γ_{33}419.33 4 (†$_\gamma$20.8 5) $\gamma_0$452.6 2 (†$_\gamma$1.74 18)
454.4, 19/2$^+$, [F] γ_{270}184.5
459.68 5, 7/2$^+$, [C] γ_{324}135.3 γ_{76}383.81 3 (†$_\gamma$100 2) γ_{33}426.47 4 (†$_\gamma$87.2 18) $\gamma_0$459.68 (†$_\gamma$12.8 11)
486.0 2, (9/2$^-$), [CD] γ_{324}161.54 10 (†$_\gamma$100) γ_{226}260.8
497.0 1, 17/2$^-$, [C] γ_{305}191.96 4 (†$_\gamma$100)
514.20 10, (3/2$^-$), [CDE] γ_{360}154.27 20 (†$_\gamma$11.7) γ_{281}232.81 5 (†$_\gamma$100 7) γ_{268}246.73 10 (†$_\gamma$52 7) γ_{60}454.66 8 (†$_\gamma$211 7) $\gamma_0$514.0 5 (†$_\gamma$57 7)
545.6 2, (5/2$^-$), [CDE] γ_{281}264.89 γ_{268}278.04 15 (†$_\gamma$38) γ_{33}512.5 3 (†$_\gamma$100 20) $\gamma_0$545.4 5 (†$_\gamma$64)
546.9, 21/2$^+$, [F] γ_{348}198.5
590.3 2, (7/2$^-$), [CDE] γ_{268}322.52 γ_{103}487.3 3 (†$_\gamma$15.4) $\gamma_0$590.28 15 (†$_\gamma$100 7)
592.5 10, 13/2$^+$, [C] γ_{453}139.44 8 (†$_\gamma$100 21) γ_{434}159.26 20 (†$_\gamma$26 10) γ_{396}197.0 2 (†$_\gamma$9.2) γ_{191}401.3 30 (†$_\gamma$9.2) γ_{130}463.22 20 (†$_\gamma$19)
598.0 2, 11/2$^+$, [C] γ_{460}138.5 γ_{192}406.35 15 (†$_\gamma$50 8) γ_{130}468.12 15 (†$_\gamma$100 8) γ_{76}522.06 15 (†$_\gamma$31 11)
618 2, [E]
646.1 2, (9/2$^-$), [CE] γ_{159}487.3 γ_{60}586.59 20 (†$_\gamma$100)
666.2 2, (5/2$^+$,7/2$^-$), [CE] γ_{268}398.64 15 (†$_\gamma$160) γ_{76}590.28 γ_{33}632.93 15 (†$_\gamma$100) $\gamma_0$666.5 5 (†$_\gamma$39)
684.4, 23/2$^+$, [F] γ_{547}137.6 γ_{454}230.0
709 5, (11/2$^-$), [DE]
721.94 4, 5/2$^-$, [CE] γ_{268}454.66 γ_{159}563.05 30 (†$_\gamma$0.20) γ_{103}619.01 2 (†$_\gamma$16.3 2) γ_{60}662.40 2 (†$_\gamma$100 1) (E0+M1+E2) γ_{33}688.72 4 (†$_\gamma$8.9 2) $\gamma_0$722.01 3 (†$_\gamma$53.8 3)
755.98 10, 7/2$^-$, [CE] γ_{159}597.48 8 (†$_\gamma$19.7 8) γ_{103}653.02 4 (†$_\gamma$100 5) γ_{76}680.10 10 (†$_\gamma$8.3 5) γ_{60}696.60 5 (†$_\gamma$14.2 5) γ_{33}722.01 $\gamma_0$755.90 5 (†$_\gamma$20.2 7)
758 6, [D]
770.57 10, [CE] γ_{324}446.43 15 (†$_\gamma$6.1 2) γ_{33}737.34 5 (†$_\gamma$100 5) $\gamma_0$770.57 10 (†$_\gamma$59 5)
787.0, 25/2$^+$, [F] γ_{547}240.1
800.0 1, 9/2$^-$, [CE] γ_{226}573.94 20 (†$_\gamma$18 5) γ_{159}641.47 5 (†$_\gamma$100 5) γ_{130}669.83 20 (†$_\gamma$5.4 17) γ_{103}696.6 γ_{33}767.00 10 (†$_\gamma$70.4 22)
805.8 2, (7/2$^+$,9/2$^+$), [C] γ_{130}676.03 30 (†$_\gamma$24 5) γ_{76}729.72 15 (†$_\gamma$50 6) γ_{33}772.4 3 (†$_\gamma$100 6) $\gamma_0$806.26 30 (†$_\gamma$11.7)
823 3, [E]
853.36 21, 11/2$^-$, [CE] γ_{324}529.17 20 (†$_\gamma$82) γ_{226}627.18 20 (†$_\gamma$100 31)
861.7 5, [CE] γ_{76}786.00 15 (†$_\gamma$46) γ_{60}801.94 20 (†$_\gamma$100) γ_{33}828.5 (†$_\gamma$18 5) $\gamma_0$862.7 5 (†$_\gamma$39 5)
906 2, [E]
914 4, [D]

$^{237}_{93}$Np (Continued)

920.9 *5*, [CE] γ860.7 *5* (†γ 37 *12*) γ887.3 *3* (†γ 100 *23*) γ921.5 *3* (†γ 86 *19*)
946 *2*, [E]
959.5, 27/2+, [D(*)F] γ172.6 γ275.1
961 *3*, [D(*)(*)]
963 *2*, [D(*)E]
984 *2*, [E]
1013 *3*, [E]
1020 *3*, [D]
1030 *3*, [E]
1040 *4*, [DE]
1066 *3*, [D(*)E(*)]
1068.2, 29/2+, [(*)E(*)F] γ281.2
1072 *6*, [D]
1112 *4*, [D]
1278.6, 31/2+, [F] γ210.5 γ319
1389, 33/2+, [F] γ321
1639, 35/2+, [F] γ249.4 γ361
1749, 37/2+, [F] γ360
2041, 39/2+, [F] γ292.7 γ401.1
2146, 41/2+, [F] γ396.9
2480, 43/2+, [F] γ334.8 γ439.0
2578, 45/2+, [F] γ431.9
2.8×10^3 *4*, 45 ns *5*, %sf>0
2955, 47/2+, [F] γ378.2 γ475.3
3043, 49/2+, [F] γ465.5
3464, 51/2+, [F] γ508.6
3541, 53/2+, [F] γ497.6
4004, 55/2+, [F] γ540.1
4069, 57/2+, [F] γ527.5

γ(^{233}Pa) ^{237}Np(0.0) α decay, 2.14×10^6 y<norm: 1.0> *5.5*, *6.68*, *8.22* *5* (†γ 9), *9.0*, *10.7*, *17.40* *5*, *22.6*, *24.14* *10*, *29.374* *20* (†γ 15.0 *10*) E1, *29.6*, *32.46*, *36.24* *10*, *43.2*, *46.53* *6* (†γ 0.11 *1*), *48.96* *10*, *54.40* *10*, *57.104* *20* (†γ 0.39 *1*) E2, *62.59* *10* (†γ 0.006 *3*), *63.90* *10* (†γ 0.012 *2*) (E2), *70.49* *10* (†γ 0.012 *3*), *74.54* *20* (†γ 0.011 *3*), *86.477* *10* (†γ 12.4 *4*) E1, *87.99* *3* (†γ 0.14 *1*), *94.64* *5* (†γ 0.6 *2*) E1, *106.15* *25* (†γ 0.053 *5*), *108.7* (†γ 0.068 *15*) M1+E2 δ<0.22 , *109.10* *10*, *115.40* *35* (†γ 0.0026 *8*), *117.702* *20* (†γ 0.16 *1*) M1+E2 δ=0.30 *9*, *131.101* *25* (†γ 0.085 *9*) E1, *134.285* *20* (†γ 0.067 *7*), *139.9* *1* (†γ ~0.005), *141.74* *10*, *143.249* *20* (†γ 0.43 *2*) M1+E2 δ=0.29 $^{+16}_{-20}$, *151.414* *20* (†γ 0.232 *12*) M1+E2 δ=0.69 *20*, *153.37*, *155.239* *20* (†γ 0.092 *9*) E1, *162.41* *8* (†γ 0.032 *4*), *169.156* *20* (†γ 0.073 *7*), *170.59*, *176.12* *6* (†γ 0.018 *3*), *180.81* *10* (†γ 0.020 *4*), *186.86*, *191.46* *5* (†γ 0.025 *4*), *193.26* *5* (†γ 0.049 *5*), *194.67* *20*, *194.95* *3* (†γ 0.184 *10*) E1, *196.86* *5* (†γ 0.020 *3*), *199.95*, *201.62* *5* (†γ 0.044 *5*) E1, *202.9* *2* (†γ 0.0048 *19*), *209.19* *5* (†γ 0.016 *2*), *212.29* *5* (†γ 0.155 *10*) E1, *214.01* *5* (†γ 0.045 *9*), *219.8*, *222.6* *2* (†γ 0.0020 *10*), *229.94* *5* (†γ 0.014 *4*), *237.86* *2* (†γ 0.063 *7*), *248.95* *10* (†γ 0.0050 *14*), *250.58*, *257.09*, *262.44* *20* (†γ 0.0068 *14*), *279.65* *20* (†γ 0.002 *2*).

α ^{237}Np(0.0) α decay, 2.14×10^6 y<norm: 1.0> α *4873.0* *20* (†0.44) α *4862.8* *20* (†0.24) α *4817.3* *20* (†2.5 *4*) α *4803.3* *20* (†1.56) α *4788.0* *15* (†47 *9*) α *4771.0* *15* (†25 *6*) α *4766.0* *15* (†8 *3*) α *4741.3* *20* (†0.019) α *4712.3* *20* α *4708.3* *20* α *4694.4* *20* (†0.48 *20*) α *4664.0* *20* (†3.32 *10*) α *4639.4* *20* (†6.18 *12*) α *4620* α *4598.6* *20* (†0.34 *4*) α *4581.0* *20* (†0.40 *4*) α *4573.8* *20* (†0.054) α *4572.1* α *4514.5* *20* (†0.04 *2*)

Part 2 of 3

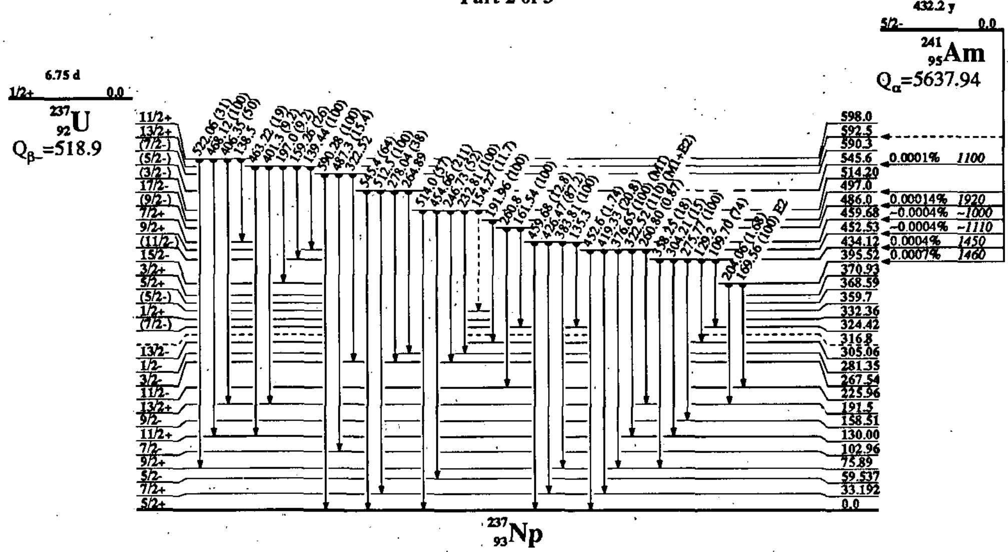

Part 1 of 3

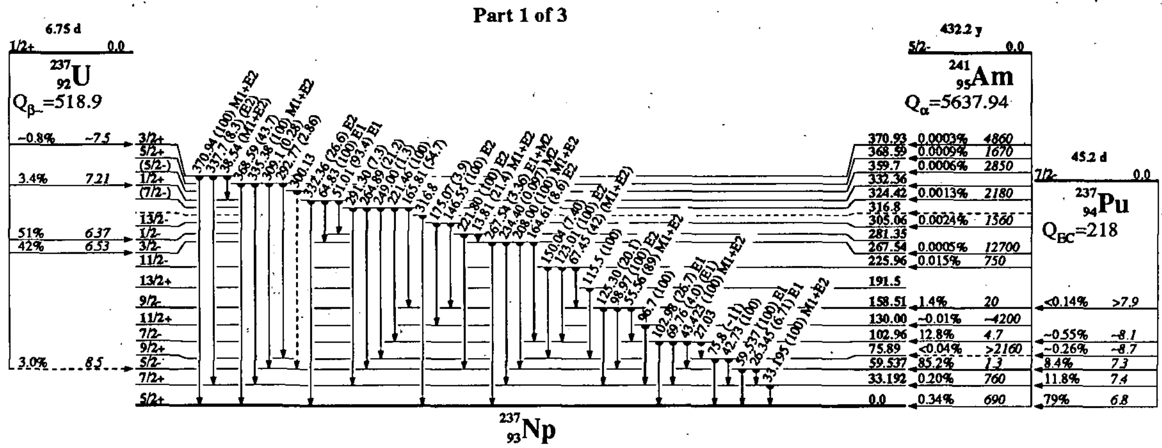

$^{237}_{94}$Pu

Reactions and References

A 237AM EC DECAY
B 241CM A DECAY
C 238PU(D,T) E=12.1 KEV 73GR26
D 239PU(P,T) E=16.5 MEV 74FR01

Adopted levels and γ rays:

0.0, 7/2⁻, 45.2 d *1*, *[ABC]*, %α=0.0042 *4*, %ε=99.9958 *4*
47.71 *4*, 9/2⁻, *[ABC]* γ_0***47.71*** *4* (†γ100) M1+E2 δ=0.24 *8*
106 *5*, 11/2⁻, *[BC]*
145.544 *10*, 1/2⁺, 0.18 s *2*, *[ABCD]* γ_0***145.544*** *10* (†γ100) E3
155.45 *2*, 3/2⁺, *[ABC]* γ_{146}***9.903*** *16* (†γ100) M1+E2 δ=0.07 *2*
175 *7*, 13/2⁻, *[BC]*
201.18 *2*, 5/2⁺, *[ABCD]* γ_{155}***45.724*** *8* (†γ46 *12*) M1+E2 δ=0.47 *13* γ_{146}***55.638*** *11* (†γ100 *16*) (E2)
224.25 *5*, 7/2⁺, *[ABCD]* γ_{155}***68.8*** *1* (†γ100) (E2)
257, 15/2⁻, *[C]*
280.22 *2*, 5/2⁺, *[AC]* γ_{201}***79.05*** *2* (†γ0.42 *7*) (M1) γ_{155}***124.72*** *5* (†γ0.59 *11*) (M1) γ_0***280.23*** *2* (†γ100 *5*) E1
304 *4*, 9/2⁺, *[BCD]*
320.97 *2*, 7/2⁺, *[A]* γ_{280}***40.748*** *6* (†γ2.0 *4*) M1+E2 δ=0.194 *50* γ_{48}***273.3*** *1* (†γ54 *4*) γ_0***321.0*** *1* (†γ100 *8*) E1
370.40 *4*, 3/2⁺, *[AB]* γ_{155}***214.9*** *2* (†γ100 *21*) (M1) γ_{146}***224.86*** *4* (†γ100 *21*) (M1)
371 *5*, 9/2⁺, *[C]*
404.19 *5*, 5/2⁺, *[ABC]* γ_{280}***123.8*** *3* (†γ~7) γ_{224}***179.94*** *2* (†γ41 *9*) (M1+E2) δ=0.7 *7* γ_{201}***203.03*** *5* (†γ71 *9*) M1+E2 δ=0.4 *4* γ_{155}***248.7*** *2* (†γ100 *10*) (M1+E2) δ=0.6 *6*
407.83 *6*, 5/2⁺, *[ACD]* γ_{280}***127.5*** *2* (†γ17 *4*) γ_{224}***183.7*** *2* (†γ30 *8*) M1+E2 δ=0.7 *7* γ_{201}***206.7*** *1* (†γ52 *7*) M1+E2 δ=0.3 *3* γ_{155}***252.2*** *2* (†γ43 *12*) M1+E2 δ~0.7 γ_0***407.8*** *1* (†γ100 *8*) (E1)
438.41 *10*, 7/2⁺, *[AC]* γ_{280}***158.3*** *3* (†γ0.8 *3*) γ_{48}***390.7*** *1* (†γ6.6 *5*) E1 γ_0***438.4*** *1* (†γ100 *5*) E1
453.2 *2*, 7/2⁺, *[AC]* γ_{224}***229.1*** *3* (†γ100 *34*) γ_{201}***252.2*** (†γ100 *34*) γ_0***453.2*** *3* (†γ67 *14*)

Part 3 of 3

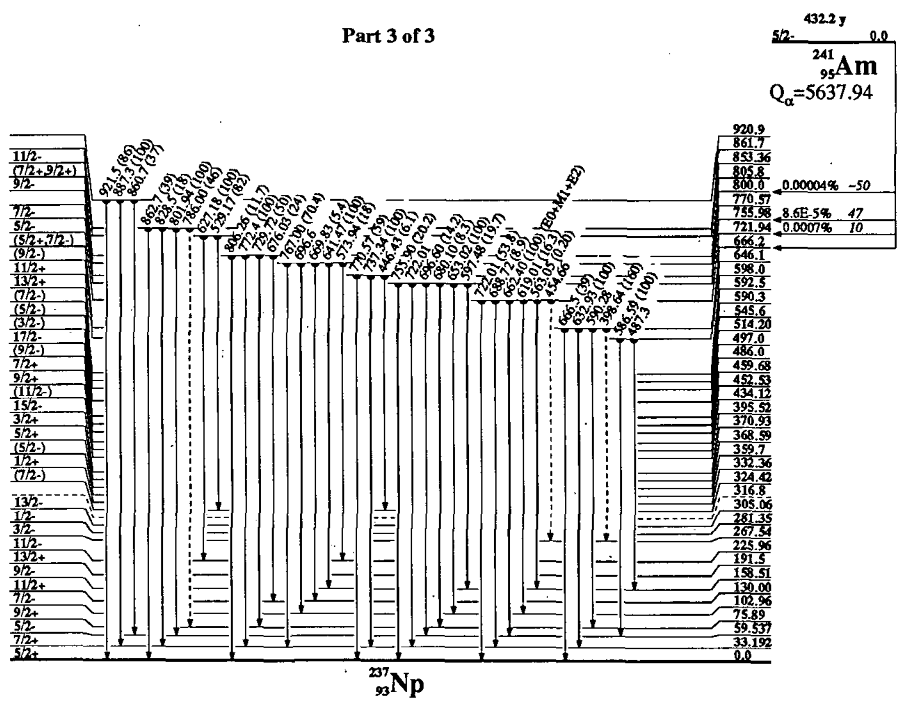

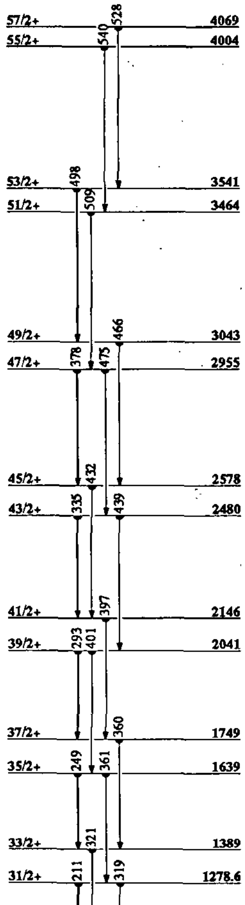

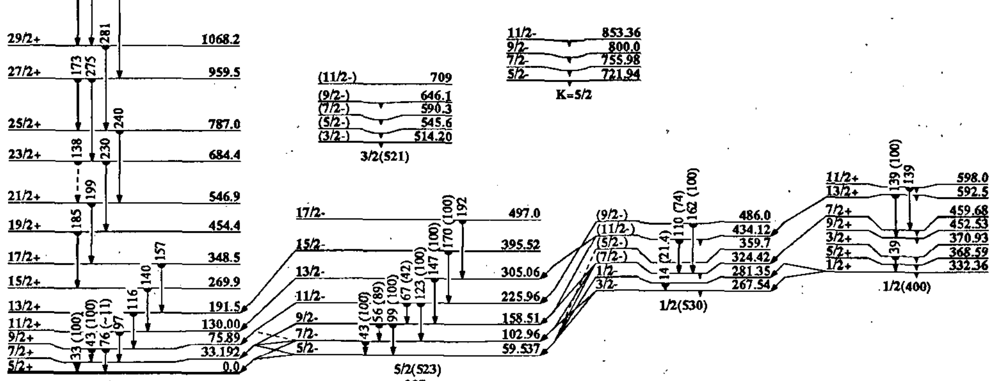

$^{237}_{93}$Np Rotational Bands

$^{237}_{94}$Pu (Continued)

473.50 *10*, 7/2$^+$, *[AC]* γ_{280}*193.4* *3* (†$_\gamma$2.1 *7*) γ_{47}*425.8* *1* (†$_\gamma$45 *3*) E1 γ_0*473.5* *1* (†$_\gamma$100 *7*) E1
486, (9/2$^+$), *[C]*
513, 9/2$^+$, *[C]*
545, (1/2$^-$), *[C]*
582, (5/2$^-$), *[C]*
591, (3/2$^-$), *[C]*
655, *[C(*)]*
655.3 *2*, (5/2)$^-$, *[AC(*)]* γ_0*655.3* *2* (†$_\gamma$100) M1
691, (7/2$^-$), *[C]*
696.2 *3*, 7/2$^-$, *[A]* γ_{655}*40.748* γ_{47}*648.5* *3* (†$_\gamma$100 *16*) M1 γ_0*696.2* *3* (†$_\gamma$77 *16*) M1
716, *[C]*
741, *[C]*
757, *[C]*
775, *[C]*
800 *2*, 1/2$^+$, *[D]*
809, *[C]*
840, *[C]*
851 *3*, (3/2$^+$,5/2$^+$), *[D]*
852, *[C]*
884, *[C]*
908.9 *2*, 7/2$^+$, *[A]* γ_{474}*435.2* *3* (†$_\gamma$9.6 *16*) M1 γ_{453}*455.8* *3* (†$_\gamma$3.5 *8*) M1 γ_{408}*501.2* *3* (†$_\gamma$10.8 *16*) M1 γ_{404}*504.8* *3* (†$_\gamma$7.3 *16*) M1 γ_{48}*861.2* *3* (†$_\gamma$14.2 *16*) γ_0*908.8* *2* (†$_\gamma$100 *6*)
933, *[C]*
964, *[C]*
998 *3*, *[C(*)D]*
1000.6 *3*, (7/2), *[AC(*)]* γ_{280}*720.4* *3* (†$_\gamma$100 *21*) γ_0*1000.6* *3* (†$_\gamma$79 *21*)
1014, *[C]*
1025 *3*, *[D]*
1053, *[C]*
1104, *[C]*
1189, *[C]*
1216, *[C]*
1250, *[C]*
1264, *[C]*
1348, *[C]*
1383, *[C]*
1397, *[C]*
1463, *[C]*
1481, *[C]*
1534, *[C]*
~2600, 85 ns *15*, %sf>0
~2900, 1.1 μs *1*, %sf≥0

γ(^{237}*Np*) ^{237}Pu(0.0) ε decay, 45.2 d<*norm: 0.0328 15*> *26.345* *1* (†$_\gamma$6.75 *20*), *27.03*, *33.195* *11* (†$_\gamma$2.27 *7*) M1+E2, *42.73* *5* (†$_\gamma$~0.090), *43.423* *10* (†$_\gamma$~0.12), *55.56* *2* (†$_\gamma$<0.05), *59.537* *1* (†$_\gamma$100 *3*) E1, *69.76* *3* (†$_\gamma$~0.0048), *75.8* *2* (†$_\gamma$~0.0096), *98.97* *2* (†$_\gamma$<0.06), *102.98* *2* (†$_\gamma$~0.032), *125.30* *2* (†$_\gamma$<0.01).

γ(^{233}*U*) ^{237}Pu(0.0) α decay, 45.2 d<*norm: 0.000009*> *21.87*, *32.9*, *40.35*, *43.7*, *51.5*, *54.8*, *58.0*, *63.1*, *76.7*, *92.0*, *114.7*, *181.8* *10* (†$_\gamma$~0.8), *198.61* *20* (†$_\gamma$7.3 *10*), *205.05* *20* (†$_\gamma$3.2 *8*), *228.56* *20* (†$_\gamma$36.2 *15*), *241* *2* (†$_\gamma$~0.5), *258.46* *20* (†$_\gamma$16.1 *12*), *261.66* *20* (†$_\gamma$18.1 *11*), *280.40* *20* (†$_\gamma$100 *2*), *298.89* *20* (†$_\gamma$72.2 *18*), *305.4* *2* (†$_\gamma$2.9 *9*), *313.34* *20* (†$_\gamma$27.8 *14*), *320.75* *20* (†$_\gamma$59.6 *18*), *411.1* *2* (†$_\gamma$1.7 *5*), *463.1* *2* (†$_\gamma$3.4 *10*), *503.9* *2* (†$_\gamma$6.9 *13*), *521.1* *20* (†$_\gamma$~0.8).

α ^{237}Pu(0.0) α decay, 45.2 d<*norm: 0.000042*> α_0*5650* *6* (†7.1) α_{40}*5610* *6* (†7.3) α_{82}*5560* *7* (†3.6) α_{155}*5498* *7* (†2.1) α_{280}*5356* *7* (†~17.2) α_{321}*5334* *7* (†~43.5) α_{354}*5302* *7* (†~12.2) α_{396}*5259* *7* (†>0.7) α_{504}*5154* *7* (†~6.4) α_{561}*5098* *7* (†~0.5)

$^{237}_{95}$Am

Adopted levels and γ rays:
0.0, 5/2($^-$), 73.0 m *10*, %α=0.025 *5*, %ε=99.975 *5*
~2400, 5 ns *2*, %sf=100

γ(^{237}*Pu*) ^{237}Am(0.0) ε+β$^+$ decay, 73.0 m<*norm: 1.00 9*> *9.903* *16* M1+E2 δ=0.07 *2*, *40.748* *6* M1+E2 δ=0.194 *30*, *45.724* *8* M1+E2 δ=0.47 *13*, *47.71* *4* M1+E2 δ=0.24 *8*, *55.638* *11* (E2), *68.8* *1* (E2), *79.05* *2* (M1), *123.8* *3* (†$_\gamma$~0.04), *124.72* *3* (†$_\gamma$0.28 *5*) (M1), *127.5* *2* (†$_\gamma$0.11 *2*), *145.552* *12* (†$_\gamma$0.48 *4*) E3, *158.3* *3* (†$_\gamma$0.07 *2*), *179.94* *2* (†$_\gamma$0.24 *5*) (M1+E2) δ=0.7 *7*, *183.7* *2* (†$_\gamma$0.19 *5*) M1+E2 δ=0.7 *7*, *193.4* *3* (†$_\gamma$0.09 *3*), *203.03* *3* (†$_\gamma$0.42 *5*) M1+E2 δ=0.4 *4*, *206.7* *1* (†$_\gamma$0.33 *4*) M1+E2 δ=0.3 *3*, *214.9* *2* (†$_\gamma$0.24 *5*) (M1), *224.86* *4* (†$_\gamma$0.24 *5*) (M1), *229.1* *3* (†$_\gamma$0.15 *5*), *248.7* *2* (†$_\gamma$0.59 *6*) (M1+E2) δ=0.6 *6*, *252.2* *2* (†$_\gamma$0.27 *7*) M1+E2 δ~0.7, *273.3* *1* (†$_\gamma$0.76 *5*), *280.23* *2* (†$_\gamma$47.3 *20*) E1, *321.0* *1* (†$_\gamma$1.4 *1*) E1, *390.7* *1* (†$_\gamma$0.55 *4*) E1, *407.8* *1* (†$_\gamma$0.63 *5*) (E1), *425.8* *1* (†$_\gamma$1.94 *12*) E1, *435.2* *3* (†$_\gamma$0.25 *4*) M1, *438.4* *1* (†$_\gamma$8.3 *4*) E1, *453.2* *3* (†$_\gamma$0.10 *2*), *455.8* *3* (†$_\gamma$0.09 *2*) M1, *473.5* *1* (†$_\gamma$4.3 *3*) E1, *501.2* *3* (†$_\gamma$0.28 *4*) M1, *504.8* *3* (†$_\gamma$0.19 *4*) M1, *648.5* *3* (†$_\gamma$0.26 *4*) M1, *655.3* *2* (†$_\gamma$1.30 *13*) M1, *696.2* *3* (†$_\gamma$0.20 *4*) M1, *720.4* *3* (†$_\gamma$0.24 *5*), *743.5* *5* (†$_\gamma$0.27 *5*), *792.0* *5* (†$_\gamma$0.16 *4*), *861.2* *3* (†$_\gamma$0.37 *4*), *908.8* *2* (†$_\gamma$2.60 *15*), *1000.6* *3* (†$_\gamma$0.19 *3*).

γ(^{233}*Np*) ^{237}Am(0.0) α decay, 73.0 m: no γ-rays.
α ^{237}Am(0.0) α decay, 73.0 m<*norm: 0.00025*> α_{50}*6042* *5* (†100)

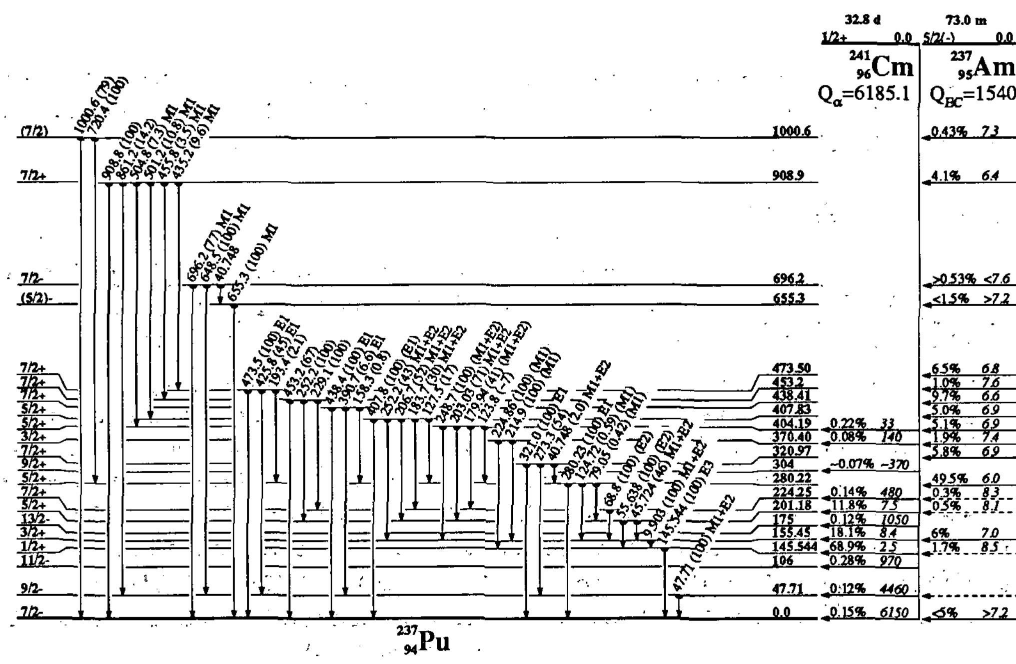

3. MacNuclide, PCNuclide, CHARTIST, and E-NUCS (R.B. Firestone and C.A. Stone)

The computer programs MacNuclide and PCNuclide are being developed to provide access to nuclear data from personal computers. Both codes are initially being developed to present basic 'wall chart' data including half-lives, decay modes, J^{π}, and thermal neutron cross-sections. The initial database for these codes (TOI/ENSDF) was derived from radioactive parent data files used to produce the Table of Radioactive Isotopes and is currently being updated. MacNuclide, a color Macintosh program, is the most sophisticated of these codes and presents data through a chart of the nuclides graphical interface. Nuclei can be selected with a mouse to create a data window which, itself, can be accessed by the mouse to obtain addition information and move about the chart. MacNuclide can create a variety of nuclear charts colored on the basis of half-life, decay mode, J^{π}, and other properties. The charts can also be colored on the basis of user generated criteria, e.g. abundance as a function of time in a reactor. The PCNuclide program will have similar capabilities but will be command driven and more suitable to less powerful personal computers. Both programs are expected to have initial release late in 1991. Future updates will include complete access to all ENSDF data, on-screen presentation of level schemes and tabular data, and a variety of accessory programs for atomic and nuclear structure calculations and applications.

The computer code CHARTIST is being developed to access the TOI/ENSDF database to prepare user tailored, color or black and white, charts of nuclei. These charts can be printed with standard POSTSCRIPT laserprinters. A series of standard charts is being prepared for general distribution in 1992.

E-NUCS will provide nuclear data via E-mail requests. This system will provide access to the Table of Isotopes and ENSDF data. More details on E-NUCS will be forthcoming.

C. SPECTROSCOPY STUDIES

1. Decay Studies of Neutron Deficient Nuclei near the Z=64 Subshell: ^{142}Dy, ^{140,142}Tb, ^{140,142}Gd, ^{140,142}Eu, ^{142}Sm, and ^{142}Pm (R.B. Firestone, J. Gilat, J.M. Nitschke, P.A. Wilmarth, and K.S. Vierinen)

The EC/β^+ and delayed proton decays of A=142 isotopes with $61 \leq Z \leq 66$ and A=140 isotopes with $63 \leq Z \leq 65$ were investigated with the OASIS facility online at the LBL SuperHILAC. Electron capture and positron decay emission probabilities have been determined for ^{142}Pm and ^{142}Sm decays, and extensive decay schemes have been constructed for ^{142}Eu^g (2.34±0.12 s), ^{142}Gd (70.2±0.6 s), ^{140}Eu (1.51±0.02 s), and ^{140}Gd (15.8±0.4 s). Decay schemes for the new isotopes ^{142}Tb^g (597±17 ms), ^{142}Tb^m (303±17 ms), ^{142}Dy (2.3±0.3 s), ^{140}Eu^m (125±2 ms), and ^{140}Tb (2.4±0.2 s) are also presented. We have assigned γ rays to these isotopes on the basis of $\gamma\gamma$ and xγ coincidences, and from half-life determinations. Electron capture and β-decay branchings were measured for each decay, and β-delayed proton branchings were determined for ^{142}Dy, ^{142}Tb and ^{140}Tb decays. Q_{EC} values, derived from the measured EC/β^+

branchings and the level schemes are compared with those from the Wapstra and Audi* and the Liran and Zeldes† mass calculation. The systematics of the N=77 isomer decays are discussed, and the intense $0^+\to1^+$ and $1^+\to0^+$ ground state beta decays are compared in figure 1 and figure 2 respectively. The shell model predictions for simple spin-flip transitions are shown in figure 1. The logft values follow the expected shell model trends but are hindered by nearly two orders of magnitude. For N=80 and N=81 the blocking of the $\nu d_{3/2}$ orbital in the daughter is also observed.

*A.H. Wapstra and G. Audi, Nucl. Phys. A432, 140 (1985).
†S. Liran and N. Zeldes, At. Data. Nucl. Data Tables 17, 431 (1976).

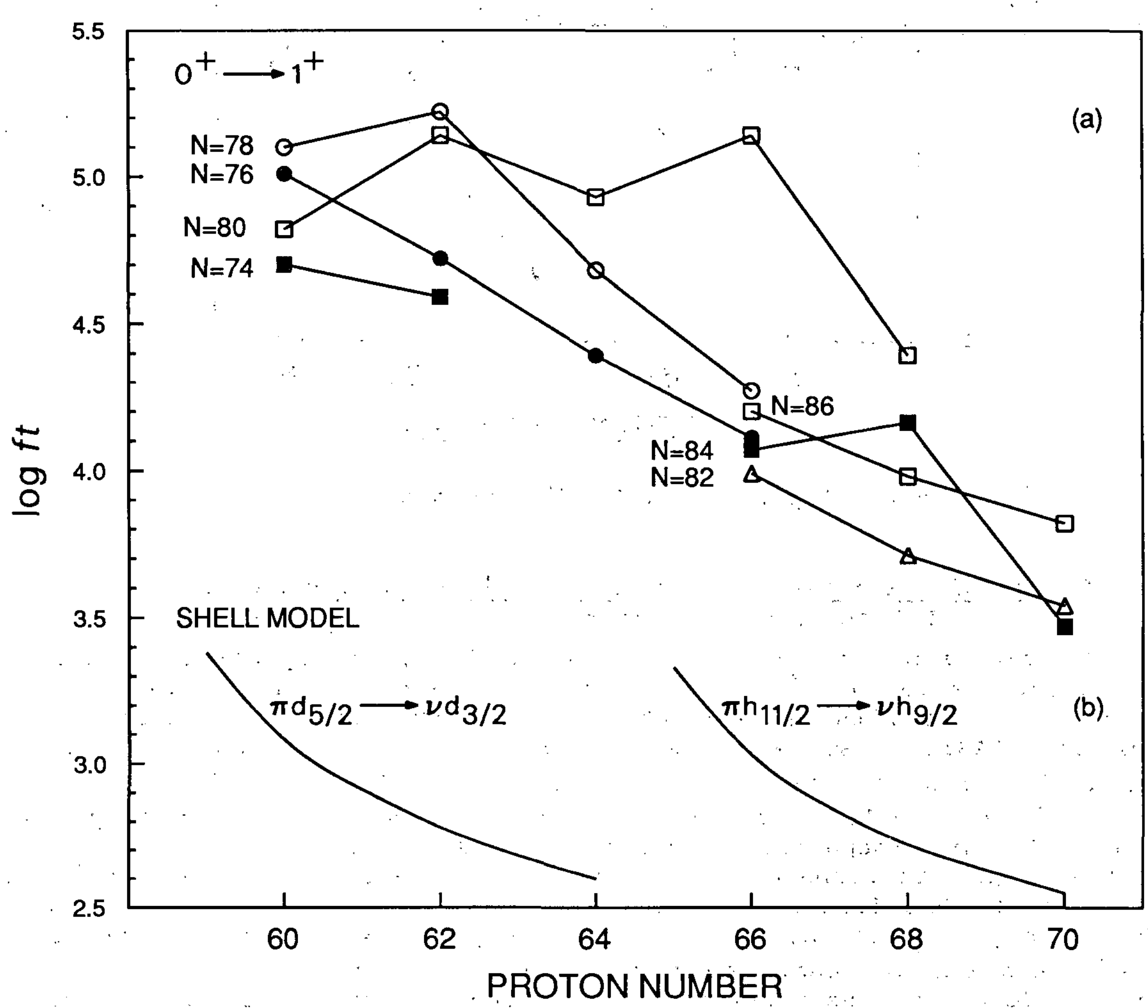

Figure 1. Ground-state $0^+\to1^+$ logft values for even-even nuclei with Z=60-70 and N=74-86. (a) Experimental logft values (b) Predicted logft values from the shell model.

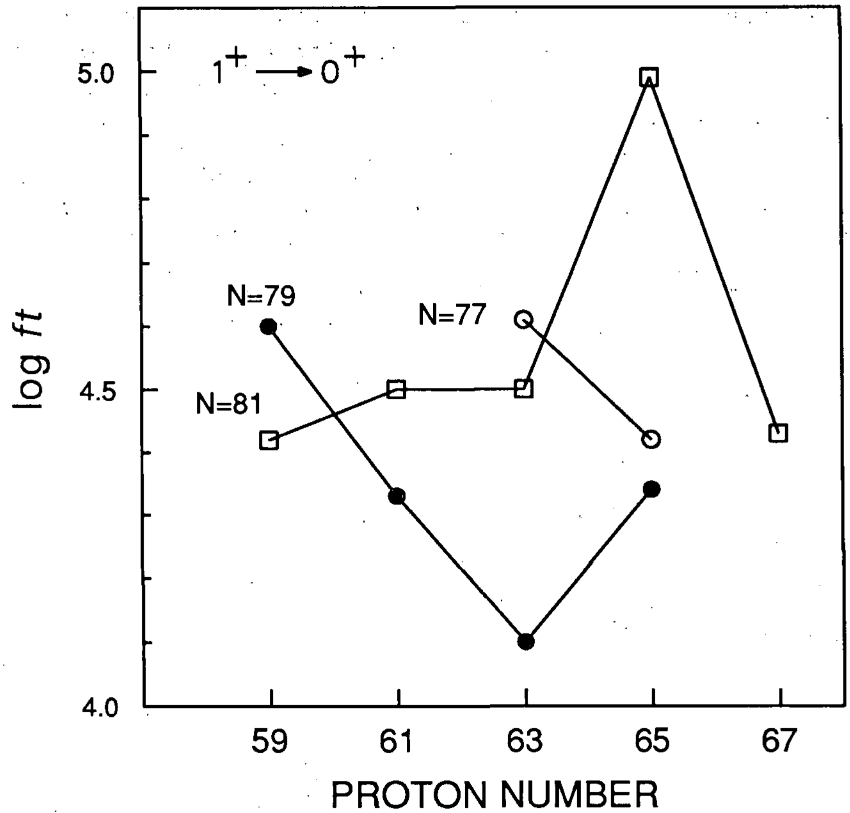

Figure 2. Experimental $1^+ \rightarrow 0^+$ ground-state logft values.

2. Total Absorption Spectrometer: First On-Line Results
(J.M. Nitschke, P.A. Wilmarth, and R.B. Firestone)

The two main objectives of the Total Absorption Spectrometer (TAS) are the determination of β-strength functions and the measurement of decay energies. In a first experiment with TAS, coupled to the on-line isotope separator OASIS, a series of neutron deficient Ba, Cs, and Xe isotopes was produced using a beam of ^{28}Si from the SuperHILAC on targets of ^{100,98,96,95,92}Mo. Only a very small subset of the results can be presented here. The mass-separated samples from OASIS were collected on a fast cycling tape and transported within 0.5 s into the center of the well in TAS. There, the following decay parameters were recorded: the total γ-ray decay energy E_{tot} in the well plus the plug, the x-ray energy, the electron energy and energy loss, and time spectra between all detectors. In the case of EC decays the x ray information together with the mass selection in the separator resulted in an unambiguous isotope identification. In some cases [i.e. ^{122}Cs(8-,1+), cf. figure 1b] it was possible to separate the isomer from the ground state based on their different half-lives (4.4 min and 21 s, respectively) by choosing the appropriate tape cycle period.

Decay energies were determined from positron spectra recorded in coincidence with E_{tot} under the condition that E_{tot}=1022 keV, as shown for ^{122}Cs

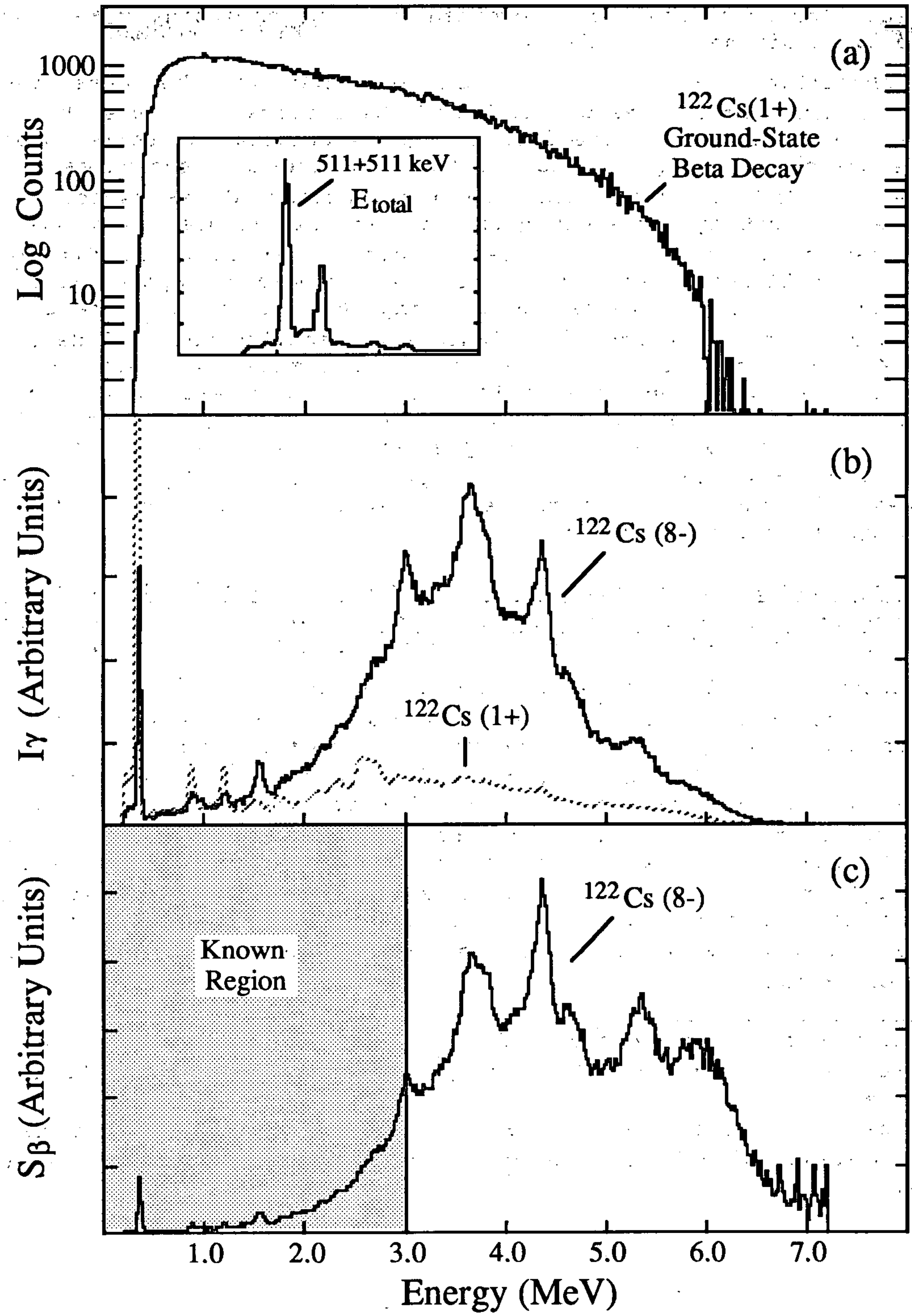

Figure 1. Results of ^{122}Cs decay: (a) positron spectrum, (b) E_{total} spectrum, and (c) beta-strength.

in figure 1a. Positron decay to an excited state at an energy x kev could be selected by requiring E_{tot}=1022+x keV.

Total absorption γ-ray spectra were measured in the mass range 116≤A≤124; as shown for the example of both ^{122}Cs isomers in figure 1b. The spectra are, in general, characterized by narrow structures, corresponding to discrete states at energies below ~2 MeV, and broader resonances up to the Q-value (7.0 MeV for ^{122}Cs); the endpoints correspond, as expected, to the Q_{EC}-value. Selecting different gates in the coincidence x-ray spectra allows a clean separation of the total absorption spectra for different elements. A preliminary evaluation of the associated approximate β-strength functions (S_β) is obtained by dividing the measured E_{tot} spectra by the Fermi function for EC decay (cf. figure 1c), assuming an ideal detector response. More realistic unfolding techniques that make use of information from the plug detector and the calculated response matrix are under development. It is evident from figure 1c that the majority of the β-strength is observed above the region previously known from β/γ studies. In the case of ^{122}Cs and several other isotopes the published β feedings and logft values will have to be corrected. Comparisons with calculated β-strength functions are in progress.

3. Decay Studies of the Neutron-Rich Isotopes ^{168}Dy and ^{168}Ho^g and the Identification of the New Isomer ^{168}Ho^m (R.M. Chasteler, J.M. Nitschke, R.B. Firestone, K.S. Vierinen, and P.A. Wilmarth)

Multi-nucleon transfer reactions between ^{170}Er ions and ^{nat}W targets with on-line mass separation at the OASIS* facility were used to produce neutron-rich A=168 isotopes. Beta and gamma spectroscopy was used to study the decay of these activities. A new isomer, ^{168}Ho^m, was identified to decay by an isomeric transition with a half-life of 132(4) s. A decay scheme for the most neutron-rich A=168 isotope, 8.8(3)-m ^{168}Dy,† was determined and is shown in figure 1. The validity of the level assignments of the ^{168}Ho daughter are supported by comparison with microscopic theoretical calculations of the quasi-particle structure of corresponding states in ^{166}Ho.‡ Also, a new $Q_{\beta-}$ value of 2.93(3) MeV for the decay of 3.0-m ^{168}Ho^g has been obtained (Figure 2).

*J.M. Nitschke, Nucl. Inst. Methods 206, 341 (1983).

†R.J. Gehrke, R.C. Greenwood, J.D. Baker, and D.H. Meikrantz, Z. Phys. A306, 363 (1982).

‡R.K. Sheline, J. Kvasil, and P.C. Sood, "Configurational Assignments in ^{168}Ho and Comparison with ^{166}Ho", submitted to Phys. Rev. C and private communication.

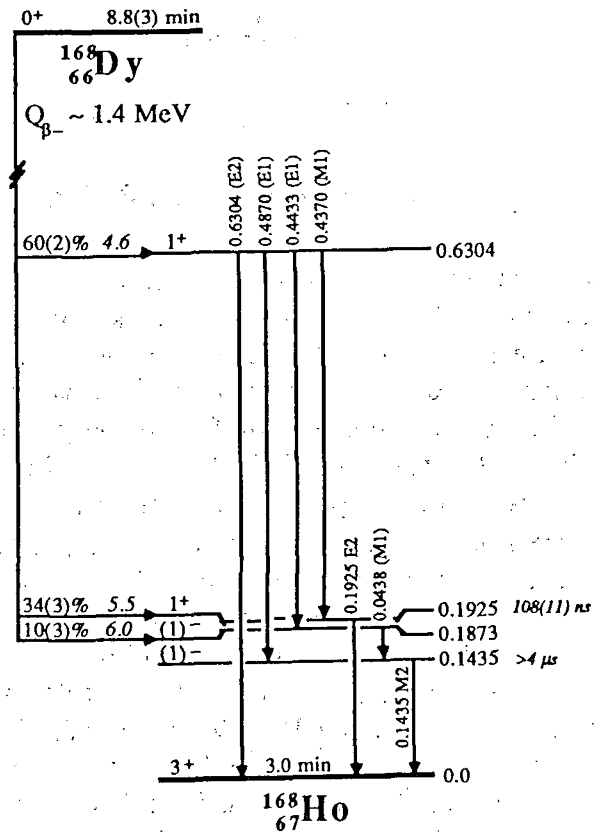

Fig. 1. Proposed decay scheme for 8.8-m ^{168}Dy. Energies are in MeV. Log *ft*'s are in italics.

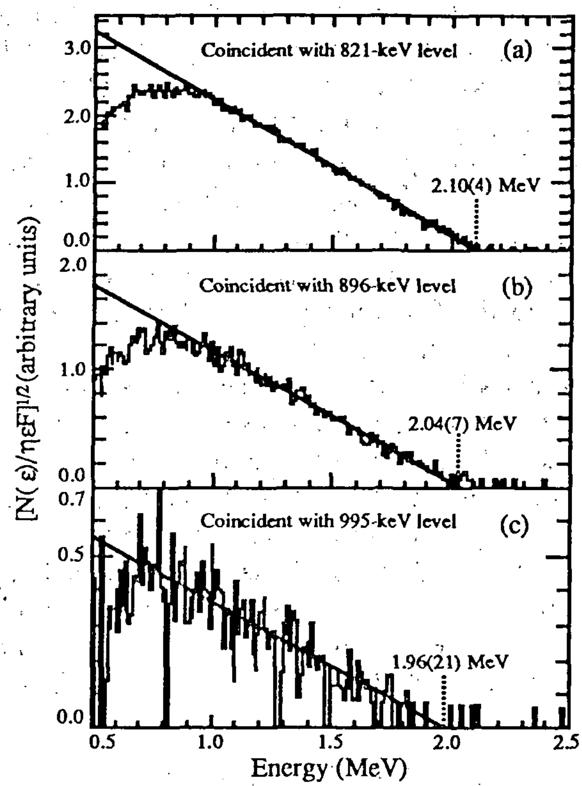

Fig. 2. Fermi-Kurie plots of γ-gated, background-subtracted beta particle spectra for ^{168}Hog β^- decays to levels in ^{168}Er; (a) 821-keV level, (b) 896-keV level, and (c) 995-keV level. The fitting intervals used in the least-squares analysis were (a) 1.0–2.0 MeV, (b) 1.0–1.9 MeV, and (c) 0.8–1.5 MeV.

A. NUCLEAR DATA EVALUATIONS AND CALCULATIONS

1. Charged-Particle Evaluations for Applications (R. M. White and D. A. Resler)

Thermonuclear reaction rates and quantities such as thermally-broadened emission spectra of secondary reaction particles as a function of plasma temperature are essential for the correct modeling of a multitude of problems ranging from fusion energy applications to astrophysics. Of primary interest to fusion applications are the reaction rates of the various isotopes of hydrogen and helium-3. We have finished new evaluations for the $^2H(d,p)^3H$, $^2H(d,n)^3He$, $^3H(d,n)^4He$, $^3He(d,p)^4He$, and $^3H(t,2n)^4He$ reactions from E_{min} to 30 MeV. E_{min} is taken as the energy where the reaction cross section is approximately 10^{-31} barns, a practical limit for many 32-bit computers. These small cross sections at low energies are due to the Coulomb penetrability and require different evaluation techniques than do neutron reactions. However, these low-energy cross sections are important in charged-particle reactions because the average interaction energy in a plasma is also low. The energy range of the cross sections described here amply covers the energies necessary to calculate Maxwellian-averaged reaction rates for plasma temperatures from 100 eV to 1 MeV. The evaluations are based on all published data known to us from 1946 to 1990 and include over 1150 measured data points from over 85 references. While there have been many parameterizations of these reactions and numerous evaluations spanning selected energy regions, we know of no work containing all measurements spanning both this time period and this energy range. A complete bibliographic listing and a detailed description of the evaluation techniques will be presented in a forthcoming LLNL report.

a. $^2H(d,p)^3H$ Evaluation

Our data base for the $^2H(d,p)^3H$ reaction contains 21 references and includes 189 integrated cross section values obtained from a variety of experimental measurements. Figure 1 shows the reference symbols (with the year in brackets) and Fig. 2 shows our evaluation of the $^2H(d,p)^3H$ reaction over the energy region from 350 eV to 200 keV plotted in terms of the astrophysical s-factor with ±3% indicated. One of the principal objectives in carrying out these evaluations is to establish the probable uncertainties (at the 95% confidence level) in the state of knowledge of each of these reactions. In this particular case, while the data appear far more discrepant in the energy region between 350 eV and 200 keV than the ±3% would indicate, the evaluation in this region is based also upon our knowledge of the structure of the ^4He compound system as well as upon numerous measurements at energies greater than 200 keV. The recent high precision measurements of Brown[90] at Los Alamos are in almost perfect agreement with this evaluation which was carried out with and without considering those data.

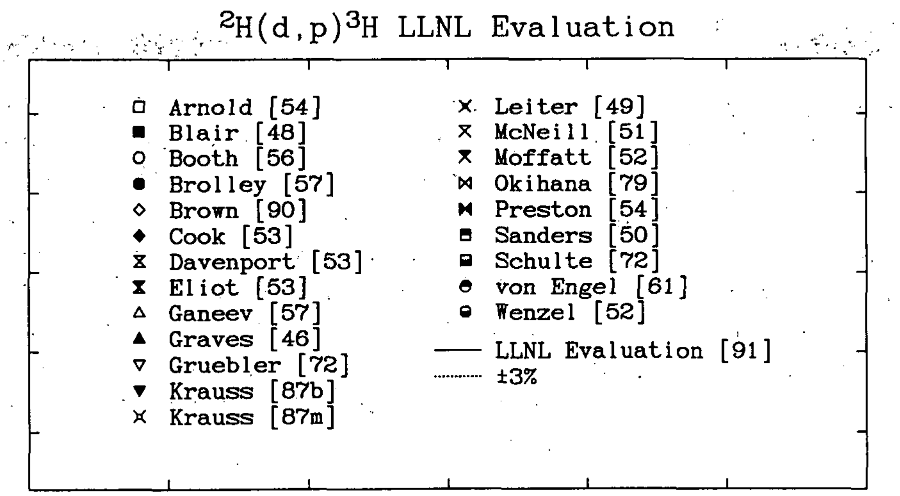

Fig. 1 Reference symbols and authors (with year of publication) for the data base used in the LLNL[91] evaluation of the $^2H(d,p)^3H$ reaction as shown in Fig. 2. A complete bibliographic listing as well as a detailed description of the evaluation techniques used for this reaction will be presented in a forthcoming LLNL report.

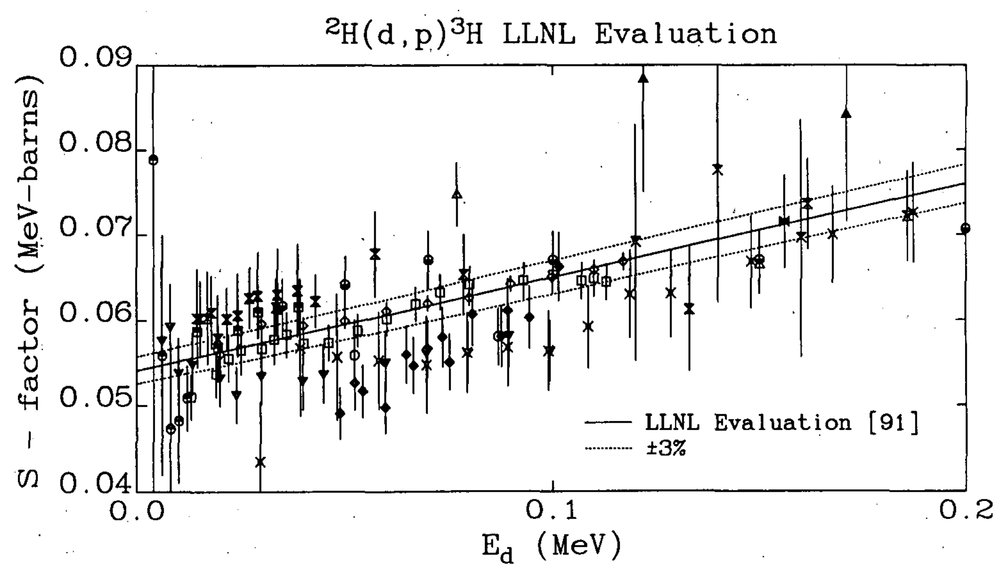

Fig. 2 Plot of the LLNL[91] evaluation of the $^2H(d,p)^3H$ reaction in terms of the astrophysical s-factor as a function of laboratory deuteron energy between 350 eV and 200 keV. The ±3% indicated on the plot represents our estimate of the uncertainty in the evaluation (at the 95% confidence level). While the $^2H(d,p)^3H$ data are most discrepant in the energy region below 200 keV, the knowledge of the structure of the ^4He compound system, as well as the data base above 200 keV, give us strong confidence in this evaluation. The recent high precision measurements of Brown[90] at Los Alamos are in almost perfect agreement with this evaluation which we made both with and without considering those data.

b. $^2H(d,n)^3He$ Evaluation

Our data base for the $^2H(d,p)^3H$ reaction contains 21 references and includes 190 integrated cross section values. Figure 3 shows the reference symbols and Fig. 4 shows our evaluation of the $^2H(d,n)^3He$ reaction from 350 eV to 200 keV plotted in terms of the astrophysical s-factor with ±3% indicated. In this reaction, several measurements in the energy range below 100 keV might indicate that the evaluation should have the slope shown here but be lowered by 6-8%. However, similarly to the $^2H(d,p)^3H$ reaction, knowledge of the structure of the compound ^4He system, as well as the data base above 200 keV, give us strong confidence in this evaluation. As in the case of the $^2H(d,p)^3H$ reaction, the recent Los Alamos measurement of the $^2H(d,n)^3He$ reaction is in excellent agreement with our evaluation which was carried out with and without considering their data.

c. $^3H(d,n)^4He$ Evaluation

Our data base for the $^3H(d,n)^4He$ reaction contains 19 references and includes 366 integrated cross section values. Figure 5 shows the reference symbols and Figs. 6 and 7 show our evaluation of the $^3H(d,n)^4He$ reaction from 300 eV to 200 keV plotted in terms of the astrophysical s-factor and cross section, respectively, with ±2% indicated. For the energy range shown, the evaluation is based on a single-level R-matrix fit to all of the available data except for three data sets whose shape and normalization are not consistent with the majority of the other measurements. Many R-matrix calculations were performed under a variety of fitting ranges and using various subsets of the main data set. The conclusion was that all of the results fell within the ±2% band indicated around the final evaluation. The Los Alamos one and two-level fits to this reaction also fall within this ±2% band. Details of the R-matrix calculations will be presented in a forthcoming LLNL report.

d. $^3He(d,p)^4He$ Evaluation

Our data base for the $^3He(d,p)^4He$ reaction contains 17 references and include 262 integrated cross section values. Figure 8 shows the reference symbols and Figs. 9 and 10 show our evaluation of the $^3He(d,p)^4He$ reaction from 1.25 keV to 1 MeV plotted in terms of the astrophysical s-factor and cross section, respectively, with ±8% indicated. Of the five reactions evaluated in this work, the data sets for this reaction are the most discrepant. The absolute values disagree by more than the experimenters' quoted errors. However, except for two full data sets and the low-energy portion of two other data sets, the shapes are in good agreement. Over the energy range from 1.25 keV to 800 keV, the evaluation is based on a single-level R-matrix fit to all of the available data except for the data which were discrepant in shape. As with the $^3H(d,n)^4He$ reaction, many R-matrix calculations were performed under a variety of conditions.

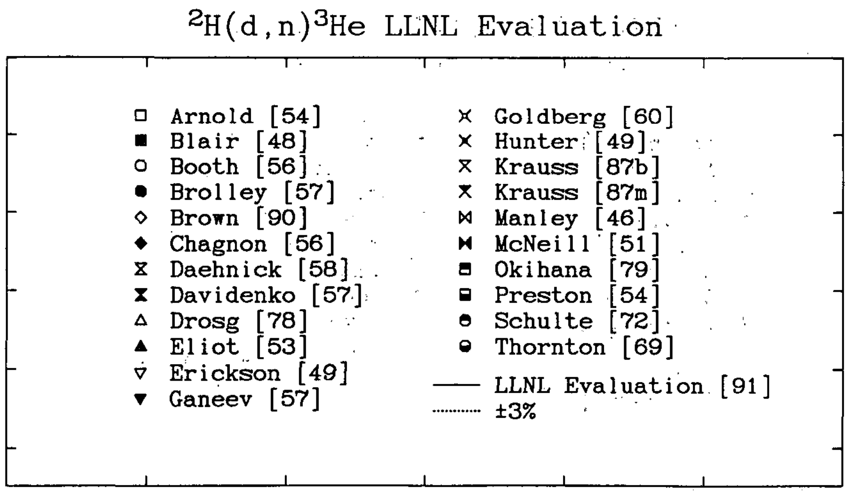

Fig. 3 Reference symbols and authors (with year of publication) for the data base used in the LLNL[91] evaluation of the ^{2}H(d,n)^{3}He reaction as shown in Fig. 4. A complete bibliographic listing as well as a detailed description of the evaluation techniques used for this reaction will be presented in a forthcoming LLNL report.

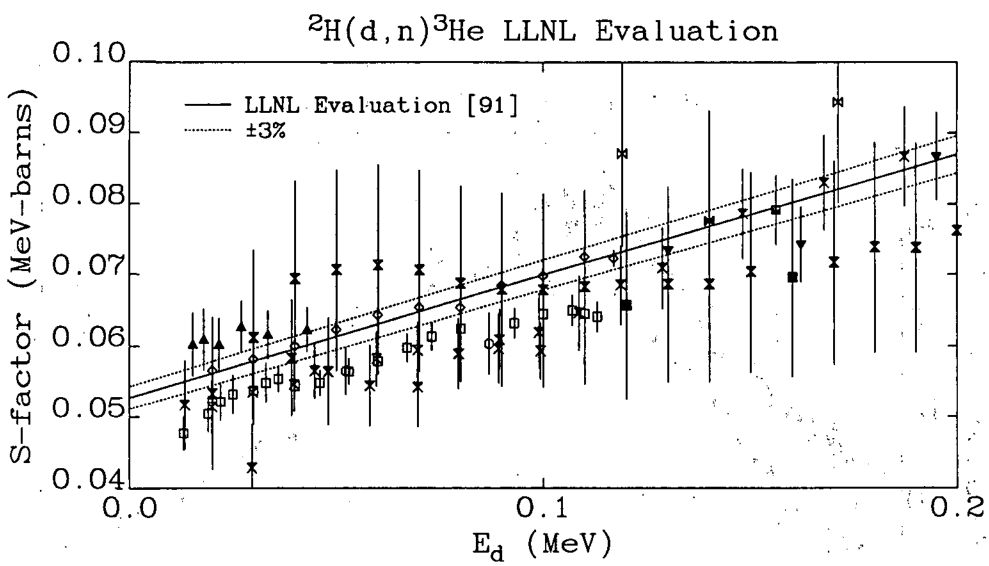

Fig. 4 Plot of the LLNL[91] evaluation of the ^{2}H(d,n)^{3}He reaction in terms of the astrophysical s-factor as a function of laboratory deuteron energy between 350 eV and 200 keV. The ±3% indicated on the plot represents our estimate of the uncertainty in the evaluation (at the 95% confidence level). In this reaction, several measurements in the energy range below 100 keV might indicate that the evaluation should have the slope shown here but be lowered by 8-10%. However, similarly to the ^{2}H(d,p)^{3}H reaction, knowledge of the structure of the ^{4}He compound system, as well as many measurements above 100 keV, indicate that there should be no significant curvature in the astrophysical s-factor in this energy region.

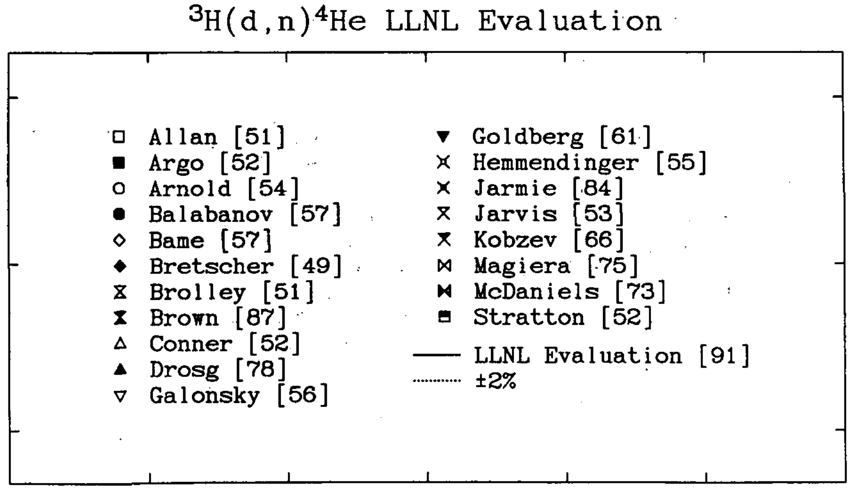

Fig. 5 Reference symbols and authors (with year of publication) for the data base used in the LLNL[91] evaluation of the $^3H(d,n)^4He$ reaction as shown in Figs. 6 and 7. A complete bibliographic listing as well as a detailed description of the evaluation techniques used for this reaction will be presented in a forthcoming LLNL report.

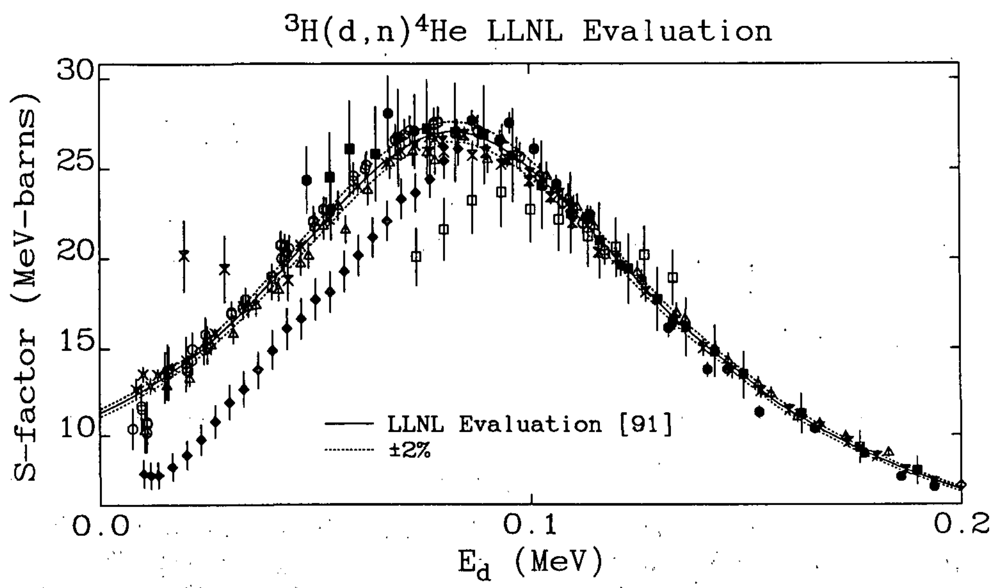

Fig. 6 Plot of the LLNL[91] evaluation of the $^3H(d,n)^4He$ reaction in terms of the astrophysical s-factor as a function of laboratory deuteron energy between 300 eV and 200 keV. The ±2% indicated on the plot represents our estimate of the uncertainty in the evaluation (at the 95% confidence level). With the exception of three data sets whose shape and normalization are not consistent with the majority of other measurements, the $^3H(d,n)^4He$ data in this region are very consistent.

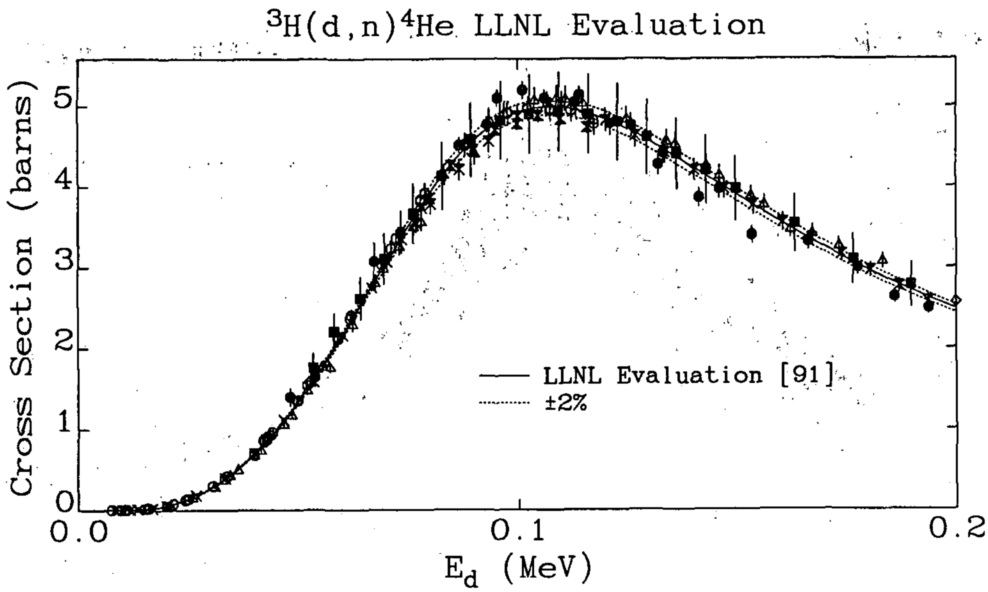

Fig. 7 Plot of the LLNL[91] evaluation of the $^3H(d,n)^4He$ reaction cross section from 300 eV to 200 keV with the three discrepant data sets removed. The evaluation procedures we used on the data base for this reaction and comparing our evaluation with other recent evaluations leads us to conclude that, unless some significant new experimental technique is developed, our estimate of the ±2% uncertainly for this reaction is unlikely to be reduced.

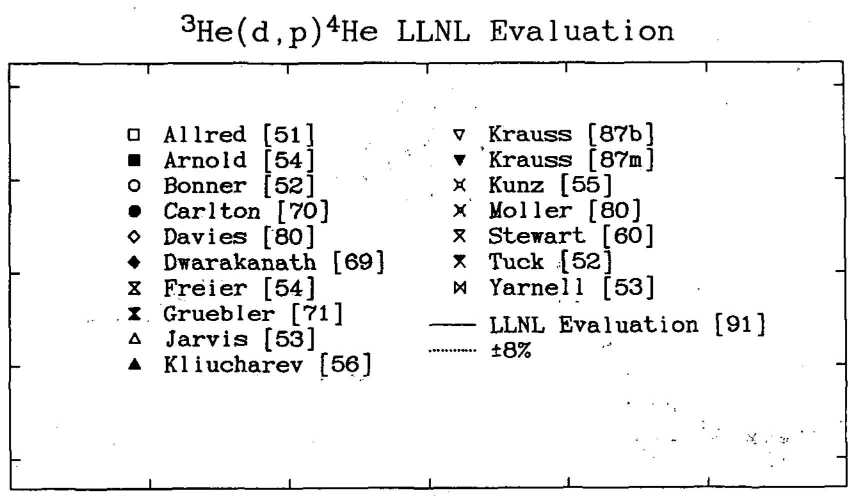

Fig. 8 Reference symbols and authors (with year of publication) for the data base used in the LLNL[91] evaluation of the $^3He(d,p)^4He$ reaction as shown in Figs. 9 and 10. A complete bibliographic listing as well as a detailed description of the evaluation techniques used for this reaction will be presented in a forthcoming LLNL report.

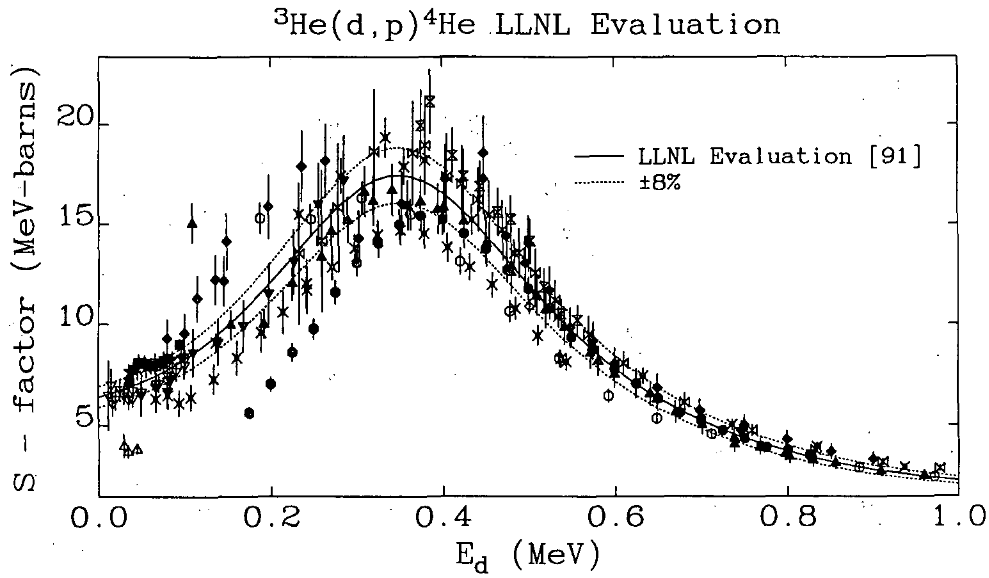

Fig. 9 Plot of the LLNL[91] evaluation of the ^{3}He(d,p)^{4}He reaction in terms of the astrophysical s-factor as a function of laboratory deuteron energy between 1.25 keV and 200 keV. The ±8% indicated on the plot represents our estimate of the uncertainty in the evaluation (at the 95% confidence level). While the data are discrepant in magnitude by more than the quoted errors, the shapes are in good agreement except for two full data sets and the low-energy portion of two other data sets.

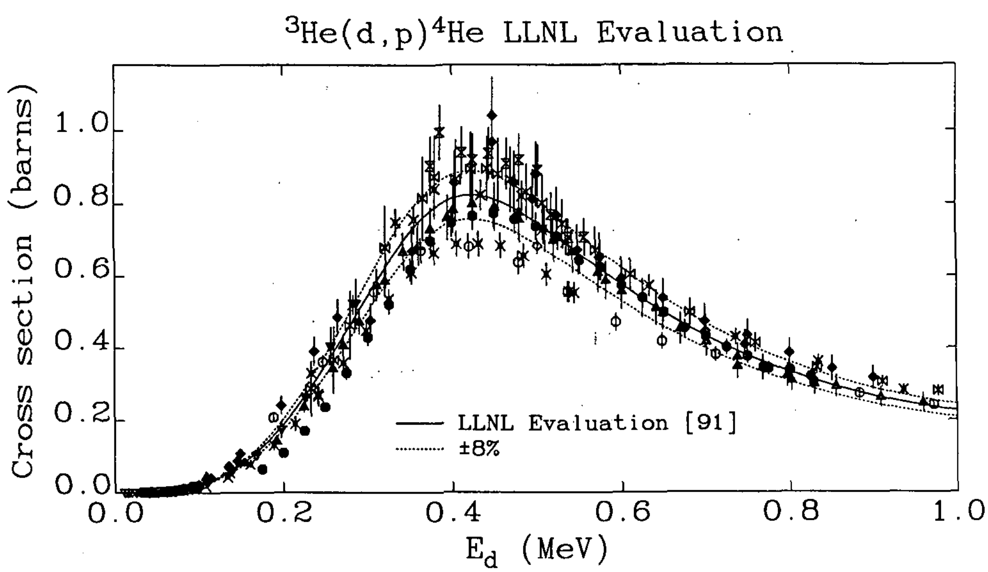

Fig. 10 Plot of the LLNL[91] evaluation of the ^{3}He(d,p)^{4}He reaction cross section from 1.25 keV to 200 keV as a function of laboratory deuteron energy. The evaluation is based on a single-level R-matrix fit to the data as is described in the text. Because of the discrepant nature of the data we have assigned ±8% as the uncertainty in the evaluation (at the 95% confidence level).

The best fit was obtained by simultaneously allowing the data set normalizations to change while fitting with the single-level R-matrix calculation. Since there were several data sets whose overall normalizations were more discrepant than the quoted errors and since it was not obvious why one measurement might be better than another, it was decided that the best one could do was assume that, on the average, the overall normalization of the entire data base was correct. Therefore, the individual data set normalizations were allowed to change subject to the constraint that the average normalization was unity.

e. ^{3}H(t,2n)^{4}He Evaluation

Our data base for the ^{3}H(t,2n)^{4}He reaction contains 6 references and includes 117 integrated cross sections values. By the nature of the reactants, this reaction is difficult to measure and experimental data extend to only 2.2 MeV. Figure 11 shows the ^{3}H(t,2n)^{4}He data up to 1 MeV and our evaluation from 500 eV to 1 MeV plotted in terms of the astrophysical s-factor with ±8% indicated. Our evaluation comes from a least-squares cubic spline fit to all the data in this region. There is a clear change in slope of the low energy data independent of any one data set. At higher energies, the evaluation follows the projection of Govorov[62] and the measurement at 1.9 MeV of Jarmie[58]. Because there exist no measured data above 2.2 MeV some estimate had to be made of the probable shape and magnitude of the high energy ^{3}H(t,2n)^{4}He reaction cross section. Figure 12 shows the high energy evaluation of the ^{3}H(t,2n)^{4}He reaction in comparison with the other four reactions.

2. Advanced Modeling of Reaction Cross Sections for Light Nuclei (D. A. Resler, S. D. Bloom, and S. A. Moszkowski)

Over the last several years we have put together a system of codes for modeling reaction cross sections for light nuclei. The technique involves starting with an effective nucleon-nucleon interaction. In general, nuclear reaction cross sections for light projectiles (n, p, d, t, ^{3}He, α) of low-energy ($E \leq 20$ MeV) incident on light nuclei ($A \leq 20$) are dominated by isolated and overlapping resonance behavior. These resonances are due to the structure of the compound nucleus. By starting with an effective nucleon-nucleon interaction, the properties of the compound nuclear structure can be obtained through the nuclear shell model. This structure information can then be transformed into the required input to an R-matrix code for the calculation of reaction cross sections. Because of the fundamental nature of the calculations, i.e., starting from a nucleon-nucleon interaction, if the method can be used to accurately calculate reaction cross sections where one has data to compare with (such as the evaluations presented in the previous section), then the method can be used with confidence where little or no data exist (such as d+^{6}Li).

In general, the model spaces needed for the shell model calculations require excitations for which current effective nucleon-nucleon interactions do not work properly. In an effort to ameleorate these problems, we are developing a new effective nucleon-nucleon

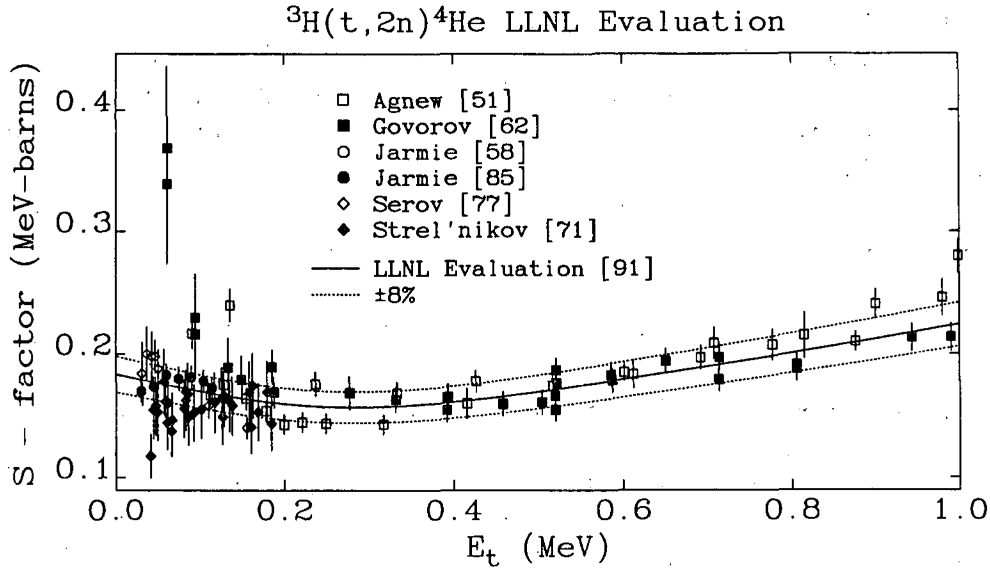

Fig. 11 Plot of the LLNL[91] evaluation of the $^{3}H(t,2n)^{4}He$ reaction in terms of the astrophysical s-factor as a function of laboratory deuteron energy between 500 eV to 1 MeV. The ±8% indicated on the plot represents our estimate of the uncertainty in the evaluation (at the 95% confidence level). Also shown are the reference symbols and authors (with year of publication) for the data base. A complete bibliographic listing as well as a detailed description of the evaluation techniques used for this reaction will be presented in a forthcoming LLNL report.

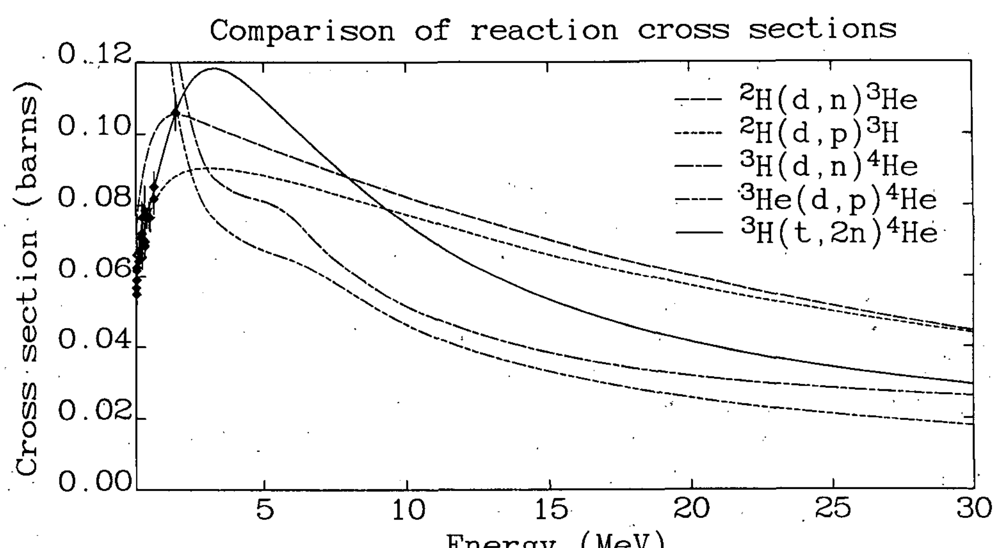

Fig. 12 Comparison of the cross sections for the five reactions considered in this work. Because there exist no measured data above 2.2 MeV for the $^{3}H(t,2n)^{4}He$ reaction some estimate has to be made of the probable shape and magnitude above 2.2 MeV. This comparison shows that what we have chosen is not unreasonable in light of the other reactions.

interaction for use in large model spaces and additionally to correctly determine basic properties of nuclei and nuclear matter (i.e., binding energies/nucleon and saturation) and to reduce to a Skyrme-like (Hartree-Fock) interaction in the short range limit. Our phenomenological interaction consists of three components (see Figure 13), each containing four parts: (1) a potential strength V, (2) a gaussian radial form factor, e^{-r^2/a^2}, (3) non-locality (gaussian in momentum space), $e^{-p^2c^2}$, and (4) a density-dependent term. The longest range (r) component is assumed to be attractive, density independent, and local (c=0). This component is constructed to look like the one pion exchange potential (OPEP). It is also this component which leads to the extra clustering that one finds in ^{4}He. The second component is of shorter range and is assumed to be attractive, density independent, and non-local. The third component is of still shorter range, repulsive, density dependent, and non-local. The last two components look much like a surface delta interaction and are required for saturation. The parameters of our interaction are being determined by least-squares techniques using the global constraints (binding energies/nucleon and saturation) for ^{4}He, ^{16}O, and nuclear matter. We have evidence that such an interaction does much to alleviate the problems previously seen in calculations performed in large model spaces.

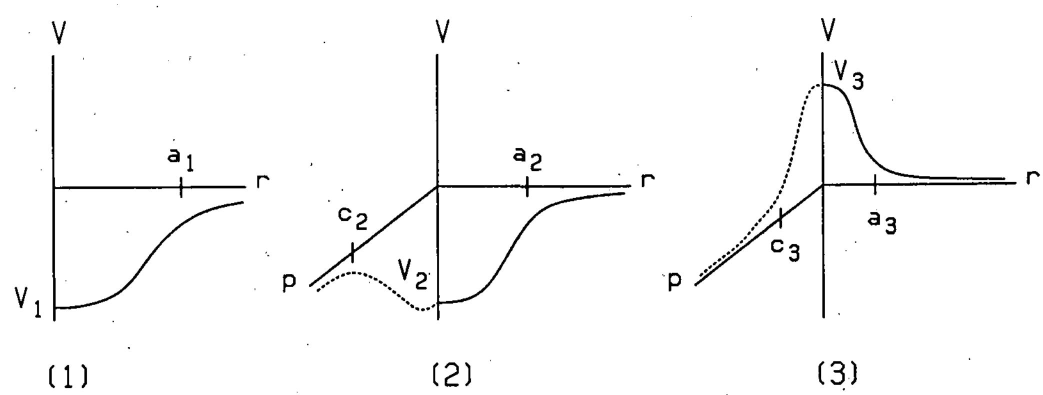

Fig. 13 Diagram of the three components being employed in the present quest for an improved nucleon-nucleon interaction. The first component is constructed to look like a one pion exchange potential and leads to the extra clustering that one finds in ^{4}He. The second and third components look much like a surface delta interaction and are required for saturation. Refer to the text for more details.

3. <u>TDF—A Processed File for Thermonuclear Applications</u> (S. I. Warshaw and R. M. White)

We have created a processed thermonuclear data file, TDF, and the computer routines, written in standard FORTRAN, with which to read this file. The TDF file contains information calculated from our evaluations such as Maxwellian-averaged reaction rates as a function of reaction and plasma temperature, the Maxwellian-averaged average energy of the interacting particles as well as the same quantities for the secondary reaction products.

Also included are routines which provide thermally-broadened spectral information for the secondary reaction products. These routines are useful for either deterministic or Monte Carlo calculations and special emphasis has been placed on making them easy to use. Documentation and availability of TDF and the routines which access it will be available to the user community by early summer 1991.

4. Evaluation of (n,2n) reactions on Isotopes of Y and Zr (M. H. MacGregor and G. Reffo)

We have carried out an evaluation of neutron-induced reactions on the isotopes $^{87,88,89}Y$ and $^{88,89,90}Zr$. These isotopes have been extensively studied in previous evaluations, and they serve as a valuable benchmark. ^{89}Y and ^{90}Zr are stable and there exists experimental information on these isotopes. The other isotopes are unstable and there exists almost no experimental information about them. Hence their cross sections must be obtained by calculational means. These isotopes occur at or near the magic neutron number N=50, which means that the nuclear systematics are varying rapidly in this region, and comprehensive studies must be made in order to extract the proper level densities. We used the Livermore version of the ENEA code set IDA for these calculations.

To calculate all the important particle decay channels, it is necessary to include 35 isotopes of Br, Kr, Rb, Sr, Y and Zr in the evaluation. The neutron resonances for these and neighboring nuclei were statistically analyzed with the IDA module ESTIMA in order to obtain the best values for the Fermi gas constant "a". The variation of "a" with neutron number is shown in Fig. 14, where the influence of the magic number N=50 is clearly apparent. The low-lying levels in these nuclei were analyzed with the IDA module AMLETO in order to obtain the correct nuclear "temperatures". These temperatures are combined with the Fermi gas constants to produce a self-consistent set of Gilbert and Cameron level densities for use in the Hauser-Feshbach formalism. A variety of optical models were also studied in order to obtain the best set of transmission coefficients for use in the Hauser-Feshbach calculations. Intercomparisons between the IDA module PENELOPE and the LLNL ALICE code were made to evaluate pre-equilibrium effects, which have a strong influence on the (n,2n) cross sections. The IDA module POLIFEMO was used to provide the width fluctuation corrections to the Hauser-Feshbach calculations. In the evaluation, the IDA nuclear density and temperature parameters were first obtained as described above, and were then adjusted so as to give the best fits to the available experimental data. These optimized parameters were used to calculate the reactions where no experimental data exist. Calculations involving isomeric-state target nuclei are still in progress. Figures 15, 16, and 17 show comparisons of our calculations for the (n,2n) cross sections of $^{87,88,89}Y$. In Figs. 15 and 16, where experimental data exist, both evaluations are in good agreement. However, in Fig. 17, where no experimental data are available to serve as normalizations, our evaluation differs by roughly 20% from other calculations. We believe this indicates the general level of accuracy that can be expected from theoretical nuclear modeling calculations in this mass region.

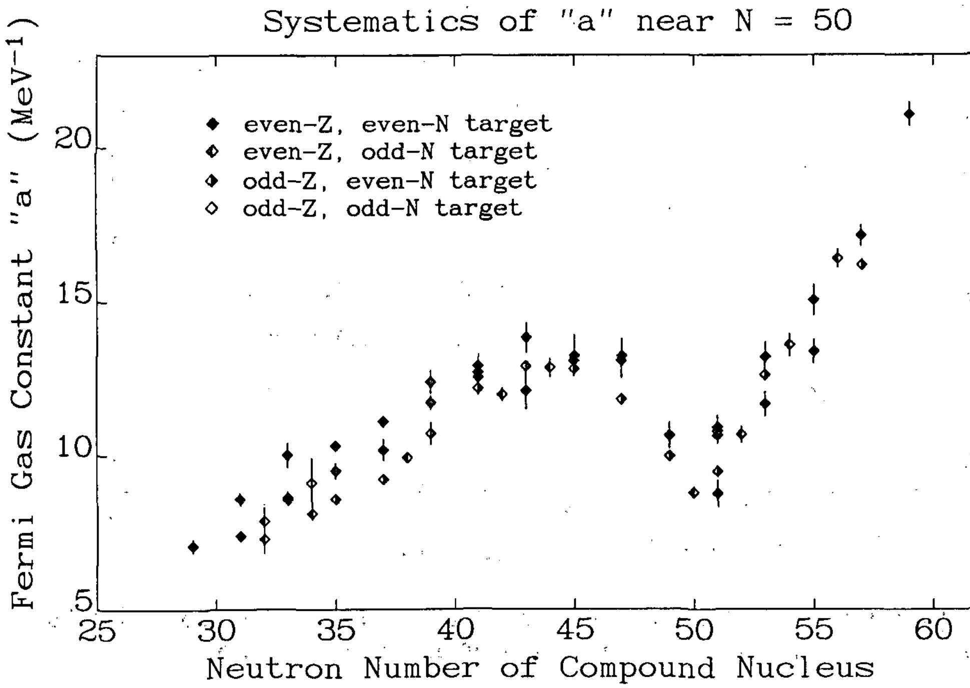

Fig. 14 Systematics of the Fermi gas constant "a" as a function of neutron number near N=50. The influence of the magic number N=50 is clearly apparent. These systematics were obtained from an analysis of neutron resonances using the IDA module ESTIMA.

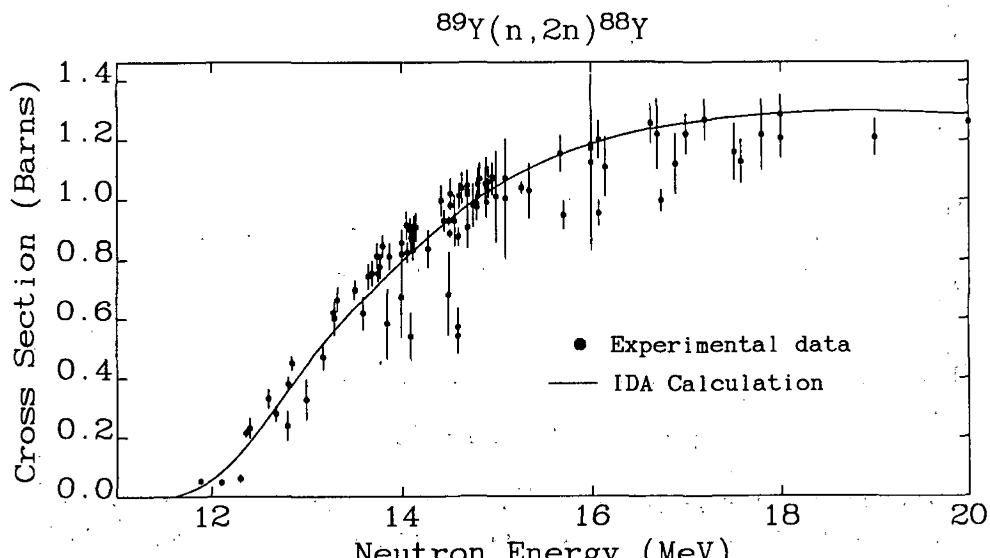

Fig. 15 Comparison of the IDA calculation to the experimental data for the $^{89}Y(n,2n)^{88}Y$ reaction. Details of the IDA calculation are given in the text.

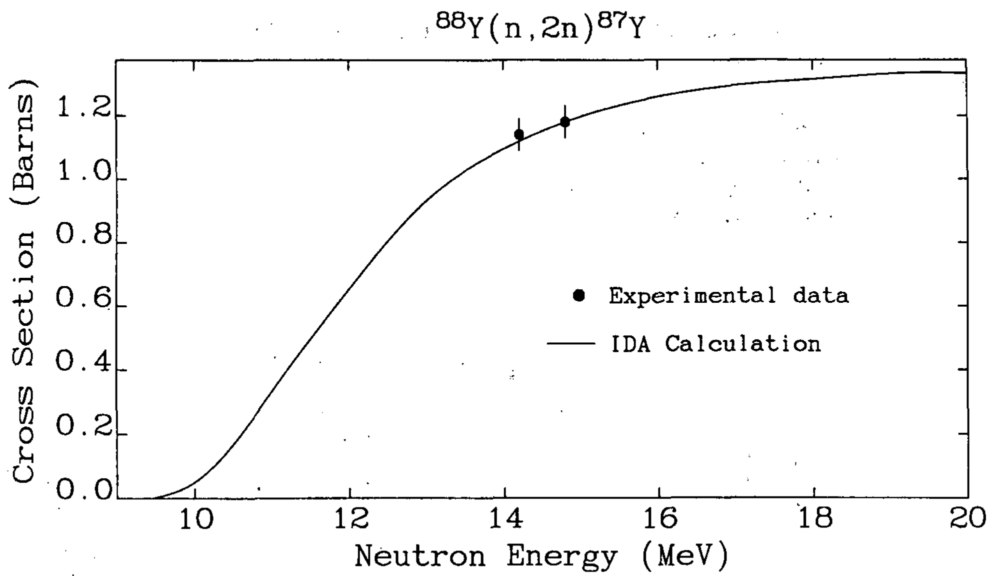

Fig. 16 Comparison of the IDA calculation to the two experimental data points for the $^{88}Y(n,2n)^{87}Y$ reaction. Details of the IDA calculation are given in the text.

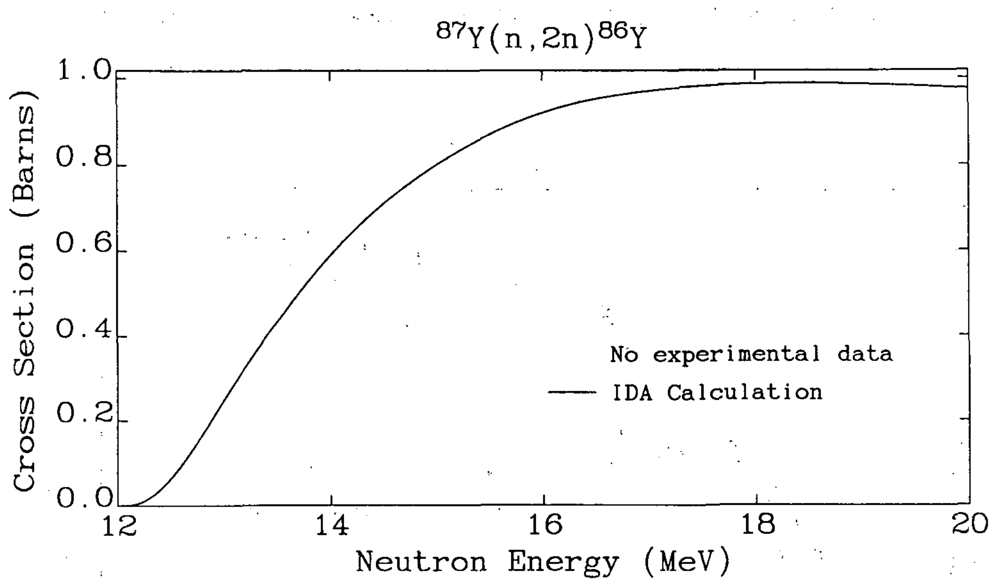

Fig. 17 Shown is the IDA calculation for the $^{87}Y(n,2n)^{86}Y$ reaction. Since there exist no experimental data to serve as normalizations, our evaluation differs by roughly 20% from other calculations and we believe this indicates the general level of accuracy that can be expected from modeling in this mass region.

5. Extension of the LLNL Evaluated Nuclear Data Base (ENDL) to 30 MeV (M. Blann and T. Komoto)

We have been extending our evaluated nuclear data base for reactions induced by neutrons up to 30 MeV. The data base will be suitable for use in transport calculations, and so must give output on an exclusive basis. We have thus far modified the ALICE code to calculate n, p, and α particle spectra with up to three successive particle emission channels (27 channels) on an exclusive basis, giving results in a format suitable for immediate inclusion into the database. We must calculate the contributions from reactions which may emit more than three n, p, or α particles at the higher energies of interest, to see if four particle exclusive reactions need to be included in the calculated data file.

For fissile nuclei we have completed code modifications to follow exclusive fission and non-fission channels up to and including third-chance fission. We have decided on algorithms for treating neutron spectra for fourth and fifth chance fission, to be encoded shortly. Additionally the Bohr-Wheeler fission treatment is being replaced by tabular fission probabilities based closely on experimental results where available.

The fission neutron spectra are now encoded to use the Watt distribution, using neutron multiplicity algorithms developed by R. J. Howerton. Prefission precompound plus compound neutrons are added to the postfission neutron spectra. The precompound plus compound channels determine the cross section vs. excitation used as input into the Howerton algorithms. We believe that reliance on experimental fission probabilities using proven neutron multiplicity algorithms through nuclear modeling will provide a reliable extrapolation to the 30 MeV incident neutron energy regime.

6. Calculated Kerma Values (R. J. Howerton)

Kerma values have been calculated from the January 1991 version of LLNL's Evaluated Neutron Data Library (ENDL). This effort is in support of the IAEA's Coordination Research Program (CRP) on Nuclear Data Needed for Neutron Therapy. Generally, the kerma for a neutron-induced reaction is defined to be the energy available from the reaction (E_n + Q) less the energy carried off by secondary neutrons and photons (E_n is the incident neutron energy and Q is the Q-value for the reaction). The kerma for a material is then obtained by summing the kermas of the individual reactions, properly weighted by isotopic or elemental abundance in the case of composite materials.

Explicit energy distributions for all secondary particles from all neutron-induced reactions are routinely entered into the LLNL ENDL data files. With these quantities, it is possible to insure energy conservation between neutron interaction and neutron-induced gamma-ray production data and to calculate average energy deposits for all secondary particles. The tolerance for energy conservation in ENDL is currently 5% or 100 keV, whichever is less.

The kerma factors are presented in the form of histograms for 175 neutron energy groups commonly used at LLNL for the isotopes and naturally occurring elemental mixtures of isotopes. For composite materials, a subset of these groups is required that eliminates neutron energies below the molecular binding energies of the materials. At these energies, different physical mechanisms than those associated with nuclear reactions are required. The histogram form was selected because it is impractical to tabulate kerma factors on a linear basis and because the kerma factors change slowly enough over the groups that linear interpolation will yield values that are within the uncertainties of the basic data from which they are calculated. Since the calculated kerma factors were derived from the evaluated data in ENDL, any errors in the kerma factors are due to errors in the evaluated library.

A. NUCLEAR DATA MEASUREMENTS

1. Low-Energy (n,charged particle) Cross Sections: The $^{17}O(n,\alpha)\,^{14}C$ Cross Section from 25 meV to Approximately 1 MeV (P.E. Koehler)

The $^{17}O(n,\alpha)^{14}C$ cross section has been measured from 25 meV to approximately 1 MeV. The measurements were made at LANSCE employing our "standard" (n,charged particle) setup[1] with a 10 μm thick solid state detector. The data are shown in Fig. A-1. This reaction may play a role in the nucleosynthesis of heavier elements in nonhomogeneous big bang models. We are currently converting the cross sections into astrophysical reaction rates.

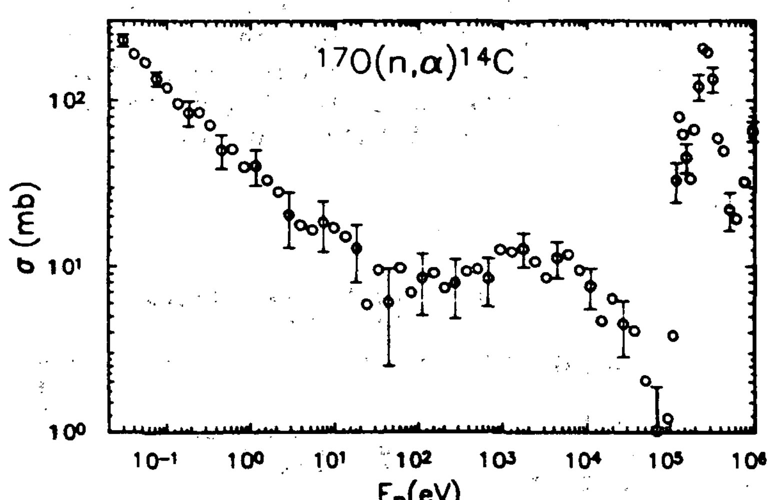

Fig. A-1. The $^{17}O(n,\alpha)^{14}C$ cross section from 25 meV to 1 MeV.

2. Development of a 4π Barium Fluoride Detector for (n,γ) Measurements on Radioactive Targets (P.E. Koehler, S.M. Graff)

During the past few years we have been developing a detector for making (n,γ) measurements at LANSCE on radioactive targets. A drawing of this detector is shown in Fig. A-2. The active region is a cube of barium fluoride, 30 cm on a side, made of 8 cubes 15 cm on a side. Each of the 8 cubes is beveled on two edges so that when the entire detector is assembled there are two 4 cm holes perpendicular to each other, passing through the center of the detector. One of the holes allows the neutron beam to pass through, while the other is for a target ladder. The radioactive target is placed at the center of the 30 cm cube, which acts as a calorimeter for the gamma-ray cascade following the neutron capture. During the past year we received the final parts for this detector and it was assembled. Tests during the 1990 run cycle revealed that the beam related background was much larger than expected. These tests together with Monte Carlo simulations using the program MCNP have identified the source of the problem to be poor collimator design. An example

[1] P.E. Koehler, C.D. Bowman, F.J. Steinkruger, D.C. Moody, G.M. Hale, J.W. Starner, S.A. Wender, R.C. Haight, P.W. Lisowski, and W.L. Talbert, Phys. Rev. C37, 917 (1988).

of the MCNP calculations for our current collimator and two improvements is shown in Fig. A-3. The calculations indicate that we can reduce the beam halo from the collimator by a factor of about 10^6. We are currently fabricating the new collimator and plan to have it installed in time for the second 1991 LAMPF run cycle.

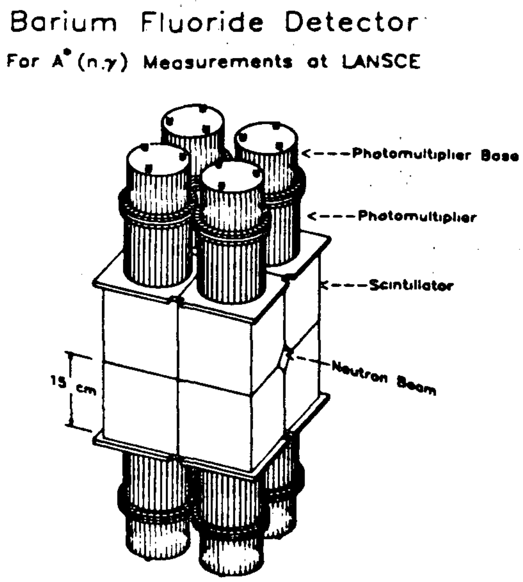

Fig. A-2. Barium fluoride detector for (n,γ) measurements on radioactive targets at LANSCE. Each of the 8 barium fluoride scintillators is enclosed in a separate box and is coupled to its own photomultiplier tube and base. The support structure which holds the 8 independent detectors together is not shown.

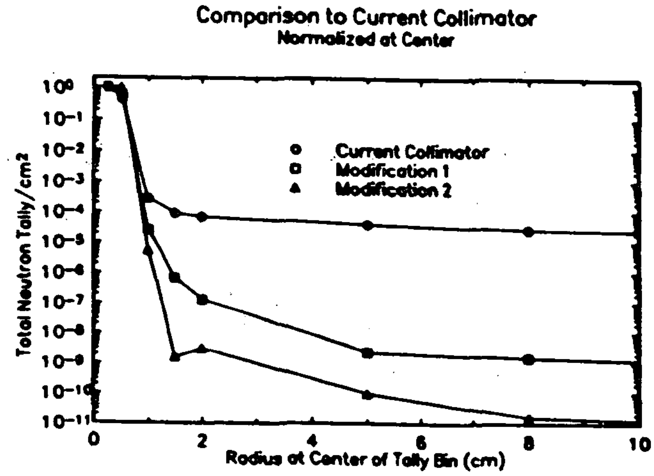

Fig. A-3. MCNP calculations for the beam profile (summed over all incident neutron energies) from the collimator on flight path 4 at LANSCE, and for two improvements to this collimator.

3. <u>Giant Resonance Studies through Neutron Capture</u> (C.M. Laymon , R.O. Nelson, S.A. Wender)

During the past year we completed work on a spectrometer for the detection of high energy gamma rays. The device consists of a 10 cm diameter by 15 cm long bismuth germanate crystal inside of an active plastic scintillator used to veto cosmic ray and escape events. During the 1990 LAMPF beam cycle we used the detector to measure a three-point angular distribution of gamma rays from the $^{40}Ca(n,\gamma)$ reaction with the specific goal of searching for evidence for the existence of the isovector giant quadrupole resonance in ^{41}Ca. Analysis of the data is in progress. Some preliminary results were presented at the Fourth International Workshop on Radiative Capture held in October at Berkeley.

4. Properties of Neutron Induced Fission on ^{238}U (A. Gavron, P. W. Lisowski, W.E. Parker, C. Zoeller)

In our ongoing program to measure various properties of fission induced by neutron reactions on ^{238}U, we have completed our analysis of mass-distribution data obtained in the 1990 run cycle at WNR. A thin (200 mg/cm^2) ^{238}U target was irradiated with neutrons between 2 and 200 MeV. Fission fragments were detected in two PIN diode arrays, and their energy was determined by comparison to ^{252}Cf fission fragments. The masses of the fragments were obtained using momentum conservation, and correcting for neutron emission and energy loss in the foil. Results of the valley-to-peak ratio are presented in Fig. A-4 as a function of the energy of the incoming neutron. We note the rapid increase that does not level off even at the highest energies.

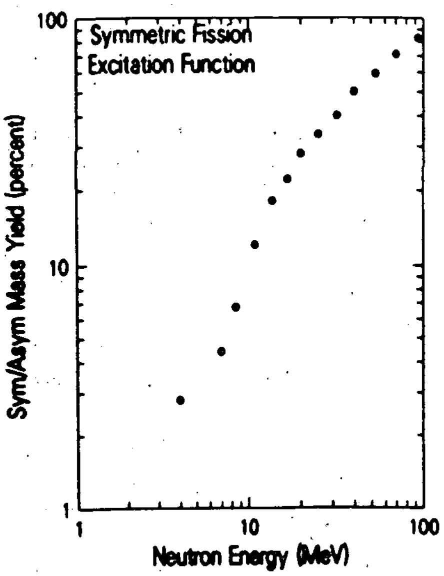

Fig. A-4. Valley to peak ratio (in percent) of fission mass yield as a function of neutron energy

5. High Resolution (n,xγ) Measurements (R.O. Nelson, S.A. Wender, C.M. Laymon, H.A. O'Brien, D.M. Drake, R.C. Haight, P.G. Young, H. Vonach,* A. Pavlik,* P. Englert **)

The program of measurements of absolute cross sections for (n,xγ) reactions begun in 1989 was continued on a longer flight path with additional data obtained for ^{56}Fe and ^{207}Pb samples. The data were measured in the neutron energy range, $3 < E_n < 200$ MeV using HPGe detectors at 90 and 125 degrees. Gamma rays from product nuclei were measured in the range $0.2 < E_\gamma < 4$ MeV. The beam was obtained from the WNR spallation neutron source facility on a 40 m flight path at 30 degrees with respect to the incident 800 MeV proton beam from LAMPF.

Analysis of the data for samples including $^{204,206,207,208}Pb$, ^{89}Y, ^{56}Fe, BN, B_4C, C, Mg, Al, Si, SiO_2, S, Ca, Ti, Cr, Mn, Fe, ^{232}Th, and ^{238}U is continuing. Preliminary results on ^{56}Fe, ^{89}Y and ^{207}Pb were presented at the International Symposium on Capture Gamma-Ray Spectroscopy and Related Topics in Asilomar, and at the International Conference on Accelerators in Research and Industry in Denton Texas.

---

* IRK, Vienna, Austria

** San Jose State University, San Jose, CA

6. Fission Cross Section Ratios For $^{233,234,236}U$ Relative to ^{235}U From 0.5 to 400 MeV (P. W. Lisowski, A. Gavron, W. E. Parker, J. L. Ullmann, S.J. Balestrini, A. D. Carlson,* * O. A. Wasson,* N. W. Hill**)

Neutron-induced fission cross section ratios for samples of $^{233,234,236}U$ relative to ^{235}U have been measured at the WNR neutron Source at Los Alamos from 0.5 to 400 MeV. The fission reaction rate was determined using a fast parallel plate ionization chamber at a 20-m flight path. Cross sections over most of the energy range were also extracted using the neutron fluence determined with three different proton telescope arrangements. Those data provided the shape of the $^{235}U(n,f)$ cross section relative to the hydrogen scattering cross section. That shape was then normalized to the very accurately known value for $^{235}U(n,f)$ at 14 MeV allowing us to obtain cross section section values from the ratio data and our values for $^{235}U(n,f)$. These results will be reported at the International conference on Nuclear Data for Science and Technology, Juelich, Germany, May, 1991.

7. Measurements of (n,charged particle) Reactions Below 50 MeV at WNR in the Study of Nuclear Level Densities (R.C. Haight, S.M. Sterbenz, S.M. Grimes,*** V. Mishra,*** N. Boukharouba,*** R. Pedroni,*** K. Doctor,*** F. Bateman ***)

Nuclear level densities can be studied in three ways through (n,p) and (n,α) reactions at MeV energies: in the residual nuclei by the study of the emission spectrum of charged particles, in the target nucleus by the study of excitation functions of these reactions, and in the compound nucleus by analyzing Ericson fluctuations measured with high resolution. In the last year we have analyzed our high resolution total cross section on silicon to derive level densities in ^{29}Si. Over much of the range, the resolution of these data is superior to that of previous works. Data on $^{28}Si(n,\alpha)$ and (n,p) to resolved final states are being analyzed in the same context. Using the 9-meter flight path for high intensity, we have obtained continuum alpha particle emission spectra from aluminum with better statistics than before. Preliminary data were taken on (n,α) reactions on iron.

8. Cross Sections for (n,α) Reactions on Carbon and ^{10}B (R.C. Haight, S.M. Sterbenz, T.M. Lee, S.M. Grimes,*** F. Bateman,*** R.S. Pedroni,*** V. Mishra,*** N. Boukharouba***)

Neutron-induced reactions on carbon that produce alpha particles are important for a wide range of applications including neutron therapy, neutron dosimetry, characterization of detector efficiencies, neutron heating of fusion materials, and helium production by neutrons. The (n,α) reaction on ^{10}B is used as a standard for flux normalization. These reactions on both targets also can shed light on basic reaction mechanisms for alpha-particle emission in neutron interactions with 1p-shell nuclides. With the 9-meter flight path at WNR/LAMPF, we have taken data on these reactions from 1 MeV to above 30 MeV. Alpha particles with energies down to 1 MeV were detected by delta-E-E coincidence counters with low pressure, windowless delta-E proportional detectors. Continuum alpha particle emission was measured from the carbon target. For the ^{10}B target, alpha particles from the $^{10}B(n,\alpha)^7Li$ (g.s.+ 0.478 MeV state) were observed. Angular distributions were measured from 30 to 135 degrees.

---

* National Institute of Standards and Technology, Gaithersburg, MD

** Oak Ridge National Laboratory, Oak Ridge, TN

*** Ohio University, Athens, OH

9. First Measurement of the (n,p) Reaction Unit Cross Section in the fp Shell from $^{64}Ni(n,p)$ at 60 to 260 MeV (A. G. Ling, D.S. Sorenson, J.L. Ullmann, R.C. Haight, N.S.P. King, P.W. Lisowski, J.Rapaport,* B.K. Park,* R.W. Finlay,* J.L. Romero,* F.P. Brady,** C. Howell*** , W. Tornow ***)

Cross sections have been measured for the reaction $^{64}Ni(n,p)^{64}Co(gs)$ at average angles of 2.6, 5.0, and 7.8 degrees and binned at three neutron energies between 60 and 260 MeV. These measurements, together with the known β^- decay strength of ^{64}Co, provide the only absolute cross section to B(GT) calibration point in the (n,p) channel for fp-shell nuclei. Since the (e^-,ν_e) channel involves the same nuclear matrix element as the (n,p) channel, the results here are important for supernova modeling codes which depend on knowledge of electron capture rates of fp-shell nuclei, such as iron, to determine the parameters of stellar collapse.

10. The Energy Dependence of Gamow-Teller Strength in p-shell Nuclei Observed in the (n,p) Reaction (D.S. Sorenson, A.G. Ling, J.L. Ullmann, R.C. Haight, N.S.P. King, P.W. Lisowski, J.Rapaport,* B.K. Park,* R.W. Finlay,* X. Aslanoglou,* J.L. Romero,** F.P. Brady,** J.R. Drummond,** C. Howell,*** W. Tornow ***)

Cross sections from zero to ten degrees (in the lab) have been measured for ground-state Gamow-Teller transitions for the reactions $^{6}Li(n,p)$, $^{12}C(n,p)$, and $^{13}C(n,p)$ from 65 to 250 MeV. The 90 meter station at Target 4 of the WNR white-neutron facility at LAMPF was used to obtain these data. Unit cross sections and volume integrals ($J_{\sigma\tau}$) for the spin-flip, isospin-flip part of the effective nucleon-nucleon interaction have been obntained. $J_{\sigma\tau}$ values extracted from these reactions agree to within 5% over the entire energy range. The unit cross sections (the cross section to B(GT) conversion factor) follow a smooth energy and mass dependence.

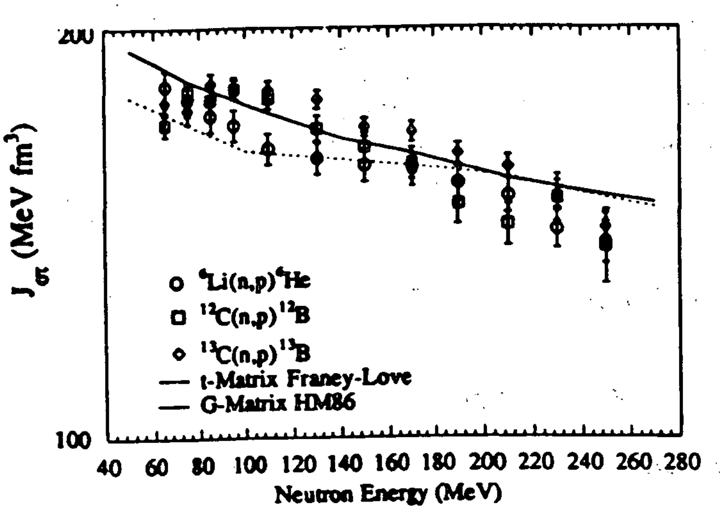

Fig. A-5. Volume integral $J_{\sigma\tau}$ for the ground state transition to the residual nucleus in the reactions $^{6}Li(n,p)^{6}He$, $^{12}C(n,p)B$, $^{13}C(n,p)^{13}B$. t-matrix and G-matrix predictions are also shown.

*Ohio Universiy, Athens, OH

** University of California, Davis, Davis, CA

*** Duke University, Durham, NC

11. Neutron-Proton Bremsstrahlung Studies at the WNR (S.A. Wender, R.O. Nelson, M.E. Schillaci, M. Blann,* D. Krofcheck,* V.R. Brown,* F.P. Brady,** D. Skopik***)

A program to study the gamma emission following neutron-proton scattering (neutron-proton bremsstrahlung) has been initiated at the WNR. The goals of the measurements are to study the effect of meson exchange currents in the nucleon-nucleon interaction over a wide range of inelasticities. These effects have been calculated to be large but have never been measured in detail. In addition, these measurements will contribute to the understanding of the source of high-energy gamma rays that have been observed in heavy-ion reactions.

The program is planned in three phases. In the first phase, the inclusive gamma-production cross section for incident neutron between 50 and 400 MeV on a liquid hydrogen target will be measured. The gamma rays will be detected in a gamma-ray telescope consisting of an active converter, two delta-E detectors and a large volume calorimeter. In the second phase, a segmented array of proton detectors will be constructed and the and the proton-gamma coincidence will be measured. This will allow identification of the NPB events. In the third phase an array of neutron detectors will be assembled and the neutron-proton-gamma coincidence will be measured. The first phase is scheduled to begin in June, 1991.

12. Direct Mass Measurements of the Neutron-Rich isotopes of Fluorine through Chlorine Jan M. Wouters, David Vieira, and Gilbert W. Butler****

The masses of the neutron-rich sodium isotopes with $N \geq 20$ manifest an enhanced binding energy anomaly that has challenged experimentalists and theorists ever since they were first reported.[1] Early interpretation assumed that this anomalous feature occured as the nucleus took on a prolate shape when neutron single-particle levels reordered and destroyed the normal $d_{3/2}$, $f_{7/2}$ magic shell gap at $N = 20$. Subsequent β-endpoint and first excited-state measurements demonstrated the existence of the anomaly in ^{32}Mg. The challenge for experimentalists has been to delineate the region of enhanced binding by measuring the masses of the neutron-rich isotopes for the adjacent elements; for theorists, the task was to reproduce the enhanced binding and understand the basic nature of these deformed nuclei. Additional mass measurements were not available until development of the recoil mass spectrometer, which has the advantages of (1) being element-independent and fast and (2) requiring little or no information about the excited states of the nuclei being studied.

Beginning in 1986, two groups using different time-of-flight recoil spectrometers

---

* Lawrence Livermore National Laboratory, Livermore, CA

** University of California, Davis, Davis, CA

*** University of Saskatchewan, Saskatoon, CAN

**** In collaboration with scientists from Utah State University, Logan, Utah; Universität München, München, Germany; Physikalisches Institut, Universität Giessen, Giessen, Germany; and Nanjing University, Nanjing, People's Republic of China

[1] C. Thibault *et al.*, *Phys. Rev.* **C12**, 644 (1975).

independently published new mass measurements that confirmed the existence of the anomaly but also suggesting that the feature was localized and smaller in magnitude than originally reported.[2,3] In this article, covering the neutron-rich isotopes of fluorine through chlorine, we attempt to resolve the limitations of previous work by presenting our recent mass measurements using the Time-of-Flight Isochronous (TOFI) spectrometer. We are reexamining this mass region now because advances in our experimental technique enable us to (1) measure more neutron-rich nuclei than we originally reported, (2) increase the accuracy of the mass values of previously measured nuclei, and (3) extend our measurements to those neutron-rich nuclei of higher atomic number. In addition, recent theoretical work has provided new insight into why the neutron-rich sodium isotopes possess enhanced binding; however, the extended predictions of these theories require verification through comparisons to the experimental mass surface.

To determine a mass, we measure the mass-to-charge, velocity, energy, and energy loss characteristics for each ion of interest passing through our experimental apparatus. This apparatus, located at the Los Alamos Meson Physics Facility, consists of a transport line, the TOFI spectrometer, and associated detector systems. A small fraction of the recoiling neutron-rich nuclei that are produced by means of fragmentation reactions are captured, prefiltered, and conveyed to the spectrometer by the transport line. This line also contains detectors for measuring the velocity of each ion. The TOFI spectrometer is isochronous; thus each ion's flight-time through TOFI is directly proportional to its mass-to-charge ratio and independent of its velocity. Because the separation in mass between isobars is small and not resolvable using TOFI, we use a Bragg detector (a special gas ionization detector) to determine the Z and to measure the energy of each ion.

Our measurements of 34 nuclei cover the Z region from fluorine to chlorine and include masses for ^{36}Al, ^{38}Si, ^{41}P, and ^{43}S, which are the most neutron-rich isotopes measured for these elements. We have compared our masses to several shell model theories and mass models in this region. Except for slight discrepancies, the masses determined for the most neutron-rich nuclei of silicon through chlorine agree quite well with theoretical masses. The most interesting results are obtained through comparisons of our experimental work and shell model theories for the sodium region.

Fig. A-6 compares our data to the shell model calculations of Wildenthal and Warburton *et al.*[4,5] The comparison with Wildenthal's calculations illustrates the reason experimentalists and theorists are interested in the sodium masses: there is good agreement between theory and experimental results throughout the entire sd-shell except for the N = 20 isotones that are centered about ^{31}Na. Extensive studies by Wildenthal *et al.* demonstrated that within the sd basis space alone the shell model could not reproduce the ground-state binding energies of these nuclei.

To date, the calculation of Warburton *et al.* is the most complete attempt to expand the shell model vector space beyond the sd shell and to account for the discrepancies described above. The interaction used in this model enables us to calculate ground-state masses by

---

[2] D. J. Vieira *et al.*, *Phys. Rev.* Lett. **57**, 3253 (1986).

[3] A. Gillibert *et al.*, *Phys. Lett.* **B192**, 39 (1987).

[4] B. H. Wildenthal, *Prog. Part. Nucl. Phys.* **11**, 5 (1984)

[5] E. K. Warburton, J. A. Becker and B. A. Brown, *Phys. Rev.* **C41**, 1147 (1990).

above. The interaction used in this model enables us to calculate ground-state masses by using separate model spaces encompassing 0, 1, 2, and 3 particle-hole neutron excitations. In Fig. A-6 we have plotted the calculation that best agrees with experiment for each nucleus; that is, the 1 neutron excitation space for Z = 10-11 N = 21, the 2 neutron excitation space for Z = 10-12 N = 20,22 and ^{33}Mg, and the 0 neutron excitation space for all other cases. The agreement is substantially improved over Wildenthal's[4] calculation for the region of the sodium anomaly and is even better than originally demonstrated by Warburton *et al.*[5] because our masses are less bound than the original sodium and magnesium mass measurements were. This result underlies the local nature (Z=10-12, n=20-22) of the enhanced binding energy effect and leads to the conclusion that the neutron/proton interaction has a strong Z-dependence.

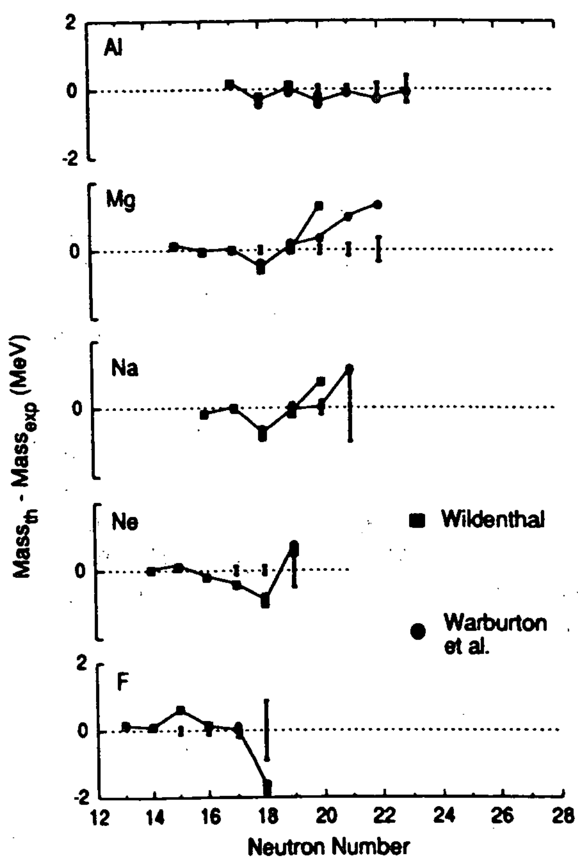

Fig. A-6. The weighted average of our data is compared to the Wildenthal and Warburton shell model calculations. In several instances, the predictions of the two calculations are virtually identical--as is indicated here by a single line but two data points, one over the other. We have added experimental error bars for our data only.

Our results demonstrate that the region of enhanced binding previously found near ^{32}Na is real, although the enhancement is roughly half as large as originally reported. Comparison of our masses to shell model calculations show that this region of enhanced binding can be understood in terms of particle-hole neutron excitations across the sd and fp shells. The systematics of low-lying energy levels from these models indicate that the nuclei with Z = 10-12 and N = 20-22 can be described as an island of inversion in which the nuclei are prolate deformed. For the neutron-rich isotopes of silicon through chlorine, our data agree well with a variety of models, demonstrating the well-behaved nature of these nuclei. The remaining discrepancies between theory and experiment, especially for the island of inversion nuclei, suggest the need for (1) full sdpf model space calculations, (2) additional masses, and (3) measurements of the spins, parities, and excitation energies of low-lying states in this region.

B. NUCLEAR DATA EVALUATION

1. Calculation of (n,xγ) Cross Sections Between Threshold and 100 MeV for Fe, Y, and Pb Isotopes (P. G. Young)

An experimental program is in progress at the Los Alamos National Laboratory WNR/LAMPF facility to perform high-resolution measurements of (n,xγ) cross sections for individual lines up to incident neutron energies in the medium-energy range for a variety of target materials.[1,2] These measurements utilize the white neutron source at WNR and make use of high resolution germanium detectors to provide signatures of individual (n,xn) reactions. In addition to providing data useful for programmatic activities such as accelerator shielding, an important goal of these measurements is to develop a data base that will permit testing of the details of nuclear models that are presently used in this energy range and to thereby facilitate improvements in the underlying nuclear theories. We have begun to perform such tests by carrying out calculations using the GNASH Hauser-Feshbach statistical theory code to 100 MeV for Fe, Y, and Pb isotopes.[3]

The calculations make use of two existing level density representations, namely, the usual level density parameterization of Gilbert and Cameron[4] that has been incorporated in many lower energy calculations, and the model of Ignatyuk *et al.*,[5] which utilizes an energy-dependent level density parameter that is more appropriate for higher energies. Standard parameterizations were used for the preequilibrium model and gamma ray transmission coefficients, and spherical optical model potentials were employed to calculate particle transmission coefficients.

Comparisons of the calculations with the WNR/LAMPF measurements of the 803-keV and 960-keV gamma rays from ^{208}Pb(n,3nγ)^{206}Pb and ^{208}Pb(n,7nγ)^{202}Pb reactions, respectively, are shown in Fig. B-1. While good agreement is found between the calculations and measurements of the (n,3n) γ-ray, the calculated values are a factor of two high for the (n,7n) γ-ray. In general, the calculations with the Ignatyuk level density were found to be superior at higher energies, as expected. In most cases agreement with experiment was reasonable at incident energies below ≈ 40 MeV but improvement in the modeling is needed at higher energies.

---

[1] R. O. Nelson, S. A. Wender, and G. L. Morgan, "High Resolution Measurement of ^{nat}Fe(n,xγ) at the WNR," *Bull. Am. Phys. Soc.* **34**, 1233, J7.12 (1989).

[2] R. C. Haight, D. M. Drake, M. Drosg, C. M. Laymon, G. L. Morgan, R. O. Nelson, S. A. Wender, P. G. Young, H. Vonach, A. Pavlik, S. Tagesen, D. C. Larson, and D. S. Dale, "Cross Sections for the Reactions ^{204,206,207,208}Pb(n,xn), 1 ≤ x ≤ 11, from Threshold to Over 100 MeV," *Bull. Am. Phys. Soc.* **35**, 1038, I6.8 (1990).

[3] P. G. Young, R. C. Haight, R. O. Nelson, S. A. Wender, C. M. Laymon, G. L. Morgan, D. M. Drake, M. Drosg, H. Vonach, A. Pavlik, S. Tagesen, D. C. Larson, and D. S. Dale, "Calculation of (n,xγ) Cross Sections Between Threshold and 100 MeV for Fe and Pb Isotopes: Comparisons with Experimental Data," presented at the *IAEA Third Research Coordination Meeting on Methods for the Calculation of Neutron Nuclear Data for Structural Materials of Fast and Fusion Reactors*, Vienna, 20-22 June 1990, LA-UR-90-2129 (proceedings to be published).

[4] A. Gilbert and A. G. W. Cameron, "A Composite Nuclear-Level Density formula with Shell Corrections," *Can. J. Phys.* **43**, 1446 (1965).

[5] A. V. Ignatyuk, G. N. Smirenkin, and A. S. Tishin, "Phenomenological Description of the Energy Dependence of the Level Density Parameter," *Sov. J. Nucl. Phys.* **21**, 255 (1975).

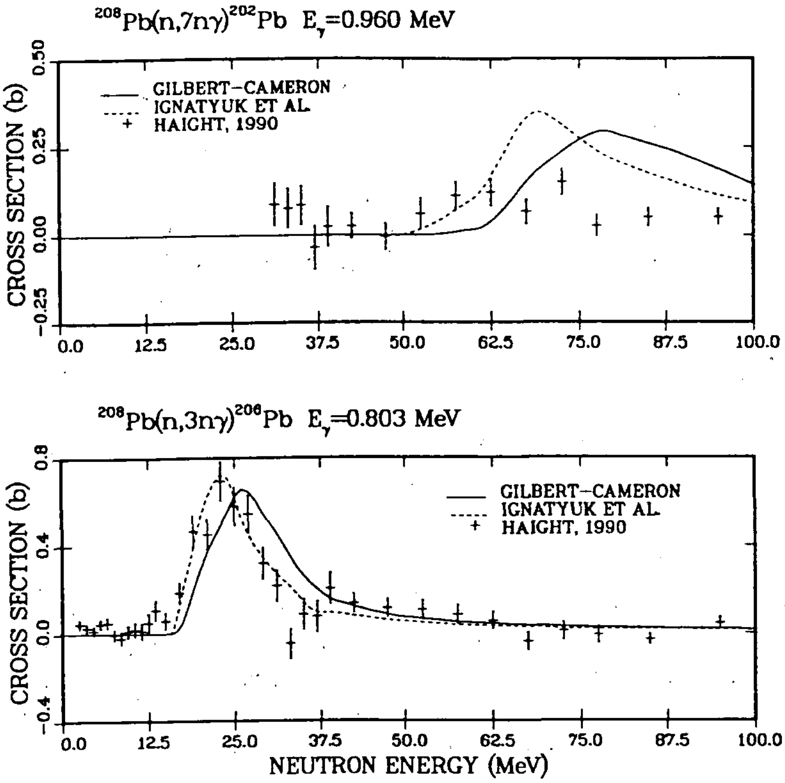

Fig. B-1. Comparison of calculated and measured values of the $^{208}Pb(n,3n\gamma)^{206}Pb$ cross section for the 0.803-MeV gamma ray and of the $^{208}Pb(n,7n\gamma)^{202}Pb$ cross section for the 0.960-MeV gamma ray. The solid curves were calculated using the Gilbert and Cameron[4] model for level densities and the dashed curves were obtained using the representation of Ignatyuk *et al.*[5]

2. Covariance Analyses for ENDF/B-VI $\bar{\nu}_p$ for ^{235}U, ^{237}Np, and ^{239}Pu and the $^{239}Pu(n,f)$ Cross Section (P. G. Young)

Covariance analyses, that is, analyses of experimental data that include consideration of uncertainties and correlations within and among experiments, were performed at Los Alamos for a number of reactions that are important in ENDF/B-VI. Included among the reactions analyzed in this manner are $\bar{\nu}_p$ for ^{235}U, ^{237}Np, and ^{239}Pu, and the $^{239}Pu(n,f)$ cross section. The motivation for these analyses was to ensure that new evaluations in ENDF/B-VI include reliable analyses of the most recent experimental data. In the case of the $^{239}Pu(n,f)$ cross section, an earlier covariance analysis had already been performed that was part of a thorough evaluation[1] of the standard cross sections for ENDF/B-VI. However, the standards analysis was completed before results from two new measurements[2,3] were available. It was discovered that inclusion of the new $^{239}Pu(n,f)$ measurements in the present covariance analysis resulted in evaluations that removed a 1% discrepancy with k_{eff} reactivity calculations for the JEZEBEL critical assembly, which occurred using the (n,f) cross section from the standards analysis. In addition, it was found that use of the new $\bar{\nu}_p$ covariance analyses for the ^{239}Pu and ^{235}U evaluations further reduced differences in calculated versus measured k_{eff} for the JEZEBEL and GODIVA assemblies.

Results from the covariance analysis of the $^{239}Pu(n,f)$ cross section (labeled ENDF/B-VI) are compared to a sampling of experimental data and to the previous ENDF/B-V.2 evaluation in Fig. B-2. Similarly, results from the $\bar{\nu}_p$ covariance analysis for ^{235}U are given in Fig. B-3. All experimental data have been corrected for ENDF/B-VI standards.

[1]R. Peelle and H. Condé, "Neutron Standards Data," *Proc. Int. Conf. on Nucl. Data for Science and Tech.*, Mito, Japan, 30 May - 3 June 1988 [Ed. S. Igarasi, Saikon Publishing. Co., Ltd., Toyko, 1988], p. 1005.

[2] P. W. Lisowski, J. L. Ullmann, S. J. Balestrini, A. D. Carlson, O. A. Wasson, and N. W. Hill, "Neutron-Induced Fission Cross-Section Ratios for ^{232}Th, ^{235,238}U, ^{237}Np, and ^{239}Pu from 1 to 400 MeV," Int. Conf. *Nucl. Data for Sci. and Tech.* Mito, Japan, May 30, 1988 (Ed., S. Igarasi, Saikon Pub.. Co., Ltd., 1988), p. 97.

[3] J. W. Meadows, "The Fission Cross Section of ^{237}Np Relative to ^{235}U from 0.1 to 9.4 MeV," *Nucl. Sci. Eng.* **85**, 271 (1983); J. Meadows, "The Fission Cross Sections of ^{230}Th, ^{232}Th, ^{233}U, ^{234}U, ^{236}U, ^{238}U, ^{237}Np, ^{239}Pu and ^{242}Pu Relative to ^{235}U at 14.74 MeV Neutron Energy," *Ann. Nucl. En.* **15**,421 (1988).

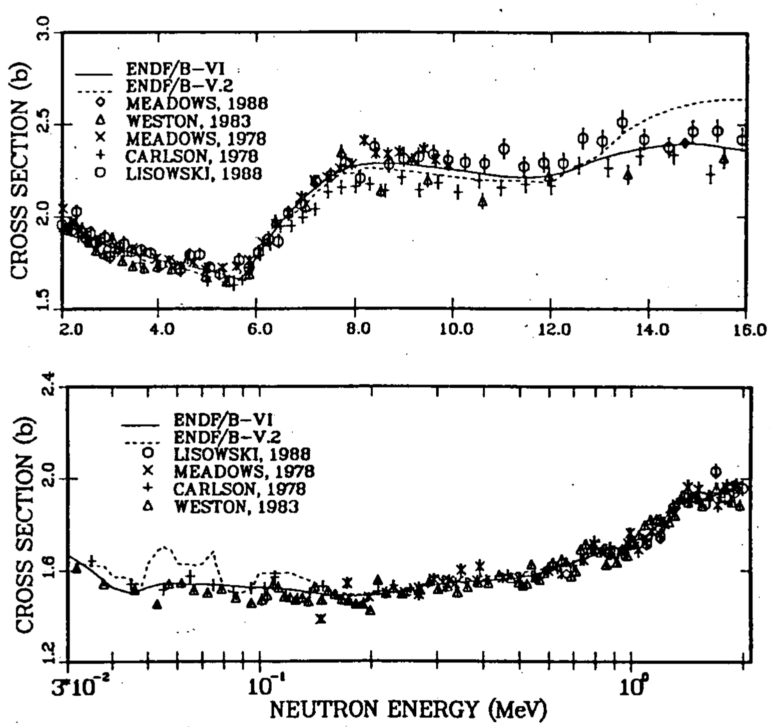

Fig. B-2. Comparison of the ENDF/B-VI evaluation of the ^{239}Pu(n,f) cross section with a sampling of experimental data, all normalized using ENDF/B-VI standards, and with the previous ENDF/B-V.2 evaluation.

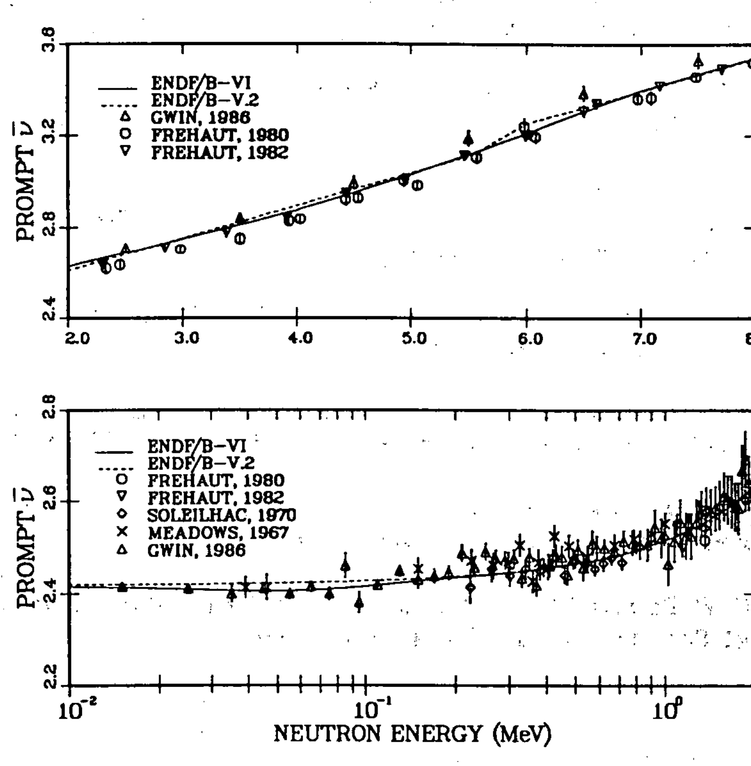

Fig. B-3. Comparison of the $\bar{\nu}_p$ evaluation in ENDF/B-VI for ^{235}U with part of the experimental data base and with ENDF/B-V.2. The experimental data were all obtained relative to ^{252}Cf $\bar{\nu}$ and have been normalized to ENDF/B-VI standards.

3. Decay and Fission-Product Yield Data [T. R. England, M. C. Brady (ORNL), J. Kakatura (JAERI), F. M. Mann (HEDL), C. W. Reich (INEL), G. Rudstam (Swedish Research Councils Lab., Studsvik, Sweden), R. E. Schenter (HEDL), and W. B. Wilson]

Work in progress was summarized in the last Los Alamos Report to the Department of Energy Nuclear Data Committee. Some files are still incomplete in the required ENDF format but have been used in local codes to test the spectra and total beta, gamma, and delayed neutron spectra. Comparisons have been made with preliminary JEF, JENDL files, Studsvik measured spectra, and theoretical data from H. V. Klapdor (Max Planck Inst. Heidelberg, Germany). Yield evaluations from the UK were supplied to us in February 1991 and have not been compared with US evaluations as yet. (The UK data base is based largely upon the data we supplied for EXFOR, but their evaluation methods differ.) The US yield data base extends through 1990.

A Los Alamos code to process all types of decay data was completed but is not documented as yet. Decay data are being expanded to include a wider range of nuclides for use in codes that are employed for SSC, ATW, NPB, etc. studies (see the contribution from HEDL).

---

[1]T. R. England and B. F. Rider, "Evaluation and Compilation of Fission Product Yields, 1990," ENDF-349, in draft form (to be published as a LANL report; this will be the primary documentation for ENDF/B-VI yields).

[2]T. R. England, F. M. Mann, C. W. Reich, and R. E. Schenter, "ENDF/B-VI Radioactive Decay and Yield Libraries," *Trans. Am. Nucl. Soc.* **60**, pp. 614-616 (Nov. 26-30, 1989).

[3]M. C. Brady and T. R. England, "Validation of Aggregate Delayed Neutron Spectra Calculated from Precursor Data," Proc. *Int. Conf. Physics of Reactions: Design and Computation, PHYSOR '90*, Marseilles, France, 23-26 April 1990 (LA-UR 89-3386).

[4]T. R. England, B. F. Rider, and M. C. Brady, "Yield Data for the Japan/US Actinides Program," Los Alamos informal document LA-UR-89-4023 (December 1989).

[5]T. R. England, B. F. Rider, C. W. Reich, F. Mann, M. C. Brady, J. Katakura, R. E. Schenter, "ENDF/B-VI Yield and Decay Data File: Status, November 1989," Los Alamos informal document LA-UR-89- 4256 (Nov. 1989).

[6]J. Katakura and T. R. England, "Augmentation of ENDF/B Fission-Product Gamma-Ray Spectra by Calculated Spectra," in draft form (to be published as a LANL report, 1991).

[7]T. R. England, B. F. Rider, and M. C. Brady, "Fission-Product Chain Yields and Delayed Neutrons: ANS 5.2 and ANS 5.8," *Trans. Am. Nucl. Soc.* **62**, p. 529.

[8]R. E. Schenter, T. R. England, and J. Katakura, "Status and Future for ANSI/ANS-5.1 Decay Heat Power in Light-Water Reactors, *Trans. Am. Nucl. Soc.* **62**, p. 534 (WHC-SA-0977-S).

[9]G. Rudstam and T. R. England, "Test of Pre-ENDF-VI Decay and Fission Yields," Los Alamos National Laboratory report LA-11909-MS (July 1990).

[10]C. W. Reich and T. R. England, "The File of Evaluated Decay Data in ENDF/B," to be presented at the Am. Nucl. Soc. Mtg., Orlando, Florida, 2-6 June 1991.

4. Ion Induced Thick-Target Nuclide Production and Radiation Sources [W. B. Wilson, M. Bozoian, R. T. Perry (N-12, LANL), and P. G. Young]

Our activity in ion reaction data has grown from low-energy reactions of decay α's in (α,n) reactions on light targets[1] to medium-energy reactions of protons and α's with a range of targets.[2-5] This extension has relied heavily upon nuclear model code results, producing reaction cross sections and thick-target yield values with rather large uncertainties but useful in a variety of applications. The range of particles and energies studied are given in Table B-I.

TABLE B-I. Targets and Energies for which Thick Target Yields Have Been Calculated

Target	Particle Energy, MeV: Protons	Particle Energy, MeV: Alphas
$_{4}$Be	≤ 100	≤ 50
$_{5}$B		≤ 50
$_{6}$C	≤ 100	≤ 50
$_{7}$N		≤ 50
$_{8}$O	≤ 100	≤ 50
$_{9}$F		≤ 50
$_{10}$Ne	≤ 100	≤ 50
$_{11}$Na		≤ 50
$_{12}$Mg		≤ 50
$_{13}$Al	≤100	≤ 50
$_{14}$Si	≤ 100	≤ 50
$_{15}$P		≤ 50
$_{17}$Cl		≤ 50
$_{26}$Fe	≤ 50	
$_{27}$Co	≤ 50	
$_{28}$Ni	≤ 50	
$_{29}$Cu	≤ 100	
$_{74}$W	≤ 50	
$_{83}$Bi	≤ 100	

[1] W. B. Wilson, M. Bozoian, and R. T. Perry, "Calculated α-Induced Thick Target Neutron Yields and Spectra, with Comparison to Measured Data," *Proc. Int. Conf. on Nuclear Data for Sci. Tech.*, May 30-June 3, 2988, Mito, Japan (1988), pp. 1193-1197.

[2] W. B. Wilson, T. R. England, R. J. LaBauve, and J. A. Mitchell, "Calculated Radionuclide Inventories of High-Exposure LWR Fuels," Nuclear Safety **29**, 177 (1988).

[3] W. B. Wilson, E. D. Arthur, M. Bozoian, R. T. Perry, and P. G. Young, "Calculated Proton-Induced Thick-Target Neutron and Gamma Yield Spectra for $E_p \leq 100$ MeV," Trans. Am. Nucl. Soc. **60**, 273 (1989).

[4] M. Bozoian, R. T. Perry, and W. B. Wilson, "Calculated α-Induced Thick-Target Neutron and Radionuclide Yields for $E_\alpha \leq 50$ MeV," Proc. *Workshop on High Energy and Heavy Ion Beams in Materials Analysis*, June 14-17, 1989, Albuquerque, New Mexico (1990), pp. 51-59.

[5] W. B. Wilson, E. D. Arthur, M. Bozoian, and R. T. Perry, "Calculated Proton-Induced Thick-Target Neutron and Radionuclide Yields for $E_p \leq 100$ MeV," *Proc. Workshop on High Energy and Heavy Ion Beams in Materials Analysis*, June 14-17, 1989, Albuquerque, New Mexico (1990), pp. 39-49.

5. Tests of the d+d Reactions at Low Energies from Muon-Catalyzed Fusion Experiments (G. M. Hale)

It is becoming apparent that muon-catalyzed fusion experiments offer the most sensitive tests of the charged-particle fusion reactions at low energies. The presence of the muon in these experiments reduces the Coulomb barrier, and selects particular spin states in some cases, giving for charged-particle reactions the same kind of information that comes from measuring spin-dependent scattering lengths for thermal neutron scattering.

In the case of the d+d reactions, for example, ddμ measurements at room temperature pick out the triplet d-d spin states, which because of the symmetry of the wavefunction, select only the P-wave states at low energies. This type of experiment[1] gives the surprising result that the neutron branch of the reaction is enhanced about 40% with respect to the proton branch. A more recent experiment[2] in which the temperature is varied, allowing an admixture of even spin states (*i.e.*, d-d S-waves), shows that the branching ratio decreases and approaches unity as the temperature is lowered. All of these observations, as well as the absolute fusion rate, can be explained by the charge-independent R-matrix analysis of reactions in the four-nucleon system that is being done at Los Alamos.

In the charge-independent A=4 analysis, the isospin-1 (T=1) parameters are first determined to fit the data for p+^{3}He elastic scattering, checked by predicting n+t scattering results,[3] then used in a large analysis of reactions in the ^{4}He system in which only the T=0 parameters are varied. In addition, isospin constraints are used to relate the p-t and n-^{3}He widths for both T=0 and T=1 levels. A small amount of internal isospin mixing is introduced by allowing slightly non-zero d-d widths (less than 0.1% of the single-particle value) to occur in the T=1 levels. These non-zero widths, which seem to be consistent with internal Coulomb mixing, become greatly amplified in the external Coulomb field by the proximity of broad P-wave levels having opposite isospin, causing large differences in the transition matrix elements for the two branches to occur for the L=1 initial d-d states.

Table B-II shows reaction constants calculated from the analysis that are appropriate for muon-catalyzed fusion experiments. One sees from the last row of the table that the predicted branching ratio for the P-waves (K_{odd}) is in excellent agreement with the room-temperature experiments, and that at low temperatures where the S-waves (K_{even}) dominate, the branching ratio should decrease to a value close to unity. The recent experimental confirmation[2] of this behavior contradicts the conjecture of some cold fusion proponents that the branching ratio is very small (10^{-9}) at low temperatures. Furthermore, the P-wave reaction constants give an overall fusion rate $\lambda_f = 3.8 \times 10^8\ s^{-1}$, compared with the experimental value of $(4.1 \pm 0.1) \times 10^8\ s^{-1}$. These results are described in a presentation[4] at the most recent international muon-catalyzed fusion conference (μCF '90) in Vienna, Austria.

Table B-II. Spin-Dependent Reaction Constants for the *d+d* Reactions.

	K_{even} (L=0)	K_{odd} (L=1)
D(d,n)	$4.55 \times 10^{22}\ fm^3\ s^{-1}$	$1.86 \times 10^{25}\ fm^5\ s^{-1}$
D(d,p)	$5.14 \times 10^{22}\ fm^3\ s^{-1}$	$1.30 \times 10^{25}\ fm^5\ s^{-1}$
$R = \frac{(d,n)}{(d,p)}$	0.886	1.43

[1]D. V. Balin *et al., Phys. Lett.* **141B**, 173 (1984); *JETP Lett.* **40**, 112 (1984).

[2]D. V Balin *et al.*, Proceedings of μCF 90 (to appear in *Muon Catalyzed Fusion*).

[3]G. M. Hale, D. C. Dodder, J. D. Seagrave, B. L. Berman, and T. W. Phillips, *Phys. Rev. C* **42**, 438 (1990).

[4]G. M. Hale, Proceedings of μCF 90 (to appear in *Muon Catalyzed Fusion*).

6. Comprehensive Calculation of Fission Barriers and Half-Lives [P. Möller, J. R. Nix, and W. J. Swiatecki (LBL)].

We have completed a comprehensive calculation of fission barriers and half-lives[1] for heavy elements ranging from plutonium to $Z = 100$. During this study we have discovered a new fission valley for ^{258}Fm and neighboring nuclei that resolves three previously existing experimental anomalies. First, for ^{258}Fm and certain nuclei beyond, the mass distribution becomes very narrow, with a single peak at symmetry. Second, the kinetic-energy distribution for some of these nuclei becomes skewed, with a peak at high energy and a broad low-energy tail. Third, the spontaneous-fission half-life decreases by several orders of magnitude. The new fission valley that appears in our calculations is associated with doubly magic fragment shell effects at 50 protons and 82 neutrons. Since these shell effects are maximum for spherical shapes, we use a shape parametrization that is capable of describing touching spherical fragments and we also take into account the finite range of the nuclear force when calculating the macroscopic contribution to the energy. The reduction in the spontaneous-fission half-lives of ^{258}Fm and neighboring nuclei arises not only from the lower and narrower barrier leading into the new valley, but also from a reduction in the nuclear inertia for motion into the new valley.

[1] P. Möller, J. R. Nix, and W. J. Swiatecki, "Fission Barriers and Half-Lives," Proc. *Conf. on 50 Years with Nuclear Fission*, Washington, D.C./Gaithersburg, Maryland, 1989 (American Nuclear Society, La Grange Park, 1989), Vol. 1, pp. 153-160.

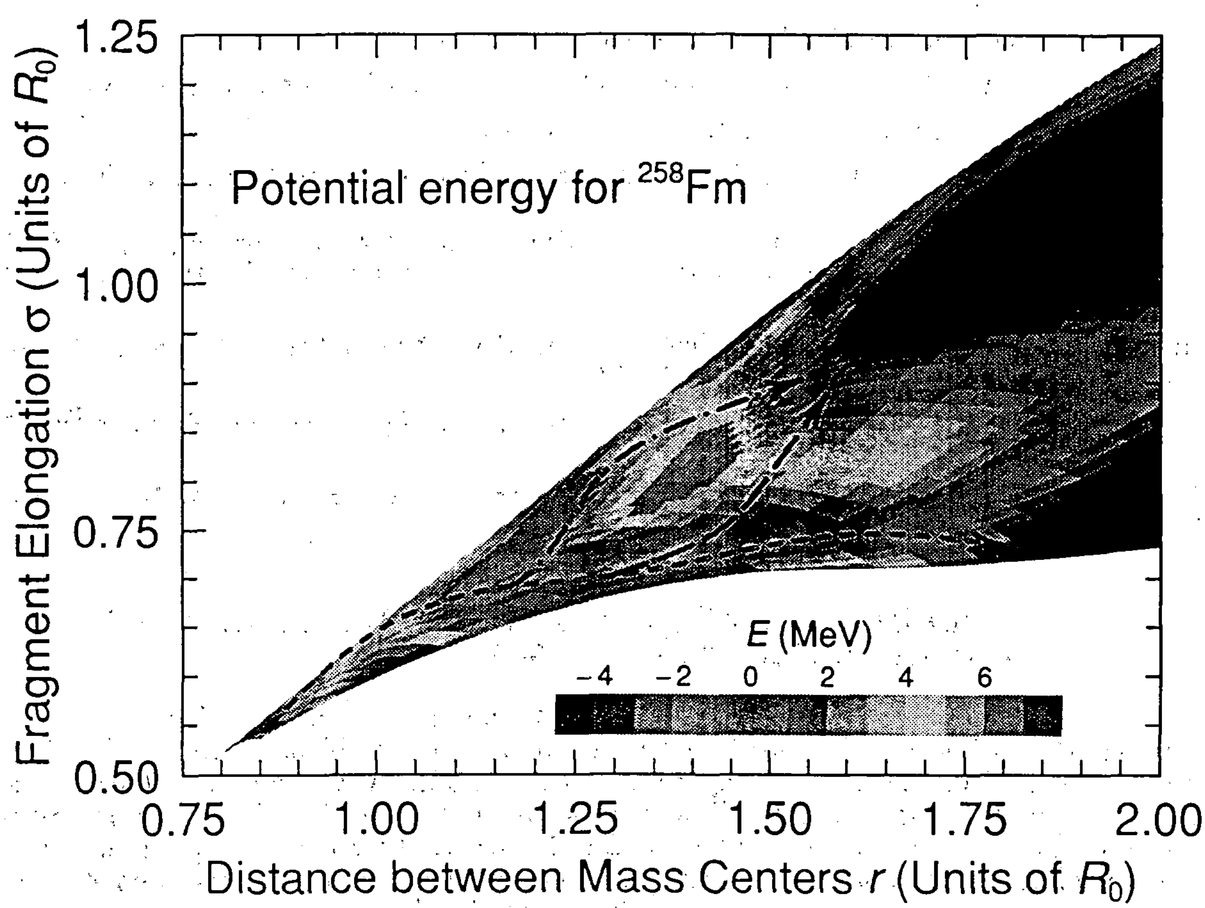

Fig. B-4. Two-dimensional fission barrier for ^{258}Fm, illustrating the paths leading into the new valley in the lower right-hand corner and into the old valley in the upper right-hand corner.

7. Theoretical Descriptions of Neutron Emission in Fission (D. G. Madland)

The current status of theoretical descriptions of the prompt fission neutron spectrum N(E) and the average prompt neutron multiplicity $\bar{\nu}_p$ has been reviewed for an IAEA Consultants' Meeting on Nuclear Data for Neutron Emission in the Fission Process.[1]

The Los Alamos model,[2] the Dresden model,[3] the Dresden version of the Los Alamos model,[4] and the Hauser-Feshbach statistical model were all studied in this review. From the study it has been concluded that, at this time, the Los Alamos model probably has the most predictive power and requires the least amount of input, and that the Dresden model can provide a very good description if sufficient experimental fission data exists for the system being calculated. Few Hauser-Feshbach calculations have been performed, but it is clear that this approach is the best known for simultaneous treatment of neutron and gamma-ray competition in fission fragment de-excitation. It is believed that, ultimately, the Hauser-Feshbach approach will probably yield the most accurate results in the calculation of N(E), N(E,E_n), $\bar{\nu}_p$, and $\bar{\nu}_p(E_n)$.

The current limitations to calculating these observables with higher accuracy than is now possible include insufficient knowledge of:

1. excitation energy partition in fission,
2. fission fragment nuclear level densities,
3. isospin dependence of global neutron optical potentials,
4. fission fragment ground state masses (for the calculation of fission energy release),
5. fission fragment mass and charge distributions, and
6. fission fragment initial excitation energy and initial angular momentum distributions.

[1]D. G. Madland, "Theoretical Descriptions of Neutron Emission in Fission," in *Proceedings of the IAEA Consultants' Meeting on Nuclear Data for Neutron Emission in the Fission Process,* Vienna, 1990 (in press) [LA-UR-91-437 (January 25, 1991)].

[2]D. G. Madland and J. R. Nix, "New Calculation of Prompt Fission Neutron Spectra and Average Prompt Neutron Multiplicities," Nucl. Sci. Eng. **81**, 213-271 (1982).

[3]H. Märten and D. Seeliger, "Analysis of the Prompt-Neutron Spectrum from Spontaneous Fission of ^{252}Cf," J. Phys. G. **10**, 349-362 (1984).

[4]H. Märten and D. Seeliger, "Description of the ^{252}Cf(sf) Neutron Spectrum in the Framework of a Generalized Madland-Nix Model," Nucl. Sci. Eng. **93**, 370-375 (1986).

8. Comparisons of Recent Experiments and the Los Alamos Model of the Prompt Fission Neutron Spectrum (D. G. Madland)

A new measurement of the prompt fission neutron spectrum for the thermal-neutron-induced fission of ^{235}U has been performed in Beijing by Wang *et al.*[1] in 1989. This spectrum was calculated[2] in 1983 using the Los Alamos model. The comparison of that calculation with the new data is shown in Figs. B-5 and B-6 wherein the best-fit Maxwellian spectrum obtained by Wang *et al.*[1] is also shown. Clearly, the best-fit Maxwellian spectrum is inferior to the Los Alamos model calculation. Since the measurement occurred six years after the calculation, no parameter adjustment has been performed. Although the agreement is reasonably good, the low energy ($E < \sim 1$ MeV) end of the spectrum is underpredicted. This may be further evidence for center-of-mass anisotropy, which is not included in the calculation.

A new measurement of the prompt fission neutron spectrum for 2-MeV neutrons incident on ^{238}U has also been performed, in Sendai, by Baba *et al.*[3] in 1990. This spectrum was calculated with the Los Alamos model using input parameters, except the value of E_n, determined[4] in 1982. The comparisons, including the best-fit Maxwellian spectrum obtained by Baba *et al.*,[3] are shown in Figs. B-7 and B-8. Again, the best-fit Maxwellian spectrum is inferior to the Los Alamos model calculation. The agreement between experiment and the Los Alamos model is reasonably good, especially given that no parameter adjustments have been made.

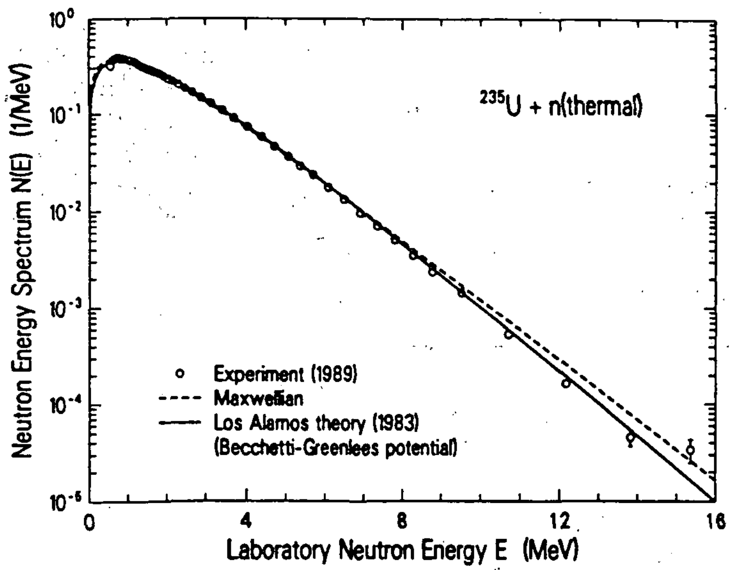

Fig. B-5. Prompt fission neutron spectrum for the fission of ^{235}U induced by thermal neutrons. The dashed curve gives the best-fit Maxwellian spectrum (T_M = 1.321 MeV) determined in Ref. 1, and the solid curve gives the Los Alamos spectrum calculated for $\sigma_c(\varepsilon)$ obtained using the optical-model potential of Becchetti and Greenless (Ref. 5). The experimental data are those of Wang *et al.*(Ref. 1).

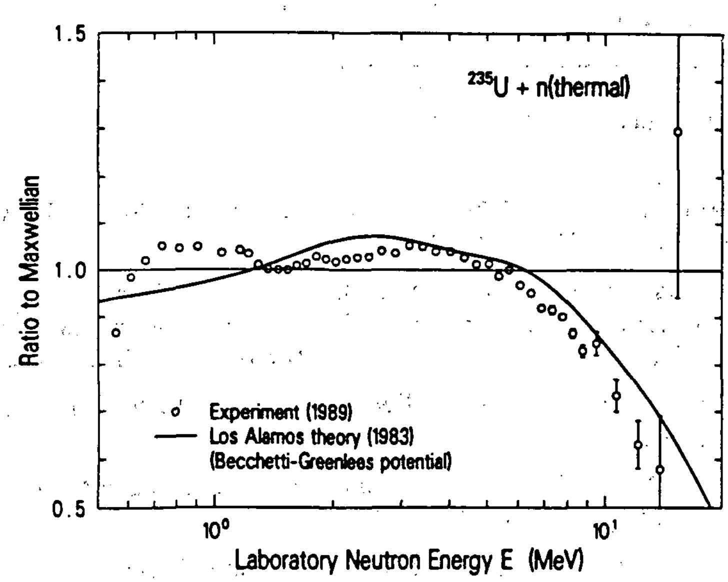

Fig. B-6. Ratio of the Los Alamos spectrum and the experimental spectrum to the best-fit Maxwellian spectrum, corresponding to the curves shown in Fig. B-5.

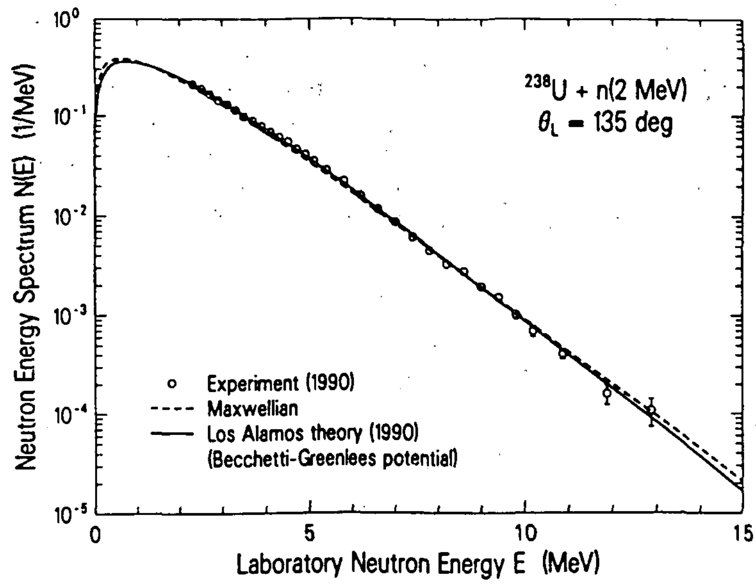

Fig. B-7: Prompt fission neutron spectrum for the fission of ^{238}U induced by 2-MeV neutrons. The dashed curve gives the best-fit Maxwellian (T_M=1.24 MeV) determined in Ref. 3, and the solid curve gives the Los Alamos spectrum calculated for $\sigma_c(\varepsilon)$ obtained using the optical-model potential of Becchetti and Greenless (Ref. 5). The experimental data are those of Baba *et al.* (Ref. 3).

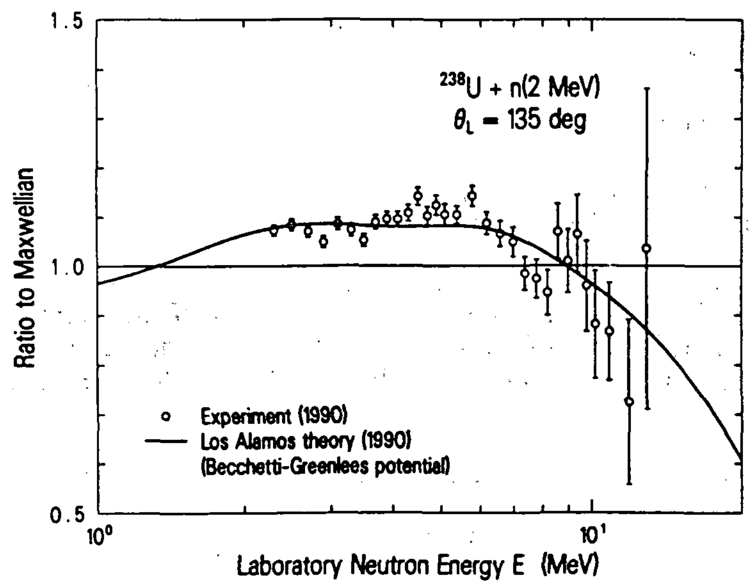

Fig. B-8. Ratio of the Los Alamos spectrum and the experimental spectrum to the best-fit Maxwellian spectrum, corresponding to the curves shown in Fig. B-7.

---

[1]Wang Yufeng *et al.*, "Experimental Study of the Prompt Neutron Spectrum of ^{235}U Fission Induced by Thermal Neutrons," Chin. J. Nucl. Phys. **11**, 47-54 (1989).

[2]D. G. Madland and J. R. Nix, "Prompt Fission Neutron Spectra and Average Prompt Neutron Multiplicities," in *Proceedings of the NEANDC Specialists' Meeting on Yields and Decay Data of Fission Product Nuclides*, Brookhaven Nat. Lab., Upton, NY, 1983, R. E. Chrien and T. W. Burrows, Eds. (BNL, 51778, 1984), p. 423.

[3]M. Baba *et al.*, "Measurement of Double-Differential Neutron Emission Spectra from Uranium-238," Jour. Nucl. Sci. Tech. **27**, 601-616 (1990).

[4]D. G. Madland and J. R. Nix, "New Calculation of Prompt Fission Neutron Spectra and Average Prompt Neutron Multiplicities," Nucl. Sci. Eng. **81**, 213-271 (1982).

[5]F. D. Becchetti, Jr. and G. W. Greenlees, "Nucleon-Nucleus Optical-Model Parameters, A > 40, E < 50 MeV," Phys. Rev. **182**, 1190-1209 (1969).

UNIVERSITY OF LOWELL

A. NEUTRON SCATTERING STUDIES

(L.E. Beghian, G.H.R. Kegel, J.J. Egan, A. Mittler, D.J. DeSimone, P.F. Dugan*, C.A. Horton, C.K.C. Jen, C. Narayan, M. O'Connor, P.A. Staples, M. Woodring and G. Yue)

1. Neutron Scattering in ^{239}Pu from 0.2 to 1.0 MeV

Neutron elastic and inelastic scattering in ^{239}Pu are being studied via the time-of-flight technique. Individual levels and level groups up to 386 keV in excitation can be resolved in the time-of-flight spectra. Neutrons were produced via the $^{7}Li(p,n)^{7}Be$ reaction. The targets are prepared by vacuum evaporation of lithium metal onto a tantalum substrate *in situ* in the accelerator beam line. The detector consists of a 1-cm thick BC418 plastic scintillator mounted on an RCA 8850 photomultiplier tube. The detector is housed in a shield of lead and paraffin loaded with lithium carbonate. The pulsed proton beam current is typically 10 μA with pulse durations less than 0.5 ns after post-acceleration Mobley bunching. Excitation function measurements are being made at 125° in the 0.2- to 1.0-MeV range with an angular distribution at 0.550 MeV. The scattering sample is a circular disk of 3.5-cm diameter and 0.2-cm thickness containing 28.7 g of plutonium. Extensive modifications have been made to our accelerator-target-sample-detector configuration in order to accommodate the small scatterer. Inelastic scattering from vanadium and bismuth scatterers provide line shapes for yield extraction from the time-of-flight spectra. Data reduction includes corrections for attenuation, multiple scattering, and fission neutron background.

2. Neutron Energy Spectra from Proton Irradiated Thick Li Targets

Recent neutron scattering experiments at Lowell have revealed the advantages of frequent checks of the time-of-flight spectrometer efficiency especially if the neutron cross sections studied are small. In the past we normally compared the response of our spectrometer to that of a U-235 fission ionization chamber so that the efficiency of our detector is based on the well known U-235 fission cross section. These comparisons are time consuming because the fission chamber efficiency is low; therefore it is not suitable for daily use. The energy spectrum of neutrons following spontaneous fission of Cf-252 has also been used to determine spectrometer efficiencies. This method also requires a considerable amount of time. In recent years we have used thick metallic lithium targets irradiated with MeV protons to generate pseudo-white neutron spectra[1]. We now use this procedure to generate standard neutron spectra suitable for rapid efficiency determinations. The method has two major advantages. (1) The neutron fluence is high i.e. 40 to 80 neutrons / (s · cm^2 · keV), in the 500- to 3500-keV range at a distance of 250 cm from the target with a 10-μA, 5.5-MeV incident proton beam. (2) Each neutron generated leaves one Be-7 atom behind, hence the neutron dosimetry is simplified by a Be-7 activity determination. The Be-7 decay scheme is simple and Be-7 has a convenient half life of 52 days. We measured neutron energy spectra from thick lithium targets using a black neutron detector[2] with a known detection efficiency.

---

* Deceased

1 G.H.R. Kegel, Nucl. Instrum. Methods <u>B40/41</u>, 1165 (1989).

2 W.P. Poenitz, Argonne Nat. Lab. Rept. ANL-7915 (1972).

We have also calculated these spectra using differential cross section data for the Li(p,n) reaction[3] and stopping cross sections[4] for protons in Li. These calculations include corrections for proton multiple scattering, for the isotopic composition of lithium, for the surface area and the time resolution of the detector, and for Li-7 depletion by proton induced nuclear transformations.

3. Neutron Target Assembly

We have installed a new target assembly on the neutron time-of-flight beam line. This assembly incorporates an oil diffusion pump, a proton beam pulse pickup, a water cooled collimator, a lithium metal resistive heating evaporator along with the target backing which consists of a 1.5 inch diameter tantalum planchette mounted on the end of the beam line held in place by an indium vacuum seal. The whole assembly was designed to minimize virtual leaks in the feed-throughs and other incorporated hardware. We have routinely achieved pressures of the order 10^{-7} torr with this assembly.

4. Determination of Lithium Isotopic Concentration

We have developed a method for determining the atomic proportions of ^{6}Li and ^{7}Li isotopes in enriched ^{6}LiF, ^{7}LiF, and lithium metallic samples. The technique is based on measuring the energy spectra of alpha particles from ^{7}Li(p,α)^{4}He and ^{19}F(p,α)^{16}O reactions and those of backscattered protons. Enriched LiF targets were prepared by thermal evaporation of thermoluminescent dosimetry chips, TLD-700 (^{7}LiF) and TLD-600 (^{6}LiF), onto self-supporting carbon substrates. Targets of metallic lithium were prepared in the same way. The ^{6}Li enriched TLD-600 sample was found to contain 4.78 at.% of ^{7}Li; however, no significant amount of ^{6}Li was found in the TLD-700 sample. A 7.57 at.% concentration of ^{6}Li in lithium metallic target was determined by using the TLD-700 as a ^{7}Li isotope content standard. This value is consistent with the reported 7.5 at.% natural abundance of ^{6}Li. A complete description of the technique will appear in a paper which is currently being prepared for publication.

5. Prompt Fission Spectra Measurements

We are commencing a program of prompt fast fission spectra measurements on the U-235, U-238, Pu-239 and Th-232 in the neutron energy range 0.5 to 3.0 MeV. The work will be carried out in two stages. In stage 1 we will measure the portion of the spectrum for energies greater than the incident energy, omitting the part of the spectrum containing elastically and inelastically scattered neutrons, via time-of-flight with a 3-m flight path using a liquid scintillator and pulse-shape discrimination to distinguish neutron from gamma-ray signals.

In stage 2 we will extend the investigations to energies less than the incident energy by using a set of BaF_2 scintillators to detect prompt gamma-rays ensuing from fission to signal the occurrence of a fission event thus discriminating against scattered neutrons. The gamma signals will not be used as start (or stop) signals for the TOF spectrometer but rather used in

---

[3] H. Liskien and A. Paulsen, Atom. Data and Nucl. Data Tables, 15, 58 (1975).

[4] H.H. Andersen and J.F. Ziegler, Hydrogen Stopping Powers and Ranges in All Elements, (Pergamon, New York, 1977).

a coincidence mode requiring simultaneous detection of gamma-rays in three BaF_2 detectors along with the arrival of a neutron burst at the fission sample. We will record flight time and neutron detector (liquid scintillator) light output (pulse height) for each fission neutron detected by combining the digital output of the TOF analog-to-digital (ADC) converter with that of the pulse height ADC to form a multi-bit word which will be transferred to a mass storage device for later analysis.

The BaF_2 scintillators have been assembled and tested achieving a time resolution of 250 ps. The two parameter data acquisition interface between the ADC's and the data storage computer has been designed and constructed and is currently being tested.

6. Theoretical Investigations (E. Sheldon)

As a follow-up to previous analyses of theoretical (n,n') excitation-functions for fast neutron scattering on the principal actinide nuclei,[5,6,7] we are examining recently measured cross sections[8] for ^{232}Th and ^{238}U at higher incident energies (E_n =2.3 - 3.0 MeV) by comparing the experimental data with calculated excitation functions for individual or grouped levels at excitation energies ranging from about 330 keV to approximately 1 MeV.

The calculations are performed without arbitrary adjustment of input parameters. Since a direct-interaction (DI) mechanism is likely to play a prominent role at these energies for such well-deformed, collective nuclei, a coupled-channels distorted-wave (DWDI) treatment is called for, as provided by Raynal's[9] program "ECIS78" or the Karlsruhe[10] variant "KARJUP" of Tamura's[11] code "JUPITOR." The CN component added incoherently to the DI contribution is computed using the program[12] "COMNUC" or[13] "CINDY." These both employ the Hauser-Feshbach formalism with provision for Moldauer level-width fluctuations and incorporate additional competing exit channels. For consistency throughout the Bruyeres-le-

---

[5] E. Sheldon, in Proc. Intenat. Conf. on Nuclear Data for Science and Technology, Antwerp, Belgium, Sept. 6-10, 1982, edited by H.K. Bockhoff (D. Reidel Publ. Co. Dordrecht. The Netherlands, 1983), pp. 518-527.

[6] Eric Sheldon, in Nuclear Data for Science and Technology, Mito, Japan, May 30-June 3, 1988, edited by S. Igarasi (JAERI, Saikon Publ. Co., Tokyo, 1988), Paper CAO1, pp. 105-110.

[7] E. Sheldon, J.J. Egan, G.C. Goswami, G.H.R. Kegel and A. Mittler in Coherent Effects in Highly Excited Nuclei (Proc. XVIII. Mikolaijki Summer School on Nuclear Physics, Mikolaijki, Masuria Poland, Sept. 1-13, 1986, edited by Z. Wilhelmi & G. Szeflinska (Harwood Academic Publ., New York, 1987), pp. 117-136.

[8] Abobakr Aliyar, "Inelastic Neutron Scattering Studies of ^{238}U and ^{238}TH on States above 300 keV for Incident Energies above 2.2 MeV", Ph.D. Dissertation, University of Lowell (1988).

[9] J. Raynal, IAEA-SMR-918, p. 281 (Saclay, 1972), and private communication.

[10] H. Rebel and G.W. Schweimer, KFK-1333 (Kernforschungszentrum Karlsruhe Report 1971).

[11] T. Tamura. ORNL-4152 (Oak Ridge National Laboratory Report 1967); and Rev. Mod. Phys. 37, 679-708 (1965).

[12] C.L. Dunford, Atomics International Report AI-AEC-12931 (1970).

[13] E. Sheldon and V.C. Rogers Computer Phys. Commun. 6, 99-131 (1973).

Chatel set[14] of optical-potential parameters and deformations (or very slightly modified versions thereof) are adopted, varying only with energy in all computations.

B. DECAY HEAT AND DELAYED NEUTRON STUDIES
(W.A. Schier, D.J. Pullen, G.P. Couchell, M.F. Villani, E.S. Jacobs and P.R. Bennett)

1. Decay Heat Study

A feasibility study was completed demonstrating the measurement of premium quality beta and gamma-ray spectra from U-235 aggregate fission products at delay times ranging from 0.1 to 1,000 s, using a helium jet/tape transport system developed over the past decade in our study of delayed neutron spectra. The study entailed:

a) measurement of gamma-ray spectra with NaI(Tl) for gamma decay heat and with Ge(Li) for individual precursor lines following the neutron induced fission of U-235;

b) ongoing development of a gamma-ray unfolding code to analyze NaI(Tl) spectra for their energy content;

c) construction and preliminary calibration of a beta spectrometer;

d) measurement of the beta count rate as a function of delay time between 0.8 s and 40,0000 s;

e) preliminary measurement of beta spectra following thermal fission of U-235 at delay times of 0.89, 12.71 and 189 s.

The successful completion of this preliminary study is the first step in a program expected to provide decay heat information from the fission of Th-232, U-233, U-235, U-238 and Pu-239. The study will extend to long delay times and thus overlap with a number of previous aggregate decay heat measurements, but more importantly will include delay times as short as 0.1-1.0 s after fission where no previous studies exist. Measurements of aggregate spectra for delay times below 10 s serve as stringent checks to predictions based on summation calculations using individual fission-product data bases. For short delay times, current summation calculations rely heavily on theoretical estimates of the gamma-ray and beta spectra of the many short-lived products for which direct spectral measurements are lacking. Furthermore, the inclusion of high-resolution Ge(Li) spectra as a function of delay time provides hundreds of tests of individual gamma-ray line intensities predicted from summation calculations.

a) Delayed Gamma-Ray Spectra of U-235

Use of the helium jet/tape transport system for transferring fission products to a low-background counting area has been exploited to acquire premium gamma-ray spectra in both the NaI(Tl) and Ge(Li) measurements. With this technique beta-gamma coincidence can be used to select a short, well defined delay-time interval, with the data accumulated

---

[14] G. Haouat, J. Lachkar, Ch. Lagrange, J. Jary, J. Sigaud and Y. Patin, Nucl. Sci. Eng. 81, 491 (1982).

continuously for that time interval until excellent statistics are obtained. In addition beta and random gamma backgrounds are excluded, while gamma-ray self absorption and secondary fission effects (from neutron backgrounds) are absent because no fission foil is transferred to the counting room.

Our preliminary measurements show that aggregate Ge(Li) spectra can provide information about individual gamma lines even for the shortest delay-time intervals, despite the enormous complexity of the spectra. This is possible because with well defined delay-time intervals, activities that are both shorter and longer lived are strongly suppressed, thus dramatically reducing the complexity of the aggregate spectrum. As a result, entire new sets of lines emerge at delay times considerably removed from one another, as shown Fig. B-1. Thus the Ge(Li) measurements of lines from isotopes whose production probability in fission and whose decay rates are well known can be used to obtain absolute fission rates for each aggregate NaI(Tl) measurement. The measurements can also serve as a check on production probabilities and decay rates for many individual isotopes having large uncertainties in one or more of these parameters.

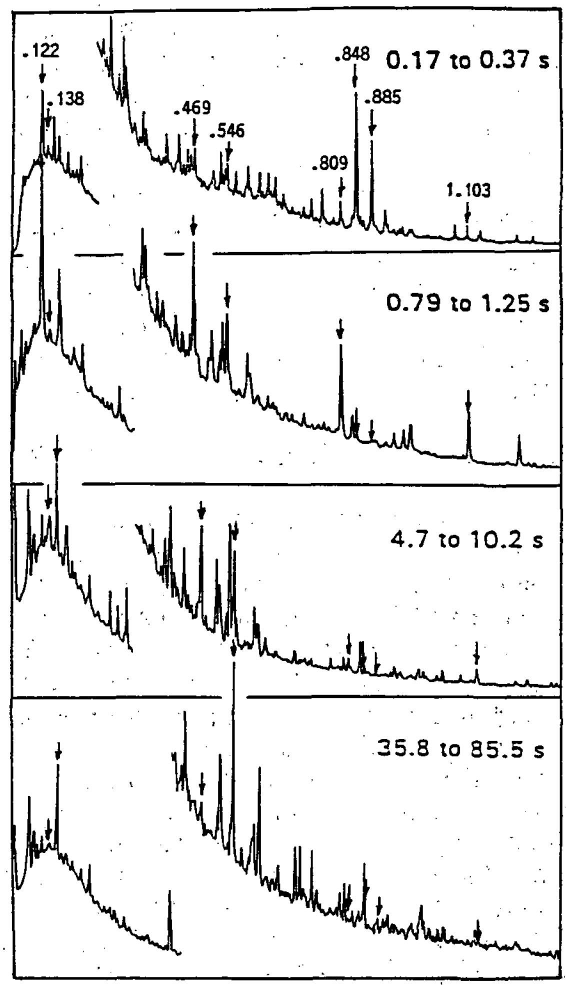

B-1. The strong delay-time dependence of selected gamma lines following U-235 thermal fission is demonstrated in the low energy portions of Ge(Li) spectra.

b) NaI(Tl) Spectrum Unfolding

In order to determine an average photon energy from a composite NaI(Tl) gamma spectrum one must remove all typical response function characteristics other than full energy peaks. We discussed our procedure for deducing response functions and full energy peaks from experimentally obtained ones in our last report. We are now investigating two possible methods for decomposing an essentially continuous gamma-ray spectrum into its full-energy-peak components: 1) by starting at the high-energy end of the spectrum, each channel is viewed as being a photopeak and a stepwise progression can be made to the low end, subtracting out a scaled response function with each step; 2) each measured spectrum can be represented in a least-squares fashion as a superposition of response functions spaced approximately a full-width-at-half-maximum apart. Computer programs for performing these analyses are under development. Each of the two methods will be investigated for decomposition reliability using complex spectra constructed by the addition of known spectra.

c) Aggregate Delayed Beta Spectra

The development of a beta spectrometer with highly effective gamma-ray discrimination was described in the last report. The spectrometer was tested by measuring the beta spectra of a number of beta emitters, several of which are also strong gamma emitters. Excellent agreement was obtained between the measured and calculated beta spectra for each source. The end-point energies of these calibration spectra varied from 0.7 to 4.81 MeV. Recently, the spectrometer was used for preliminary measurements of aggregate beta spectra at delay times of 0.89, 12.7 and 189 s after the thermal fission of U-235. The spectra were of premium quality because a short, well defined delay time interval was selected by use of the helium-jet/tape-transport system, gamma-ray discrimination was effective, and no self absorption or secondary fission effects were present since the fission foil is not transferred to the counting area. The measured spectra showed considerable hardening of energy in proceeding from longer to shorter delay times. Although the spectra have not been corrected for detector response, the corrections are expected to be small, and so in Fig. B-2 our raw spectrum at 189 s is compared with that obtained by Dickens et al.[15] for approximately the same delay time. The agreement is excellent except at the end points where response function effects (e.g., energy resolution) give rise to a small deviation.

d) Beta Count Rate as a Function of Delay Time

The variation of the beta activity with delay time after fission is a straight-forward measurement using the helium jet/tape transport system, and its determination serves as a useful check to the overall transfer efficiency and relative normalization of the system. Since the beta activity is sprayed by the helium jet onto a moving transport tape, for a constant tape velocity, a given distance along the tape downstream from the spray point corresponds to specific delay time. The measurement was performed using two thin scintillator detectors, one placed at a fixed position (the monitor detector) and the other that was movable along the tape to sample various delay-time intervals. Beta count rates were acquired for each detector in a multiscaling mode and a ratio of the corresponding portions of the multiscaler outputs provided relative normalization. The 0.25-mm thick plastic scintillators were insensitive to gamma rays, and the scintillator geometry entered only in calculating the small delay-time interval spanned. The system was also used to measure beta count rates in a more conventional manner. In this second method the tape bearing the activity was stopped, and the beta activity remained stationary at the beta detector. The time dependence of the activity was measured by multiscaling. Good agreement was obtained between the two techniques.

---

[15] J.K. Dickens, T.A. Love, J.W. McConnell, J.F. Emery, K.J. Northcut, R.W. Peelle and H. Weaver, "Delayed Beta- and Gamma-Ray Production Due to Thermal-Neutron Fission of U-235, Spectral Distributions for Times After Fission Between 2 and 14000 sec: Tabular and Graphical Data", ORNL/NUREG-39, Oak Ridge National Laboratory (1978).

B-2. Comparison of the U. of Lowell beta spectrum at a mean delay time of 189 s with that of Dickens et al.[15], referred to as PRESENT DATA, having a mean delay time of 190 s. The LASL, 1976 calculation was by T.R. England and M.G. Stamatelatos.

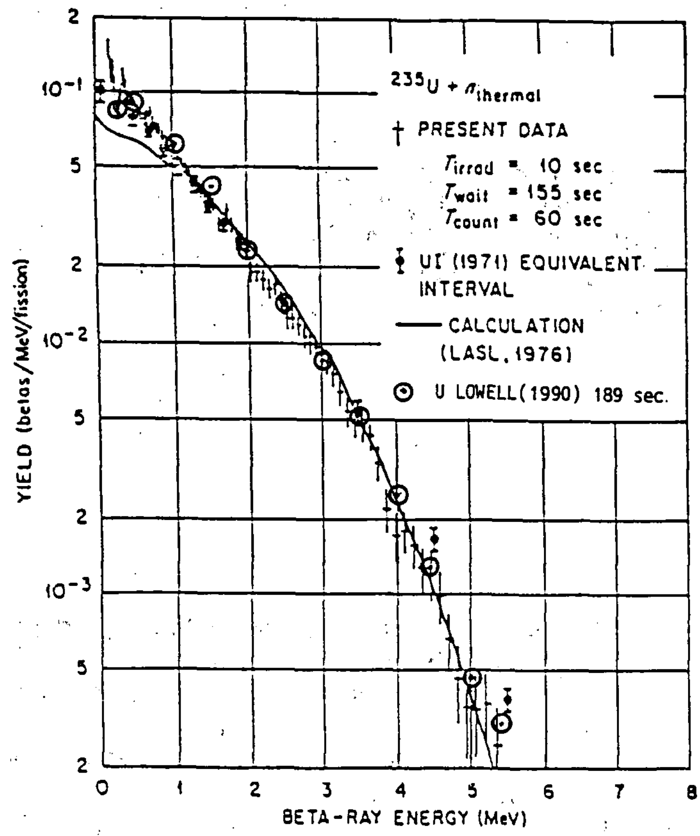

e) Preliminary Measurement of Beta Spectra

Our preliminary measurements of the beta count rate spanned the delay-time range, 0.75-40,000 s. It is conventional to plot the product, activity x delay time, versus delay time since this product remains roughly constant. Our results are compared to those of Dickens et al.[16] in Fig. B-3. Both data sets display essentially the same character and agree well for the most of the range of overlap. Each data set has been corrected for a loss of the noble gasses, krypton and xenon. The most noticeable discrepancy is for short delay times where our values are somewhat higher than those of Ref. 16. This discrepancy will be given further study.

2. Six-Group Decomposition of Aggregate Delayed Neutron Spectra

In our last report we discussed methods developed for decomposing eight U-235 aggregate delayed neutron (DN) Spectra into six spectra based on the Keepin Six-Group model using parameters from ENDF/B-VI.[17] Previous attempts at producing U-235 six-group

---

[16] J.K. Dickens, T.A. Love, J.W. McConnell and R.W. Peelle, Nucl. Sci. Eng. 74, 106 (1980).

[17] T.R. England, Los Alamos National Laboratory, private communication (1988).

B-3. Comparison of our preliminary beta count rate following thermal fission of U-235 with that of Dickens et al.[16] Both data sets include small corrections for lost noble gasses.

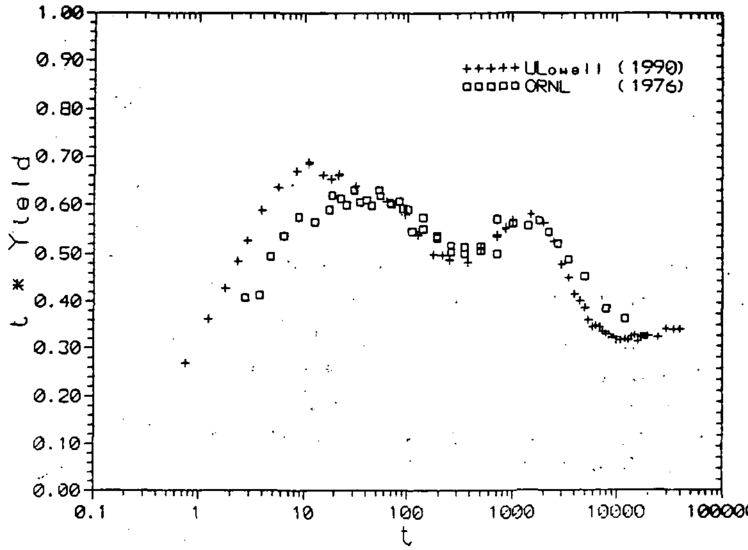

spectra using standard least-squares methods produced solutions that were overly oscillatory and often negative. The addition of a constraint condition to the least-squares problem yielded solutions that were physically acceptable. The constrained least-squares method has been well-studied with many different constraint conditions producing similar acceptable solutions. However, there is a degree of subjectivity in the method insofar as the choice of constraints is concerned. Recently, a Monte-Carlo simulation program was developed to further investigate whether the unstable six-group solutions were produced by the experimental uncertainties in the U-235 measured aggregate spectra and/or by a non-linearity in the Keepin Model. Furthermore, the Monte-Carlo method requires no preconceived notion of spectrum shape as is invoked in the constrained least-squares method.

The Monte-Carlo procedure involved the random generation of synthetic aggregate spectra based on our measured spectra as the "mean" spectra and assuming a normal distribution about that mean with a standard deviation based on the experimental uncertainties. The synthetic aggregate spectra were then subjected to six-group decomposition using the method of unconstrained least-squares. After 1,000 such computer simulations, the resultant six-group solutions were averaged and compared to the six-group solutions also obtained using unconstrained least squares from the measured aggregate spectra. The two independent solutions are numerically equivalent, suggesting the measured uncertainties were not responsible for the unstable solutions attained in the unconstrained condition. The Monte-Carlo procedure was repeated for several constrained least-squares cases, and all were essentially identical to the respective constrained solutions obtained from the measured composite spectra. The Monte-Carlo study thus gives us confidence in our previous six-group solutions obtained by the constrained least-squares procedure discussed in our last report.

THE UNIVERSITY OF MICHIGAN
DEPARTMENT OF NUCLEAR ENGINEERING

A. PULSED 14 MeV NEUTRON FACILITY (J. Yang, N. Tsirliganis, E. Christodoulou, D. Wehe, G. Knoll)

Since our report of last year, we have shifted our major emphasis from the measurements using photoneutron sources reported then to the continuing development of a unique facility for production of nanosecond pulsed 14 MeV neutrons. The system consists of a 150 kV Cockcroft-Walton accelerator, quadrupole doublet, sweeper, high voltage pulser, mass analysis magnet, two-gap klystron buncher, and quadrupole triplet. The long-term goals of this project were outlined in our report of a year ago. These goals remain essentially as described at that time, and only a summary will be given here.

Over the past year, our experimental progress has been slowed by a series of equipment problems that have delayed the start of actual data taking. These have included a serious problem with vacuum leaks in the main accelerator column, difficulties with the stability of the high voltage pulser used in our beam line, and the need to make design changes in the ion source to enhance the extracted current. While addressing these problems, we have also taken the opportunity to carry out some major upgrades in the vacuum system, ion source, and pulsing system that we expect will help ensure greater reliability in the long term. We have continued to improve the performance of the pulsing system, and our most recent measurements have demonstrated the ability of the klystron buncher to produce pulses with a time width of 0.9 to 1.1 ns. We have completed the development of a large NE-213 scintillation detector for use in the time-of-flight neutron energy measurements, and have incorporated an effective scheme for pulse shape discrimination to suppress gamma ray backgrounds.

An essential part of this effort has been the establishment of low-scatter environment in the vicinity of the neutron source. We believe that many of the discrepancies in current data are due to unrecognized complications due to scattering in the target and structural materials near the source. As a result, we have taken extreme measures to insure that the target assembly is of minimum mass, and that the beam line terminates on a low-mass gridded support located 4 meters above the floor of our heavily-shielded laboratory.

The first phase of our experimental work will involve the measurement of elastic scattering angular distributions in a variety of materials having significant interest either for nuclear model verification or because of their technological importance. Priority candidates include iron, vanadium, cobalt, yttrium, niobium, indium, and bismuth. Because of intensity limitations, we expect to carry out these initial measurements using "ring geometry" in which relatively massive targets can be employed. This geometry also dictates the application of Monte Carlo codes to accurately model the experiment in order to properly account for complications due to multiple scattering in the target. In the longer term, we are planning to extend our program to include measurements of direct neutron inelastic scattering yields and continuum neutron spectra induced by 14 MeV neutrons. Many of these measurements will require an improvement in available neutron yield, and we are exploring several possibilities to increase the pulsed beam intensity.

B. <u>ACTIVATION CROSS SECTION MEASUREMENTS IN COOPERATION WITH ARGONNE NATIONAL LABORATORY</u> (G. Piccard, D. Smith[ANL], J. Meadows [ANL])

We are continuing a cooperative program with the Applied Physics Division of Argonne National Laboratory measuring activation cross sections using the ANL FNG facility. First efforts are directed toward a determination of the $^{89}Y(n,p)$ differential cross section, and an integral measurement of the $^{89}Y(n,p)$ to the $^{59}Co(n,p)$ cross section ratio. Irradiations have been completed using targets of natural yttrium at a series of energies between 5.5 and 10 MeV. The induced activity has been determined using 4π beta counting, with particular attention paid to determining self-absorption corrections. The neutron flux is measured using a ^{238}U fission chamber located directly behind the samples. Monte Carlo codes are used to determine the contribution of scattered neutrons during the irradiations.. Analysis of the results is underway, and should be completed by the end of this summer.

NATIONAL INSTITUTE OF STANDARDS AND TECHNOLOGY
(formerly the National Bureau of Standards)

A. NUCLEAR DATA MEASUREMENTS

1. The $^{10}B(n,\alpha_1\gamma)$ Cross Section from 200 keV to 4 MeV (R. A. Schrack and O. A. Wasson, NIST; D. C. Larson, J. K. Dickens and J. H. Todd, Oak Ridge National Laboratory)

The measurement of this important cross section standard has been completed in the neutron energy range from 0.2 to 4 MeV using the ORELA facility at Oak Ridge National Laboratory. The results are being prepared for presentation at the International Conference on Nuclear Data for Science and Technology to be held in Julich, Germany May 13 - 17 of this year. Figure 1 shows a comparison of the new results and ENDF/B-VI evaluation. The present results are in good agreement with the ENDF/B-VI values below about 2 MeV. Discrepancies greater than 40% occur at higher energies.

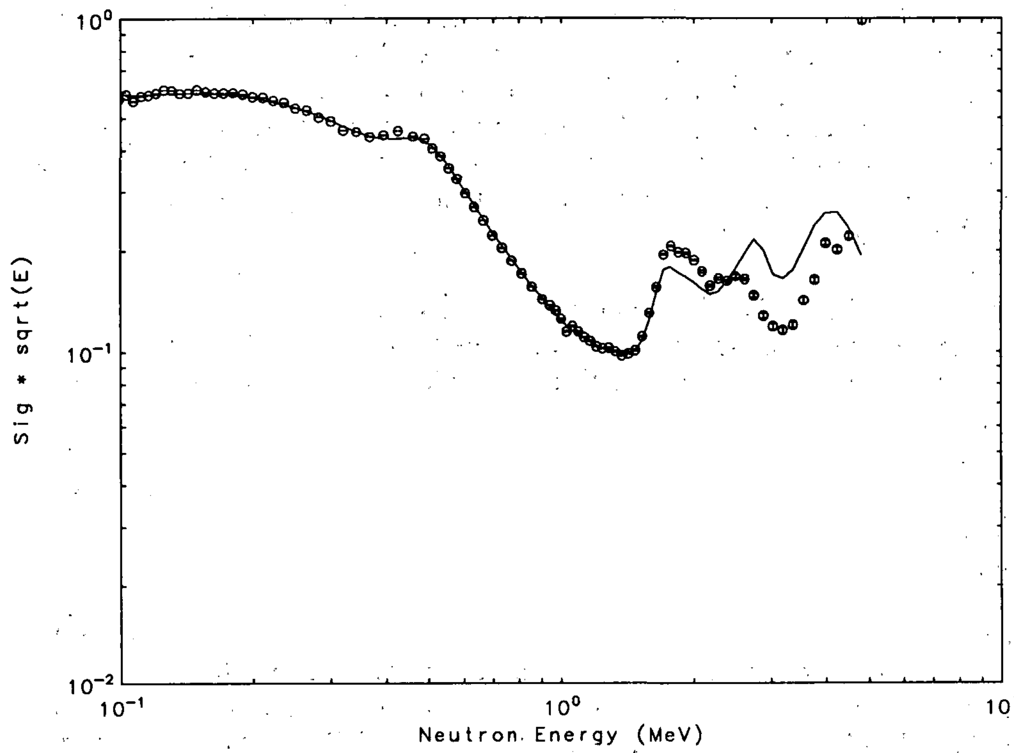

Figure 1. The $^{10}B(n,\alpha_1\gamma)$ cross section experimental results shown as open circles. The error bars represent statistical errors only. The solid line shows the values given by the ENDF/B-VI evaluation. The experimental data are normalized to the ENDF/B -VI values in the neutron energy region from 200 to 360 keV.

The experiment is currently being extended down to 4 keV neutron energy in order to improve the normalization of the higher energy experiment. A well-characterized hydrogen gas proportional counter[1] has replaced the scintillation detector used in the higher energy experiment for neutron flux monitoring. Preliminary test runs indicate that everything is working correctly and that a good new measurement of the cross section will obtained as a companion to the higher enery measurement. The new low energy measurement, while valuable in its own right, will facilitate the normalization of the high enery measurement.

2. ^{235}U Fission Cross Section Measurements (A. D. Carlson and O. A. Wasson, NIST; P. W. Lisowski, J. L. Ullmann and A. Gavron, LANL; N. W. Hill, ORNL)

The analysis of the data runs is essentially finished for the ^{235}U(n,f) cross section experiment performed at the target 4 neutron facility of the Los Alamos Meson Physics Facility. This experimental work was done at the same time as the fission cross section ratio measurements for ^{232}Th, ^{233}U, ^{234}U, ^{236}U, ^{238}U, ^{237}Np and ^{239}Pu which cover the neutron energy region from about 1 to 400 MeV. These ratio measurements and the work involving the LET and MET fluence detectors which were described in last year's report will be discussed in the Los Alamos National Laboratory contribution to this Status Report. A large amount of data obtained in earlier runs with an IBM-PC acquisition system has been analyzed for the ^{235}U fission cross section. For these analyses special computer programs had to be written in order to process the large data files. The neutron fluence was measured with the NIST Annular Proton Telescope (APT). Above 30 MeV neutron energy, it became more difficult to resolve background from the foreground, partly due to the geometry of the detector which produced only moderate pulse height resolution. Thus the cross section data will terminate at 30 MeV.

The use of the MICROVAX-XSYS computer-data acquisition system at LANL has significantly improved the data accumulation process. The dead-time for data acquisition is less and the options for monitoring the quality of the data are significantly better than were available previously. Using this acquisition system with the APT, an effort was made to improve our understanding of the backgrounds. Data obtained with polystyrene (CH) and polyethylene (CH_2) films were analyzed to determine the background contribution from the carbon in the sample. This was quite successful for all but the highest neutron energies where there were statistical problems due to the subtraction of comparable numbers.

An exhaustive examination of the corrections to the experimental data is nearly complete. The final results of this work will be presented at the nuclear data conference at Jülich. In figure 2 the present work is compared with the ENDF/B-VI evaluation. The agreement is generally good except above about 15 MeV where the database used for the ENDF evaluation is rather poor.

---

[1]Nucl. Sci. Eng. 68, 170-182 (1978).

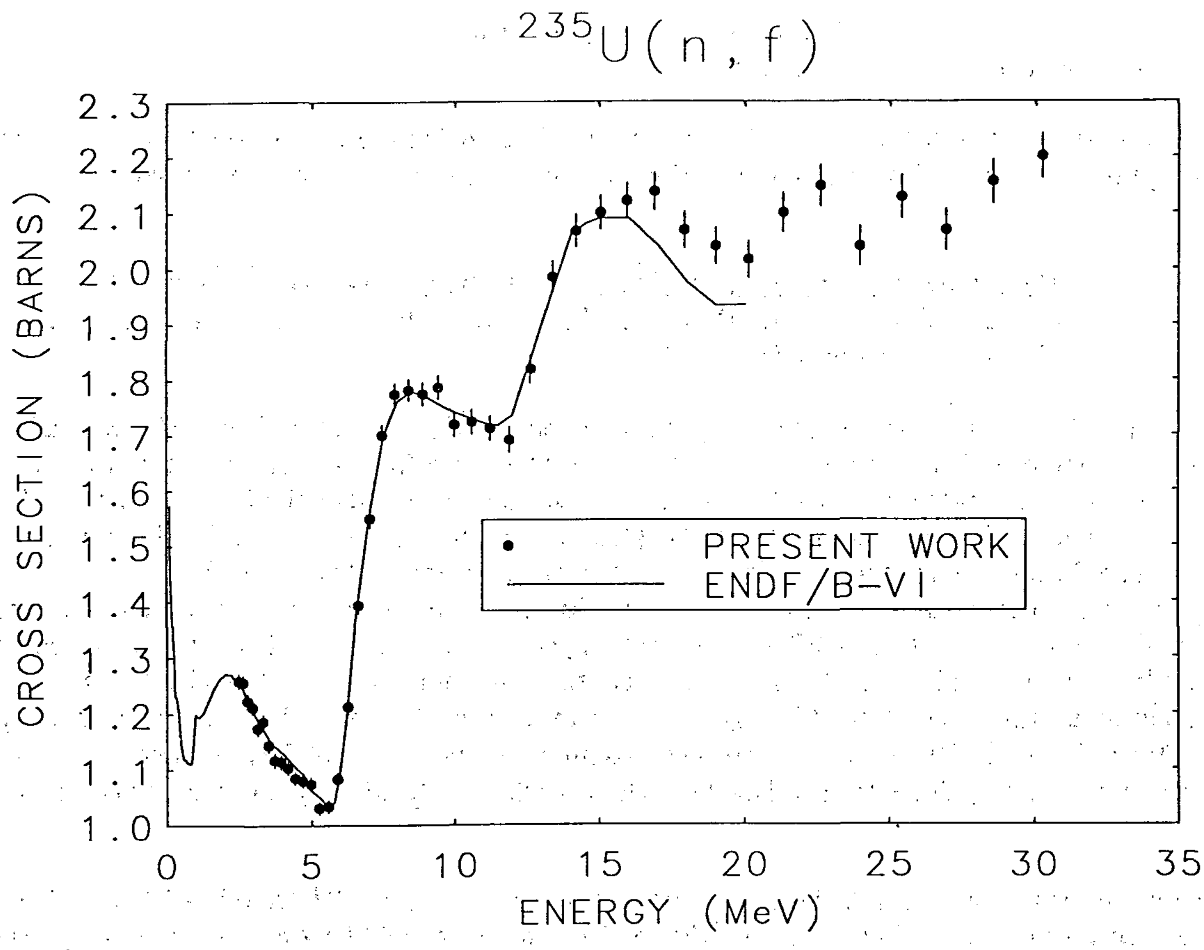

Figure 2. Comparison of the present measurement with the ENDF/B-VI evaluation. The error bars represent statistical uncertainties only.

3. <u>^{237}Np Fission Cross Section Measurements Below 1 MeV</u> (A. D. Carlson, NIST; G. L. Morgan, W. E. Parker, P. W. Lisowski, and S. J. Baelistrini, LANL; N. W. Hill, ORNL)

Measurements have been made of the $^{237}Np(n,f)$ cross section at the Los Alamos Neutron Scattering Center (LANSCE). These data extend from about 1 MeV down to the resonance region. This work was done as in conjunction with a measurement of the subthreshold fission cross section of ^{236}U. A discussion of the ^{236}U experiment is given in the LANL status report. The work on the ^{237}Np cross section was motivated by the need to improve the accuracy of this important materials dosimetry standard. This cross section has been utilized in crucial detectors for investigating pressure vessel degradation problems and providing information on the lifetime of these pressure vessels.

The measurements were made relative to the $^{235}U(n,f)$ standard cross section and will be absolute ratios. In addition to the fission deposits, a thin ^{10}B deposit was placed in the ionization chamber so that the $^{10}B(n,\alpha)$ standard cross section could be used to establish the shape of the neutron fluence.

The $^{10}B(n,\alpha)$ response which has a smooth energy dependence, also allows estimates of the background to be obtained with notch filters.

The data were stored in event mode so that they could be analyzed after the conclusion of the data-taking under different biasing conditions. The measurements are now being analyzed.

4. Measurement of the H(n,n)H Angular Distribution (A. D. Carlson, NIST; S. M. Grimes, Ohio U.; C. R. Howell, Duke U.; R. Pedroni, Ohio U.; W. Tornow, Duke U.; O. A. Wasson, NIST)

The evaluation of the hydrogen scattering cross section by Hopkins and Breit in 1971 was the basis for the ENDF evaluations from II through V. It has been used for many years by the cross section community. To improve the ENDF H(n,n)H cross section, a recently completed evaluation of this cross section by Dodder and Hale was adopted for use in the new ENDF/B-VI library. The maximum difference between these evaluations is almost 2% for a neutron energy of about 11 Mev and a center of mass angle of 180°. Ryves and Kolkowski of the NPL have reported preliminary measurements of the hydrogen differential scattering cross section at 14.5 MeV. The data measured were the ratio of the differential cross sections at center of mass angles of 180 and 110 degrees, and the absolute cross section at 180 degrees. The ratio measurement is in better agreement with ENDF/B-V than ENDF/B-VI. The absolute measurement lies about midway between the evaluations. Both the Hopkins-Breit and Dodder-Hale evaluations rely strongly on rather dated measurements.

To improve the database for the hydrogen scattering cross section, a NIST-Ohio U.-TUNL collaborative experiment is now being designed. The spectrometer which will be used for the initial measurements has been recently used for $^2H(n,n)^2H$ cross section measurements. In the analysis of these data the subtle properties of this spectrometer have been thoroughly investigated and understood. It is expected that measurements on this program will be initiated this year.

B. NEUTRON DETECTOR DEVELOPMENT AND FACILITIES FOR NUCLEAR DATA MEASUREMENTS

1. A 2.5 MeV Neutron Source for Neutron Cross Section Measurements (R. J. Biss, C. D. Dick, and O. A. Wasson, NIST; K. J. Lee, Korean Standards Research Institute)

A 2.5 MeV neutron source continues to be available at the 100-kV, 0.5-mA ion generator at NIST. Neutrons are produced by the $D(d,n)^3He$ reaction with a yield of 3×10^6 s^{-1}. The Time-Correlated Associated-Particle method is used for neutron fluence determination and for background elimination. Measurements to apply nuclear data to the detection of rare materials in bulk samples continue.

2. Absolute Thermal Neutron Counter Development (D. M. Gilliam, G. L. Greene and G. P. Lamaze, NIST; J. Richardson, Harvard University)

An accurate neutron fluence monitor for the measurement of cold and thermal neutrons is being developed. A gamma-alpha coincidence technique is employed to make an accurate calibration of a totally-absorbing ^{10}B capture gamma detector system. This neutron detector is being developed as part of a neutron lifetime experiment, but it also has potential applications for improved thermal neutron cross section measurements, improved calibration of the NIST manganous bath, and possible implications for ^{252}Cf nubar data. One important feature of the absolute calibration of this system is that the alpha-gamma coincidence method can be checked by intercomparisons with standard alpha-particle sources. The combination of these two methods is expected to permit uncertainties of less than 0.1%. Encouraging preliminary results have been reported.[2] A much more elaborate experimental arrangement is now operational.[3] This new arrangement includes two germanium detectors to greatly reduce gamma-ray detector efficiency dependence on neutron beam position, two alpha-particle detectors to permit optimization of calibrations by both the coincidence and standard source methods, and much better boron target positioning precision. The new apparatus has been thoroughly tested at the NIST Reactor in a thermal beam, and is being installed in the new Cold Neutron Guide Hall as one of the first experiments to use that new facility.

A second totally absorbing detector based on cryogenic calorimetry with a ^{6}Li target will be compared with the $^{10}B(n,\alpha_1\gamma)$ device. This calorimeter is a dissertation research project for J. Richardson of Harvard University.

C. NUCLEAR DATA COMPILATIONS, EVALUATIONS AND MEETINGS

1. The Evaluation of The Standards for ENDF/B-VI (A. D. Carlson; W. P. Poenitz, Argonne National Laboratory: R. W. Peelle, Oak Ridge National Laboratory; G. M. Hale, Los Alamos National Laboratory)

The ENDF/B-VI evaluation of the standard neutron cross sections has been completed. These standards were accepted for use in ENDF/B-VI by the Cross Section Evaluators Working Group (CSEWG). There had been some concern expressed in the phase I review of these standards about the rather small values of some of the uncertainties. These uncertainties were obtained from the combination of the simultaneous and R-matrix evaluations. The uncertainties for the output from the simultaneous and R-matrix evaluations were increased by the square root of chi squared per degree of freedom before these results were combined in order to take into account the spread of the experimental input values and thus produce more realistic uncertainties. Comments have been made by some individuals that they felt that users would not use these uncertainties but instead would arbitrarily increase them to what they considered a more acceptable level. A strong statement was

---

[2]J. Radioanalytical and Nucl. Chem., 123 (1988) 551-559.

[3]Nuc. Instr. and Meth. in Phys. Res., A284, No.1 (1989) 220-222.

made that the standards subcommittee should provide such expanded uncertainties since they have had the closest contact with the data base and could make better estimates of more "acceptable" values. The standards subcommittee did supply these expanded uncertainties at the last CSEWG meeting. These uncertainties are estimates such that if a modern day experiment were performed today on a given standard using the best techniques, those results should fall within these expanded uncertainties (2/3 of the time). They take into account data inconsistencies and concerns about R-matrix parameters. These expanded uncertainties will be put in file 1 and in the documentation for the standards.

The covariance files for the combination output are available but very large. The matrix will be collapsed keeping most of the covariance elements located near the diagonal and those in the regions where the covariance elements are changing most rapidly.

After the acceptance of the cross section standards by CSEWG, a revision to the carbon scattering standard became available which takes into account the two small resonances in ^{13}C. The standard is the natural carbon scattering cross section. This revision was phase I reviewed and and accepted for use in ENDF/B-VI.

The documentation of the ENDF/B-VI standards is nearly completed. Discussions held at the last CSEWG meeting led to changes in this documentation which are now being made.

The Mannhart evaluation of the 252Cf spontaneous fission neutron spectrum was accepted for use in ENDF/B-VI. This evaluation was recently put into ENDF/B-VI format.

2. <u>NEANDC Endorsed Working Group on The $^{10}B(n,\alpha)$ Cross Section Standards</u> (A. D. Carlson, Chairman)

A large number of nuclear cross sections have been measured relative to the $^{10}B(n,\alpha)$ standard cross sections, particularly in the low energy region. At the higher neutron energies, the quality of the standard is significantly reduced due to inconsistencies in the experimental measurements. There is general interest on the part of the community of cross section measurers, evaluators and users in improving these neutron cross section standards. The ^{10}B standard has received much attention lately as a result of its relatively poor data base and the problems it caused in the ENDF/B-VI standards evaluation process.

An Inter-Laboratory working group has been formed in order to provide a mechanism for improving these cross sections. The working group was endorsed by the NEANDC. Representatives from the measurement, evaluation and user communities are members of this working group.

In the first meeting of this group, concerns were expressed about the problems with the data base. There are discrepancies in the $^{10}B(n,\alpha_1\gamma)$, $^{10}B(n,\alpha_0)$ and even the total cross sections. It was noted that many of the discrepancies present in the total cross sections may be largely due to poor quality transmission samples. New measurements and analyses are now underway in an effort to remove the problems with the boron cross sections.

A meeting of this working group is planned during the Jülich nuclear data conference. Presentations are expected on the status of the $^{10}B(n,\alpha)$ standard cross sections, recent measurements of the $^{10}B(n,\alpha_1\gamma)$ cross section, new results of the branching ratio, preliminary angular distribution determinations, work on the fabrication of highly characterized transmission samples and plans for new highly accurate total cross section measurements. This should be an appropriate time to coordinate the needs of a number of groups interested in obtaining well characterized transmission samples. The progress which has been made will be reviewed and there will be an opportunity to critically judge the next steps in improving our understanding of these important cross sections.

3. Photon and Charged-Particle Data Center (S. M. Seltzer, M. J. Berger, J. H. Hubbell)

a. Proton and Alpha Particle Stopping Powers and Ranges

As part of the work of the ICRU Stopping Power Committee, an extensive set of proton and alpha-particle stopping powers (electronic and nuclear), ranges and penetration depths has been prepared for 25 elements and 48 compounds of dosimetric interest. The energy regions covered are 1 keV to 10000 MeV for protons and 1 keV to 1000 Mev for alpha particles. The results incorporate current theoretical and experimental information on heavy charged-particle stopping powers. A draft manuscript has been accepted by the ICRU, and a final version is nearly complete.

b. Photon Energy-Absorption Coefficients

The program to prepare a new compilation of photon energy-absorption coefficients nears completion. The methods are based on: (1) our current database of photon interaction cross sections, (2) a critical evaluation of the underlying secondary electron and positron spectra, (3) our recent calculations of the bremsstrahlung yields of electrons and positrons slowing down, (4) updated calculations of positron annihilation-in-flight corrections, and (5) current data on the x-ray fluorescence yield. An earlier, preliminary collaborative effort with P.D. Higgins, C.H. Sibata and F.H. Attix resulted in the preparation of tables for selected materials of dosimetric interest. The goal of the new work is improve on these results and to develop a PC code to allow users to calculate results for any material.

c. Electron and Positron Elastic-Scattering Cross Sections

A database of elastic-scattering cross sections has been newly organized from the results of recently completed exact phase-shift calculations, using Hartree-Fock potentials. The results cover all neutral atoms with atomic numbers from 1 to 100, and electron and positron energies from 1 keV to 1 MeV (above which simpler methods are adequate).

1. OAK RIDGE NATIONAL LABORATORY

Highlights of this past year include completing the measurement of the polarizability of the neutron (with Schmiedmayer and Riehs of the Technical University, Vienna, via a 0.1% precision lead transmission measurement from 0.1 to 500 keV) with a result of $(1.20 \pm 0.25) \times 10^{-3}$ fm^3. This measurement has an uncertainty 5 times smaller than any previous result, and is the first time a significant value has been obtained for this quantity. The ^{10}B$(n, \alpha\gamma)$ measurement and analysis (with Wasson and Schrack of NIST) was completed, providing accurate data up to $E_n = 4$ MeV. Preliminary analysis of high-precision η measurements for ^{235}U from 0.002 to 0.4 eV (with Moxon of Harwell) show agreement with previous Harwell results, and disagree with Geel results. These, and other results from this past year, are presented below as abstracts of published papers and reports.

New experimental efforts include further measurements to pin down the normalization of the high-resolution ^{239}Pu fission data (part of a cooperative program with Geel), a measurement of the capture to fission ratio in ^{235}U from subthermal to several keV using the photon multiplicity detector, a measurement of the capture width of the 2.25 keV ^{60}Ni resonance with the redesigned 40-m capture system, and an extension to lower energies of the ^{10}B$(n, \alpha\gamma)$ measurement (with NIST).

Significant time was spent developing and issuing safety reports and procedures manuals, cleaning and tidying up experimental areas in an attempt to meet OSHA standards, sorting and salvaging old equipment, labeling chemicals, etc., and being trained (and performing training) as required to prepare for the DOE Tiger Team Inspection last October. We are pleased to note that, as a result of this work, no significant problems were found at our facility during the Inspection. The amount of time required for the Tiger Team activity was not foreseen last year, hence some planned activities had to be delayed.

A. CROSS SECTION MEASUREMENTS

1. Capture, Total and Reaction

a. Cross Sections for Production of 70 Discrete-Energy Gamma Rays Created by Neutron Interactions with ^{56}Fe for E_n to 40 MeV: Tabulated Data[1]
(J. K. Dickens, J. H. Todd, and D. C. Larson)

Inelastic and nonelastic neutron interactions with ^{56}Fe have been studied for incident neutron energies between 0.8 and 41 MeV. An iron sample isotopically enriched in the mass 56 isotope was used. Gamma rays representing 70 transitions among levels in residual nuclei were identified, and production cross sections were deduced. The reactions studied were ^{56}Fe$(n, n')^{56}$Fe, ^{56}Fe$(n, p)^{56}$Mn, ^{56}Fe$(n, 2n)^{55}$Fe, ^{56}Fe$(n, d+n, np)^{55}$Mn, ^{56}Fe$(n, t+n, nd+n, 2np)^{54}$Mn, ^{56}Fe$(n, \alpha)^{53}$Cr, ^{56}Fe$(n, n\alpha)^{52}$Cr, and ^{56}Fe$(n, 3n)^{54}$Fe. Values obtained for production cross sections as functions of incident neutron energy are presented in tabular form.

---

[1] ORNL/TM-11671 (September 1990).

b. Experimental and Calculated Excitation Functions for Discrete-Line Gamma-Ray Production Due to 1–40 MeV Neutron Interactions with ^{56}Fe[1] (J. K. Dickens, C. Y. Fu, D. M. Hetrick, D. C. Larson, and J. H. Todd)

Measuring cross sections for gamma-ray production from tertiary reactions is one of the ways to gain experimental information about these reactions. To this end, inelastic and other nonelastic neutron interactions with ^{56}Fe have been studied for incident neutron energies between 0.8 and 41 MeV. The experiment was carried out on a 20-m flight path of the ORELA pulsed neutron time-of-flight facility located at Oak Ridge National Laboratory. A beryllium target neutron source was used to provide increased neutron flux, particularly at the high end of the neutron energy range, and to reduce the gamma flash intensity. A high-purity germanium detector having 25% efficiency was used to measure yields for 70 individual gamma rays having energies between 126 and 2470 keV. A 63-g iron sample isotopically enriched in the mass 56 isotope was used. The effects of neutron scattering in the iron sample have been extensively studied in the analysis. Absolute cross sections have been determined for each of the 70 gamma rays. The reactions studied were ^{56}Fe$(n,n')^{56}$Fe, ^{56}Fe$(n,p)^{56}$Mn, ^{56}Fe$(n,2n)^{55}$Fe, ^{56}Fe$(n,d+n,np)^{55}$Mn, ^{56}Fe$(n,t+n,nd+n,2np)$ ^{54}Mn, ^{56}Fe$(n,\alpha)^{53}$Cr, ^{56}Fe$(n,n\alpha)^{52}$Cr, and ^{56}Fe$(n,3n)^{54}$Fe.

Experimental excitation functions have been compared with cross sections calculated using the nuclear reaction model code TNG, with generally favorable results.

c. Measurement of the ^{10}B$(n,\alpha\gamma)$ Cross Section in the 0.3–4-MeV Neutron Energy Interval[1] (R. A. Schrack,[2] O. A. Wasson,[2] D. C. Larson, J. K. Dickens, and J. H. Todd)

This new measurement was performed in order to improve the accuracy of this important neutron cross section standard in the neutron energy region above 600 keV. The experiment was carried out at the 150-m flight path of the ORELA pulsed neutron time-of-flight facility located at Oak Ridge National Laboratory. The relative cross section was measured in the neutron energy region from 0.3 to 4 MeV. A beryllium target neutron source was used to provide increased neutron flux at the high end of the neutron energy range and to reduce the gamma flash intensity. A high purity germanium detector having 30% efficiency was used to measure the 478-keV γ ray from the ^{10}B(n,$\alpha\gamma$) reaction in the sample, which was positioned 19 m from the neutron source. The neutron fluence incident on the sample was determined from measurements using the NIST Black Detector which was positioned at 150 m on the same flight path. The efficiency and response of this detector have been carefully determined in a series of previous measurements and calculations at NIST. The neutron flight time and pulse amplitude for each event in both detectors were recorded in the new ORELA data acquisition system based on a microcomputer. The data reduction and analysis was performed at NIST using a newly written series of programs. The effects of neutron scattering in the boron sample have been extensively studied in the analysis. The absolute cross section, which was obtained from normalization to the ENDF/B-VI evaluation in the lower neutron energy region, will be presented and compared with previous measurements.

---

1 Accepted for the International Conference on Nuclear Data for Science and Technology, Jülich, Germany, May 13–17, 1991.

2 National Institute of Standards and Technology, Gaithersburg, MD 20899.

d. Measurement of the $^{10}B(n, \alpha_0)/^{10}B(n, \alpha\gamma)$ Ratio Versus Neutron Energy[1]
(L. W. Weston and J. H. Todd)

The ratio of ground state transitions to excited state transitions following neutron absorption in ^{10}B has been measured for the neutron energy region from 20 to 1000 keV. Face-to-face silicon surface-barrier detectors were used to detect reactions and measure the total energy of the emitted alpha and Li particles. ORELA was used as a white neutron source and time-of-flight was used to determine the neutron energy. The ratio varied from 0.064 at the lowest energies to 0.72 at 920 keV. The present measurements tend to be smaller than the presently accepted values by 10 to 30% in the 100 to 600 keV energy region.

e. Measurement of the Nitrogen Total Cross Section from 0.5 eV to 50 MeV[2]
(J. A. Harvey, N. W. Hill, and N. M. Larson)

The recent (1990) ENDF/B-VI evaluation of cross sections for nitrogen again emphasized the lack of reliable total cross-section data in the low energy region. Nitrogen total cross-section data are needed for investigating problems involving transport of neutrons through air. The most recent measurement was thirteen years ago, and the most recent measurement below 500 keV was in 1961. The Oak Ridge Electron Linear Accelerator (ORELA) neutron source was used for a series of transmission measurements to provide data from 0.5 eV to 50 MeV. A nitrogen gas sample was used. For the low-energy measurements from 0.5 eV to 300 keV the 80-m flight path was used, collimated to view the water moderator portion of the tantalum neutron producing target. A lithium glass detector was used to register the neutrons. To obtain the higher energy data, the 200-m flight path was used, collimated directly on the tantalum portion of the neutron target. A separate high-energy measurement using the beryllium block target was also done, to provide improved statistics above 20 MeV. A new advance in neutron detectors was used, consisting of a detector coupled to two photomultiplier tubes which are biased just above the single photoelectron level. These detectors are operated in a coincidence mode, which eliminates background due to photomultiplier noise. This results in a detector with low background, a narrow resolution function, and sensitive to neutrons from about 30 keV to tens of MeV. Overall backgrounds were low, ranging from 0.1% to 1% of the total counts at a given energy for the sample-out measurement. The corrected counts were normalized to a monitor counter, and converted to total cross sections. An uncertainty analysis and associated covariance matrix are available.

Results of these measurements differ by up to 10% with earlier data and support the R-matrix analysis results used in the ENDF/B-VI evaluation, including energy regions where no data were available.

---

[1] Accepted for publication in *Nucl. Sci. Eng.*

[2] Accepted for the International Conference on Nuclear Data for Science and Technology, Jülich, Germany, May 13–17, 1991.

f. Total Cross Section and Neutron Resonance Spectroscopy for $n+^{40}Ar$[1]
(R. R. Winters,[2] R. F. Carlton,[3] C. H. Johnson,[4] N. W. Hill, M. R. Lacerna[5])

The neutron total cross section for ^{40}Ar has been measured over the incident neutron energy range 0.007 to 50 MeV. R-matrix analysis of the cross section from 0.007 to 1.52 MeV provides resonance parameters which provide a complete description of the neutron scattering functions for the $s_{1/2}$, $p_{1/2}$, and $p_{3/2}$ scattering channels and less nearly complete scattering functions for the $d_{3/2}$ and $d_{5/2}$ channels. The back-shifted Fermi gas model is used to model the level densities for *s*-, *p*-, and *d*-wave resonances.

g. Measurement of the Electric Polarizability of the Neutron[6] (J. Schmiedmayer,[7] P. Riehs,[8] J. A. Harvey, and N. W. Hill)

The electric polarizability of the neutron was determined to be $\alpha_n = (1.20 \pm 0.15 \pm 0.20) \times 10^{-3}$ fm^3 from its characteristic influence on the energy dependence of the neutron ^{208}Pb scattering cross sections, as measured in a neutron time of flight transmission experiment at the Oak Ridge Electron Linear Accelerator (ORELA) pulsed neutron source.

h. Measurement of T_{eff} for Cu in $YBa_2Cu_3O_7$ Neutron Resonance Absorption[9]
(H. A. Mook, J. A. Harvey, and N. W. Hill)

i. Observation of Phonon Softening at the Superconducting Transition in $Bi_2Sr_2CaCu_2O_8$[10] (H. A. Mook, M. Mostoller, J. A. Harvey, N. W. Hill, B. C. Chakoumakos, and B. C. Sales)

---

[1] *Phys. Rev.* **C43**, 492 (1991).

[2] Department of Physics, Denison University, Granville, OH 43023.

[3] Middle Tennessee State University, Murfreesboro, TN.

[4] Consultant.

[5] Ohio State University, Columbus, OH.

[6] *Phys. Rev. Letters* **25**, 1015 (1991).

[7] Harvard University, Cambridge, MA.

[8] Institut für Kernphysik der Technischen Universität Wien, Wien, Austria.

[9] *Phys. Rev.* **B41**, 764 (1990).

[10] *Phys. Rev. Letters* **65**, 2712 (1990).

j. Cold Fusion Studies – Part 1: Preliminary Results From an Investigation of the Possibility of Electrochemically Induced Fusion of Deuterium in Palladium and Titanium Cathodes[1] (D. M. Hembree, Jr., E. L. Fuller, Jr., F. G. Perey, G. Mamantov,[2] and L. A. Burchfield)

A series of experiments designed to detect the by-products expected from deuterium fusion occurring in the palladium and titanium cathodes of heavy water (D_2O) electrolysis cells is reported. The primary purpose of this account is to outline the integrated experimental design developed to test the cold fusion hypothesis and to report preliminary results that support continuing the investigation.

Apparent positive indicators of deuterium fusion were observed, but could not be repeated or proved to originate from the electrochemical cells. In one instance, two large increases in the neutron count rate, the largest of which exceeded the background by 27 standard deviations, were observed. In a separate experiment, one of the calorimetry cells appeared to be producing ~18% more power than the input value, but thermistor failure prevented an accurate recording of the event as a function of time. In general, the tritium levels in most cells followed the slow enrichment expected from the electrolysis of D_2O containing a small amount of tritium. However, after 576 hours of electrolysis, one cell developed a tritium concentration approximately seven times greater than the expected level.

k. Tests for 'Cold Fusion' in the Pd-D2 and Ti-D2 Systems at 40 to 380 MPa and −196 to 27°C[3] (J. G. Blencoe, M. T. Naney, D. J. Wesolowski, and F. G. Perey)

l. Lack of Evidence for Cold Fusion Neutrons in a Titanium-Deuterium Experiment[4] (F. G. Perey, M. T. Naney, J. G. Blencoe, and D. J. Wesolowski)

2. Actinides

a. Resonance Structure in the Fission of $(^{235}U + n)$[5] (M. S. Moore,[6] L. C. Leal,[7] G. de Saussure, R. B. Perez,[8] and N. M. Larson)

---

[1] Y-12 Report Y/DK-669 (June 1990).

[2] Chemistry Department, University of Tennessee, Knoxville, TN.

[3] *Journal of Fusion Energy* **9**, 149 (1990).

[4] Accepted for publication in *Journal of Fusion Energy*.

[5] *Nucl. Phys. A* **502**, 443c (1989).

[6] Los Alamos National Laboratory, Los Alamos, NM.

[7] Argonne National Laboratory, Argonne, IL 60439.

[8] Oak Ridge National Laboratory and University of Tennessee, Knoxville, TN.

b. Resonance Analysis and Evaluation of the ^{235}U Neutron Induced Cross Sections[1] (L. C. Leal[2])

Neutron cross sections of fissile nuclei are of considerable interest for the understanding of parameters such as resonance absorption, resonance escape probability, resonance self-shielding, and the dependence of the reactivity on temperature.

In the present study, new techniques for the evaluation of the ^{235}U neutron cross sections are described. The Reich-Moore formalism of the Bayesian computer code SAMMY was used to perform consistent R-matrix multilevel analyses of the selected neutron cross-section data. The Δ_3-statistics of Dyson and Mehta, along with high-resolution data and the spin-separated fission cross-section data, have provided the possibility of developing a new methodology for the analysis and evaluation of neutron-nucleus cross sections. The result of the analysis consists of a set of resonance parameters which describe the ^{235}U neutron cross sections up to 500 eV.

The set of resonance parameters obtained through a R-matrix analysis are expected to satisfy statistical properties which lead to information on the nuclear structure. The resonance parameters were tested and showed good agreement with the theory.

It is expected that the parameterization of the ^{235}U neutron cross sections obtained in this dissertation represents the current state of art in data as well as in theory and, therefore, can be of direct use in reactor calculations.

c. Resonance Analysis of the ^{239}Pu Neutron Cross Sections in the Energy Range 300 to 2000 eV[3] (H. Derrien[4] and G. de Saussure)

A recent high-resolution measurement of the neutron fission cross section of ^{239}Pu has allowed the extension from 1 to 2 keV of a previously reported resonance analysis of the neutron cross sections, and an improvement of the previous analysis in the range 0.3 to 1 keV. Extensive tabular and graphical comparisons between results of measurements and calculations with the resonance parameters are given. The evaluation in ENDF-6 format is available at the nuclear data centers (NNDC at Brookhaven National Laboratory and NEADB at Saclay).

[1] ORNL/TM-11547 (June 1990).

[2] Argonne National Laboratory, Argonne, IL 60439.

[3] ORNL/TM-11490 (June 1990).

[4] Retired from Centre d'Etudes Nucleaires de Cadarache, France.

3. Experimental Techniques

a. White Source Gamma-Ray-Production Spectral Measurement Facilities in the U.S.[1] (D. C. Larson, J. K. Dickens, R. O. Nelson,[2] and S. A. Wender[2])

The two primary neutron sources for measuring gamma-ray-production (GRP) cross sections for applied work in the U.S. are the Oak Ridge Electron Linear Accelerator (ORELA) located at Oak Ridge National Laboratory and the Weapons Nuclear Research (WNR) Facility located at Los Alamos National Laboratory. Both facilities are based on white neutron sources and collectively cover the energy range from thermal to 800 MeV. The paper describes the capabilities of both facilities.

The ORELA facility came on line in 1970 and has been involved in GRP measurements since its inception. The neutron energy range covered is from thermal to 40 MeV. Measurement capabilities exist for thermal capture, using a barium fluoride multicrystal spectrometer, a liquid scintillator tank, or high-resolution spectral studies with germanium detectors. Capture cross sections and low-resolution spectra in the resonance region are measured with a newly designed C_6D_6 detector system to replace the older C_6F_6 system, or a germanium system for high-resolution work. Fission chambers, ^{6}Li, and ^{10}B detectors are used for flux normalization. Gamma rays from nonelastic reactions are measured using an intrinsic germanium detector system, with plastic scintillators for flux determination. Flight paths from 10- to 150-m are used for GRP measurements. A new data acquisition system based on personal computers has been implemented.

The WNR facility covers the neutron energy range from <1 MeV to 800 MeV. Two flight paths, 18- and 40-m long, are currently used for GRP measurements. The measurements performed may be divided into four gamma-ray energy ranges. For $0.2 < E_g < 10$ MeV germanium detectors are used for high-resolution measurements of inelastic excitation processes. For $1 < E_g < 25$ MeV a five-crystal BGO spectrometer is used to measure GRP cross sections and angular distributions. For $E_g > 10$ MeV a large, actively-shielded BGO spectrometer on a rotating mount is utilized for fast-neutron capture gamma-ray studies. For $20 < E_g < 200$ MeV, construction is underway of a multi-element detector for high energy gamma rays from nucleon Bremsstrahlung and pion production. The flux is monitored during experiments using fission ionization chambers containing foils of ^{235}U and/or ^{238}U.

The paper will provide details on each of these capabilities, and outline results obtained.

b. Scintillation Detector Efficiencies for Neutrons in the Energy Region Above 20 MeV[3] (J. K. Dickens)

The computer program SCINFUL (for SCINtillator FULl response) is a program designed to provide a calculated complete pulse-height response anticipated for neutrons

[1] Accepted for the International Conference on Nuclear Data for Science and Technology, Jülich, Germany, May 13–17, 1991.

[2] Los Alamos National Laboratory, Los Alamos, NM 87545.

[3] Accepted for the Meeting on Neutron Cross Section Standards for the Energy Region Above 20 MeV, Uppsala, Sweden, May 21–23, 1991.

being detected by either an NE-213 (liquid) scintillator or an NE-110 (solid) scintillator. The detector is in the shape of a right circular cylinder. The neutron source is considered to be a point source; however, it may be placed at any location with respect to the detector, even inside of it. The neutron source may be monoenergetic, or it may be Maxwellian distributed, or it may be uniformly distributed between chosen lower and upper bounds. The calculational method uses Monte Carlo techniques, and it is relativistically correct. Extensive comparisons with a variety of experimental data have been made. There is generally overall good agreement (less than 10% differences) of results from SCINFUL calculations with measured integral detector efficiencies for the design incident neutron energy range of 0.1 to 80 MeV. Calculations of differential detector responses, i.e., yield versus response pulse height, are generally within about 5% on the average for incident neutron energies between 16 and 50 MeV and for the upper 70% of the response pulse height. For incident neutron energies between 50 and 80 MeV, the calculated shape of the response agrees with measurements, but the calculations tend to underpredict the absolute values of the measured responses. Extension of the program to compute responses for incident neutron energies greater than 80 MeV will require data on neutron interactions with carbon, such as those currently being measured at the Svedberg Laboratory at Uppsala University.

c. Time Dependent Monte Carlo Calculations of the ORELA Target Neutron Spectrum[1] (S. N. Cramer and F. G. Perey)

The time dependent spectrum of neutrons in the water-moderated Oak Ridge Electron Linear Accelerator (ORELA) target has been calculated using a modified version of the MORSE multi-group Monte Carlo code with an analytic hydrogen scattering model. Distributions of effective neutron distance traversed in the target are estimated with a time and energy dependent algorithm from the leakage normal to the target face. These data are used in the resonance shape analyses of time-of-flight cross section measurements to account for the experimental resolution function. The 20 MeV-10 eV energy range is adequately represented in the MORSE code by the 174 group VITAMIN-E cross section library with a P_5 expansion. An approximate representation of the ORELA positron source facility, recently installed near the target, has been included in the calculations to determine any perturbations the positron source might create in the computed neutron distributions from the target. A series of coupled Monte Carlo calculations was performed from the target to the positron source and back to the target using a next-event estimation surface source for each step. The principal effect of the positron source was found to be an increase in the distance for the lower energy neutron spectra, producing no real change in the distributions where the ORELA source is utilized for experiments. Different configurations for the target were investigated in order to simulate the placement of a shadow bar in the neutron beam. These beam configurations included neutrons escaping from: (1) the central tantalum plates only, (2) the entire target with the tantalum plates blocked out, and (3) only a small area from the water. Comparisons of the current data with previous calculations having a less detailed model of the tantalum plates have been satisfactory.

---

[1] *Proceedings of Conference on Monte Carlo Methods for Neutron and Photon Transport Calculations, Budapest, Hungary, September 25–28, 1990.*

d. Gaseous Radionuclide Activity in the Building 6010 Exhaust Determined by Gamma-Ray Assay of Cryogenic Liquified Samples[1] (J. K. Dickens)

Samples of gaseous components in the exhaust stack of Building 6010 at the Oak Ridge National Laboratory were obtained for two conditions, (a) the Oak Ridge Electron Linear Accelerator in a normal operating mode, and (b) the accelerator shut down. The decay of one radionuclide, ^{222}Rn, was observed equally in both measurements. The decay of three radionuclides, namely ^{11}C, ^{13}N, and ^{41}Ar, was observed during accelerator operation but not during shutdown. Gamma-ray assay measurements were obtained using a calibrated, high-resolution, Ge detector system. Background data were obtained to ascertain quantitatively the sample-independent contributions to the measurements. Data reduction utilized a combination of computer and manual methods. A complete analysis was carried out to determine the actual measured isotope radioactivity density (in pCi/ℓ) for the particular conditions existing at the time the samples were collected. Corrections were applied to these results to account for non-constant sample collection rates and for sample transfer losses. A complete report of all facets of the experiment is given.

e. Electron Linear Accelerators for Fast Neutron Data Measurements in Support of Fusion Energy Applications[2] (K. H. Böckhoff,[3] A. D. Carlson,[4] O. A. Wasson,[4] J. A. Harvey, and D. C. Larson)

Continuing improvements in electron linear accelerators, and associated targets, detectors, and data acquisition systems, make facilities based on these neutron sources very productive in meeting nuclear data needs for fusion energy development. The operation of an electron linear accelerator is briefly outlined, and specific information about neutron-producing targets, available detector systems, and data acquisition capabilities for several of the most productive facilities is given. Data needs are reviewed in terms of reactions important to the fusion energy program, and several examples are given of data acquired at these facilities for these reactions. Much of the experimental data upon which nuclear data evaluations are based are measured at electron linacs, and they continue to be a valuable source of nuclear data for fusion reactor design.

f. Safety Study for the Oak Ridge Electron Linear Accelerator[5] (J. A. Harvey, T. A. Lewis and R. W. Peelle)

This Safety Study (SS) has been prepared in response to Department of Energy, Oak Ridge Operations Report OR 5481.1B, entitled *Safety Analysis and Review System*, for DOE facilities that involve hazards that are not routinely encountered and accepted by the general public. This SS is issued in conjunction with a second document entitled *Operational Safety Guidelines for the Oak Ridge Electron Linear Accelerator*, ORNL/CF-90/50. Both documents are concerned with the Oak Ridge Electron Linear Accelerator (ORELA),

[1] ORNL/TM-11738 (February 1991).

[2] *Nucl. Sci. Eng.* **106**, 192 (1990).

[3] Central Bureau for Nuclear Measurements, Steenweg op Retie, 2440 Geel, Belgium

[4] National Institute of Standards and Technology, Gaithersburg, MD 20899.

[5] ORNL/CF-90/49 (May 1990).

a low-hazard accelerator facility operated by the Oak Ridge National Laboratory (ORNL) in Building 6010 at the X-10 site.

g. Procedures at the Oak Ridge Electron Linear Accelerator Facility[1] (J. A. Harvey, T. A. Lewis and R. W. Peelle)

Work at the Oak Ridge Electron Linear Accelerator (ORELA) is covered by regulations and procedures that relate to employee and public safety, the safeguarding of sensitive materials, and the security for the federal property within the ORELA building. The goal of this manual is to make the procedures of particular concern conveniently available to persons working at ORELA. However, this manual does not cover procedures for optimization of accelerator performance or research projects.

h. A Data Acquisition Work Station for ORELA[2] (B. D. Rooney, J. H. Todd, R. R. Spencer, and L. W. Weston)

B. DATA ANALYSIS

1. Theoretical

a. ^{56}Fe and ^{60}Ni Resonance Parameters[3] (C. M. Perey, F. G. Perey, J. A. Harvey, N. W. Hill, and N. M. Larson)

High-resolution neutron measurements for ^{56}Fe-enriched iron targets were made at the Oak Ridge Electron Linear Accelerator (ORELA) in transmission below 20 MeV and in differential elastic scattering below 5 MeV. A natural iron target was used in transmission below 160 keV. The data were analyzed from 5 to 850 keV with the R-matrix codes SAMMY for the transmissions and RFUNC for the scattering. Parameters were obtained for 33 $\ell = 0$ and 242 $\ell = 0$ resonances.

The distribution of the reduced widths for the 33 s-wave resonances is consistent with a Porter-Thomas distribution and the distribution of the nearest neighbor spacings agrees with a Wigner distribution. The average s-wave level spacing is equal to 25.4 ± 2.2 keV. The Porter-Thomas distribution and the Fermi-gas model suggest that several s-wave levels may have been missed but the Dyson-Metha Δ_3 statistics test fails to confirm this possibility. The distributions of the reduced neutron widths for the $\ell = 1$ and $\ell = 2$ resonances were also consistent with Porter-Thomas distributions.

Even though modulations are observed in the staircase plot of the reduced s-wave level widths and in the plot of the Lorentz-weighted strength functions, these modulations do not provide a clear indication of the presence of doorway states because of the small number of resonances. The s-wave strength function is equal to $(2.3 \pm 0.6) \times 10^{-4}$.

[1] ORNL/CF-90/95 (July 1990).

[2] ORNL/TM-11454 (September 1990).

[3] Accepted for the International Conference on Nuclear Data for Science and Technology, May 13-17, 1991, Jülich, Germany.

New ^{6}Li glass transmission data were acquired for two ^{60}Ni-enriched sample thicknesses. These new data are fully consistent with each others but are not consistent with earlier ORELA ^{6}Li glass transmission data. Our new ^{6}Li glass transmission data and the earlier proton recoil transmission data above 150 keV were analyzed with the code SAMMY to update the ^{60}Ni resonance parameters. For the 2.253-keV resonance the neutron width was determined to be 59.3 ± 0.8 meV and the radiation width 553 ± 50 meV.

b. <u>Multilevel Resonance Analysis of ^{59}Co Neutron Transmission Measurements</u>[1]
(G. de Saussure, N. M. Larson, J. A. Harvey, and N. W. Hill)

High-resolution neutron transmission measurements through several thicknesses of ^{59}Co were performed by Harvey at the Oak Ridge Electron Linear Accelerator (ORELA) in conjunction with the ENDF/B-VI evaluation of ^{59}Co. These measurements have much better energy resolution than previously published transmission measurements. The results of some of the measurements of Harvey were used in the ENDF/B-VI evaluation of the total cross section above 100 keV, but the data were not used below 100 keV where the ENDF/B-VI cross sections are represented by resolved resonance parameters. These resonance parameters were based instead on the compilation of Mughabghab et al.

The ENDF/B-VI resolved resonance parameters were used to compute the transmission measurements of Harvey, and very large discrepancies were observed between these computations and the results of the measurements. Consequently, six transmission measurements of Harvey were analyzed, in the neutron energy range from 200 eV to 100 keV, using the multilevel R-matrix computer code SAMMY which utilizes Bayes' theorem for the fitting process. The parameters of four fictitious bound levels and a few levels above 100 keV were adjusted to account for the contribution in the region 0 to 100 keV of the levels outside that region and to reproduce the evaluated cross sections in the thermal energy region and over the well-known first resonance at 132 eV.

The transmission measurements are not very sensitive to the values of the resonance capture widths; therefore, the capture widths obtained in this analysis have large uncertainties. An attempt was made to adjust the capture widths to give results consistent with the capture areas reported by Spencer et al.; however, the attempt was not successful because the correspondence between the resonances observed in transmission and those observed in capture is not always unambiguous, and the capture areas measured by Spencer et al. often have large multiple scattering corrections.

c. <u>Multilevel Resonance Analysis of ^{59}Co Transmission Measurements</u>[2]
(G. de Saussure and N. M. Larson)

High-resolution neutron transmission measurements through several thicknesses of ^{59}Co were performed by Harvey at the Oak Ridge Electron Linear Accelerator (ORELA) in conjunction with the ENDF/B-VI evaluation of ^{59}Co. These measurements have much better energy resolution than previously published transmission measurements. The

[1] ORNL/TM-11762 (in preparation).

[2] Accepted for the International Conference on Nuclear Data for Science and Technology, May 13-17, 1991, Jülich, Germany

ENDF/B-VI resolved resonance parameters were used to compute the transmission measurements of Harvey, and very large discrepancies were observed between these computations and the results of the measurements. Consequently, six transmission measurements of Harvey were analyzed, in the neutron energy range from 200 eV to 100 keV, using the multilevel R-matrix computer code SAMMY which utilizes Bayes' theorem for the fitting process. The parameters of four fictitious bound levels and a few levels above 100 keV were adjusted to account for the contribution in the region 0 to 100 keV of the levels outside that region and to reproduce the evaluated cross sections in the thermal energy region and over the well-known first resonance at 132 eV.

d. Pairing Corrections and Spin Cutoff Parameters in Exciton Level Densities for Two Kinds of Fermions[1] (C. Y. Fu)

Pairing corrections in particle-hole (exciton) state-density formulas used in precompound nuclear reaction theories are, strictly speaking, dependent on the nuclear excitation energy U and the exciton number n. A general formula for (U, n)-dependent pairing corrections has been derived in an earlier paper for the exciton state-density formula for one kind of fermion. In the present paper, a similar derivation is made for two kinds of Fermions. In this formulation, it is assumed that neutrons and protons occupy different sets of single particle states. It is shown that the constant-pairing-energy correction used in standard state-density formulas, such as U_0 in Gilbert and Cameron, is a limiting case of the present general (U, n)-dependent results. Spin cutoff factors are calculated using the same pairing theory and parameterized into an explicit (U, n)-dependent function, thereby defining the exciton level-density formula for two kinds of Fermions. The results show that the ratios in the exciton level densities in the one-Fermion and two-Fermion approaches vary with both U and n, thus likely leading to differences in calculated compound to precompound ratios. However, the differences in the spin cutoff factors in the two cases are found to be rather small.

e. Analysis of Beta-Ray Data Important to Decay Heat Predictions[2] (J. K. Dickens)

Recently obtained experimental total beta-ray spectra for 77 radionuclides created during fission of ^{235}U have been compared with predicted total beta-ray spectra based on beta-ray transition energies and intensities of individual components currently available in the Evaluated Nuclear Structure Data File (ENSDF). In addition, experimental average beta-ray energies, $< E_\beta >$, for 100 radionuclides are compared with evaluated/theoretical $< E_\beta >$ from four compilations, namely (a) a 1982 compilation by the author, (b) the current ENSDF (1989), (c) a compilation of the Japanese Nuclear Data Committee (1988), and (d) predictions using the microscopic theory of Klapdor and coworkers. No one of these evaluations/predictions is superior in reproducing the experimental data. A comparison of the experimental $< E_\beta >$ with the total available beta decay energies, Q_β, indicates that the approximation $< E_\beta > \approx Q_\beta/3$ somewhat overestimates $< E_\beta >$ on the average; however, the ratio $R = < E_\beta > /q_\beta$ varies between 0.11 and 0.46, and there is no discernible

[1] *Nucl. Sci. Eng.*, accepted October 1990.

[2] Accepted for publication in *Nucl. Sci. Eng.*

trend in R vs Q_β or $< E_\beta >$, nor a discernible difference for radionuclides having $T_{1/2} \leq 2$ sec compared with those having $T_{1/2} > 2$ sec. Lastly, the intensities of possible ground-state decay transitions were estimated for 47 radionuclides and compared with similar data in ENSDF. In 14 cases, a non-zero ENSDF value is supported by the experimental data, and in 8 cases a zero value in ENSDF is supported by the lack of experimental data suggesting a high-energy ground-state beta-ray transition. Of the remaining 25 radionuclides the experimental data for nine cases suggests increases are needed in the ENSDF, and for 16 radionuclides the data indicate the need for smaller values of the ground-state transition intensities from those given in the ENSDF, being zero for 4 nuclides (^{80,81}Ga, ^{84}As, and ^{145}Cs).

f. An R-Matrix Analysis of the ^{235}U Neutron Induced Cross Sections Up to 500 eV[1] (L. C. Leal,[2] G. de Saussure, and R. B. Perez[3])

A detailed evaluation of the R-matrix resonance parameters describing the interaction of neutrons with ^{235}U has been performed up to 500 eV using the most recent high-resolution measurements of the ^{235}U neutron cross sections. The availability of ^{235}U spin-separated neutron cross-section data, in conjunction with the use of the Δ_3-statistics of Metha and Dyson, has made possible a detailed study of the statistical distribution of the resonance parameters and their average values. The present R-matrix resonance parameters have been converted into equivalent sets of Adler-Adler parameters and multipole momentum space expansion parameters. Extensive validation of our evaluation has been performed by comparing self-shielded fission rates computed with our R-matrix parameters with the measurements of Czirr; a test of the ENDF/B unresolved resonance formalism for the calculation of ^{235}U self-shielding factors is also presented.

g. URR Computer Code: A Code to Calculate Resonance Neutron Cross-Section Probability Tables, Bondarenko Self-Shielding Factors, and Self-Indication Ratios for Fissile and Fertile Nuclides[4] (L. C. Leal,[2], G. de Saussure, and R. B. Perez[3])

The URR computer code has been developed to calculate cross-section probability tables, Bondarenko self-shielding factors, and self-indication ratios for fertile and fissile isotopes in the unresolved resonance region. Monte Carlo methods are utilized to select appropriate resonance parameters and to compute the cross sections at the desired reference energy.

The neutron cross sections are calculated by the single-level Breit-Wigner formalism with s-, p-, and d-wave contributions. The cross-section probability tables are constructed by sampling the Doppler broadened cross sections.

The various self-shielding factors are computed numerically as Lebesgue integrals over the cross-section probability tables.

---

[1] Submitted to *Nucl. Sci. Eng.*, July 1990.

[2] Argonne National Laboratory, Argonne, IL

[3] Oak Ridge National Laboratory and University of Tennessee, Knoxville, TN.

[4] ORNL/TM-11297/R1 (February 1990).

h. Statistical Properties of the ^{235}U Fission Widths: A Search for Intermediate Structure in the ^{235}U Compound Nucleus[1] (R. B. Perez,[2] G. de Saussure, L. C. Leal,[3] and M. S. Moore[4])

Resonance parameters were obtained from a consistent Reich-Moore analysis of a set of ^{235}U neutron cross sections up to 500 eV. Within this energy interval 905 s-wave levels were identified, of which 356 correspond to J=3 and 549 to J=4.

In the presence of a double-humped barrier, the fission width $\bar{\Gamma}_f(E)$, averaged over the fine structure of the dense Class-I states is characterized by a Lorentzian

$$\bar{\Gamma}_f(E) = \frac{A}{(E - E_{II})^2 + W^2}$$

where E_{II} is the location of the Class-II state and W is its half width. In the absence of intermediate structure, the average fission width should be constant over the energy interval considered.

The fission width for both spin states were averaged over several energy intervals. No energy dependence of the $J = 3$ average fission width was observed. The Wald-Wolfowitz runs test, $J = 4$ showed the fission widths to be consistent either with an energy independent average or with the initial portion of a Lorentzian function arising from a far-away Class-II state. For the $J = 4$ state the averaged fission widths increased monotonically with energy. A fit of the cumulative sum of the fission widths to the function, $\int_{-\infty}^{E} dE\, \bar{\Gamma}_f(E)$, demonstrated that the energy dependence of the average spin-4 fission width can be interpreted in terms of a Class-II state at 750 eV with a half-width of 233 eV. This result is consistent with a previously analysis by Moore et al. of the ^{235}U average fission widths. The Wald-Wolfowitz runs test showed that the distribution of the $J = 4$ state resolved fission widths around the Lorentzian average, is consistent with a random distribution, hence supporting the hypothesis on the Lorentzian dependence of the average fission width.

Within the restrictions imposed by the size of the available statistical samples, the analysis of the resolved fission widths performed in this work supports the presence of intermediate structure only in the case of the $J = 4$ spin state of the ^{235}U compound nucleus.

---

[1] Accepted for International Conference on Nuclear Data for Science and Technology, Jülich, Germany, May 13-17, 1991.

[2] Oak Ridge National Laboratory and University of Tennessee, Knoxville, TN.

[3] Argonne National Laboratory, Argonne, IL.

[4] Los Alamos National Laboratory, Los Alamos, NM 87545.

2. ENDF/B Related Work

a. Description of Evaluations for Natural Carbon Performed for ENDF/B-VI[1] (C. Y. Fu)

An evaluation of data for neutron induced reactions on natural carbon was performed for ENDF/B-VI and is briefly described. The evaluation is based on R-Matrix fits to measured cross sections for $E_n < 5$ MeV, on least-squares adjustment of the ENDF/B-V data to new experimental information, including KERMA factors, for E_n between 5 and 20 MeV, and on experimental data and theory from 20 to 32 MeV. Evaluated data are given for neutron induced reaction cross sections, angular and energy distributions of the secondary neutrons, and gamma-ray production cross sections and spectra. Uncertainty files are included for the file 3 cross sections. Resonances in ^{13}C below 2 MeV were added. Important improvements to ENDF/B-V were made for the $(n, n'3\alpha)$ cross sections. The upper incident energy was extended to 32 MeV, resulting in the addition of cross sections for many more reactions.

b. Description of Evaluations for $^{50,52,53,54}Cr$ Performed for ENDF/B-VI[1] (D. M. Hetrick, D. C. Larson, N. M. Larson, and C. Y. Fu)

Isotopic evaluations for $^{50,52,53,54}Cr$ performed for ENDF/B-VI are briefly reviewed. The evaluations are based on analysis of experimental data and results of model calculations which reproduce the experimental data. Evaluated data are provided for neutron induced reaction cross sections, angular and energy distributions, and for gamma-ray production cross sections associated with the reactions. File 6 formats are used to represent energy-angle correlated emission and recoil spectra. Uncertainty files are included for all File 3 cross sections.

c. Description of Evaluations for $^{54,56,57,58}Fe$ Performed for ENDF/B-VI[1] (C. Y. Fu, D. M. Hetrick, C. M. Perey, F. G. Perey, N. M. Larson, and D. C. Larson)

Isotopic evaluations for $^{54,56,57,58}Fe$ performed for ENDF/B-VI are briefly reviewed. The evaluations are based on analysis of experimental data and results of model calculations which reproduce the experimental data, including data for the isotopes and the natural element. Evaluated data are given for neutron-induced reaction cross sections, angular and energy distributions of secondary particles, and gamma-ray production cross sections associated with the reactions. File 6 formats are used to represent energy-angle correlated data and recoil spectra. Uncertainty files are included for all File 3 cross sections. A detailed description of the evaluation is given for ^{56}Fe and results of calculations for the major reactions are used for evaluations of the minor isotopes, with particular attention paid to inelastic scattering to the low-lying levels in ^{57}Fe.

---

[1] Submitted for inclusion in BNL Report ENDF-201 (1991).

d. Description of Evaluations for ^{58,60,61,62,64}Ni performed for ENDF/B-VI[1]
(D. C. Larson, C. M. Perey, D. M. Hetrick, and C. Y. Fu)

Isotopic evaluations for ^{58,60,61,62,64}Ni performed for ENDF/B-VI are briefly reviewed. The evaluations are based on analysis of experimental data and results of model calculations which reproduce the experimental data. Evaluated data are given for neutron induced reaction cross sections, angular and energy distributions, and for gamma-ray production cross sections associated with the reactions. File 6 formats are used to represent energy-angle correlated data and recoil spectra. Uncertainty files are included for all File 3 cross sections.

e. Description of Evaluations for ^{63,65}Cu Performed for ENDF/B-VI[1]
(D. M. Hetrick, C. Y. Fu, and D. C. Larson)

Isotopic evaluations for ^{63,65}Cu performed for ENDF/B-VI are briefly reviewed. The evaluations are based on analysis of experimental data and results of model calculations which reproduce the experimental data. Evaluated data are given for neutron-induced reaction cross sections, angular and energy distributions, and for gamma-ray production cross sections associated with the reactions. File 6 formats are used to represent energy-angle correlated data and recoil spectra. Uncertainty files are included for all File 3 cross sections.

f. Description of Evaluations for ^{206,207,208}Pb Performed for ENDF/B-VI[1]
(C. Y. Fu, D. C. Larson, and N. M. Larson)

An evaluation of data for neutron induced reactions on ^{206,207,208}Pb was performed for ENDF/B-VI and is briefly described. The evaluation is based on experimental data guided by model calculations. Evaluated data are given for neutron induced reaction cross sections, angular and energy distributions of the secondary neutrons, recoil spectra, and gamma-ray production cross sections and spectra. File 6 formats are used to represent energy-angle correlated data for the outgoing neutrons. Uncertainty files are included for all File 3 cross sections. New data are available for $(n, 2n)$ cross sections and energy-angle correlated neutron emission spectra. Resonance parameters, absent from the previous evaluations, have been added. Serious energy imbalance problems in ENDF/B-V have been completely removed by using isotopic evaluations, by using calculated gamma-ray production spectra instead of adopting experimental data directly, and by using the File 6 formats.

g. Generation of Covariance Files for the Isotopes of Cr, Fe, Ni, Cu, and Pb in ENDF/B-VI[2] (D. M. Hetrick, D. C. Larson, and C. Y. Fu)

The considerations that governed the development of the uncertainty files for the isotopes of Cr, Fe, Ni, Cu, and Pb in ENDF/B-VI are summarized. Four different approaches were used in providing the covariance information. Some examples are given

---

[1] Submitted for inclusion in BNL Report ENDF-201 (1991).

[2] ORNL/TM-11763 (February 1991).

which show the standard deviations as a function of incident energy and the corresponding correlation matrices.

h. Accurate Calculations of Neutron KERMA and Damage from ENDF/B-VI Evaluations for Silicon, Chromium, Iron, and Nickel, and Comparison with ENDF/B-V Results[1] (D. C. Larson, D. M. Hetrick, C. Y. Fu, S. J. Epperson,[2] and R. E. MacFarlane[3])

i. Improvements to ENDF/B-VI Iron and Possible Impacts on Pressure Vessel Surveillance Dosimetry[4] (C. Y. Fu, D. M. Hetrick, C. M. Perey, F. G. Perey, N. M. Larson, and D. C. Larson)

The ENDF/B-VI cross-section evaluations for the four iron isotopes are summarized, emphasizing the major improvements over ENDF/B-V. The evaluations were mostly based on a preliminary file generated in 1986 for natural iron that has been used for re-calculating several neutron-transport experiments, all of which showed improved agreement. These re-analyses, including those for pressure-vessel surveillance dosimetry, are also discussed.

j. Evaluated Cross Sections for Neutron Scattering from Natural Carbon Below 2 MeV Including R-Matrix Fits to ^{13}C Resonances[5] (C. Y. Fu)

k. Calculated Cross Sections for Neutron Induced Reactions on ^{19}F and Uncertainties of Parameters[6] (Z. X. Zhao,[7] C. Y. Fu, and D. C. Larson)

Nuclear model codes were used to calculate cross sections for neutron-induced reactions on ^{19}F for incident energies from 2 to 20 MeV. The model parameters in the codes were adjusted to best reproduce experimental data and are given in this report. The calculated results are compared to measured data and the evaluated values of ENDF/B-V. The covariance matrix for several of the most sensitive model parameters is given based on the scatter of measured data around the theoretical curves and the long-range correlation error of measured data. The results of these calculations form the basis for the new ENDF/B-VI fluorine evaluation.

---

[1] Accepted for publication in Proceedings of the 7th ASTM-EURATOM Symposium on Reactor Dosimetry, Strasbourg, France, August 1990.

[2] University of Florida, Gainesville, FL.

[3] Los Alamos National Laboratory, Los Alamos, NM 87545.

[4] Invited paper accepted for publication in Proceedings of the 7th ASTM-EURATOM Symposium on Reactor Dosimetry, Strasbourg, France (August 1990).

[5] *Nucl. Sci. Eng.* **106**, 489 (1990).

[6] ORNL/TM-11671 (September 1990).

[7] Chinese Nuclear Data Center, Institute of Atomic Energy, P. O. Box 275(41), Beijing, People's Republic of China.

l. Comparisons of Experimental Beta-Ray Spectra Important to Decay Heat Predictions with ENDSF Evaluations[1] (J. K. Dickens)

Graphical comparisons of recently obtained experimental beta-ray spectra with predicted beta-ray spectra based on the Evaluated Nuclear Structure Data File are exhibited for 77 fission products having masses 79–99 and 130–146 and lifetimes between 0.17 and 23650 sec. The comparisons range from very poor to excellent. For beta decay of 47 nuclides, estimates are made of ground-state transition intensities. For 14 cases, the value in ENDSF gives results in very good agreement with the experimental data.

m. Test of the ENDF/B Unresolved Resonance Formalism for ^{235}U[2] (L. C. Leal,[3] G. de Saussure, R. B. Perez,[4] and R. Q. Wright)

n. Evaluations of ^{28,29,30}Si Neutron Induced Cross Sections for ENDF/B-VI[5] (D. C. Larson, D. M. Hetrick, S. J. Epperson,[6] and N. M. Larson)

o. Proposed Improvements to ANSI/ANS-5.1, Decay Heat Power in Light Water Reactors[7] (J. K. Dickens)

The American National Standard ANSI/ANS-5.1 "Decay Heat Power in Light Water Reactors," had as its impetus the concern about consequences of a Loss-of-Coolant Accident (LOCA) and the desire to replace the earlier "draft" standard. The earlier (1973) "draft" standard had already been adopted by the AEC/NRC in regulatory requirements for evaluation of Emergency Core Cooling System (ECCS) performance in a hypothetical LOCA. The 1979 adopted Standard was a distinct improvement over the 1973 "draft" Standard.

In the intervening period, new experimental results have been reported, and computational capabilities have been substantially improved not only in calculational technique but also in a greatly expanded evaluated data base. Last year the ANS-5.1 Working Group reviewed plans for improving the Standard not only prior to its next renewal, but also for the future. The directions of proposed improvements have been guided by the needs of the reactor community, not only to provide a more accurate basis for ECCS requirements, but also for intermediate and longer cooling times after shutdown. These improvements will be guided by the results of recent experiments and will be augmented by summation calculations using up-to-date evaluated fission-product decay and cross-section data.

The list of improvements represents an ambitious program, particularly within the time frame required for the upcoming renewal.

---

1 ORNL/TM-11414 (March 1990).

2 *Trans. Am. Nucl. Soc.* **61**, 395 (1990).

3 Argonne National Laboratory, Argonne, IL 60439.

4 Oak Ridge National Laboratory and University of Tennessee, Knoxville, TN.

5 ORNL/TM-11825 (in preparation).

6 University of Florida, Gainesville, FL.

7 Abstract of invited paper, *Trans. Am. Nucl. Soc.* **62**, 536 (1990).

p. International Evaluation Cooperation Task 1.1: Intercomparison of Evaluated Files for ^{52}Cr, ^{56}Fe, and ^{58}Ni[1] (C. Y. Fu, D. C. Larson, D. M. Hetrick, H. K. Vonach,[2] J. Kopecky,[3] S. Iijima,[4] N. Yamamuro,[5] and G. Maino[6])

Task 1.1 (indicated in the title) is one of six initial tasks in a joint NEACRP/NEANDC Task Force on Evaluation Cooperation organized to promote international evaluation collaboration. The purpose of Task 1.1 is to graphically compare selected evaluations for structural materials in ENDF-VI (USA), JEF-II/EFF-II (Europe), and JENDL-III (Japan). The isotopes ^{52}Cr, ^{56}Fe, and ^{58}Ni are especially interesting because they are important components of steel and because new evaluations for them have recently been completed for each library.

Large discrepancies have been found in some areas. For example, the spreads in the evaluated ^{56}Fe(n,α) cross sections around 10 MeV and in the neutron emission spectra for ^{58}Ni for $E_n = 8$ MeV and $E_n' = 1.5$ MeV are more than 30%. Communications among the participants have been initiated for improving the evaluations in individual libraries, for assessing differences associated with present-day evaluation techniques, and for more consistent utilization of the formats.

q. Evaluation of the Silicon Isotopes for ENDF/B-VI[1] (D. M. Hetrick, D. C. Larson, N. M. Larson, C. Y. Fu, and S. J. Epperson[7])

Silicon is an important semiconductor material, so understanding neutron-induced radiation damage effects is very important. There is considerable interest in the cross sections for secondary charged particle production (including recoil nuclei) for radiation damage calculations in electronic components. Since silicon is a major constituent of concrete and soils, neutron and gamma-ray transport information is also important. For these reasons, much effort was put into the ENDF/B-VI evaluations for the three stable isotopes of silicon. The evaluations are based on analysis of experimental data, supplemented by results of nuclear model calculations which reproduce the experimental data.

The new file 6 format of ENDF/B is used to represent energy-angle correlated data and recoil spectra, both present for the first time in the silicon evaluations. Also, for the first time, all necessary nuclear data are given to allow KERMA (Kinetic Energy Released in MAterials) and displacement cross sections to be calculated directly from information

---

[1] Accepted for the International Conference on Nuclear Data for Science and Technology, May 13-17, 1991, Jülich, Germany.

[2] Institut fur Radiumforschung und Kernphysik, Boltzmanngasse 3, A-1090 Vienna, Austria.

[3] Department of Physics, Netherlands Energy Research Foundation, 3 Westerduinweg, P.O.B. 1, NL-1755 ZG Petten, The Netherlands

[4] Naig Nuclear Research Laboratory, Naig Co., Ltd. 4-1 Ukishima-Cho, Kawasaki-Ku, Kawasaki-Shi 210, Japan

[5] Data Engineering Inc., 60 Kitahassaku, Midori-Ku, Yokohama 226, Japan

[6] ENEA, Bologna, Italy.

[7] University of Florida, Gainesville, FL.

available in the evaluation, dependent only upon the quality of the evaluated data. These quantities are fundamental to studies of neutron heating and neutron radiation damage.

This paper reviews the structure of the evaluations, notes important measured data considered, gives a summary of the model codes used, and shows examples of calculations compared to measured data. Preliminary results for radiation damage show the overall quality of the silicon evaluation is much improved over ENDF/B-V and should meet the present needs of the user community.

r. Current Status and Proposed Improvements to the ANSI/ANS-5.1 American National Standard for Decay Heat Power in Light Water Reactors[1]
(J. K. Dickens, T. R. England,[2] and R. E. Schenter[3])

The American National Standard for Decay Heat in Light Water Reactors (ANSI/ANS-5.1) was issued in 1979 and has been used extensively for the past decade. Since the standard was issued there have been new experimental decay-heat measurements, and new and improved calculational capabilities have been developed. In this report the standard is compared with these new data and with calculations based on improved methods. Three foreign standards or proposed standards have also been developed, and these are compared in content with the present ANSI/ANS standard. Proposals for improving the standard are presented and discussed.

[1] In preparation for *Nuclear Safety*.

[2] Los Alamos National Laboratory, Los Alamos, NM 87545.

[3] Westinghouse Hanford Company, Richland, WA 99352.

OHIO UNIVERSITY

A. MEASUREMENTS

1. n–d Elastic Scattering at Backward Angles (S.M. Grimes, R.S. Pedroni, C.E. Brient, N. Al–Niemi*, C.R. Howell**, W. Tornow** and H.R. Setze**)

We are in the process of making high–accuracy cross sections (an accuracy better than ± 5%) for n–d elastic scattering at backward angles. The angular range is 140° to 180° in the center–of–mass system. Some measurements have already been made at $E_n = 8$ and 10 MeV. We plan to complete the measurements at 8 and 10 MeV soon. Measurements are also anticipated at $E_n = 14$ MeV. The measurements are being made by detecting the recoiling deuteron using a charged–particle time–of–flight spectrometer in which a triple coincidence is required between two Δ–E detectors (proportional counters) and a stopping E detector (BC–404 plastic scintillator).

2. Neutron Total Cross Section Measurements at Intermediate Energy[1] (R.W. Finlay, G. Fink, W. Abfalterer, P. Lisowski†, G.L. Morgan† and R.C. Haight†)

New measurements of neutron total cross sections have been performed as a function of neutron energy up to 600 MeV using the WNR facility at Los Alamos National Laboratory. Spallation induced by the 800 MeV LAMPF proton beam in a thick tungsten target produces a continuous or "white" spectrum of source neutrons. A tightly–collimated beam line at 30° to the incident proton direction was used for a series of transmission measurements on about twenty target nuclei ranging in A from beryllium to bismuth. A small, fast scintillation counter was used to detect neutrons by time of flight at a flight path of 40 m. With a micropulse spacing of 1.8 μsec, the practical energy range of the measurements extends from about 4.5 to 600 MeV. While the goal of the experiment was to measure total cross sections above 100 MeV in 1% energy bins and with 1% statistics, much of the data at lower energy is significantly better than that. Particular emphasis was given to isotopically separated samples of closed–shell nuclei (^{40}Ca, ^{90}Zr, ^{208}Pb) for which a substantial body of intermediate–energy proton scattering data already exists. Preliminary analysis of these data in terms of energy–dependent isovector effects in Schroedinger and Dirac optical potentials are presented. Additional applications of these data to shielding, transport, dosimetry, intermediate structure, etc. are discussed.

---

* Physics Department, Kent State University, Kent, OH 44242

** Triangle Universities Nuclear Laboratory, Duke University, Durham, NC 27706

† Los Alamos National Laboratory, Los Alamos, NM 87545

1 Accepted for the International Conference on Nuclear Data for Science and Technology, 13–17 May 1991, Jülich

3. Scattering of Polarized Protons from ^{6}Li at 200 MeV[1] (C.W. Glover*, C.C. Foster,**, P. Schwandt**, J.R. Comfort†, J. Rapaport, T.N. Taddeucci††, D. Wang#, G.J. Wagner##, J. Seubert@, A.W. Carpenter@@, J.A. Carr‡, F. Petrovich‡, R.J. Philpott‡ and M.J. Threapleton‡)

New cross section and analyzing power data have been obtained for elastic and inelastic scattering of 200 MeV protons from ^{6}Li. The elastic data are well described by a standard, spherical, 12–parameter phenomenological Woods–Saxon (WS) optical potential. Microscopic folding–model optical potentials, obtained by convoluting free and Pauli–corrected effective nucleon–nucleon (NN) interactions with ^{6}Li ground–state densities constrained by electromagnetic data, produce satisfactory descriptions of the elastic data. The effects of the spin–spin optical potential, estimated via the distorted wave approximation (DWA), are small but not negligible. The inelastic transitions leading to the 3^+, T = 0 state at 2.18 MeV and the 0^+, T = 1 state at 3.56 MeV are also examined within the framework of the microscopic folding model using the DWA. Transition potentials are generated by convoluting the two effective NN interactions considered with target transition densities constrained by weak and electromagnetic data. These are employed in DWA calculations using both folded optical potentials consistent with the transition potentials and the WS optical potential. The self–consistent calculation with the Pauli–corrected interaction provides a good description of the data for the 3^+ excitation. The results for the 0^+ excitation provide a clear indication that shell model configurations outside the p shell are important for a complete description of this transition.

4. Scattering of Polarized Protons from ^{7}Li at 200 MeV (C.W. Glover*, C.C. Foster**, P. Schwandt**, J.R. Comfort†, J. Rapaport, T.N. Taddeucci††, D. Wang#, G.J. Wagner##, J. Seubert@, A.W. Carpenter@@, J.A. Carr‡, F. Petrovich‡, R.J. Philpott‡, M.J. Threapleton‡)

New cross section and analyzing power data have been measured for elastic and inelastic scattering of 200 MeV protons from ^{7}Li, which have a $3/2^-$, T = 1/2 ground state. A microscopic folding–model optical potential, obtained by convoluting a Pauli–corrected effective nucleon–nucleon (NN) interaction with ^{7}Li ground state densities constrained by weak and electromagnetic data, produces a satisfactory description of the elastic data. The effects of the non–spherical terms in the optical

---

* Oak Ridge National Laboratory, Oak Ridge, TN 37831
** Indiana University Cyclotron Facility, Bloomington, IN 47405
† Physics Department, Arizona State University, Tempe, AR 85287
†† Los Alamos National Laboratory, Los Alamos, NM 87545
# Physics Department, University of Kentucky, Lexington, KY 40506
Physikalisches Institut der Universität Tübingen, 7400 Tübingen, Germany
@ Physics Department, Indiana University–Purdue University at Indianapolis, Indianapolis, IN 46223
@@ Physics Department, Austin Peay State University, Clarksville, TN 37044
‡ Physics Department and Supercomputer Computations Research Institute, The Florida State University, Tallahassee, FL 32306
1 Phys. Rev. C 41, 2486 (1990)

potential, estimated via the distorted wave approximation (DWA), are appreciable. The elastic transitions leading to the $1/2^-$, T = 1/2 and $7/2^-$, T = 1/2 states at 0.48 and 4.63 MeV, respectively, are also examined within the framework of the microscopic folding model and the DWA. Transition potentials are generated by convoluting the effective NN interaction considered with target transition densities constrained by weak, electromagnetic, and low energy proton and neutron scattering data. These potentials are employed in DWA calculations along with the folded optical potential that is consistent with the transition potentials. These self–consistent calculations also provide a good description of the inelastic data. The results provide a clear indication that there are important shape differences between the ^{6}Li and ^{7}Li radial densities and that the two inelastic transitions in ^{7}Li, which are primarily quadrupole in character, have $\rho^m_{2n}/\rho^m_{2p} \approx 0.9$ and 0.9–1.2.

5. Neutron Scattering from ^{90,91,92,94}Zr*[1] (Y. Wang** and J. Rapaport)

Neutron elastic and inelastic scattering differential cross sections from zirconium isotopes, ^{90,91,92,94}Zr, have been measured at neutron incident energies E_n = 8.0, 10.0 and 24.0 MeV. The obtained neutron energy resolutions were 135, 188 and 410 keV (FWHM) for neutron scattering at 8.0, 10.0 and 24.0 MeV, respectively. The elastic scattering data are used to study the isospin dependence of the empirical OMP. The inelastic data are compared with results of DWBA calculations to obtain deformation length values, δ_L, for low–lying collective states. The ratio of neutron and proton transition matrix element, M_n/M_p, are deduced for these low–lying collective states in ^{90,92,94}Zr using the present neutron data and published results of proton data DWBA analyses. An excited–core model analysis of inelastic neutron scattering data from ^{91}Zr is presented.

6. Determination of the Level Density of ^{29}Si from Ericson Fluctuations[2] (V. Mishra, N. Boukharouba, S.M. Grimes, K. Doctor†, R.S. Pedroni and R.C. Haight††)

Neutron total cross section measurements for ^{28}Si have been made with the white neutron source at WNR for neutron energies between 4 and 600 MeV. Very good resolution (≈ .02 ns/m) was obtained. The detailed structure at low energies is found to be different than obtained in previous measurements, although at energies $7 < E_n < 15$ MeV the agreement is quite good. The cross section becomes quite smooth above 15 MeV. An Ericson analysis is performed to yield values for the level density of ^{29}Si between 13 and 22 MeV.

---

* Partially supported by the National Science Foundation

** Presently at Indiana University Cyclotron Facility, Bloomington, IN 47405

† Present address: 1710 Jefferson Avenue, Pt. Pleasant, WV 25550

†† Los Alamos National Laboratory, Los Alamos, NM 87545

1 Nucl. Phys. A517, 301 (1990)

2 Submitted to Phys. Rev. C

7. Isovector Effective Interactions from $^{14}C(p,n)^{14}N$ Studies Between 500 and 800 MeV[1] (E. Sugarbaker*, D. Marchlenski*, T.N. Taddeucci**, L.J. Rybarcyk**, J.B. McClelland**, T.A. Carey**, R.C. Byrd**, C.D. Goodman†, W. Huang†, J. Rapaport, D. Mercer††, D. Prout††, W.P. Alford#, E. Gülmez##, C.A. Whitten## and D. Ciskowski@)

Cross sections at 0° for the pure Fermi (0^+, 2.31 MeV) and Gamow–Teller (1^+, 3.95 MeV) states in the $^{14}C(p,n)^{14}N$ reactions have been measured at $E_p = 494$, 644 and 795 MeV using the LAMPF neutron time–of–flight facility with a new 617–m neutron flight path. The measured cross sections per unit transition strength, $\hat{\sigma}$, provide a measure of the isovector spin–flip and non–spin–flip central components of the effec–tive nucleon–nucleon interaction. Cross sections and the ratio $R^2 = \hat{\sigma}_{GT}/\hat{\sigma}_F$ are compared to lower energy measurements and to calculations using a free N t–matrix.

8. Cross Sections and Spectra for the ^{54}Fe and ^{56}Fe (n,xp) and (n,xα) Reactions Between 8 and 15 MeV[2] (S.K. Saraf@@, C.E. Brient, P.M. Egun@@@, S.M. Grimes, V. Mishra and R.S. Pedroni)

Cross sections and spectra for the (n,xp) and (n,xα) reactions on targets of ^{54}Fe and ^{56}Fe are measured at 8, 9.5 and 11 MeV bombarding energies. The bulk of the spectra appears to be the result of compound nuclear reactions, based on their angular and emission energy dependence. A single set of level density parameters is deduced which fits not only these data but also the data recently obtained at 15 MeV. Very small (n,d) cross sections are found in this energy region.

9. Analog (p,n) Cross Sections of Even–Even Palladium Isotopes at 26 MeV[3] (J.D. Anderson‡, V.R. Brown‡, R.W. Bauer‡, B.A. Bohl‡, C.H. Poppe‡, S. Stamer‡‡, E. Mordhorst‡‡, W. Scobel‡‡, S.M. Grimes and V.A. Madsen‡‡‡)

The differential cross sections for the (p,n) reaction to the ground–state and first 2^+ excited analogs of the four even palladium isotopes (104, 106, 108, 110) have

---

* Physics Department, The Ohio State University, Columbus, OH 43210
** Los Alamos National Laboratory, Los Alamos, NM 87545
† Indiana University Cyclotron Facility, Bloomington, IN 47405
†† Physics Department, University of Colorado, Boulder, CO 80309
# Physics Dept., Univ. of Western Ontario, London, Ontario, Canada N6A 3K7
Physics Department, University of California, Los Angeles, CA 90024
@ Physics Department, University of Texas, Austin, TX 78712
@@ Thomas Jefferson University, Philadelphia, PA 19107
@@@ Institute für Mittelenergiephysik, Zürich, Switzerland
‡ Lawrence Livermore National Laboratory, Livermore, CA 94550
‡‡ I. Institut für Experimentalphysik, University of Hamburg, Hamburg, Germany
‡‡‡ Physics Department, Oregon State University, Corvallis, OR 97331
1 Phys. Rev. Lett. 65, 511 (1990)
2 Nucl. Sci. and Eng. (in press)
3 Phys. Rev. C 41, 1993 (1990)

been measured at a proton bombarding energy of 26 MeV. Integrated cross sections for the analog states deviate from the linear dependence of neutron excess as was previously found in other sets of isotopes, e.g., the molybdenum and zirconium isotopes. The observed dependence on deformation of the ground–state analog transition is in quantitative agreement with calculations, which include the inelastic couplings originally used to explain the molybdenum results. Detailed ten–coupled–channels calculations including the ground state, the one– and two–quadrupole phonon collective states in Pd, and their analogs in Ag give excellent agreement simultaneously with proton elastic scattering, proton inelastic scattering to the first 2^+ state, ground–state analog transitions and 2^+ analog state transitions. The effect of the one–step isovector deformation was too small to be extracted from these data.

10. n+^{209}Bi Mean Field Between –20 and 60 MeV[1] (R.K. Das* and R.W. Finlay)

New measurements of differential elastic neutron scattering for ^{209}Bi at energies between 7.5 and 24.0 MeV are presented along with new measurements of σ_T up to 60 MeV. These data, taken together with earlier measurements at lower energy, provide a very large data set for testing and extending the dispersive optical model analysis. The dispersion correction to the optical model has been obtained from the scattering and total cross section data. The potential is extrapolated to negative energy for comparison with bound state properties. A very good description of all of the data is obtained from –20 to 60 MeV. The present analysis suggests somewhat less depletion of the Fermi sea in this mass region than has been obtained from electron scattering data and from other recent treatments of the dispersion correction to the optical model.

B. MODEL CALCULATIONS AND ANALYSIS

1. Comment on "Testing" the Gamow–Teller Sum Rule[2] (C.D. Goodman**, J. Rapaport and S.D. Bloom†)

Several recent papers purport to "test" the Gamow–Teller sum rule. They compare the differences between incomplete strength function integrals for the β^- and β^+ directions with the quantity 3(N–Z) and interpret discrepancies as degrees of failure of the sum rule. We point out that the Gamow–Teller sum rule is an exact operator relationship, not a model to be tested. It is useful for determining whether a measured strength function is complete.

---

* Physics and Astronomy Department, University of North Carolina at Chapel Hill, Chapel Hill, NC 27599–3225

** Indiana University Cyclotron Facility, Bloomington, IN 47408

† Lawrence Livermore National Laboratory, Livermore, CA 94550

1 Phys. Rev. C 42, 1013 (1990)

2 Phys. Rev. C 42, 1150 (1990)

2. Energy Dependence of the Nuclear Level Density at Energies Above 100 MeV[1] (S.M. Grimes)

Level densities are calculated for the nucleus ^{40}Ca using an exact iterative method for non–interacting fermions. Various single–particle energies are tested. It is found that the conventional Fermi–gas energy dependence provides a good representation of the actual level density only up to energies above 100 MeV. Above this point, the deviations rapidly grow, reaching many orders to magnitude at energies above 200 MeV. One calculation has also been made for ^{90}Zr. These results are similar, with the point of breakdown of the Fermi–gas from raised to about 200 MeV. The present results should have significant consequences for heavy–ion reaction studies of equilibration and for astrophysics.

---

1 Phys. Rev. C 42, 2744 (1990)

A. INTRODUCTION

To a large extent the following contributions have been excerpted from the annual TUNL progress report. Further details and pertinent graphs are included there. Additional information can be obtained by contacting the first author of the respective sections.

B. AVERAGE LEVEL DENSITIES IN MEDIUM-MASS NUCLEI (Li, Bilpuch, Mitchell)

Average statistical properties of nuclei, such as level densities, are important for pure and applied nuclear physics. However, existing phenomenological descriptions have serious limitations. Since most level-density information arises from s-wave neutron resonances, the models are tested only for these limited circumstances. It is not clear how reliable it is to extend phenomenological models to different excitation energies, mass, or angular momentum. Our high-resolution proton-resonance studies at TUNL provide information on nuclei for which no neutron data are available. In order to test the parity dependence and J dependence of the level density, we chose the nuclide ^{49}V (^{48}Ti+p). The ^{48}Ti(p,p) and (p,p') reactions were measured at six angles from E_p = 3.08 to 3.86 MeV. Resonance energies, spins, total widths, and partial widths were determined for 716 resonances. The $1/2^-$ and $3/2^-$, and the $3/2^+$ and $5/2^+$ sequences appear to be less mixed than we observed previously for ^{45}Ca. The level densities for $1/2^+$ and $1/2^-$ states are approximately equal. After correction for missing levels, the experimental J dependence is in agreement with the standard Bethe level density equation. These ^{49}V results provide the *most extensive set of resonances ever measured* and in principle provide the best data for tests of the parity and J dependence of the level density. More extensive calculations with phenomenological models are planned.

C. DISPERSION RELATIONS AND THE MEAN-FIELD POTENTIAL IN NUCLEON SCATTERING

A current development in understanding the optical-model (OM) potential for nucleon-nucleus scattering is the inclusion of dispersion relations (DR) in describing the potential. The DR relates the real and imaginary parts of the mean field as follows:

$$\mathcal{M}(r, E) = \mathcal{V}(r, E) + i\, \mathcal{W}(r, E)$$
$$\mathcal{V}(r, E) = \mathcal{V}_{HF}(r, E) + \Delta\mathcal{V}(r, E)$$
$$\Delta\mathcal{V}(r, E) = (P/\pi) \int_{-\infty}^{\infty} [\mathcal{W}(r, E') / (E' - E)]\; dE' .$$

Here $\mathcal{W}(r, E)$ is the usual absorptive potential that is a combination of a surface and volume contributions, $\mathcal{V}_{HF}$ (r, E) is the Hartree-Fock contribution, $\Delta\mathcal{V}(r, E)$ is the dispersive contribution to the mean field, $\mathcal{V}(r, E)$, and P denotes a principal value integral. The DR introduces a surface contribution to the real central potential and this contribution has a moderately strong variation with energy below 10 MeV. In the following contributions we summarize our results to refine the description of the OM potential.

1. The Dispersive Optical Model for n + ^{27}Al (Nagadi, Delaroche,* Howell, Tornow, Walter)

Spin-spin cross sections for ^{27}Al measured at TUNL by Gould *et al.*[1] using a polarized target and polarized neutrons between 5 and 17 MeV. They attempted to fit the data using the spherical OM parameters of Varner *et al.* and using a complex spin-spin potential with a volume form factor. The ^{27}Al spin-spin cross section was also measured recently by Heeringa *et al.*[2] between 20 and 50 MeV, and they attempted to describe their data and the low energy data of Gould *et al.* using the spherical OM parameters of Martin and confining the spin-spin potential to be real and localized at the surface.

The common difficulty faced in these two analyses was the lack of an OM potential appropriate for ^{27}Al below 14 MeV. One of the early goals of the present work was to develop a more suitable OM for performing spin-spin calculations. In addition, we are interested in extending the dispersion relation (DR) optical model to investigate the applicability of the DR to deformed nuclei, such as ^{27}Al. In fact, our preliminary calculations show that the strength of the spin-spin potential that one obtains in fitting the spin-spin data is sensitive to the inclusion of these dispersive terms. Our dispersive model gives a good description of $\sigma(\theta)$ data over the energy range from 7 to 26 MeV, the latter energy being the highest for which $\sigma(\theta)$ data are available. The ^{27}Al(n,n) analyzing power data from TUNL at 14 and 17 MeV were also used, in particular, to constrain spin-orbit parameters. Table 1 lists the parameters of our OM potential. Here V_{HF} is the so called Hartree-Fock potential of the nuclear mean field.

Although the dispersive OM fit to σ_T data is very good for $E_n > 7$ MeV, the data below 5 MeV are not fit as well. This total cross-section discrepancy is symptomatic of all dispersive OM studies so far.

From sensitivity calculations with this new dispersive OM, we concluded that both the magnitude and the nature of the spin-spin potential obtained from fitting spin-spin total cross section data is dependent on the inclusion of the DR corrections. We were able to describe the qualitative features of the spin-spin total cross section using a real interaction of a strength $V_{ss} = 1$ MeV. We did not explore other contributions of V_{ss} and W_{ss} at this time because of the problem of fitting the total cross section

---

* Centre d'Études de Bruyères-le-Châtel, France.

1 C.R. Gould *et al.*, Phys. Rev. Lett. 57 (1986) 2371

2 W. Heeringa *et al.*, Phys. Rev. Lett. 63 (1989) 2456

below 7 MeV. We are attempting to improve the OM at low energies by including differential cross sections below 8 MeV in the data base and by more carefully accounting for the compound-nucleus contributions to these data.

Table 1. Dispersive optical model parameters[a)] for ^{27}Al.

$\mathcal{V}_{HF}(r,E) = V_{HF}(E)\ f(r) + \Delta\mathcal{V}(r,E)$
$V_{HF}(E) = V_{HF}(E_F)\ \exp[-\alpha\ (E - E_F)/V_{HF}(E_F)]$
$f(r) = [1+\exp((r-R_{HF})/a_{HF})]^{-1}$
$V_{HF}(E_F) = 54.0$, $\alpha = 0.39$, $r_{HF} = 1.19$, $a_{HF} = 0.66$
$W_v = a_v\ (E - E_F)^4 / [(E - E_F)^4 + b_v{}^4]$
$a_v = 9.13$, $b_v = 50.0$
$W_D = g\ (E - E_F)^6 \exp(-c\ E) / [(E - E_F)^6 + h^6]$
$g = 10.413$, $h = 12.98$, $c = 0.0186$
$r_D = 1.28$, $a_D = 0.55$, $V_{so} = 5.7$, $r_{so} = 1.0$, $a_{so} = 0.41$

a) Potentials are in MeV and geometries in fm.

2. Determining the Mean Field for n + ^{28}Si (Alohali, Delaroche,* Howell, Tornow, Walter)

Previously[3] we reported a conventional spherical optical model and a coupled-channels analysis for the reactions $n + {}^{28}Si$ and $p + {}^{28}Si$ in the energy range from 8 to 40 MeV. One aim of the combined analyses was to test for charge-symmetry breaking and to study isospin-dependent effects in the absorptive term for nucleon scattering from ^{28}Si. The two models gave good representations of the data for $\sigma(\theta)$ and $A_y(\theta)$ for both projectiles and for σ_T for $n + {}^{28}Si$. One assumption in these models was that the strength of the surface and volume absorptive terms should vary linearly with energy. However, with such energy dependences the OM fails to reproduce σ_T below about 5 MeV.

One advantage of newer formulations that relate the strength of the absorptive potential to the Fermi energy E_F is that the absorptive potential can be constrained to drop to zero at $E = E_F$ in some smooth fashion (as is expected from basic principles). The dispersive optical model that we are studying uses an $(E - E_F)^n$ dependent form for the absorptive potential. To date we applied dispersive methods to $n + {}^{28}Si$, but not to $p + {}^{28}Si$. The data base was $\sigma(\theta)$, $A_y(\theta)$, and σ_T data measured at TUNL and several other labs. The energy range for $\sigma(\theta)$ was 2 to 40 MeV, for $A_y(\theta)$ it was 10 to 17 MeV, and for σ_T it was 0.2 to 80 MeV. As in the ^{27}Al and ^{54}Fe cases, we have found that the model is not capable of explaining σ_T data at low energies. We plan to investigate other energy dependences for W_D and W_V and to determine whether the radii and diffusenesses must be E-dependent.

* Centre d'Études de Bruyères-le-Châtel, France

[3] C.R. Howell *et al.*, Phys. Rev. C38 (1988) 1552

3. The Proton Mean Field in p + ^{40}Ca from -60 to 200 MeV (Tornow, Chen,* Delaroche,†)

In continuation of our previous dispersive OM analyses of $n + {}^{40}Ca$ and $p + {}^{40}Ca$, we studied the properties of quasibound proton particle states in ^{40}Ca. Our analysis predicts root-mean-square radii, occupation probabilities, absolute spectroscopic factors and spectral functions. We find that our model predicts a 15% depletion of the Fermi sea. It is interesting to compare our results to those for ^{208}Pb, since a wealth of data exists for ^{208}Pb and ^{40}Ca, two nuclei which are widely considered as testing grounds in nuclear structure studies. The most striking feature emerging from this comparison is that the 15% depletion of the Fermi sea for ^{40}Ca is considerably lower than that previously found in the ^{208}Pb region. There, the $3s_{1/2}$ proton orbit (the hole state closest to E_F) has an occupancy of 0.7.[4,5] In ref. 4, short-range and tensor correlations are explicitly considered, while the dispersive OM includes these correlations and others in a global and implicit manner. Therefore, our phenomenological results suggest that the microscopic calculations[4] overpredict the depletion of the Fermi sea. Our conclusion is consistent with the 12% depletion deduced recently by Grabmayr *et al.* [6] for ^{208}Pb. Recent calculations[7] performed in nuclear matter indicate a 13% depletion originating from short-range correlations. This result would be consistent with our phenomenological estimate if the effects of the long-range correlations on the entire depletion were to be a few percent.

4. A Dispersion Analysis to Determine the n + ^{54}Fe Mean Field (Howell, Delaroche,† Walter)

The observed energy dependence of the radius parameter of the real potential in our OM analysis of $n+{}^{54}Fe$ scattering data[8] indicated that dispersion corrections should be applied to the real potential. We are currently re-analyzing the $n+{}^{54}Fe$ data with a model which includes such corrections. Our goal is to determine the Hartree-Fock potential for the $n+{}^{54}Fe$ interaction by fitting the positive-energy scattering data and the negative-energy bound-state data for the ^{55}Fe system. The optical-model parameters are adjusted to fit σ_T data from 0.5 to 80 MeV, $\sigma(\theta)$ from 2 to 26 MeV, and $A_y(\theta)$ data at 10, 14, and 17 MeV. The description of the differential scattering data by our model is very good. However, our dispersive OM predictions of σ_T are 5% low at high energies, i.e., E ~ 50 MeV and 20% low at low energies, i.e., E ~ 1.5 MeV. A deeper V_{HF} than is represented by our exponential function is needed in order to fit σ_T at the extreme energies. Sensitivity tests revealed that the calculated σ_T in both energy regions is strongly influenced by changes in ΔV_D. Since ΔV_D is critically dependent on our knowledge of W_D at all energies, we are including

* Tsinghua University of Beijing, The People's Republic of China

[4] S. Fantoni and V.R. Pandharipande, Nucl. Phys. A427 (1984) 473

[5] V.R. Pandharipande et al., Phys. Rev. Lett. 53 (9184) 1133

[6] P. Grabmayr *et al.*, Nucl. Phys. A494 (1989) 244

[7] A. Ramos, A. Polls, and W.H. Dickhoff, Nucl. Phys. A503 (1989) 1

† Centre d' Ètudes de Bruyères-le-Châtel, France

[8] Howell, Delaroche, and Walter, TUNL Annual Report XXVIII (1988) 70

integrated elastic-scattering cross sections in our analysis below E = 8 MeV to better determine the energy dependence of W_D at low energies.

5. The n + ^{93}Nb Interaction: Conventional and Dispersion Optical Models (Pedroni,* Byrd,† Honoré,‡ Howell, Walter)

We have recently submitted a report for publication in Phys. Rev. C describing measurements of $\sigma(\theta)$ and $A_y(\theta)$ for ^{93}Nb(n,n)^{93}Nb in the range $8 \leq E \leq 17$ MeV, and an OM analysis of these data and σ_T data from 1 to 40 MeV. Three conventional potentials are presented, each based on different initial starting parameters for the OM search routine. The data are also compared to predictions based on potentials reported previously. The data are quite well described by the global model of Walter and Guss (Nuclear Data Symposium, Santa Fe, 1985) and are very well described by the present models. The combined data set, which includes the only $A_y(\theta)$ for n + ^{93}Nb, is described best with the spin-orbit parameters V_{SO} = (6.74 - 0.015 E)MeV, r_{SO} = 1.13 fm, and a_{SO} = 0.511 fm. In addition, the data favor a small, positive absorptive spin-orbit potential, $W_{SO} \approx 0.9$ MeV.

In an extension of the above work, we recently initiated a dispersive optical model analysis of this data set. For this study we also included σ_T data up to 80 MeV. We have had difficulty converging on a model that satisfactorily describes all these data. The major problem is σ_T below 5 MeV. Curiously, these data were quite well described by one of our conventional models mentioned above. We are continuing this dispersion analysis.

6. The Neutron Mean Field in n + ^{208}Pb from -20 to 40 MeV (Roberts, Felsher, Weisel, Zemin Chen, Howell, Tornow, Walter, Horen**)

We have performed a series of optical-model analyses for ^{208}Pb(n,n), starting with a conventional spherical optical model and increasing in complexity to a dispersive OM with an ℓ-dependent absorption. These models were developed using $A_y(\theta)$ data recently measured at TUNL at 6, 7, 8, 9 and 10 MeV, and earlier TUNL measurements of $A_y(\theta)$ at 10 and 14 MeV and of $\sigma(\theta)$ at 9, 10, 14 and 17 MeV. We also included $\sigma(\theta)$ data from Ohio University from 4 to 8 MeV and from 20 to 26 MeV and from MSU at 30 and 40 MeV. High-accuracy σ_T data from 0 to 40 MeV were also used. For the dispersive OM analysis, we included empirically derived properties of the single-particle states of the n+^{208}Pb system.

Both the conventional spherical OM and the dispersive OM give quite good descriptions of the appropriate data. However, precise detailed agreement at all energies still evades us when we restrict the model to one in which the parameters

---

* Pres. address: Dept. of Physics, Ohio University, Athens, Ohio

† Pres. address: Physics Division, Los Alamos National Laboratory, Los Alamos, NM

‡ Pres. address: Bowman Gray School of Medicine, Winston-Salem, NC

** Oak Ridge National Laboratory

vary smoothly with energy. A major problem to be faced in carrying the dispersive OM farther is the lack of sensitivity at the 2% level of determining parameters. It is not clear if it is valid to assume that the imaginary surface potential has a Woods-Saxon form factor, which is a problem tied to excitation of collective surface nodes and to partial-wave nodes in the nuclear surface region. Also, it is now clear that to push the model beyond the simple fixed-geometry representations will be difficult. It would be important to have more and better $A_y(\theta)$ data above 14 MeV to help fix the energy dependence of the interaction. A manuscript which reports on the new TUNL measurements mentioned above and on progress with the optical models and nuclear mean field determination has been submitted for publication.

D. ANALYZING POWERS FOR $^{120}Sn(n,n)^{120}Sn$ AT 17 MeV (Pedroni, Howell, Walter)

A paper summarizing the results of this research was recently published in Phys. Rev. C. The abstract reads: "Measurements of $A_y(\theta)$ have been made for the elastic scattering of neutrons from ^{120}Sn at 17 MeV. The data were corrected for finite geometry and multiple scattering effects and are compared to predictions derived from the coupled-channels analysis for $^{116,120}Sn$ of Guss *et al.*"

E. ANALYZING POWERS FOR $^{209}Bi(n,n)$ AND TESTS OF COMPOUND-NUCLEUS MODELS
(Weisel, Tornow, Howell, Roberts, Felsher, Alohali, Walter, Mertens, Horen*)

The development of nucleon-nucleus OM potentials has been a major concern of TUNL for the past two decades. In recent years, the task of comparing contesting approaches has become one of increasingly small effects, especially with the application of dispersion relations. Effects of the dispersion relation are observed with the best sensitivity at low incident nucleon energies, E ≤ 10 MeV. A concern at low energies is how closely the data base represents direct-reaction or shape-elastic scattering. For this reason it is important to know the compound-elastic contribution exactly. The purpose of the present study is to test our ability to properly account for the compound-nucleus (CN) effect. Our approach is to compare angular distributions of analyzing powers $A_y(\theta)$ for the special case of neighboring heavy nuclei for which the CN contribution are known to be appreciably different. The CN elastic contributions can be calculated with available computer programs based on the Hauser-Feshbach statistical model and subtracted from measured data to leave only direct-reaction elastic scattering. If the two neighboring nuclei behave statistically in the region of measurement, and if the CN model is accurate, their resultant direct-reaction scattering data should be virtually identical.

We performed high-accuracy measurements of $A_y(\theta)$ for $^{209}Bi(n,n)^{209}Bi$ data at 6 and 9 MeV to compare to companion TUNL data for ^{208}Pb. Our reason for choosing 9

* Oak Ridge National Laboratory

negligible here for both ^{208}Pb and ^{209}Bi. The 9-MeV ^{209}Bi data closely agree with the 9 MeV ^{208}Pb data.
At 6 MeV the compound-reaction contributions are significant. The most sensitive input to the CN calculation are the parameters modeling the continuum of excited states. We determined the parameters for the constant-temperature (CT) formula by three criteria: a) extrapolation from a plot of the number of available states *vs* excitation energy, b) agreement between inelastic-scattering data and results of the CN calculation, c) consideration of the $A_y(\theta)$ data, which sets an upper limit to the CN correction, since the magnitude of $A_y(\theta)$ cannot exceed 1.0. The CN correction for ^{209}Bi is relatively straightforward. For ^{208}Pb a wider range of CN corrections is allowed by the third criterion. Although we allow for the option of missing 35% of the discrete levels up to 6 MeV when establishing the CT formula, we still find that the $A_y(\theta)$ data for ^{208}Pb suggest the CN contribution is underestimated when compared to the $A_y(\theta)$ data for ^{209}Bi. The investigation of these systems is continuing.

F. MICROSCOPIC DESCRIPTIONS OF NUCLEON-NUCLEUS SCATTERING FOR A = 6 - 208 FROM 8 to 80 MeV (Walter, Hansen,* Dietrich*)

As part of a program to characterize the nature and strength of microscopic potentials, we have studied such models in connection to neutron-nucleus scattering for about 10 nuclei over the energy range 8 to 40 MeV. We used a large portion of the TUNL $\sigma(\theta)$ and $A_y(\theta)$ measurements in the 8 to 17 MeV range. The main focus lately has been the Jeukenne, Lejeune and Mahaux (JLM) and the Yamaguchi (YAM) potentials. The former is based on the Reid hard-core nucleon-nucleon (NN) interaction and an M3Y spin-orbit term, whereas the latter is based on the Hamada-Johnson NN interaction and uses a spin-orbit term derived from the NN interaction.

For near-spherical nuclei with $A \geq 54$, reasonable fits are obtained to both $\sigma(\theta)$ and $A_y(\theta)$ data if the strengths of the three potentials of the models (V, W, V_{SO}) are scaled by factors [$\lambda_V(E)$, $\lambda_W(E)$, $\lambda_{SO}(E)$] that have a monotonic energy dependence. The $\lambda_V(E)$ is close to unity, ranging between 0.95 and 1.05. The $\lambda_W(E)$ falls rapidly from about 0.8 at 12 MeV and above to about 0.6 (0.45) for JLM (YAM) as the incident nucleon energy is decreased to 8 MeV. The λ_{SO} is probably independent of energy, and is about 1.2 to 1.4 for both models. For ^{28}Si(n,n)^{28}Si qualitative agreement was also obtained. However, for ^{40}Ca several details in $\sigma(\theta)$ and $A_y(\theta)$ were not predicted; in particular, the reaction might be too complicated at the lower energies to be explained with this approach.

Very little is known about the quality of the predictions of existing microscopic models for nucleon-nucleus scattering for A < 12. More recently, we tested the model for (n,n) and (p,p) scattering from ^{6}Li, ^{10}B and ^{11}B. Results for ^{10}B and ^{11}B were surprisingly good, and the ^{6}Li data were moderately well fit. Our next step is to incorporate data for ^{9}Be and ^{27}Al, and to summarize our findings in publications.

* Lawrence Livermore National Laboratory

G. <u>A GLOBAL NUCLEON OPTICAL MODEL POTENTIAL FOR A = 40 - 209, E = 10 - 65 MeV</u> (Varner,* Thompson, McAbee, Ludwig, Clegg)

We have completed a new parameterization of the nucleon-nucleus OM potential based on data for A = 40 - 209, proton energies of 16 - 65 MeV, neutron energies of 10 - 26 MeV, and including extensive polarized-beam data. This parameterization is based on current understanding of the basis of the optical potential, such as the folding-model and nuclear-matter approaches. The potential differs significantly from previous global parameterizations, especially in the weakness of the isovector potential, the parameterization of potential radii, and the smooth variation of the imaginary potential depths with energy. We also describe an OM parameter search system, MINOPT, based on the minimization program MINUIT. It was applied to simultaneously analyze all 300 angular distributions in the large database.

For the first time in a global OM analysis, we have estimated parameter uncertainties and correlations between parameters, using the non-parametric statistical technique known as the bootstrap. Our OM potential is intended to serve as a starting point for definitive tests of models of the mean potential field in nuclei, and to be used for applications such as modeling *r*-process nucleosynthesis in stars and engineering design of fusion reactors. An extensive description of this research has been accepted for publication in Physics Reports.

H. <u>NUCLEAR DATA EVALUATIONS FOR A = 4 - 20</u> (Tilley, Weller, Hale,† Atkinson)

The project for the evaluation of nuclear data in the mass range A = 3 - 20, carried out for many years by Dr. Fay Ajzenberg-Selove, is in the process of being moved to TUNL. Some details of the evaluations are as follows.

The new compilation on the A = 4 system is nearing completion. The reaction-by-reaction tables of measurements, discussions, and reference lists are essentially complete. Several copies of a preliminary version were circulated at the Washington APS Meeting in April 1990. The reaction sections are now being revised and updated at TUNL while the General sections (which will contain discussions of excited states in the A = 4 system) are being prepared at Los Alamos. A paper will be prepared for submission to Nuclear Physics.

Reference lists, drawings, and other material for A = 5 - 20 are being transferred to TUNL, and we have begun the A = 16 - 17 evaluation while Dr. Ajzenberg-Selove is working on A = 13 - 15, which she expects to complete soon. She continues literature coverage for A = 5 - 20 and is providing us updated reaction-by-reaction bibliographical listings. In addition, the TUNL group is carrying out a parallel review of the current

---

* Oak Ridge National Laboratory

† Los Alamos National Laboratory

literature. To the extent possible within current personnel constraints, we will comply with the recommendation that the A = 16-17 evaluation be in the ENSDF format.

I. GAMOW-TELLER STRENGTH FUNCTIONS FOR LIGHT- AND MEDIUM-MASS NUCLEI (Howell, Aslanoglou,* Brady,† Drummond,† Finlay,* Haight,‡ King,‡ Lisowski,‡ Morris,‡ Rapaport,* Romero,† Sorenson,† Tornow, Ullmann‡)

We have developed a facility at the Los Alamos National Laboratory (see ref. 9 for details) to measure forward-angle cross sections for the (n,p) reaction for neutrons in the range from 50 to 250 MeV. The measurements use the continuous energy neutron beam at LAMPF/WNR. The goal is to provide complementary information on the isovector parts of the nucleon-nucleus interaction to that obtained from (p,n) charge-exchange data.

The $^{12,13}C(n,p)$ measurements reported[9] last year are being prepared for publication. The $^{12}C(n,p)$ reaction is important for several reasons. First, the "unit cross section" (discussed in ref. 10) $\hat{\sigma}_{GT}$ can be calibrated with reference to the known β^- decay strength, since ^{12}C is the product of an allowed Gamow-Teller (GT) β^- decay ($^{12}B \rightarrow \beta^- + {}^{12}C$). Second, it is a convenient reaction for investigating the quenching of the GT strength which was observed in (p,n) reactions. The complete GT strength for the $^{12}C(n,p)$ reaction can be extracted with little error. Third, the $\hat{\sigma}_{GT}$ was found to be about 50% larger for the $^{13}C(p,n)$ reaction than for $^{12}C(p,n)$. The difference between the $^{12,13}C(p,n)$ reactions has been attributed to "odd-even" effects[10]. This 50% effect was not observed in our $^{12,13}C(n,p)$ data.

This summer we are finishing measurements on $^{32}S(n,p)$. In addition to having a strong Gamow-Teller strength, the β^+ and β^- strengths should be equal since ^{32}S is a self-conjugate nucleus. This implies that the ratio of the zero-degree cross sections for the $^{32}S(n,p)$ and $^{32}S(p,n)$ reactions gives the ratio of $\hat{\sigma}_{GT}$ for these reactions. We are also measuring forward-angle (n,p) cross sections for ^{60}Ni and ^{64}Ni. In addition to providing a testing ground for nuclear-structure calculations, ^{64}Ni is the only nucleus in the *fp* shell to be the product of a strong beta decay to the ground state of the daughter nucleus ($^{64}Co \rightarrow \beta^- + {}^{64}Ni$).

J. REACTIONS IN VERY LIGHT NUCLEAR SYSTEMS

Because of space limitations, this year no details have been given here about studies at TUNL involving light nuclear systems. Some of the work underway is

---

* Ohio University, Athens, OH

† University of California, Davis, CA

‡ Los Alamos National Laboratory, Los Alamos, NM

9 C.R. Howell et al., TUNL Annual Report XXVIII (1989) 90

10 T.N. Taddeucci et al., Nucl. Phys. A469 (1987) 125

outlined in the TUNL annual report. A list of work reported therein that is pertinent to the present report is listed here with only one author's name.

1. A Test of NN Potentials Using Backward-Angle *n-d* Scattering, C.R. Howell
2. Three-Nucleon-Force and Off-Shell Effects in *d(n,nnp)* Breakup, C.R. Howell
3. Analyzing Powers in *d(d,pn)d* at 12 MeV, P.D. Felsher
4. Spin Effects in $d(d,p)^3He$ and $d(d,n)^3He$ at Very Low Energies, H.J. Karwowski
5. The D state in ^{3}H from Sub-Coulomb *(d,t)*, E.J. Ludwig
6. The $d(d,\gamma)^4He$ Reaction with Polarized Beams, H.R. Weller
7. The $^3H(p,\gamma)^4He$ Reaction and the $(\gamma,p)/(\gamma,n)$ Ratio in ^{4}He, H.R. Weller
8. Ground-state Widths of ^{5}He and ^{5}Li from $^3H(d,\gamma)^5He$ and $^3He(d,\gamma)^5Li$, D.R. Tilley
9. Radiative Capture Observables and the Resonating-Group Model, H.R. Weller

WESTINGHOUSE HANFORD COMPANY

Activation Cross Section Library, F.M. Mann and D.E. Lessor (Westinghouse Hanford Company).

Using the REAC*2 cross section library, the latest version of the ECN-REAC activation library, and general purpose evaluations from ENDF/B-VI, a large point-wise activation cross section library is being developed. All stable isotopes and all isotopes with half-lives greater than 100 days and mass less than radon will be included. A future version will include the actinides. All significant reactions below 20 MeV will be present. The library will extend to 40 MeV for the most important targets. The point-wise library will be processed into a 89-group library for use in activation codes.

Master Decay Library, F.M. Mann and F. Schmittroth (Westinghouse Hanford Company), T.R. England (Los Alamos National Laboratory), and C.R. Reich (Idaho National Engineering Laboratory).

Using the ENDF/B-VI decay file and the ENDSF nuclear structure file, a decay library based upon ENDF/B-VI for all isotopes reached by neutron-induced reactions or by high energy proton-induced reactions is being developed. A version based on the preliminary ENDF/B-VI decay data and ENDSF was created and tested. Preliminary comparisons with other data files in common use have shown that the new file is more comprehensive and accurate, especially for nuclides less frequently encountered.